Anaerobic digestion of petroleum refinery sludge: Effect of pretreatment and co-digestion

A thesis submitted

in partial fulfillment of the requirement for the degree of

Doctor of Philosophy

By

Shinjini Paul Choudhury

Department of Civil Engineering

Indian Institute of Technology Guwahati

Guwahati-781039, Assam, India

August -2023

In loving gratitude to

My beloved parents

whose unwavering love, blessings, and continual encouragement have been the guiding light leading to my achievements and growth

Department of Civil Engineering
Indian Institute of Technology Guwahati
Guwahati – 781039, Assam, India

Dr. Ajay Kalamdhad
Professor
Email: k.ajay@iitg.ac.in
Phone: +91-361-258-2431

CERTIFICATE

This is to certify that the thesis entitled **"Anaerobic biodegrability of petroleum refinery sludge: Effect of pretreatment and co-digestion"** submitted by Shinjini Paul Choudhury (186104030), a Research Scholar of Department of Civil Engineering, Indian Institute of Technology Guwahati, for the award of the degree of Doctor of Philosophy, is a record of an original research work carried out by under my supervision and guidance. The thesis has fulfilled all requirements as per the regulations of the institute and, in my opinion, has reached the standard needed for submission. The results embodied in this thesis have not been submitted to any other University or Institute for the award of any degree or diploma to the best of my knowledge and belief.

Date:
Place: IIT Guwahati

Prof. Ajay Kalamdhad

Department of Civil Engineering
Indian Institute of Technology Guwahati
Guwahati – 781039, Assam, India

STATEMENT

I, Shinjini Paul Choudhury, declare that this thesis titled "**Anaerobic biodegrability of petroleum refinery sludge: Effect of pretreatment and co-digestion**" and the work presented in it are my own. I confirm that:

- This work was done wholly while in candidature for a research degree at this Institute.
- In full or in portions, the contents of this thesis have not been submitted to any other University or Institute for the award of any degree or diploma.
- Where I have consulted the published work of others, this is always clearly attributed.
- Where I have quoted from the work of others, the source is always given. With the exception of such quotations, this thesis is entirely my own work.
- I have acknowledged all main sources of help.
- Where the thesis is based on work done by myself jointly with others, I have made clear exactly what was done by others and what I have contributed myself.

Date: Signed

Shinjini Paul Choudhury
Registration No.: 186104030

ACKNOWLEDGEMENT

I am truly privileged to have this opportunity to express my profound gratitude to the individuals who have wholeheartedly supported me in my journey towards completion of this thesis. I firmly believe that without their support, the successful completion of this work would not have been possible.

First and foremost, I am profoundly grateful to my supervisor, **Prof. Ajay Kalamdhad**, for his exceptional guidance and mentorship throughout my research journey. His invaluable expertise, constructive feedback, and unwavering encouragement have played a pivotal role in shaping the direction of this thesis and driving me to reach my fullest potential. His dedication, patience, and commitment to excellence have been a constant source of inspiration, and I consider myself incredibly fortunate to have had such an outstanding supervisor who believed in my capabilities and nurtured my academic and personal growth. Working under his supervision has been an honour, and I am deeply indebted to him for his significant contribution to my overall development.

I would also take this opportunity to thank my Doctoral Committee Members, **Dr. Anil Kumar Mishra** (Chairman), **Dr. Bimlesh Kumar**, and **Dr. Senthilkumar Sivaprakasam**, for their exceptional suggestions and encouragement in propelling my research work forward. Their thought-provoking questions have inspired me to explore my research from diverse perspectives, leading to a more comprehensive and enriched study. I also express my sincere thanks to **Prof. Sharad Gokhale**, Head of the Department of Civil Engineering for providing me with the necessary research facilities. I gratefully acknowledge the unstinted help provided by **Mr. Chitaranjan Medhi**, **Mr. Payodhar Pathak** and **Ms. Jonali Saikia** during all phases of my research work. Furthermore, I would like to thank the **Mr. Susanta Sarma** and other office staffs of the Department of Civil Engineering for their support in administrative work.

I express my gratitude to **Prof. Parameswar K. Iyer**, Director of IITG, for providing necessary facilities and creating a conducive academic environment within the institution that facilitated my research journey. Additionally, I acknowledge the Central Instrument Facility, Centre for Environment, School of Agro and Rural Technology, Mechanical Workshop, and Lakshminath Bezbaroa Central Library at IIT Guwahati for offering state-of-the-art infrastructure for conducting advanced research in the field of study.

I extend my sincere appreciation to all the members of the **Waste Management Research Group (WMRG)** for their invaluable support, engaging research discussions, and assistance in my laboratory work. Being a part of the WMRG family has enriched my research experience in

countless ways. Words will fall short to express my gratitude to **Mr. Nayan**, **Mr. Rontu** and **Mr. Sujit** for their constant assistance during experimental setup and sample collection.

Throughout this journey, I have formed a special bond with **Mr. Sugato Panda**, a former master's student in the School of Agro and Rural Technology, IIT Guwahati. His valuable contributions to my research work have been instrumental in the progress of my study. I would also appreciate the efforts of **Ms. Bandita Dalasingh**, **Mr. Amlan Buragohain** and **Mr. Pranav Gautam,** former master's students of NIT Agartala and IIT Guwahati for their contribution during my academic journey, especially during collection of raw materials and assisting in the experimental work. I extend my best wishes to them for their future endeavours.

I extend my heartfelt gratitude to **Dr. Izharul Haq**, former IPDF, IIT Guwahati, for his expert guidance in bacterial pretreatment, toxicity evaluation and microbiological studies. His assistance has been instrumental for completion of this thesis.

I must take this opportunity to thank my seniors, **Dr. Biswanath Kumar Saha, Dr. Mayur Shirish Jain**, **Dr. Kunwar Raghvendra Singh, Dr. Dhamodharan Kondusamy**, **Dr. Visva Bharati Barua**, **Dr. Jyoti Kainthola**, **Dr. Chejarla Venkatesh Reddy**, **Dr. Saswati Ray, Dr. Heena Kauser,** and **Dr. Ankit Goswami** for their support and mentorship during my journey.

I must say thanks to my supportive friends, juniors and labmates, **Mr. Maturi Krishna Chaitanya**, **Ms. Ashmita Kundu**, **Ms. Silvia Saikia**, **Mr. Suryateja Pottipati, Mr. Arun Sathyan**, **Mr. Induchoodan T.G.**, **Mr. Prakash Singh**, **Mr. Ankit Kumar**, **Ms. Sumona Koley**, and **Ms. Jyoti Beniwal**, whose support and respect during my research journey at IITG have been encouraging.

Lastly, I am deeply grateful and indebted to my mother, **Mrs. Sampa Paul Choudhury**, and my father, **Mr. Bijan Paul Choudhury**, for their unconditional love, unwavering support, continuous encouragement, and blessings throughout my years of study and the entire research journey leading up to this thesis. Their presence has been the cornerstone of my achievements, and I cannot thank them enough for existing in my life. I also extend my heartfelt appreciation to my close friends, **Ms. Ayushi Sharma**, **Mr. Om Prakash Vats** and **Ms. Vipasha Maholia** whose direct or indirect support has played a significant role in making this journey worthwhile.

Above all, I humbly acknowledge the **ALMIGHTY** for bestowing upon me the wisdom, strength and patience to undertake this research and complete it with His divine grace and blessings.

Shinjini Paul Choudhury

ABSTRACT

Rapid industrialization in conjunction with urbanization is devouring natural resources worldwide and their processing or refining into useful products are leading to mounting global waste generation. Petroleum refinery sludge (PRS), an egregious solid residue generated from the effluent treatment plants (ETPs) of petrochemical refineries, poses an environmental hazard owing to its intricate hydrocarbon composition, necessitating competent treatment for secure disposal. The PRS generated from the biological treatment units of the ETPs has enormous potential for biogas production through anaerobic digestion. Selection of appropriate inoculum is crucial to foster a well-balanced environment with favourable microbial communities for initiating the anaerobic digestion process. In order to select an appropriate inoculum, the biodegradation of PRS was compared between undigested residue of animal manure, and anaerobically acclimated or digested sludge from an operational anaerobic reactor. Upon performing 1L batch anaerobic biodegradation assays, digested sludge provided a better seeding environment exhibiting maximum biogas yield with higher organic fraction removal resulting in improved biodegradability. 16S metagenome sequencing of digested sludge revealed significant predominance of *Proteobacteria*, *Bacteroidetes* and *Firmicutes* at phylum level possessing hydrocarbon-degrading properties.

However, the hydrolysis phase of the complex PRS substrate was lengthy due to its recalcitrant nature. To overcome this, different pretreatment techniques were applied (thermal, electrokinetic, and microbial). Thermal pretreatment involved the optimization of different modes of heat application (dry heat, pressurized moist heat, agitated open moist heat and microwave irradiation). Dry heat at 140 °C for 60 min proved most effective, leading to a 40% increase in biogas production and 48.7% organic matter removal. Electrokinetic pretreatment was optimized using central composite design- response surface methodology (CCD-RSM) to ascertain a combined variation of applied voltage (40-80 V), exposure duration (20-120 min) and distance between graphite electrodes (8-16 cm). Electrokinetic pretreatment at 60 V, 83.5 min, and 11.6 cm electrode spacing resulted in maximum solubilization, leading to 61% enhancement in biogas production. Furthermore, microbial pretreatment was optimized utilizing two bacterial strains, Laccase enzyme-producing *Pseudomonas putida* 7525, and novel lignin peroxidase (LiP) enzyme-producing *Kosakonia oryziphila* IH3 (MZ605201) to optimize the accelerated solubilization of PRS. Pretreatment utilizing *P. putida* at a dosage of 10^8 colony forming units per mL (CFU/mL) resulted in maximum solubilization within 6 d, leading to 54.6% biogas augmentation. Consequently, pretreatment with *K. oryziphila* at a dosage of 10^8 CFU/mL maximized solubilization within 4 d of pretreatment, leading to 50.2% biogas enhancement. Scaled up (20 L) anaerobic biodegradability batch studies revealed maximum removals of total petroleum

hydrocarbon (57.3%), and oil and grease (71.5%) for electrokinetically pretreated PRS whereas, utmost removal of total phenol (91.7%) was observed for *P. putida* pretreated PRS. The phytotoxicity assay conducted on batch digestates using *Vigna radiata* L. showed concentration-dependent decrease in seed germination, shoot length, root length and biomass compared to control (untreated PRS), thereby, suggesting dilution of toxicant concentrations.

Initial characterization of PRS expressed the restriction of biodegradability due to lack of nutrient balance and substrate recalcitrance. Anaerobic co-digestion of nitrogen-rich PRS was performed with carbon-rich yard waste (YW), balancing the nutrients and moisture content for efficient microbial proliferation. Using CCD-RSM, anaerobic biodegradability batch experiments were conducted with varying carbon/nitrogen (C/N) ratios and pH to achieve maximum biogas at C/N= 32.5 and pH = 7.0. However, the sluggish biogas recovery (40%) indicated a slow rate-limiting hydrolysis in absence of pretreatment. Electrokinetically-assisted co-digestion process, when optimized at an applied voltage of 53.5 V for 53 min maximized solubilization of PRS mixed with YW at optimum co-digestion condition. Upscaled batch studies resulted in 84.2% enhancement in biogas production compared to monodigestion of PRS with significant total petroleum hydrocarbons, emulsions, and lignocellulosic degradation. Consequently, when microbially-assisted pretreatment was conducted utilizing two bacterial strains isolated from PRS (LiP enzyme-producing *Bacillus subtilis* IH1, MZ618640 and Lac enzyme-producing *Bacillus velezensis* IH2, MZ605121), *B. subtilis* IH1 strain led to maximum improvement in solubilization, resulting in 76% enhancement in biogas against monodigestion of PRS. Further identification of major organic pollutants in the batch digestate revealed significant degradation of the toxic organic hydrocarbon pollutants apotheosizing the efficacy of the synergistic sustainable technique for the management of PRS.

In order to ascertain the feasibility of anaerobic biodegradation of PRS, a lab-scale 20 L anaerobic biphased baffled reactor (ABBR) was operated in semi-continuous mode for 200 d. The ABBR was operated with untreated PRS for 100 d resulting in average methane content of 47.5%, at an OLR of 1.6 kg COD m^{-3} d^{-1} along with a mere 19.5% COD removal. Operation of electrokinetically pretreated PRS at optimum condition obtained from the electrokinetic pretreatment (60V, 83.5 min, 11.6 cm electrode spacing) resulted in average methane content of 61% at optimum OLR of 1.5 kg COD m^{-3} d^{-1}, along with 70.6% COD removal. Electrokinetic pretreatment of PRS resulted in enhanced solubilization with average methane enhancement by 1.3-folds suggesting enhanced degradability and improved process stability.

Keywords: *Anaerobic digestion; petroleum refinery waste; hydrocarbon; phytotoxicity; yard waste; co-digestion; pretreatment; biogas*

TABLE OF CONTENTS

LIST OF FIGURES

LIST OF TABLES

LIST OF ABBREVIATIONS AND SYMBOLS

ABBR	Anerobic biphased baffled reactor
AD	Anaerobic digestion
AnCoD	Anaerobic co-digestion
ANOVA	Analysis of Variance
BMP	Biochemical methane potential
C/N	Carbon/Nitrogen
DS	Digested sludge
EK	Electrokinetic
FESEM	Field Emission Scanning Electron Microscope
FTIR	Fourier Transform Infrared
GS-MS	Gas Chromatography-Mass Spectroscopy
HRT	Hydraulic retention time
I/S	Inoculum/Substrate
I/F	Inoculum/(substrate+co-substrate)
O&G	Oil and grease
OLR	Organic loading rate
PAH	Polyaromatic hydrocarbon
PRS	Petroleum refinery sludge
sCOD	Soluble chemical oxygen demand
TPH	Total petroleum hydrocarbon
TS	Total solids
UR	Undigested residue
VFA	Volatile fatty acids
VS	Volatile solids
YW	Yard waste

Chapter 1

INTRODUCTION

This chapter discusses about petroleum refinery sludge (PRS) generated from the effluent treatment plants of petrochemical refineries, different types of PRS, and the problems associated with their management. This discussion further proceeds towards suitability of anaerobic digestion for PRS and different types of enhancement techniques for energy recovery. Finally, this chapter has been incorporated with the objectives, need and the scope of the study.

1.1 OVERVIEW

Rapid industrialization and urbanization have accentuated the energy demand worldwide. Implausible exhaustion of fossil fuels due to their rapid utilization in food, agriculture and industrial sectors has fueled the environmental pollution and greenhouse gas emissions causing energy insecurity globally (Baykara, 2018). In addition to that, comprehensive production of colossal quantities of waste from different types of industrial activities are cumulative to the environmental pollution demanding critical research for their efficient and cost-effective management (Hu et al., 2020).

During the exploration and production of petroleum in petrochemical industries, various wastes are generated which cannot be disposed of without treatment since they are contemplated as hazardous waste (Islam, 2015; Roy et al., 2015). These waste oils having the potential to be reused are recirculated to the refining plants and the portions losing their usage potential are treated in the Effluent Treatment Plant (ETP) of the refineries. The focus of an ETP is to reduce oil and grease, remove suspended pollutants and degrade dissolved contaminants from these wastes, decreasing their concentrations to the acceptable limits of discharge. The ETP is an amalgamation of physical, chemical and biological processes. During each process certain wastes or solid residues are generated which can be regarded as 'effluent treatment plant sludge' or 'bottom tank sludge' or 'petroleum refinery sludge'. Petroleum refinery sludge generated from mechanical treatment of petroleum refinery wastewater involving physical processes to remove heavy solids and immiscible liquids (free and emulsified oil) in separation tanks such as dissolved air floatation unit is known as oily sludge (Diya'uddeen et al., 2011; Bhattacharyya and Shekdar, 2003). Treatments involving physico-chemical processes for removal of dissolved oil and lighter solids, such as floatation or clariflocculation, generate chemical sludge (El-Naas et al., 2014). Petroleum refinery biosludge is generated from treatments involving biological processes such as activated sludge process responsible for the removal of dissolved organic pollutants (Islam, 2015; El-Naas et al., 2014). The

sludge generated by the petroleum refineries have garnered an increased attention in recent years because their composition is very complex which comprises of a mixture of petroleum hydrocarbons, asphaltenes, long chain paraffinic wax, sediments and heavy metals. The high concentration of petroleum hydrocarbons along with few recalcitrant components present in refinery sludges make them cytogenic, mutagenic and carcinogenic in nature (Johnson and Affam, 2018). Their improper treatment or disposal can pose serious threats to human health and environment.

Petroleum refinery sludge (PRS) consists of complex hydrocarbons which include linear and cyclic alkanes (40-52%), polyaromatics (28-31%), resins (7-22%) and ashphaltenes (8-10%) (Kriipsalu et al., 2008; Janajreh et al., 2020). Oily sludge from petrochemical industries consists of total petroleum hydrocarbon (aliphatic and aromatic) (15-50%) along with water (30-85%) and solids (5-50%) (Hu et al., 2013). Due to high calorific values of PRS (17000-19000 kJ/kg^2), combustion technologies such as incineration or pyrolysis for its treatment at a high temperature range of 500-1100°C seem to be advantageous options (Hu et al., 2013; Li et al., 2020; Zuo et al., 2021). But the characteristics of PRS vary greatly not only in calorific values but also in moisture content (6% - 80%) and oil content (35% - 92%) due to which the combustion technology becomes inefficient at high moisture and low oil contents (Sankaran et al., 1998; Kriipsalu et al., 2008; Hu et al., 2020). Also, due to the high viscosity of oily sludge, they are heated before being fed into incinerators to maintain their flow requiring energy-intensive pretreatment (Sankaran et al., 1998). Combustion of auxiliary fossil fuels and organic sludge at high temperatures generates hazardous residues and leads to toxic gaseous emissions (GHG, SO_2, and NO_x) which require additional treatment (Hu et al., 2020). Land disposal of PRS without treatment can reduce hydraulic conductivity, water availability and exchange of water-air into the soil hampering the physical as well as the nutritional profile of soil matrix, all of which have always been a matter of concern for many years (da Silva et al., 2012; Kriipsalu et al., 2008). The multi-phasic and heterogeneous properties of these sludge make any particular treatment approach highly inconsistent. Few treatment options explored for management of PRS are centrifugation, froth-floatation, oxidation and plasma gasification as described in Hu et al. (2013) which again are either energy-intensive or cost-intensive and therefore, biological remediation options are in dire need for the overall management of these sludge (Elektorowicz and Habibi, 2005). Anaerobic digestion (AD) is one such biological treatment option explored by various researchers for improved digestibility, sludge dewaterability and toxicity removal of PRS through biogas production (Haak et al., 2016; Janajreh et al., 2020). In AD, suitable microbial consortium decay biodegradable fraction of a substrate in the absence of any terminal electron acceptor (sulfate, nitrate, and oxygen) generating methane-

rich biogas and the process is carried out in four stages: hydrolysis, acidogenesis, acetogenesis, and methanogenesis (Appels et al., 2008). Hydrocarbons are found to purvey the source of electron donors and carbon for the functioning of bacteria under redox conditions during anaerobic biodegradation (Holliger and Zehndert, 1996). But AD of PRS is challenging since it depends on the concentration of toxicants which become inhibitory for the methane-producing bacteria, and the presence of recalcitrant compounds (Kriipsalu et al., 2008). The recalcitrant nature of hydrocarbons is attributed to unfavourable environmental conditions and lesser application of microbes utilizing hydrocarbons under anaerobic conditions. Therefore, providing a favourable microbial inoculation for AD of PRS is necessary since it will not only increase microbial diversity but also improve the biodegradation efficiency with improved solubilization (Wang et al., 2016).

The action of consortium of anaerobic microorganisms for stabilization of sludge is often limited to low organic matter removal efficiency (30-45%), long hydraulic retention time (20-40 days) and recalcitrant properties of sludge which can be attributed to rate-limiting hydrolysis stage necessitating pretreatment. (Haak et al., 2016; Ennouri et al., 2016; Heng et al., 2017). PRS is a complex mixture of hydrocarbons, water/oil emulsions, heavy metals and recalcitrant components, and therefore, to reduce the lengthy hydrolysis phase pretreatment is vital to solubilize the complex intracellular components (hydrocarbons) and transform the recalcitrant organic content into biodegradable fraction thereby amplifying energy production. A wide range of pretreatments have been studied which can be classified as, physical (Ye et al., 2008; Yang et al., 2019), chemical (Heng et al., 2017), physico-chemical (Yu et al., 2014; Zeng et al., 2019), thermal (Yeshanew et al., 2016; Ennouri et al., 2016), and biological pretreatments (Kavitha et al., 2014).

Besides, PRS lacks the nutrient balance in terms of carbon and nitrogen (C/N) ratio due to low carbon and high nitrogen content inhibiting the microbial action and decreasing the organic loading rate resulting in diminished biogas yield (Janajreh et al., 2020). For suitable AD, C/N is desired to be in the range of 20-35 (Lee et al., 2022). Unfavourable C/N ratio leads to the production of inhibitors such as, ammonia or sulphides, and accumulates high amount of volatile fatty acids (VFAs) delaying the activation of methanogenesis process. In absence of favourable conditions for any feedstock, anaerobic co-digestion (AnCoD) in presence of a suitable co-substrate to optimize the C/N, F/M or pH would augment the biogas yield, accelerate the biodegradability and improve the microbial diversity inside an anaerobic reactor (Dioha et al., 2013). Since PRS has a low carbon or high nitrogen content, co-digestion with suitable co-substrate having high carbon or low nitrogen content reportedly increase the methane yield but the percentage enhancement varies with the choice of co-substrate and the optimization of the factors (such as, F/M, C/N, pH and inoculant concentrations) affecting it. The AnCoD of PRS with food waste, corn stover, swine manure and

sugarcane bagasse reportedly enhanced biogas from 2.1 folds to 3.45 folds against monodigestion (Yang et al., 2020; Ghaleb et al., 2020; Castro et al., 2022; Lee et al., 2022). Except food waste, co-substrates being utilized till date are commonly available in rural areas but the co-digestion of PRS would be economically viable with co-substrates from urban regions as rightly perceived by Janajreh et al. (2020) who performed the AnCoD of petroleum hydrocarbon waste with municipal wastewater treatment sludge in the ratio of 60:40 (w/w) at 35°C. But the lower percentage of energy recovery and lesser utilization of organic fraction of the feedstock during the process indicated potential for further augmentation in PRS biodegradation. Pretreatment in conjunction with co-digestion might lead to an appreciable enhancement in energy recovery which is still a grey area in the field of biogas production.

In conclusion, the adoption of anaerobic digestion and co-digestion techniques for management of PRS has the potential to offer economic benefits, efficient waste management, organic matter reduction, and a valuable source of biogas production, making it an indispensable and vital component of a sustainable and environmentally responsible degradation approach.

1.2 OBJECTIVES OF THE STUDY

The main objective of the study was to enhance the biogas production of PRS through different types of pretreatment (thermal, electrokinetic and microbial), and co-digestion strategies that utilizes carbon-rich co-substrate for enhancement in solubilization, improvement in biodegradability and consequent reduction in toxicity. The scope of the present study was limited to:

- BMP (1L) test of PRS with undigested residue (UR) and digested sludge (DS) as inoculums followed by 16S rRNA metagenomics comparison study of inocula.
- Pretreatment studies (thermal, electrokinetics and microbial) for accelerated hydrolysis during anaerobic digestion of PRS.
- Combination of co-digestion of PRS (with a suitable substrate) and different pretreatment techniques (electrokinetics and microbial) for nutritional balance and biogas enhancement.
- Fabrication and operation of lab-scale semi-continuous anaerobic biphased baffled reactor (ABBR) and its feasibility study.

1.3 NEED OF THE STUDY

Anaerobic digestion (AD) of industrial wastes provides a means of stabilization, yielding a renewable energy source in the form of methane-enriched biogas. AD proves highly advantageous for industries, offering an alternative energy option, waste reduction, and economic sustainability. While various treatment processes have been explored in the petrochemical industry for management of refinery wastes, their application has mostly been limited to cleanup operations for contaminated land or water. At a typical petroleum refinery effluent treatment plant, the generated sludges are highly heterogeneous and multi-phasic in nature. The organic fraction present in hydrocarbon-rich petroleum refinery waste activated sludge, or biosludge, is conducive to AD due to high moisture content, high organic content and low emulsion content, resulting in biogas production through the decomposition of volatile solids. AD enhances sludge stabilization and dewaterability by reducing organic suspended solids and increasing sludge particle density. However, the AD process may encounter challenges such as extended hydrolysis phases due to inadequate inoculation and nutrient imbalances. Additionally, the presence of complex hydrocarbons and recalcitrant compounds in the sludge can lengthen the AD process, leading to suboptimal utilization of this technology. To address these issues, various pretreatment techniques (mechanical, thermal, electrochemical, and biological) have been explored. These techniques increase solubilization, shorten hydrolysis phases, and subsequently enhance biogas production. Furthermore, co-digestion of refinery sludge with a suitable co-substrate can balance nutrient levels, foster diverse microbial proliferation, and dilute toxicant concentrations. Co-digestion followed by pretreatment has further potential to improve the overall efficiency and effectiveness of the AD process for petroleum refinery waste.

1.4 SCOPE OF THE STUDY

To maximize biogas yield, it is essential to implement pre-treatment strategies crucial for dissociating the intricate hydrocarbon structure of petroleum refinery sludge, which can hinder enzyme accessibility and microbial activity. Additionally, co-digestion helps address any nutritional imbalances that might hinder the growth rate of microbes involved in the biogas production process. The scope of the present study is limited to characterization of PRS collected from a nation-wide petrochemical refinery, Assam, India, and inoculums (UR of animal manure, and DS from an operation anaerobic digester) collected from the Amingaon village near Indian Institute of Technology Guwahati (IITG) campus, Assam, India. To conduct the biochemical methane potential (BMP) test (1L capacity) studies for untreated PRS with UR and DS as

inoculums, optimizing the best result from the study. Effects of different pretreatment techniques on the hydrolysis of PRS with respect to pH, soluble chemical oxygen demand (sCOD), volatile fatty acids (VFA), volatile solids (VS) etc. and its characterization using Field Emission Scanning Electron Microscopy (FESEM) and Fourier Transform Infrared spectroscopy (FTIR) was studied to determine the best pretreatment technique. Based on the above studies, scaled-up batch study (20L capacity) was done to quantify the oil and grease, total phenol and total petroleum hydrocarbons removal. Additionally, combined pretreatment and co-digestion of nitrogen-rich PRS with suitable carbon-rich co-substrate was performed for nutrient balance and improved biodegradability. Finally, operation of lab-scale anaerobic biphased baffled reactor in semi-continuous mode was performed with untreated followed by pretreated PRS. The organic loading rate (OLR) was optimized based on biogas production, methane composition, COD removal and hydrocarbon degradation.

1.5 THESIS ORGANIZATION

The present thesis covers eight chapters with appropriate sections and subsections and also contains references and visible research outputs. A brief description of these chapters is mentioned as follows:

- **Chapter 1** gives a brief discussion about the problems associated with the improper management and disposal of PRS, proposed anaerobic digestion techniques, objectives, need of the study and scope of the thesis.
- **Chapter 2** includes the detailed literature review on the treatment and management approaches practiced for PRS, potential of PRS in anaerobic digestion, pretreatment techniques, co-digestion, enhancement in inoculation efficiency, optimum parameters in anaerobic digestion process and various biogas reactors.
- **Chapter 3** deals with the experimental flowchart of different phases of the study (I, II, III, IV) and the methodologies adopter for their successful accomplishment. The detailed procedures of physio-chemical analysis and instrumental analysis are provided.
- **Chapter 4** presents a discussion about phase I, the anaerobic biodegradability assay to ascertain the efficacy of different inoculums, in order to select the most efficient inoculum.
- **Chapter 5** presents the effect of different pretreatment techniques i.e., thermal, electrokinetic and microbial pretreatment on solubilization of PRS for enhanced biogas yields and pollutant removals.

- **Chapter 6** presents the anaerobic co-digestion of PRS with suitable co-substrate for enhanced biogas production. This process was further augmented by combining with different pretreatments for improved biodegradability.
- **Chapter 7** deals with the operation of lab-scale anaerobic biphased baffled reactor (ABBR) with untreated PRS and pretreated PRS with the optimum technique observed from Chapter 5.
- **Chapter 8** lists the overall conclusions obtained from different phases of the research work and recommendations for future work.

Chapter 2

LITERATURE REVIEW

This chapter discusses the available relevant literature on the problems associated with the management, treatment and secure disposal of the PRS generated from the effluent treatment plants of the petrochemical industries. This chapter thereby steers towards the utilization of PRS as a feedstock for AD and AnCoD processes followed by different types of pretreatment techniques for enhanced biogas production. This chapter also includes the effects of these techniques on hydrocarbon degradation and emulsion removal.

2.1 GROWING DEMAND OF OIL AND NEED FOR ALTERNATIVE ENERGY SOURCES

Crude oil is extracted directly from the oil wells and purified by fractional distillation to give out petroleum products by separation of liquid mixture into different fractions of different boiling points. Crude oil consists of naturally occurring hydrocarbons of different molecular weights and including certain miscellaneous organic compounds which exist as a liquid in natural underground reservoirs. Petroleum products such as diesel, kerosene, gasoline, fuel oil etc., are produced from crude oil processing at petroleum refineries and liquid hydrocarbon extraction at natural gas processing plants (Hu et al., 2013). Due to rising incomes over the past decade and the increasing number of vehicles with soaring consumption of fuel in developed countries, oil demand keeps rising by about 1.2% per year (Hu et all, 2020). Developing countries of Asia, Latin America and Africa will keep growing across most fuels, strongest being liquefied petroleum gas and naphtha, and transport fuels. The fastest growth will be in Africa and Southeast Asia, with demand increasing at 2.0% per year within 2035 (Janajreh et al., 2020; Laherrère et al., 2022).

The global demand for crude oil, a finite fossil fuel resource, continues to increase while new reserves are becoming increasingly difficult to discover. In fact, sixteen of the twenty largest oil fields worldwide have already reached peak production levels, unable to meet the global demand adequately (Raugei et al., 2012). The current global consumption of fossil fuels, primarily derived from crude oil, surpasses a staggering 11 billion tonnes annually. Unfortunately, crude oil reserves are depleting at a rate exceeding 4 billion tonnes per year. If consumption continues at this pace, all known oil deposits would be exhausted within a mere 53 years as per a report from International Renewable Energy Agency, 2020. Consequently, there is a pressing need to explore and utilize alternative, green, and sustainable sources of energy on various scales—ranging from small to medium to large as per a report from World Energy Council, 2019. This imperative arises from the

necessity to meet the ever-growing energy demands while reducing reliance on dwindling oil reserves. By embracing innovative and eco-friendly energy solutions, a more sustainable future for our energy requirements can be ensured.

2.2 GENERATION OF PETROLEUM REFINERY SLUDGE

Petrochemical industries generate a considerable amount of solid residue, commonly known as 'petroleum refinery sludge' (PRS) during the exploration, production and refining processes of crude oil, and also from the effluent treatment plants (ETPs) of refineries (Xu et al., 2008, Mrayyan et al., 2005). In recent years, the PRS generated during the ETP processes has received increasing attention due to its high concentration of petroleum hydrocarbons and other recalcitrant components. Typically, an increase in refining capacity correlates with a proportional rise in the generation of PRS. Studies indicate that, on average, approximately one ton of PRS is produced for every 500 tons of crude oil processed (Hu et al., 2013). This estimation highlights the substantial volume of PRS generated as a by-product of petroleum refining operations. PRS is a complex mixture of oil-in-water (O/W) emulsions, water-in-oil (W/O) emulsions, suspended solids and heavy metals (Nour et al., 2006). The petroleum hydrocarbons are an amalgamation of aromatic hydrocarbons, polyaromatic hydrocarbons, resins and asphaltenes, which are toxic in nature (Colberg, 1995; Ayotamuno et al., 2007). PRS, a highly viscous hazardous waste, basically comprises of about 55% of water, 2% of asphaltenes, and 23% of light hydrocarbons including heavy metals such as vanadium, iron and nickel making the sludge harmful for the organisms and environment (Subramanian et al., 2007). Therefore, due to the hazard potential, PRS cannot be disposed of without proper treatment (Xu et al., 2008; Mrayyan et al., 2005; Mater et al., 2006; Rocha et al., 2010).

2.3 CLASSIFICATION OF PETROLEUM REFINERY SLUDGE

Petroleum refineries generate various types of sludge during their operations in ETPs, which include oily sludge, chemical sludge, and biosludge. These sludges pose significant challenges in terms of their management and proper disposal (Rodan-Carrillo et al., 2012).

- **Oily sludge:** It is a by-product of the oil refining process and is primarily composed of a mixture of oil, water, and solid particles. It is not only generated from the physical treatment process of the ETPs [such as such as the American Petroleum Institute (API) separator, parallel plate interceptor, corrugated plate interceptor (CPI), dissolved air floatation unit (DAF)], but also gets accumulated in different parts of the refining processes, such as storage tanks, oil-water separators, and other wastewater treatment units. Oily sludge

contains huge concentrations of hydrocarbons, heavy metals, and other contaminants. The handling and disposal of oily sludge require specialized techniques, including separation, dewatering, remediation and treatment processes to recover valuable hydrocarbons and minimize environmental impacts (Hu et al., 2013; Islam, 2015).

- **Chemical sludge:** This type of sludge is generated as a result of various chemical treatment processes employed in the ETPs. It consists of residues from coagulation, flocculation, precipitation, and neutralization steps used to remove impurities and contaminants from the wastewater such as flocculation–flotation units (FFU) of the ETPs. Chemical sludge contains suspended solids, precipitated metals, and residual chemicals, which require proper treatment and secure disposal to prevent pollution and comply with the environmental regulations (Johnson and Affam, 2019).
- **Bio-sludge:** Bio-sludge, also known as biological sludge or activated sludge, is produced during the secondary treatment stage as excess activated sludge from on-site wastewater biological treatment plant of the ETPs in refineries. It is a mixture of microorganisms, organic matter, and excess biomass that results from the biological degradation of organic compounds in the wastewater. Bio-sludge contains beneficial bacteria and can be recycled or further treated to recover energy or valuable resources. However, its disposal also requires careful consideration to minimize environmental impacts (Kriipsalu et al., 2008; Hu et al., 2013; Haak et al., 2016; Wang et al., 2016).

Managing these different types of sludge involves implementing appropriate treatment processes to reduce their volume, separate valuable components (oil and hydrocarbons), and minimize the environmental risks associated with their disposal. Techniques such as centrifugation, sedimentation, filtration, and thermal treatment (e.g., incineration), pyrolysis are commonly employed to treat and manage PRS (Sankaran et al., 1998; Gong et al., 2018; Hu et al., 2020). Additionally, recycling and reusing certain components of the sludge, such as recovering oil or extracting valuable metals, can help in achieving more sustainable waste management practices (Kriipsalu et al., 2008). Overall, the proper management of oily sludge, chemical sludge, and biosludge is essential for petroleum refineries to ensure compliance with environmental regulations, protect water resources, and minimize the impact on ecosystems. One of the prima facie goals of petroleum refining industries is to implementing effective treatment processes and explore innovative technologies which can contribute to more sustainable and responsible sludge management practices.

2.3 COMPOSITION OF PETROLEUM REFINERY SLUDGE

PRS is a complex residue that exhibits the characteristics of a stable water-in-oil (W/O) emulsion, comprising water, solids, petroleum hydrocarbons (PHs), and heavy metals. The stability of W/O emulsions primarily relies on a protective film that prevents the coalescence of water droplets. This interfacial film consists of various natural emulsifiers, including certain PHs constituents like asphaltenes and resins, fine solids, oil-soluble organic acids, and other finely dispersed materials (Kralova et al., 2011). The pH of the sludge varies within the range of 6.5 to 7.5, and its chemical composition varies extensively depending on factors such as the source of the crude oil, refining processes employed, and the equipment and reagents used. The TPH content in PRS can range from 5% to 86.2% by mass, the water content can vary between 30% and 85%, while the solids content can range from 5% to 46% (Tahhan et al., 2011). PRS consists of four main fractions: aliphatics, aromatics, NSO-containing compounds, and asphaltenes. Aliphatics and aromatics make up around 75% of the PHs in refinery sludge Kriipsalu et al., 2008). These fractions include alkanes, cycloalkanes, benzene, toluene, xylenes, naphthalene, phenols, and various PAHs. The NSO fraction contains polar compounds like naphthenic acids, mercaptans, thiophenes, and pyridines (Kriipsalu et al., 2008). PRS also contains asphaltenes, which are complex mixtures of polyaromatic and alicyclic molecules with alkyl substitutes. Asphaltenes and resins contribute to the stability of the emulsion (Hu et al., 2013). The composition of oily sludge typically includes 40-52% alkanes, 28-31% aromatics, 8-10% asphaltenes, and 7-22.4% resins (Hu et al., 2013; Johnson and Affam, 2019).

The chemical composition of oily sludge is highly diverse, leading to substantial variations in its physical properties, including density, viscosity, and heating value rendering it to be highly heterogenous and multiphasic in nature (Haak et al., 2016). However, physical properties can be empirically estimated based on the polarity and molecular weight of the chemical constituents of the sludge. It is essential that each sample of sludge collected from different sources on different d be evaluated independently to ensure accurate understanding and appropriate management of its physical properties.

2.4 TOXIC IMPACT OF PETROLEUM REFINERY SLUDGE ON ENVIRONMENT

The improper disposal of PRS presents a grave environmental hazard due to its high concentration of toxic substances. Upon entering the terrestrial environment, this sludge can disrupt the physical as well as chemical properties of receiving soils, triggering alterations in soil morphology. Contaminated soils exhibit nutrient deficiencies, hindered seed germination, and

impaired plant growth upon contact with oily sludge (Dettenmaier et al., 2009; Tang et al., 2012). The viscous nature of the sludge components allows them to adhere to soil surfaces, obstruct soil pores, and form hydrophobic crusts, resulting in diminished moisture retention, reduced hydraulic conductivity, and compromised soil wettability (Robertson et al., 2007). These hydrophobic crusts persist for extended periods, impeding water availability and impeding the exchange of water and air in affected agricultural soils. Hence, the proper management and treatment of refinery sludge are crucial to mitigate detrimental impacts on soil quality and ensure the sustainability of terrestrial ecosystems.

Improper disposal of PRS poses significant risks to the environment due to the presence of PAHs and heavy metals, which have cumulative and toxic impacts. PAHs, known for their genotoxic nature to humans and ecological receptors, can migrate through the soil profile and contaminate groundwater and interconnected aquatic systems (Haider et al., 2021). Soil enzymes, crucial for soil health, can be hindered by the presence of PHs, leading to adverse effects on soil microorganisms. Over time, weathered residues form stable compounds through covalent bonding with soil humic polymers, such as long-chain alkanes, and fatty acids, resisting microbial degradation (Hu et al., 2013). These persistent interactions between the sludge and soil components amplify the environmental concerns associated with their disposal.

2.5 PETROLEUM REFINERY SLUDGE TREATMENT

Treatment of petroleum refinery sludge involves various methods aimed at reducing its environmental impact and recovering valuable resources. It is necessary to select the appropriate treatment method depending on the specific characteristics of the petroleum refinery sludge, environmental regulations, and desired outcomes. A combination of different treatments may also be employed to achieve the desired results effectively. Some common treatments for petroleum refinery sludge have been enlisted below.

(A) Oil recovery methods

Some of the oil recovery methods from PRS include chemical treatments, various distillation processes, cracking, solvent treatment and bioremediation (Elektorowicz and Habibi, 2006, Elektorowicz et al., 2006; da Silva et al., 2012; Conrardy et al., 2016; Johnson and Affam, 2019; Hu et al., 2020). Some of these are briefly summarized in Table 2.1. The salient features of each method include a brief description about the method with major advantages and limitations.

Table 2.1. A summary of various treatment methods applied to petroleum refinery sludge

Methods	Salient features	Advantages	Limitations	References
Manual cleaning	○ Cleaning is done by entering the tank and sludge is moved out using pumps or manually.	○ Economic	○ Time-consuming. ○ Difficult hydrocarbon recovery.	Hu et al. (2013)
Solvent extraction	○ Solvent-based treatment breaks down complex molecules in oily sludge into oil, water, and particulates. ○ The sludge is mixed with a solvent, impurities settle down, and the oil-solvent mixture is distilled to separate the oil. ○ The solvent is recycled, and the recovered oil is obtained.	○ Short process time ○ Large volume of sludge can be treated	○ Cost-intensive. ○ High-end requirements to prevent solvent vapour emission. ○ Heating requirements for recycling of the solvent.	Da Silva et al. (2012)
Froth-floatation	○ The oily sludge is mixed with water to form a slurry, and air is pumped in to create air bubbles that trap oil particles. ○ The oil and air conglomerate rises to the surface, allowing the accumulated oil to be skimmed off.	○ Simple ○ Economic	○ Ineffective at higher viscosities. ○ High moisture in the recovered oil.	Hu et al. (2013)

			○ Limited field-scale applicability.	
Microwave irradiation	○ Microwave energy directly reaches to the material through molecular interactions with electric field. Microwave heating converts electromagnetic energy to heat energy. ○ The heat is generated throughout the volume of material leading to destabilization of oil-water emulsion.	○ Fast and efficient	○ Requires specific equipment. ○ Energy-intensive. ○ Meagre treatment capacity.	Fang and Lai. (1995); Aburahman et al., (2006); Siddique et al. (2017)
Ultrasonic irradiation	○ Ultrasonic irradiations create compactions and rarefactions, exerting positive and negative pressures on the molecules. The resulting shock waves from the collapse of microbubbles increase pressure and temperature, enhancing mass transfer and destabilizing water and oil emulsion.	○ Fast and efficient	○ Costly equipment. ○ Meagre treatment capacity.	Xu et al. (2008); Jin et al. (2012); Kapusta (2018)
Centrifugation	○ Centrifugal forces separate sludge constituents based on density, and demulsifying agents can reduce viscosity. Heat pre-treatments and multiple centrifugation cycles result in lower viscosity and produce liquid effluent as a significant portion of waste volume.	○ Efficient and fast	○ Energy-intensive. ○ High capital and maintenance cost. ○ Ineffective at higher viscosities	Johnson and Affam (2019)

	○ Cambiella et al. (2006) reported that small amount of coagulant salt (calcium chloride) can improve water-oil separation by 92-96%.			
Electrokinetic process	○ It utilizes low-intensity direct current (DC) across a pair of electrodes (cathode and anode) on a pervious medium. ○ It works on three mechanisms: electromigration (movement of ions), electrophoresis (movement of suspended or dissolved particles), and electro-osmosis (movement of fluid through pores in the charged matrix). ○ Firstly, the colloidal particles are broken down under the influence of an electrical field directing the colloidal and solid particles of PRS towards anode area (electrophoresis). The separated liquid phase consisting of water and oil move towards the cathode area (electro-osmosis), directed by the nature of the charges on the surface of solid particles i.e., the anions move towards the anode and the cations shift towards cathode.	○ Fast ○ Highly efficient ○ Economic ○ Energy-saving	○ System application is complex and uneasy.	Yang et al. (2005); Elektorowicz et al. (2006); Glendinning et al. (2007); Gill et al. (2014); Conrardy et al. (2016)

(B) Disposal methods

Petroleum refinery sludge is disposed using various methods, some of which are described in Table 2.2.

Table 2.2. A summary of various disposal methods applied to petroleum refinery sludge

Methods	Salient features	Advantages	Limitations	References
Incineration	○ Oily wastes are combusted in presence of excess oxygen and auxiliary fuels in rotary kilns (for around 30 min at a temperature range of 980-1200˚C) and fluidized bed incinerators (for many d at a temperature range of 730-760˚C).	○ Fast ○ Efficient	○ Energy-intensive ○ Cost-extensive ○ Emission of hazardous flue gases requiring additional treatment	Hu et al. (2013)
Oxidation	○ Addition of reactive chemicals to the oily sludge which can change the nature of the sludge rendering it harmless (inorganic salts or CO_2, water etc.). Some of the oxidizing agents commonly used for chemical treatment are Fenton's reagent, hypochlorite and permanganate.	○ Fast ○ Efficient	○ High chemical dosage ○ Energy-intensive ○ Cost extensive ○ Disposal issues due to application of chemical agents	Johnson and Affam, 2019
Stabilization	○ In this process, contaminants are made immobile by converting them into less toxic form. This process abridges the waste using a	○ Economic ○ Efficient	○ Process becomes inefficient for high moisture contents	Islam, 2015

	binder in order to prevent its leaching into the environment thus converting the products into sustainable construction materials or non-hazardous waste which can thereby be safely disposed in landfills.		○ Proper management of stabilized product.	
Biodegradation	○ Some biodegradation techniques involve- i. **Land farming**- This process enables physical, chemical and biological degradation of hydrocarbon contaminants by mixing it with soil. This type of treatment proved to have removed 80% of total petroleum hydrocarbons (PHC) within 11 months in a semi-arid climate. About 70-90% PHC degradation was achieved in 2 months through oily sludge land farming treatment.	○ Low cost. ○ Large volume of sludge can be stabilized.	○ Very slow. ○ Underground water pollution due to leachability of pollutants. ○ Requires large land areas for remediation	Marin et al., 2005; Admon et al., 2001;
	ii. **Composting**- In this process, micro-organisms degrade petroleum waste to convert them to compost.	○ Fast ○ Efficient ○ Less land requirement than land-farming	○ Problems associated with leachability of volatile organic hydrocarbon compounds	Islam, 2015; Johnson and Affam, 2019

2.5.1 Multi-phasic nature of petroleum refinery sludge

The PRS is highly heterogeneous and multi-phasic due to the application of a complex treatment approach in the ETPs (Haak et al., 2016). Due to high calorific values of PRS (17000-19000 kJ/kg), combustion technologies such as incineration or pyrolysis for its treatment at a high temperature range of 500-1100°C seem to be attractive options (Hu et al., 2013; Li et al., 2020; Zuo et al., 2021). But the characteristics of PRS vary greatly not only in calorific values but also in moisture content (6% - 80%) and oil content (35% - 92%) due to which the combustion technology becomes inefficient at high moisture and low oil contents, e.g., excess activated sludge release from biological treatment unit of ETPs (Sankaran et al., 1998; Kriipsalu et al., 2008; Hu et al., 2020). Also, due to the high viscosity of oily sludge, they are heated before being fed into incinerators to maintain their flow requiring energy-intensive pretreatment (Sankaran et al., 1998). Combustion of auxiliary fossil fuels and organic sludge at high temperatures generates hazardous residues and leads to toxic gaseous emissions (GHG, SOx and NOx) which require additional treatment (Hu et al., 2020). Few treatment other treatment options such as centrifugation, froth-floatation, oxidation and plasma gasification are either again either energy-intensive or cost-intensive. Land disposal of PRS without treatment can reduce hydraulic conductivity, water availability and exchange of water-air into the soil hampering the physical as well as the nutritional profile of soil matrix, all of which have always been a matter of concern for many years (da Silva et al., 2012; Kriipsalu et al., 2008). The improper disposal of PRS may modify both the physical and chemical properties of the surrounding soils changing the overall morphology. If treatment is ineffective and disposal into the environment is improper then it may lead to a major health concerns due to intricate hydrocarbons constituents which are genotoxic and mutagenic to both animal and mankind (Robertson et al., 2007). Hydrocarbons if disposed in landfills without treatment then, it can also lead to groundwater infiltration thus causing a menace to the environment (Trofimov and Rozanova, 2003). The multi-phasic and heterogeneous properties of these sludge make any particular treatment approach highly inconsistent and therefore, biological remediation options are in dire need for the overall management of these sludge for their efficient hydrocarbon degradation and overall process stabilization into less harmful by-products.

2.6 ANAEROBIC DIGESTION

2.6.1 Definition and process

In AD, suitable microbial consortium decay biodegradable fraction of a substrate in the absence of any terminal electron acceptor (sulphate, nitrate, and oxygen) generating methane-rich biogas.

This process is facilitated by a diverse consortium of microorganisms, including bacteria, archaea, and fungi, which work together in a symbiotic relationship. The process is carried out in four phases: hydrolysis, acidogenesis, acetogenesis, and methanogenesis. The stages of anaerobic digestion process are presented briefly below and illustrated in a flowchart as shown in Fig. 2.1.

a) **Hydrolysis-** In the hydrolysis stage, complex organic compounds, such as proteins, carbohydrates, and lipids, are broken down into simpler molecules by enzymes produced by hydrolytic bacteria. This stage is crucial for converting insoluble polymers to soluble dimers and monomers that can be further metabolized by the hydrolytic bacteria. The hydrolytic bacteria secrete extracellular enzymes that convert proteins to amino acids, polysaccharides to monosaccharide, and lipids to fatty acids. The chemical reaction carried out during this phase is mentioned in Reaction 2.1. Hydrolysis is a rate-limiting step, being an important parameter in the reaction kinetics of the AD process, and this phase is time-consuming. A variety of pretreatment methods are used to optimize the rate-limiting hydrolysis phase for the enhancement in methane yield.

$$nC_6H_{10}O_5 + nH_2O \longrightarrow nC_6H_{12}O_6 \qquad [2.1]$$

b) **Fermentation-** The next step after hydrolysis is called as acidogenesis or fermentation. The products from hydrolysis get absorbed by the cell membrane of acidogenic bacteria to produce intermediate short-chain VFAs and other products. The chemical reaction carried out during this phase is mentioned in Reaction 2.2. The specific concentrations of intermediates produced during acidogenesis phase depends on the condition of the digester (Huang., 2015). The organic substrates act as both electron donor and acceptors. (Metcalf and Eddy., 2003). The products from this process are mainly, acetic acid, butyric acid, propionic acid, valeric acid, isovaleric acid and some traces of alcohols and aldehydes. One of the important products of amino acids breakdown is the production of ammonia from deamination, which, at sufficiently high concentrations, acts as an inhibitor of AD process (Kovacs et al., 2013).

$$nC_6H_{12}O_6 \longrightarrow 3nCH_3COOH \qquad [2.2]$$

c) **Acetogenesis-** This is termed as a preparatory step for methanogenesis. In this process, short-chain VFAs and other intermediates are converted to acetate and hydrogen. Based on the bacterial metabolisms, there are two types of acetogenic bacteria, proton-reducing acetogens and homoacetogens. The chemical reaction carried out during this phase is mentioned in Reaction 2.3.

$$2CO_2 + 4H_2 \longrightarrow CH_3COOH + 2H_2O \quad [2.3]$$

d) **Methanogenesis-** Methanogenic microorganisms finally convert the accessible intermediates from acid fermentation to biogas. Methanogenic organisms are a group of obligate anaerobic achaea, and they are principally two types of organisms, *Methanothrix* and *Methanosarcina*, which convert acetate to methane (CH_4) and carbon dioxide (CO_2). There are two types of methanogenic bacteria, acetoclastic methanogens and hydrogenotrophic methanogens. Typically, acetate from acetoclastic methanogenesis accounts for about 67% of the CH_4 production (Reaction 2.4) and that from hydrogenotrophic methanogenesis accounts for about 33% of the CH_4 production (Reaction 2.5).

$$CH_3COOH \longrightarrow CH_4 + CO_2 \quad [2.4]$$

$$CO_2 + 4H_2O \longrightarrow CH_4 + 2H_2O \quad [2.5]$$

2.6.2 Syntrophic relationships among organisms

Methanogens are able to maintain a very low partial pressure of H_2, which allows the equilibrium of fermentation reactions to shift towards the formation of more oxidised end-products such as acetate and formate. The utilisation of H_2 produced by acidogens and other species of microorganisms by methanogens is known as inter-species hydrogen transfer. Methanogenic organisms (hydrogenotrophic) act as a proton sink that allows fermentation reactions to proceed, but if the process delays in utilising the H_2, then VFA accumulation occurs. and the reactor pH falls upsetting the process stability and buffer capacity.

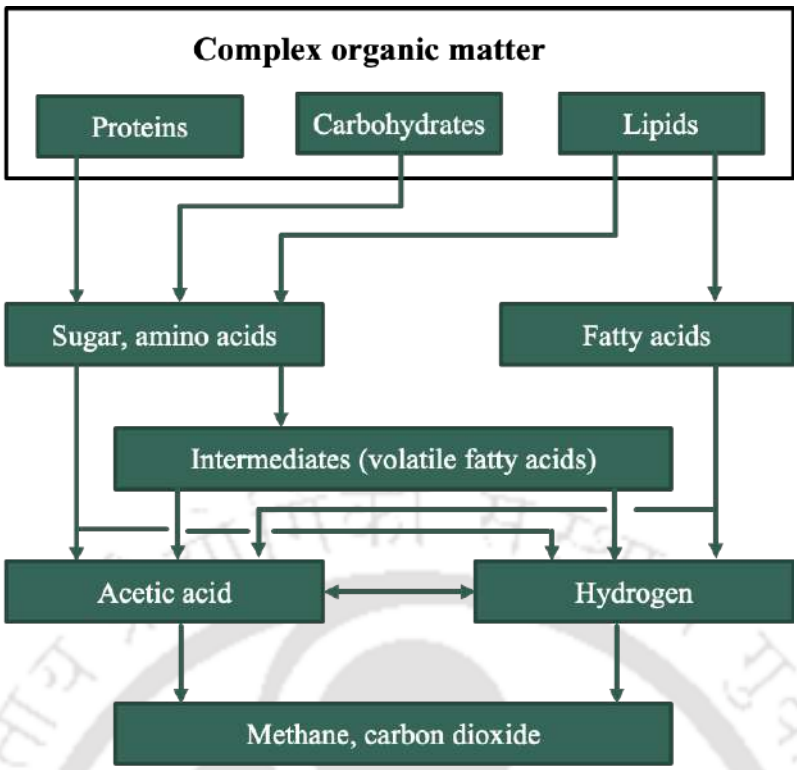

Fig. 2.1. Steps involved in the anaerobic digestion process

2.6.3 Factors affecting anaerobic digestion process

- **Temperature**- AD occurs in a varied range of temperature profiles, psychrophilic (< 20°C), mesophilic (20-45°C), thermophilic (45-65°C). Most commonly used temperature profiles for AD process are mesophilic and thermophilic. Temperature plays a major role in the physical and chemical properties of an organic substrate which affects the thermodynamic and kinetics reactions inside an anaerobic reactor. Increasing the temperature improves diffusivity, increases rate of liquid to gas transfer due to increase in gas solubility, and improves liquid-solid-biomass separation. The hydrolysed soluble products become more accessible to the micro-organisms, and hence the reaction rate increases resulting in lower reaction time. This decreases the HRT of the reactor. But increase in temperature might lead to free ammonia formation that can freely diffuse through the cell membrane resulting in proton imbalance within the bacteria hampering the methanogenic activity.

- **pH**- The pH level significantly affects the efficiency of the AD process. Acetoclastic methanogens thrive within a pH range of 6.5 to 7.5 (Hwang et al., 2004). The pH can vary due to factors such as VFA concentration, bicarbonate levels, alkalinity, and CO_2 production. Maintaining a stable pH is crucial by controlling the VFA and bicarbonate concentrations to preserve the digester's buffering capacity. Excessive accumulation of VFAs can lead to digester failure as acidogenic bacteria proliferate, lowering the pH below

5.0 and inhibiting methanogen growth. pH levels above 8 can also hinder the biological functions of anaerobes. Therefore, maintaining the optimal pH range is essential for efficient biogas production in AD.

- **C/N ratio**- Nitrogen is an important element for the production of amino acids and proteins to be converted to ammonia, a buffer compound for neutralization of acidification process. Microbial populations would be low, if the nitrogen content is very low, and a lot of time will be consumed in digesting the available carbon present in the substrate. C/N ratio range of 20-35 has been found to be mostly suitable for various types of substrates.
- **Organic loading rate (OLR)** – The OLR is the amount of VS fed into the reactor each day. Increased OLR increases the activity of acid formers and inhibits methane formation. Lower OLR signifies underutilization, i.e., reduction in the rate of AD. Loading is done based on the type of waste that will be fed into the reactor as the nature of the waste will determine the level of biochemical activity.
- **Solids retention time (SRT)** – The average period of time for which the solids remain within the bio-reactor is defined as SRT. The SRT should be long enough to provide sufficient methanogenic activity. Methanogenesis starts at a SRT between 5-15 d at 25°C and 30-50 d at 15°C (Halalsheh et al., 2005).
- **Hydraulic retention time (HRT)**- HRT is the average time that the organic substrate remains in the digester. It is the ratio of the volume of the digester to the flow rate of the digester. A shorter HRT results in a higher loading rate (Meegoda et al., 2018). A shorter HRT would result in greater process efficiency and decreased capital costs; a longer HRT improves the process efficiency when feedstock utilized are complex (lignocellulosic biomasses).
- **Sulphate reduction**- Sulphate reduces to sulphide which has a negative effect on the methanogens as the methanogenic bacteria compete with the sulphate-reducing bacteria for the production of intermediate acetic acid due to presence of high concentration of sulphur. The reduction of sulphate increases pH and buffer capacity, and leaves the system as hydrogen sulphide (H_2S) gas which acts as an inhibitor in the AD process.

2.6.4 Petroleum refinery waste as a substrate for anaerobic digestion process

The rate of biodegradability of any substrate depends on the composition of the feedstock. There are various types of techniques available for estimation of biochemical methane potential (BMP) of a complex substrate as petroleum refinery waste including molecular composition,

simulation and modelling or an extensive literature review of biogas yields obtained experimentally. The aim of obtaining optimum methane production through AD of any substrate can be governed by parameters such as pH, VS reduction, or VFA accumulation for production of methane (Mruto et al., 2004). However, several demerits of these process variables are highlighted by various researchers due to less sensitivity and consistency. Dhamodharan et al. (2015) found that higher the VS reduction, higher is the probability of biogas production. VS is also a parameter to design the size of a reactor. sCOD, pH, VFA and moisture contents are also some of the factors affecting the AD process. Various studies have been carried out by different researchers all around the globe on the biogas production of petroleum industry wastewater PRS with different types of inoculums.

Siddique et al. (2014) conducted anaerobic digestion with petrochemical wastewater as a substrate and activated manure (dairy and beef manure) as an inoculum. The authors varied food/inoculum (F/M) ratio from 0.25 to 2.0 and organic loadings from 6.31 to 32 gVS/L. At mesophilic temperature of 37ºC, the cumulative methane was enhanced by 17.5 times whereas the same at thermophilic temperature of 55ºC, only improved by 6.5% by the end of 145 d of digestion period.

Siddique et al. (2015) performed anaerobic digestion of petrochemical wastewater using dairy and beef manure as inoculums which enhanced methane production by 50%, followed by sCOD reduction of 98% at HRT of 10 d. Under mesophilic conditions, methane enhanced by 50-60% whereas under thermophilic conditions, the same increased by 65% during the AD process.

Haak et al. (2016) conducted anaerobic co-digestion of ozone pretreated dissolved air floatation (DAF) unit float (oily sludge) and waste activated sludge (WAS). DAF and WAS were anaerobically digested using digested sludge as an inoculum source (collected from an operational anaerobic digester) for assessing the toxicity and biogas production potential. They concluded that due to high toxic potential (presence of high TPH content), mono-digestion of DAF is not possible. Methane production was much higher from the mono-digestion of WAS compared to that of DAF suggesting the feasibility of anaerobic digestion of biosludge over oily sludge.

Janajreh et al. (2020) used two substrates for AD with digested sludge as an inoculum and this process is commonly known as anaerobic co-digestion (simultaneous mixing of two or more substrates overcoming the drawbacks of monodigestion) enhancing the economic feasibility to maintain a positive synergism in an anaerobic digester. The authors conducted AD of petroleum hydrocarbon waste (PHW) as a substrate and wastewater treatment sludge (WWTS) as a co-substrate and reported that the biogas generation was at the maximum when 60% PHW and 40%

WWTS were co-digested at 35˚C. The authors also performed thermal gravimetric analysis of the digestate and the results before and after the incubation showed VS degradation of 43%.

2.7 PRETREATMENT

Pretreatment is a process of initiating or improving the efficiency of microbial attack on a substrate. Pretreatment constitutes a pivotal stage in augmenting the microbial degradation of organic substrate and optimizing the overall efficiency of AD process. During the pretreatment process, the compact structure of substrate is disrupted, thus facilitating improved solubilization, rendering it more amenable to microbial attack. These alterations effectively overcome the inherent biological limitations encountered in AD. Pretreatment measures yield manifold benefits, not only amplifying biogas production but also enhancing the calorific value of the generated gas. Pretreatment reduces sludge retention time, thereby enhancing biogas yield (Kondusamy and Kalamdhad, 2014). Various pretreatment methodologies can be employed, encompassing physical techniques (comminution and irradiations), chemical processes (alkali treatment, acid hydrolysis, and wet oxidation), as well as biological approaches (application of fungi or enzymes) (Kavitha et al., 2014; Wang et al., 2016; Kapusta, 2018). The implementation of pretreatment techniques reduces the demands and complexities associated with subsequent gas purification, particularly in the context of bio-methane production.

The effects on biodegradability of substrate vary with the feedstock characteristics. Easily available organics (food waste) takes lesser time to degrade in comparison with complex feedstock (agricultural residue, pulp and paper mill sludge, lignocellulosic biomasses), which are difficult to degrade due to presence of recalcitrant lignin content. The PRS is composed of huge concentrations of aliphatic, polycyclic, and polyaromatic hydrocarbons, most of which are recalcitrant because of their heavy molecular weights, compact molecular bonds, hydrophobicity and low solubility in water (Johnson and Affam, 2019). The anaerobic degradation of petroleum sludge without pretreatments has been found to be very complex. The hydrolysis stage known as rate limiting stage has been found to be very long as the micro-organisms find the complex substrate very difficult to degrade (Wang et al., 2016). Pretreatment modifies the overall physical, chemical and biological properties of any substrate thus improving its biodegradability (Roy et al., 2016). Some of the pretreatments that are in application are: thermal, chemical, ultrasonic and ozonation (Taiwo and Otolorin, 2009; Siddique et al., 2015; Hu et al., 2016; Kapusta, 2018), out of which few are discussed below.

2.7.1 Ultrasonication

Ultrasonication is a type of mechanical pretreatment which disrupts the structure of cell and floc matrix. There are two types of processes involved with ultrasonic treatment; cavitation, which occurs at low frequencies, and at high frequencies chemical reactions take place due to the formation of hydroxyl radicals. Low frequencies in the range of 20–40 kHz are efficient for ultrasonication of sludge which leads to disintegration of sludge. Removal of adsorbed materials from solid particles, separating solid/liquid in high-concentration suspensions, and decreasing W/O emulsion stability are some of the key functions of ultrasonic treatment (Ye et al., 2008). Ultrasonication of oily sludge depends on a variety of factors such as, ultrasonic frequency, power, temperature, moisture content in emulsion and exposure time of ultrasonic irradiation (Hu et al., 2013). Very low or high temperatures are not suitable for oily sludge treatment.

Wang et al. (2016) conducted ultrasonic pretreatment on petroleum refinery waste activated sludge using an ultrasonic homogenizer operating at a frequency of 20 kHz, and power applied 1 W/mL. They reported that ultrasonic pretreatment led to 40% VS degradation.

Siddique et al. (2017) performed ultrasonic pretreatment for methane enhancement from the co-digestion of petrochemical wastewater and waste activated sludge. Pretreatment was conducted using an ultrasonic homogenizer at a frequency of 20 kHz, 60% amplitude, and 350 W power. Each sample was exposed to ultrasonic pretreatment for 15-30 min to attain specific energies of 15 and 25 MJ/kg TS. Ultrasonic pretreatment increased biogas production by 25% compared to untreated co-digestion.

Pretreatment helps to improve biogas production and increases the removal rate of PAHs. For research, ultrasonication treatment has been widely applied as pretreatments. Ultrasonic irradiation has the capacity to process oily sludge in a short exposure period. Application of ultrasonic irradiation for oil recovery from petroleum sludge at field-scale has not been widely corroborated. It is more common in laboratories by the usage of an ultrasonic probe for treating a small quantity of oily sludge (Hu et al., 2013). Table 2.2 shows few studies pertaining to the effect of ultrasound irradiation on the oil and hydrocarbon recovery.

Table 2.2 Effects of ultrasound irradiation on hydrocarbon recovery

Ultrasound frequency	Power	Time	Temp	Major effects	References
28 kHz	-	-	40˚C	55.6 % oil recovery rate obtained with an optimal acoustic pressure of 0.10 MPa.	Xu et al. (2008)
20 kHz	66 W	10 min	-	Oil recovery rate was up to 80% from oily sludge and water ratio of 1:2.	Zhang et al. (2012)
28 kHz	400 W	15 min	60˚C	Oil recovery rate was above 95%. No further enhancement in the recovery of oil was observed when the ultrasonic power and treatment duration increased beyond 400W and 15 min.	Jin et al. (2012)
20 kHz	480 W	20 min	-	PAHs removal efficiencies of phenanthrene, paranaphthalene, fluoranthene, benzofluoranthene, and benzopyrene from ultrasound pretreated sludge were 28.5%, 25.9%, 16.0%, 22.0%, 18.5% after 20 d of anaerobic digestion with petrochemical sludge.	Zhou et al. (2015)

2.7.2 Thermal pretreatment

Thermal pretreatment partially solubilizes sludge enhancing the AD process (Fang and Lai, 1995; Tanaka et al., 1997). Thermal pretreatment degrades the gel structure of sludge, releasing the linked water thereby improving sludge dewaterability. Optimal temperature range of 160–180°C with an exposure time of 30 to 60 min is suitable for the application of thermal pretreatment. Biogas enhancement after thermal pretreatment is directly related to COD solubilization (Carrère et al., 2008). Increasing temperature above 150°C increased solubilization, but no further enhancement in methane was observed (Dwyer et al., 2008). Excessive high temperatures (>170–

190˚C) decrease sludge biodegradability therefore, optimization of thermal pretreatment conditions is crucial for any particular substrate.

Zhou et al. (2015) concluded from their study that thermal pretreatment proved to be a prospective enhancement method for the degradation of aromatic hydrocarbons, biogas production, and improvement of dewaterability during petroleum sludge anaerobic digestion. The authors conducted thermal pretreatment at 130°C for 20 min in an autoclave. VS removal efficiency was 28.1% as compared to control. Removal efficiencies of paranaphthalene was highest (55%) followed by phenanthrene, fluoranthene, benzofluoranthene and benzopyrene after thermal pretreatment. Increase in aromatic hydrocarbon biodegradation was either due to transfer of the aromatics from sorption sites with low desorption rates to those with high ones, or transformation of slow-sorption sites into fast-sorption ones through thermal pretreatment (Bonten et al., 1999). Additionally, pretreatment broke down the microbial cells of sludge thereby facilitating decomposition reaction and enabling greater amount of intracellular organic matter to release to the liquid phase of sludge. This, in turn, increased the sCOD enhancing biodegradation of more PAHs in the anaerobic digester (Zhou et al., 2015).

Wang et al. (2016) conducted thermal pretreatment of petroleum refinery waste activated sludge for its anaerobic digestion at 170°C for 60 min in a muffle furnace. The authors also conducted pretreatments of the same sludge with ultrasound irradiation and alkali. At the same time, a combination pretreatment of ultrasound-thermal was also performed. The concentration of sCOD in thermal treated sludge was almost 1.25 times higher than that in ultrasonic treated sludge and 6 times higher than that in alkaline treated sludge. The VS removal efficiency was highest for combined ultrasonic-thermal pretreatment (54.5 %) compared to only thermal, only ultrasonic ultrasonic and alkaline treatments. Besides, alkaline pretreatment showed very poor VS degradation (6%).

2.7.3 Ozone pretreatment

Ozone pretreatment partially solubilizes the sludge thereby enhancing the methane yield from the sludge. Ozonation is done at an optimal ozone dose. If the dosage becomes too high, then it will reduce apparent solubilization and therefore increase destruction of ozone at the expense of methane yield. Optimal ozone dose for enhanced biodegradability of substrates were reported to vary from 0.1-0.2 g O_3 g^{-1} TS (Hu et al., 2013; Johnson and Affam, 2019). Ozonation can be used as a pretreatment or post-treatment for AD. Ozone pretreatment improves biodegradability and methane production thereby reducing toxicity of hydrocarbons (Haak et al., 2016). Ozonation leads

to physicochemical changes in sludge such as lower pH (due to production of volatile fatty acids) and viscosity (Kianmehr et al., 2010).

Haak et al. (2016) conducted anaerobic co-digestion of ozone pretreated dissolved air floatation (DAF) unit float (oily sludge) and waste activated sludge (WAS). DAF and WAS were anaerobically digested using digested sludge as an inoculum source (collected from an operational anaerobic digester) for assessing the toxicity and biogas production potential. Ozonation as a pretreatment increased solubilization of both sludges decreasing the toxicity or inhibition percentages but toxicity of mono-digestion of DAF sludge was reduced through ozone pretreatment. Methane production was higher from monodigestion of WAS compared to that of DAF.

Roy et al. (2016) conducted the anaerobic digestion of two waste streams acquired from a petrochemical refinery. The waste streams comprised of dissolved air flotation (DAF) unit float (oily sludge) and waste activated sludge (WAS) from the biological treatment unit of the petroleum refinery. Pretreatment through ozonation improved the digestion of DAF float at higher hydraulic retention time (HRT) thereby increasing the solids percentage removal. Ozonation enhanced toxic organic compounds removal from DAF float.

2.7.4 Biological pretreatment

Biological pretreatment involves the application of microorganisms, such as fungi, yeast, or specific enzyme-producing bacteria, to selectively degrade complex organic compounds present in organic substrates. Biological pretreatment circumscribes both aerobic and anaerobic processes which include both sludge destruction or pretreatment prior to AD process. Improvement of the hydrolysis process is what a biological pretreatment aims at prior to the main digestion process (Appels et al., 2008).

Petrochemical waste is a complex mixture consisting of complex hydrocarbon compounds (aliphatics, nitrogen–oxygen–sulphur (NSO), aromatics, and asphaltenes). Asphaltenes are recalcitrant compounds and does not undergo degradation. Aliphatic hydrocarbons include n-alkanes, isoalkanes and cyclic alkanes (naphthenes). Isoalkanes and cyclic alkanes are difficult to degrade compared to n-alkanes. Microorganisms attack hydrocarbons following the order: n-alkanes > isoalkanes > low molecular weighted aromatics > naphthenes (Gojgic-Cvijovic et al., 2012). A broad spectrum of micro-organisms such as, bacteria, fungi and yeast utilize petroleum hydrocarbons as carbon and energy sources (Das and Chandran 2011). Individual microorganisms or consortiums of microbial strains belonging to the same or different genera can selectively

metabolize hydrocarbons. There are specific enzymatic systems that can degrade petroleum hydrocarbons (Das and Chandran 2011). An initial attack typically occurs by a combination of mechanisms: attachment of microorganisms to substrates, and production of emulsifiers, biosurfactants, solvents, gases and acids (Varjani, 2017). Aerobic microbial degradation of petroleum hydrocarbons can be followed by various pathways (terminal oxidation, sub-terminal oxidation, β- oxidation, ω-oxidation). A generalized aerobic pathway of hydrocarbon degradation by microbes has been illustrated in Fig. 2.2. An oxidative process initiates the intracellular attack on organic hydrocarbon pollutants, facilitated by oxygenases and peroxidases that activate and incorporate oxygen. Step-by-step peripheral degradation pathways then convert the pollutants into intermediates of the tricarboxylic acid (TCA) cycle, while central precursor metabolites such as, succinate, acetyl-CoA, and pyruvate contribute to the synthesis of cell biomass (Varjani and Upasani, 2017).

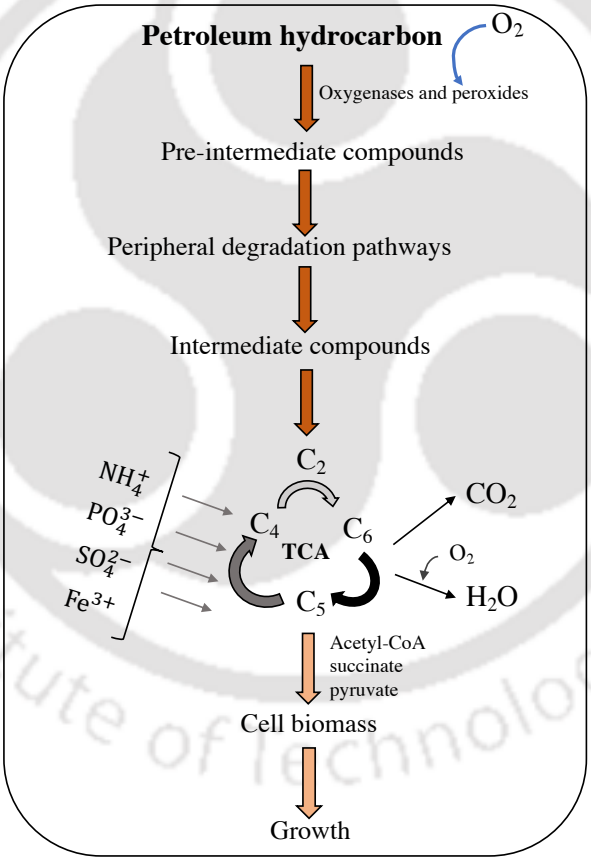

Fig. 2.2. Aerobic metabolic pathway of hydrocarbon degradation (Das and Chandran, 2011)

During anaerobic microbial degradation, petroleum hydrocarbons are activated through four general enzymatic pathways: (a) substrate addition to fumarate, catalyzed by a glycyl radical enzyme, to produce aromatic-substituted succinates, (b) methylation of unsubstituted aromatics,

(c) hydroxylation of alkyl substituents by a dehydrogenase, and (d) direct carboxylation. As a result of these activation reactions, pathways for ring saturation, β-oxidation, or ring cleavage are activated, and central metabolites such as benzoyl-CoA are produced either completely getting oxidized or getting incorporated into the biomass (Mbadinga et al., 2011; Varjani, 2017). The potential of specific microbial strain/consortium to degrade petroleum refinery wastes have garnered a lot of attention in recent years of research, some of which are briefly highlighted below.

Gojgic-Cvijovic et al. (2012) conducted a 12-week experiment where TPH degradation was studied by a consortium of bacteria (*Pseudomonas*, *Achromobacter*, *Bacillus* and *Micromonospora*) isolated from PRS. About 88% of TPH content was observed to be degraded in the PRS. Biodegradation of PRS can be affected by the type of microorganisms, temperature, treatment duration, nutrients, characteristics and concentration of PRS. Any single microbial strain might not have the metabolic capacity to degrade all of the components present in the sludge. A specific group of micro-organisms may initially convert the petroleum hydrocarbons into intermediate compounds which can then be further degraded by a different group of microorganisms.

Mukred et al. (2008) employed a mixed bacterial culture and compared that with pure cultures only to report the advantages of the mixed culture. Also, they indicated that the treatment duration plays an important factor in biodegradation of hydrocarbons. With time the degradation rate of petroleum hydrocarbons decreases reaching a threshold after which the recalcitrance nature is visible in the degradation rate. The characteristics of hydrocarbons also affect the rate of biodegradation. Degradation order was found to be saturates/alkanes> light aromatics> high aromatics> polar compounds> asphaltenes (Hu et al., 2013).

The most active agents in petroleum degradation are bacteria. Several bacteria exclusively feed onto hydrocarbons (Das and Chandran, 2011). Joseph and Joseph (2009) isolated two strains of *Bacillus* from petroleum-contaminated soils and the bacteria successfully separated oil with an efficiency of 97% at less than 5% level of sludge in the mixture of sludge and sand. *Bacillus* sp. exhibited highest rate of oil recovery or separation during the first 48 h but the rate became constant after that. *Acinetobacter* sp. has the potential to utilize carbon source in the chain length of C_{10}–C_{40} (Throne-Holst et al., 2007). The bacterial genera of *Gordonia*, *Aeromicrobium*, *Brevibacterium*, *Burkholderia*, *Dietzia*, and *Mycobacterium* are potential organisms for hydrocarbon degradation. *Sphingomonas* sp. also has the potential to degrade polyaromatic hydrocarbons (Daugulis and McCracken, 2003). *Arthrobacter*, *Mycobacterium*, *Burkholderia*, *Pseudomonas*, *Rhodococcus* and *Sphingomonas*, species reportedly degraded aromatic

hydrocarbons (Jones et al., 1983). Such genera of bacteria can be utilized as a pretreatment technique for enhancement of biogas as indicated in few studies below.

In one such study, **Merrylin et al. (2013)** conducted *Bacillus licheniformis* pretreatment on non-flocculated municipal solid waste sludge on a 5L fermenter, and reported 57% biogas enhancement with 64% VS removal.

Kavitha et al. (2014) conducted surfactant-mediated (0.02 g/g SS of sodium dodecyl sulfate) enzymatic pretreatment on waste activated sludge. They reported 19.8% reduction in sCOD with 2.2-fold increment in biogas yield.

In absence of any source of hydrocarbon-degrading bacteria, the AD of oil refinery substrate has a high hydrolysis phase leading to a very long HRT and also much quantity of substrate remains unutilized by the end of the digestion period. This is because the bacteria genera are not robust enough to degrade higher weighted hydrocarbons. So, if the higher-weighted hydrocarbons are made simpler with potential strains of bacteria then the enhancement in biogas can inevitably be achieved.

2.8 ANAEROBIC CO-DIGESTION

2.8.1 Anaerobic co-digestion with different substrates

Co-digestion is a process that involves the simultaneous AD of multiple organic substrates or feedstocks in a single biogas digester. This approach allows for the efficient utilization of diverse organic materials, including agricultural residues, food waste, animal manure, energy crops, including industrial wastes. The co-digestion process offers several benefits over monodigestion. By combining different feedstocks, the overall biogas production can be significantly increased, maximizing the energy potential of the system (Mehryar et al., 2017a). Additionally, co-digestion helps to balance the nutrient content of the digester, as different substrates often have varied nutrient profiles. This nutrient balance improves the stability and performance of the AD process. The success of co-digestion relies on careful selection and optimization of the substrate combination. The feedstocks should complement each other in terms of their physical and chemical characteristics, as well as their degradation rates. It is essential to consider the carbon and nitrogen ratio (C/N), moisture content, pH, particle size, toxicant concentrations, and other factors to achieve an ideal substrate mixture that promotes a stable and efficient digestion process (Janajreh et al., 2020). For efficient anaerobic co-digestion process, C/N ratio is desired to be in the range of 20-35 (Lee et al., 2022). An unfavourable C/N ratio leads to the production of inhibitors such as ammonia or sulphides, and accumulates the high amount of VFAs delaying the activation of the

methanogenesis process. The biogas yield is highly dependent on factors such as food/microorganism (F/M) ratio, C/N ratio, pH, temperature, and VS content. In absence of favourable conditions for any feedstock, anaerobic co-digestion (AnCoD) in presence of a suitable co-substrate to optimize the C/N, F/M, or pH would augment the biogas yield, accelerate the biodegradability and improve the microbial diversity inside an anaerobic reactor (Dioha et al., 2013). For instance, substrates with low carbon or high nitrogen content, co-digestion with a suitable co-substrate having high carbon or low nitrogen content reportedly increases the methane yield, but the percentage enhancement varies with the choice of co-substrate utilized and the optimization of the factors (such as F/M, C/N, pH and inoculant concentrations) affecting it. Few studies that have explored the co-digestion of PRS for nutrient balance and reduction of toxicant concentrations are given below.

Yang et al. (2020) performed anaerobic co-digestion of oily sludge with corn stover and the inoculum utilized was a fermentation substrate. They evaluated that with the increase in the mass ratio of corn stover and oily sludge, the biogas yield increased showing a positive co-relation between corn stover and biogas production. The addition of organic fraction and balancing the lack of nutrients improved the biodegradability of oily sludge.

Ghaleb et al. (2021) performed anaerobic co-digestion of biosludge from oil refinery with sugarcane bagasse (highly lignocellulosic biomass) in order to balance the C/N ratio for efficient biodegradation. The co-substrate being complex in nature due to the presence of 28% lignin, the authors utilized thermochemical pretreatment employing 1% (w/v) sodium hydroxide being maintained at 100°C, 150 rpm for 1 h. The pretreatment led to delignification of lignin and exposed the more soluble hemicellulose and cellulose for improved microbial proliferation during the co-digestion process. This eventually incremented the biogas yield by 70% for C/N = 30 compared with C/N = 20.

Castro et al. (2022) conducted anaerobic co-digestion of oil refinery waste activated sludge (ORWAS) (biosludge) with food waste and observed that biogas enhancement was 2.1-fold compared with mono-digestion of ORWAS with 52% VS degradation at substrate:cosubstrate ratio of 80:20 (v/v%), within 30 d of digestion period.

Lee et al. (2022) conducted anaerobic co-digestion of oil scum (oily sludge) and secondary sludge (biosludge) with food waste (or swine manure). Due to presence of high TPH content (>87% wet weight of sludge) in the oil scum, it was not feasible for AD. Due to the presence of lesser fractions of TPH in secondary sludge including diverse microbial community, it was rendered

suitable for AD. The co-digestion of secondary sludge with food waste or swine manure increased methane potential from 10% - 40% at different mixing ratios, improving the synergy indices.

2.8.2 Microbial community dynamics in anaerobic co-digestion process

The microbial community dynamics in anaerobic co-digestion process plays a pivotal role in the efficient degradation of organic substrates and the generation of valuable biogas. Understanding the intricate interactions and shifts within these microbial communities is crucial for optimizing co-digestion systems. Studies have shed light on the microbial diversity dynamics during anaerobic co-digestion, unveiling the intricate web of microbial species and their functional roles. Bacterial species, such as *Firmicutes* (e.g., *Clostridium* and *Lactobacillus*), *Proteobacteria* (e.g., *Enterobacter* and *Pseudomonas*), and *Bacteroidetes* have been identified as prominent players throughout the co-digestion process (Joseph et al., 2020). In addition to bacteria, archaeal communities have been investigated due to their essential role in methanogenesis, the production of methane gas. *Methanobacterium* and *Methanosarcina* species have been observed to dominate the archaeal populations, demonstrating their active involvement in methane production during co-digestion (Li et al., 2021). The dynamics of microbial communities are influenced by various factors, including the composition of the substrate, operating conditions, and process parameters. These factors shape the community structure, leading to shifts in the relative abundance of specific bacterial species and archaeal groups. Temperature is a critical parameter that affects the microbial community dynamics in anaerobic co-digestion. Different microbial species have varying temperatures, optimal for growth and metabolic activities. Mesophilic conditions (35-40°C) favor the growth of mesophilic bacteria, while thermophilic conditions (50-60°C) promote the proliferation of thermophilic microorganisms. Studies have shown that shifts in temperature can result in changes in microbial community composition, with specific species adapting and thriving under different temperature regimes (Supaphol et al., 2011). Even VFA concentrations, particularly acetic acid, propionic acid, and butyric acid, also play a significant role in shaping the microbial community dynamics during co-digestion, as VFAs are intermediate metabolites produced during the anaerobic breakdown of organic matter. High VFA concentrations can have inhibitory effects on certain microbial populations, causing shifts in community structure. Some microorganisms, such as acetogens and homoacetogens, are specialized in utilizing VFAs as their primary carbon sources, while methanogens convert VFAs into methane. The balance between these functional groups is crucial for efficient biogas production (Yan et al., 2018).

2.8.3 Optimization of anaerobic co-digestion parameters

Optimization models have been widely utilized for the optimization of anaerobic co-digestion parameters to enhance the performance and efficiency of the process. These models help in identifying the optimal operating conditions and parameter settings by considering microbial community dynamics, temperature, and VFA concentrations that maximize biogas production, minimize substrate degradation time, and improve overall process stability (Mehryar et al., 2017b). Several optimization techniques and models have been employed in this regard as listed below.

- ✓ **Mathematical programming models**- Mathematical programming models, such as linear programming (LP) and nonlinear programming (NLP), have been used to optimize anaerobic co-digestion parameters. These models consider multiple objectives, such as maximizing biogas yield, minimizing substrate utilization time, and maximizing process stability, while considering constraints related to substrate availability, reactor capacity, and process limitations (Tufaner and Demirci, 2020).

- ✓ **Response Surface Methodology (RSM):** RSM is a statistical modelling technique that helps in optimizing process parameters by fitting mathematical models to experimental data. RSM involves the design of experiments, data analysis, and fitting of response surfaces to identify the optimal combination of parameters that yield maximum biogas production or desired process performance (Güven et al., 2008; Behera et al., 2018; Kainthola and Kalamdhad, 2019). RSM has been utilized to optimize various parameters, including substrate composition, mixing ratio, C/N ratio; pretreatment process parameters, and hydraulic retention time (HRT) of reactors (Jiménez et al., 2014; Jacob and Banerjee, 2016; Feng et al., 2017; Ghaleb et al., 2021).

- ✓ **Artificial Intelligence (AI) and Machine Learning (ML) techniques**: AI and ML techniques, such as genetic algorithms, neural networks, and fuzzy logic, have been employed for optimization in anaerobic co-digestion (Jacob and Banerjee, 2016; Andrade Cruz et al., 2022). These techniques can handle complex systems with multiple parameters and objectives, allowing for the identification of optimal operating conditions. AI and ML models can learn from historical data and optimize the anaerobic digestion process parameters such as rate of biogas production in anaerobic digesters and design considerations based on patterns and relationships within the data (Sappl et al., 2023).

- ✓ **Genetic Algorithm (GA):** GA is a computational optimization method inspired by natural selection and genetics. It involves the generation of a population of potential solutions,

which are then evolved through iterations to identify the best solution. It has been applied to optimize parameters such as substrate composition, loading rates, temperature, and retention time in anaerobic digestion and co-digestion processes (Jacob and Banerjee, 2016).

Various other studies utilized mathematical programming models, response surface methodology, and other optimization techniques to determine the optimal operating conditions, for maximizing biogas/methane yield and improving process efficiency in anaerobic co-digestion. By considering the microbial community dynamics, temperature, pH, C/N ratio, sCOD and VFA concentrations, these optimization models contribute to the effective management of organic feedstock in anaerobic condition.

2.9 BIOGAS REACTORS

Efforts and exploration have been committed towards design and performance of a biogas digester for different types of feedstock for nearly two to three decades. The major complication to put up a challenge for various researchers was the hydrolysis phase in particular with the complex polymer substances. The feedstock quantity that can be utilized is not only performance and stability dependent but also cost-dependent majorly. Various types of anaerobic reactors are used to utilize different types of organic substances such as, single stage, dual stage, upflow anaerobic sludge blanket (UASB) reactor, anaerobic sequencing batch reactors (ASBRs), baffled reactors and hybrid reactors, some of which might be suitable for petroleum sludge treatment as well (Kondusamy and Kalamdhad, 2014; Wang et al., 2016).

Petroleum refinery sludge contains high calorific values in the range of (17 to 19) x 10^3 kJ/kg, which is mainly due to the presence of high oil content making it a valuable energy source. Few types of petrochemical sludge (e.g., biosludge) also consist of huge percentage of moisture content. Conventional single-phase AD of petroleum sludge is challenging due to the presence of the refractory organics and emulsions (Wang et al., 2016). Methane generation efficiency is higher from a dual stage anaerobic reactor compared to that of a single stage reactor. A single stage reactor demands neutral pH and long retention time since methanogens are slow-growing and sensitive and they show better stability and greater methane yield in a dual stage reactor (Maspolim et al., 2015).

The performance and efficiency of anaerobic reactors are influenced by various factors. These include the organic loading rate (OLR), hydraulic retention time (HRT), temperature, pH, substrate characteristics, and the presence of inhibitors or toxic compounds (Liang et al., 2019; Barua and

Kalamdhad, 2019). Temperature plays a critical role in the activity of anaerobic microorganisms, with mesophilic (around 35-40°C) and thermophilic (around 50-60°C) conditions being the most commonly used (Siddiqui et al., 2016; Veluchamy et al., 2019). pH affects the microbial community composition and metabolic pathways, and optimal pH ranges vary depending on the reactor type and the specific microorganisms involved (Liang et al., 2019). The characteristics of the substrate, such as its composition, nutrient content, and biodegradability, significantly influence the reactor performance. Certain inhibitors or toxic compounds present in the feedstock can inhibit the activity of anaerobic microorganisms and affect the overall efficiency of the process (Roy et al., 2016). Few prominent studies have been summarized in Table 2.3 which have utilized petroleum refinery waste for AD in different types of reactors. Overall, understanding and controlling these factors is essential for optimizing the performance of anaerobic reactors and achieving efficient and stable biogas production or organic waste treatment.

2.10 CONCLUDING REMARKS

Colossal quantities of PRS, containing intricate and persistent organic compounds, pose significant risks and demand effective treatment and management. Separating oil and grease from the sludge is costly and challenging on a large scale, while alternative methods such as, land farming and bioremediation have limitations due to slow compound degradation and soil accumulation. This accumulation raises soil toxicity, leaches into groundwater, and endangers human health. Improper disposal also threatens coastal areas and marine ecosystems. Hence, inadequate treatment and disposal of petroleum refinery sludge have profound environmental implications for both land and water ecosystems.

PRS has a very high calorific value, making techniques such as pyrolysis and incineration appear appealing for its treatment. However, these methods demand substantial energy consumption, high capital and maintenance cost, and high-end equipments, rendering them cost-intensive. Furthermore, the heterogeneous and multiphasic nature of the sludge, with varying emulsion and moisture content, hinders the effectiveness of conventional combustion or landfilling approaches. In contrast, anaerobic digestion emerges as an eco-friendly and cost-effective alternative, with researchers worldwide highlighting its significant methane generation potential from petroleum refinery sludge. Nonetheless, the absence of appropriate pretreatment techniques results in prolonged hydraulic retention times and sluggish degradation due to extended hydrolysis phases and inadequate inoculation, leading to minimal methane production. Even lack of nutrient balance and appropriate inoculation hinders the microbial proliferation reducing the degradation efficiency. Henceforth, it is imperative to engage in comprehensive research endeavors aimed at

Table 2.3. Different types of reactors and its characterization parameters

Substrate	Type of reactor	Reactor size (Working volume)	HRT or OLR	Operation period	Pretreatment	Biogas or methane enhancement	Remarks	References
Petrochemical wastewater	Continuous stirred tank reactor (CSTR)	4.5 L (2.7 L)	10 d/ 6.31 kg COD/m^3 /d	140 d	Oxidation (peroxide) (Dose = 1% for 2.5 h)	(50-60)%	✓ sCOD removal =98% ✓ Methane =83.45%	Siddiqui et al. (2014)
Petrochemical wastewater	Continuous stirred tank reactor (CSTR)	5 L (2.8 L)	5 d	109 d	-	131%	✓ sCOD removal =98% ✓ Methane enhancement = 124.5%	Siddiqui et al. (2015)
Petroleum refinery waste activated sludge (WAS)	Completely mixed semi-continuous reactor	4.0 L (3.0L)	1.3 gCOD/L/d (Ozonated WAS)	280 d	Ozonation (Dose = 0.05 g O_3/g TS_{sample})	160%	✓ TS removal increment = 25% ✓ sCOD removal increment = 32%	Roy et al. (2016)
Oil refinery WAS	Two-phase and single-phase batch reactor	1.0 L	-	30 d	Thermal (170°C, 60 min) ✓	67% for bi-phase compared to single-phase	✓ Methane = 60% (two-phase) ✓ Methane = 40% (single-phase).	Wang et al. (2016)

								✓ sCOD removal= 77.8% for two-phased reactor (2.1 times that of single-phase reactor)	
Petrochemical wastewater	Continuous stirred tank reactor (CSTR)	4.5 L (2.7 L)	(6.3-32) gVS/L/d	145 d	-	✓ 49.7% (Mesophilic) ✓ 46.7% (Thermophilic)		✓ VS removal = 77% (Mesophilic) ✓ TS removal =53% (Mesophilic) ✓ VS removal = 79% (Thermophilic) ✓ TS removal =46% (Thermophilic)	Siddiqui et al. (2016)

innovating novel pretreatment methodologies to augment the efficacy of sludge degradation processes, thereby facilitating enhanced energy recovery. Notably, petroleum refinery biosludge, characterized by a low carbon-to-nitrogen (C/N) ratio, necessitates exploration of anaerobic co-digestion strategies involving suitable co-substrates boasting a higher C/N ratio. This endeavor seeks to foster optimal microbial proliferation, thereby mitigating nutrient deficiencies, modulating moisture content, and diluting inhibitors, improving process stability. Nonetheless, the selection of appropriate co-substrates and the optimization of process parameters necessitate meticulous investigation and experimental investigation. Research is necessary to comprehend the impact of factors such as, C/N ratio, pH, hydraulic retention time, and substrate composition on large-scale anaerobic reactor performance, enhancing biogas production, reducing toxicity, and improving overall efficiency. Therefore, research efforts should focus on developing effective techniques, optimizing process parameters, and evaluating environmental impacts for economically viable waste management.

Chapter 3

MATERIALS AND METHODS

Different experimental approaches were used to accomplish the stipulated objectives. The research was carried out in different phases using petroleum refinery sludge as a substrate and digested sludge as an inoculum. The detailed methodology summarized below.

3.1 EXPERIMENTAL FLOWCHART

In order to achieve the desired goals, the proposed research work was accomplished in different phases as shown in Fig. 3.1.

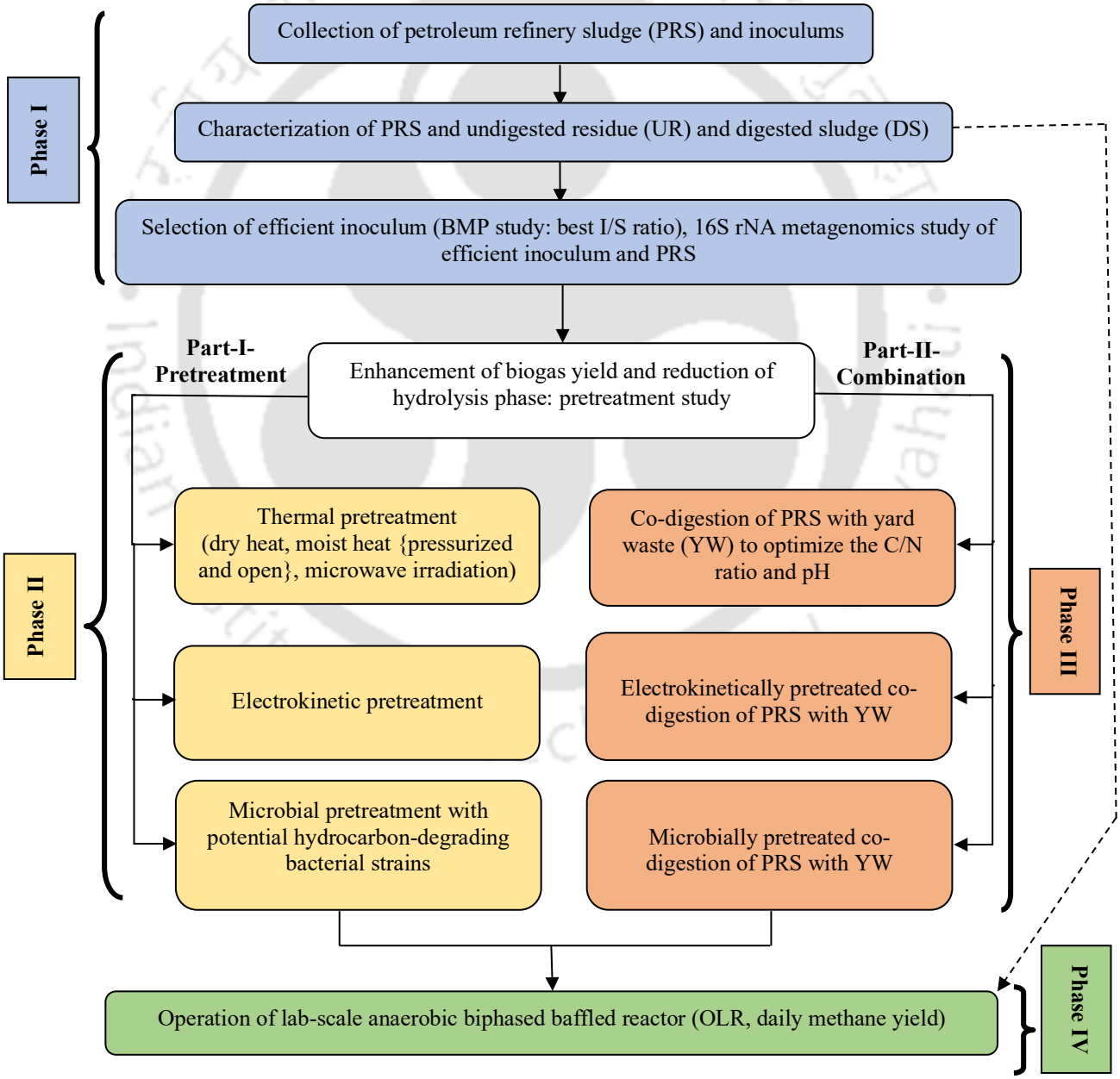

Fig. 3.1. Experimental flowchart of the research work

In phase I, the BMP test was conducted to check the efficacy of undigested residue of animal excreta, and digested (degassed) sludge from an operational steady-state anaerobic digester treating animal residue as inoculums, and exploring the optimum inoculum and feedstock (I/F) ratio based on VS content. In phase II, the effect of different pretreatments on the hydrocarbon degradation and enhanced biogas production from PRS was estimated with the most efficient inoculum from phase I. In phase III, the effect of different pretreatments on the anaerobic co-digestion of PRS and YW was evaluated to further estimate the enhancement in biogas. In phase IV, a lab-scale semi-continuous anaerobic reactor was operated at different organic loading rates (OLRs) to optimize the OLR resulting in maximum methane yield.

3.2 SUBSTRATE, CO-SUBSTRATE AND INOCULUM

Grab samples of PRS was collected in 10L high-density polyethylene containers from the biological wastewater treatment unit of ETP of a large-scale refinery in Guwahati, Assam, India. Collected PRS samples were dark brown in colour having a semi-solid consistency.

The yard waste (YW) was collected from the residential colony of the same petroleum refinery from which the substrate was collected, and located in Guwahati, Assam, India. The collected mixed YW was firstly screened for any plastic or metals. The screened YW consisted of tree leaves (fresh and fallen) (55% by weight), small branches of trees and twigs (20% by weight), grass clippings (23% by weight) and remaining consisted of some unknown weeds. The screened YW was sun-dried for 24 hrs, ground using a mixer grinder (Philips HL7756/03, 750W) to obtain particle size within 5-10 mm and stored in airtight bags at room temperature. The initial characterization of YW revealed pH, moisture content, VS, TS, sCOD, VFA and C/N ratio as 5.13, 7.6%, 89.5(%TS), 92.4%, 7800 mg/L, 1500 mg/L, and 46.8 respectively.

The inoculums selected for the study were undigested residue (UR) of animal excreta and anaerobically digested sludge (DS), rich in methanogens from an anaerobic digester treating animal residue as feedstock. UR was collected from Amingaon village situated near the Indian Institute of Technology Guwahati, India campus. A pre-inoculated degassed anaerobically well-acclimated DS was collected from a steady operational anaerobic digester located in Maligaon, Guwahati, India. The sludge samples and inocula were stored at 4ºC until further use.

3.3 PHASE I- INOCULUM STUDY

The inoculum study emphasizes on the comparative exploration of PRS for efficient biogas production with two different inoculums: (a) undigested residue (UR) of animal excreta and (b)

anaerobically acclimated digested sludge (DS) from an operational steady-state anaerobic digester treating animal residue as feedstock, under different inoculum and feedstock (I/F) ratios.

3.3.1 Experimental setup of anaerobic biodegradability batch test

Biochemical methane potential assay (BMP) signifies anaerobic biodegradation of any substrate. It measures the maximal amount of biogas recouped from any substrate per mass of organic matter present in that substrate as chemical oxygen demand (COD) or volatile solids (VS) (Koch et al., 2020). BMP batch tests were carried out in 1L batch reactor for both types of inocula. Separate but similar BMP experiment was formulated for both the inocula (UR and DS) to attain a standard comparison. Five different mixing ratios of inoculum and sludge (0.3, 0.4, 0.5, 0.7 and 1) were selected for the comparative study of both the inocula. Based on VS, the amount of PRS and inocula (UR and DS) were optimized and presented in Table 3.1. Vital macro and micronutrients were added to individual reagent bottle for optimum microbial growth and maintenance of buffer capacity (Distefano and Ambulkar, 2006). The reactors were incubated in mesophilic temperature conditions. Anaerobic condition was created by purging nitrogen gas and sealing with airtight rubber corks. The 1L anaerobic reactors were then affixed to 1L aspirator bottles comprising 1.5N sodium hydroxide to engross produced carbon dioxide and remove other trace gases such as ammonia, nitrogen, hydrogen sulphide, etc. The principle of water displacement method is applied for the quantification of biomethane from the above-mentioned experimental setup using thymol blue as an alkali indicator (Fig. 3.2). The inocula experiments were conducted for 70 d in triplicates.

Table 3.1. Feedstock composition for BMP test for inoculum study

AD with UR				AD with DS		
UR:PRS or DS:PRS	**Quantity of PRS (g)**	**Quantity of UR (g)**	**Quantity of de-ionized water (g)**	**Quantity of PRS (g)**	**Quantity of DS (g)**	**Quantity of de-ionized water (g)**
0.3	465.07	100	234.93	195.91	100	504.09
0.4	387.56	100	312.44	163.26	100	536.74
0.5	310.05	100	389.95	130.61	100	569.39
0.7	221.47	100	478.53	97.95	100	602.05
1	155.02	100	544.98	65.30	100	634.70
C1	100	0	700.00	100	0	700.00
C2	0	100	700.00	0	100	700.00

NB: For digestion with both inocula, total weight for all the ratios is 800g; C1- $Control_{sludge}$; C2- $Control_{inoculum}$

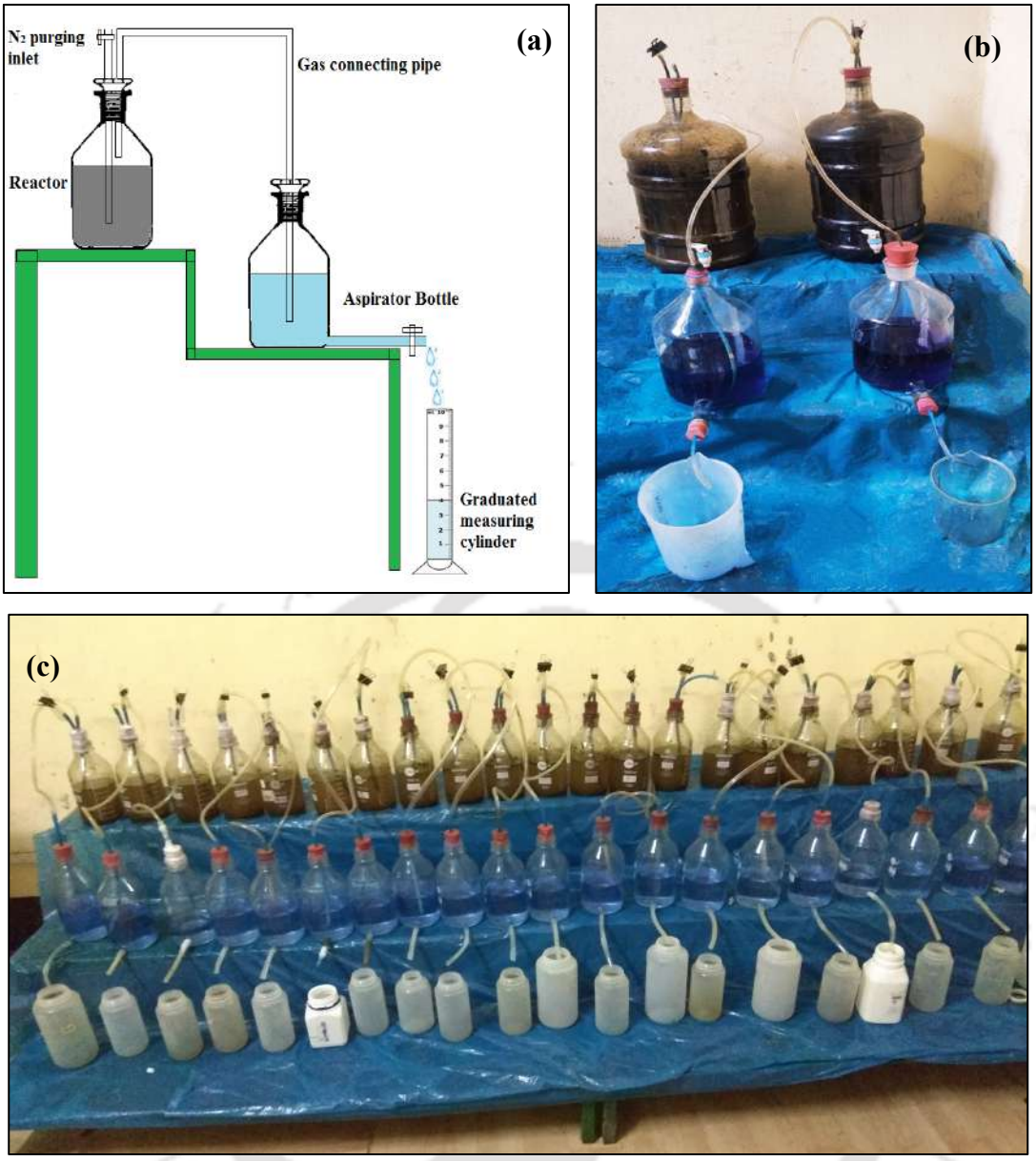

Fig. 3.2. (a) Diagrammatic representation, and pictorial representations of (b) 20L and (c) 1L batch tests

3.3.2 Metagenomic study

3.3.2.1 Metagenomic DNA isolation, qualitative and quantitative analysis

Sample of the most efficient inoculum from the BMP study was sent for 16S metagenomics profiling. The metagenomic DNA was isolated from the received inoculum sample by commercially available soil Kit (Nucleospin Soil). The qualities of the isolated metagenomic DNA samples were quantified using Nano Drop.

3.3.2.2. Preparation of 2 x 300 MiSeq library

The amplicon libraries were prepared using Nextera XT Index Kit (Illumina inc.). Primers for the amplification of the bacterial 16S V3-V4 region were designed and synthesized at Eurofins Genomics Lab. Amplification of the 16s gene was carried out. 3µl of PCR product was resolved on 1.2% Agarose gel at 120V for approximately 60 min or till the samples reached 3/4th of the gel. The forward and backward primers used for the study were GCCTACGGGNGGCWGCAG and ACTACHVGGGTATCTAATCC respectively. The quality check (QC) passed amplicons with the Illumina adaptor were amplified using i5 and i7 primers that add multiplexing index sequences as well as common adapters required for cluster generation (P5 and P7) as per the standard Illumina protocol. The amplicon libraries were purified by AMPure XP beads and quantified using Qubit Fluorometer.

3.3.2.3 Quantity and quality check (QC) of library on Agilent 4200 Tape Station

The amplified libraries were analyzed on 4200 Tape Station system (Agilent Technologies) using D1000 Screen tape as per manufacturer instructions.

3.3.2.4 Cluster Generation and Sequencing

After obtaining the mean peak sizes from Tape Station profile, libraries were loaded onto MiSeq at appropriate concentration (10-20pM) for cluster generation and sequencing. Paired-End sequencing allows the template fragments to be sequenced in both the forward and reverse directions on MiSeq. The kit reagents were used in binding of samples to complementary adapter oligoes on paired-end flow cell. The adapters were designed to allow selective cleavage of the forward strands after re-synthesis of the reverse strand during sequencing. The copied reverse strand was then used to sequence from the opposite end of the fragment.

3.3.2.5 Bioinformatics analysis

i. The raw reads were processed using the Quantitative Insights into Microbial Ecology (QIIME) pipeline (v1.8).
ii. Trimmomatic (v0.38) was employed to obtain high-quality, clean pair-end (PE) reads, followed by the merging of PE data into single-end reads using FLASH (v1.2.11).
iii. Operational taxonomic units (OTUs) were identified by comparing the sequences to the Greengenes database (version 13_8).
iv. Utilizing the UCLUST algorithm at a 97% sequence similarity threshold, all sequences from the samples were clustered into Operational Taxonomic Units (OTUs).

3.4 PHASE II- PRETREATMENT STUDY

In order to determine the most efficient pretreatment technique for biogas production from PRS, three different types of pretreatment studies were conducted. The three different type of pretreatment techniques investigated were thermal pretreatment, electrokinetic pretreatment and biological pretreatment. Depending on the increase in biogas production and hydrocarbon degradation, the most efficient pretreatment technique for biogas production from PRS was determined with the most efficient inoculum from the inoculum study.

3.4.1 Thermal pretreatment

The study evaluated the effect of three different modes of heat application on the solubilization and hydrolysis of PRS. The optimum operating condition of the most efficient mode of heat application was chosen as a method of thermal pretreatment for anaerobic biodegradability of PRS. Each mode of heat application was evaluated in two phases- (a) Temperature variation (b) Exposure time variation. The ranges of temperature and exposure period for each mode were chosen based upon previous studies (Kuglarz et al., 2013; Ennouri et al., 2016). An untreated sample (control) was examined as reference.

3.4.1.1 Dry heat

To study the effect of dry heat on PRS, a hot air oven (ICT-WB) was employed (Fig. 3.3a) which works on the principle of conduction. 100g of sludge samples were taken in 500 mL wide-mouth glass bottles in three replicates. To study the effect of temperature variation, each sample was subjected to temperatures:70, 80, 90, 100, 110, 120,140 and 160°C for 50 min. Upon evaluation of the optimum temperature through maximum solubilization and volatile fatty acids accumulation, the samples were then heated for different time intervals: 30, 60, 90,120 and 180 min to evaluate the optimum exposure time.

3.4.1.2 Moist heat

(i) Pressurized moist heat

For temperature study of pressurized moist heat on PRS, different temperatures were set at 80, 90, 100, 110 and 120°C for 30 min. 100g samples in triplicates were taken in closed wide-mouth glass bottles of 500 mL capacity and kept inside an 'autoclave' (REICO-83114) (Fig. 3.3b) under 15 psi pressure, which works on the principle of saturated steam under pressure. Temporal study

was conducted at the optimum temperature for 20, 40, 60 and 80 min to determine the optimum exposure period.

(ii) Agitated open moist heat

To study the effect of moist heat without pressure on PRS, a temperature study was conducted at 60, 70, 80, 90, and 100 °C for 40 min. 100g samples were taken in 250 mL conical flasks, in triplicates and kept inside a reciprocating water bath (ICT, WB-P098) ((Fig. 3.3c) and uniformly agitated at 100 rpm. Reciprocating water baths transfer moist heat to a substance on the principle of conduction and convection. Upon evaluation of the optimum temperature, the temporal study was investigated for 30, 60, 90 and 120 min to assess the optimum exposure time.

3.4.1.3 Microwave irradiation

A microwave oven (SAMSUNG-CE1041DSB2) (Fig. 3.3d) was used for the temperature and temporal study of this pretreatment process. Temperatures were set at 100, 140, 160, 180, 200,220 and 250°C for 2 min giving a standing time of 10 min. Upon examining the optimum temperature, microwave radiations were exposed to PRS for 3, 5, 10, 15, 20 min. The optimum operating condition of microwave irradiation pretreatment was evaluated after the temporal study.

Fig. 3.3. (a) Hot air oven, (b) autoclave, (c) hot water bath, and (d) microwave

3.4.1.4 Experimental setup of anaerobic biodegradability batch test

The influence of the most efficient mode of heat as pretreatment was assessed on the anaerobic biodegradability of PRS by measuring the accelerated biogas production from the 1L BMP setup for different inoculum and pretreated substrate (I/S) ratios (0.3, 0.4, 0.5 and 0.7) at optimum pretreatment conditions (temperature and time). Untreated PRS was kept as control. The quantities of substrate and inoculum utilized are shown in Table 3.2. The experimental set up has been done

as per section 3.3.1 for 1L BMP batch test with the most efficient inoculum. Upon achieving the most efficient I/S ratio from the 1L BMP study, it was upscaled to 20L capacity (14L working volume) with the intention of evaluating the compositional alterations throughout the digestion period. Fig. 3.2(b) is a representation of the 20 L anaerobic batch experimental setup.

Table 3.2. Substrate composition for 1L BMP test assay

I/S ratio	PRS (g)	DS (g)	De-ionized water (g)
0.3	198.2	100	401.8
0.4	165.17	100	434.83
0.5	132.14	100	467.86
0.7	99.10	100	500.9
Control	100	0	600.00

NB: Total weight for all the ratios is 700g

3.4.1.5 Energy assessment

For evaluating the energy requirement and scalability of the pretreatment used for enhanced biogas production from PRS, an energy assessment study is carried out assuming the sludge to be homogeneous and no loss of mass during the pretreatment process. The amount of energy produced due to methane production from the pretreated sludge after subtracting the energy produced due to raw sludge based on the highest methane yield can be represented as Q_B (kJ) and calculated as per Eq. (3.1) (Passos and Ferrer, 2015)

$$Q_B = \rho(Y_P - Y_S)\S * V * \eta \quad [3.1]$$

where, ρ is density of PRS (kg/m^3), Y_P and Y_S are the highest methane yields produced during anaerobic digestion of pretreated and untreated PRS respectively (m^3 CH_4/kg VS), § is lower heating value of methane (kJ/m^3), V is usable volume of reactor (m^3), η is energy conversion efficiency (assumed 90%). The amount of energy utilized in the form of heat can be denoted as Q_H (kJ) and evaluated as per Eq. (3.2) (Kuglarz et al., 2013)

$$Q_H = C_S(T_P - T_D)M_s \quad [3.2]$$

where, C_S is the specific heat capacity of sludge (kJ/kg/ºC), T_P is the temperature (ºC) at which the pretreatment is conducted, T_D is the digestion temperature (ºC), M_S is the mass of sludge used

in the pretreatment process (kg). The amount of energy expended during the pretreatment process of sludge can be represented as Q_U (kJ) and calculated as per Eq. (3.3) (Passos and Ferrer, 2015)

$$Q_U = \frac{\omega * E_T}{W} \quad [3.3]$$

where, ω is the power consumption (Watt) by the efficient mode of heating evaluated from the pretreatment study, E_T is the optimum exposure time (s) for the efficient mode of thermal pretreatment, W is the weight of volatile solids fraction of PRS (g-VS).

The energy consumption due to the thermal pretreatment process during anaerobic digestion of PRS can be represented as Q_T (kJ) and evaluated by Eq. (3.4)

$$Q_T = Q_B + Q_H - Q_U \quad [3.4]$$

3.4.2 Electrokinetic pretreatment

3.4.2.1 Electrokinetic (EK) pretreatment optimization by CCD-RSM

CCD-RSM is a decisive sequential technique applied based on the design of experiments for performance optimization of the design matrix thereby reducing the number of experimental runs leading to a faster and more systematic investigation of the process variables as compared to conventional optimization approaches (Güven et al., 2008). For EK pretreatment study on PRS, CCD-RSM was used to investigate the combined effects of applied voltage, time and electrode spacing on the compositional changes in PRS. A five-level-three-factorial experiment was designed by CCD. The independent variables included were: applied voltage (X_1), exposure time (X_2) and electrode spacing (X_3), and each variable was coded at five levels: the high level (+1), the low level (−1), the center point (0) and two outer points corresponding to 'α' where, $\alpha = 2^{n(1/4)}$ (n = 3 in this study, α = ±1.681) as shown in Table 3.3. The regression model was developed according to the following equations of the levels: $x_1 = [(X_1-60)/40]$; $x_2 = [(X_2-70)/50]$ and $x_3 = [(X_3-12)/4]$ as explained by Behera et al. (2018). ±1 corresponds to factorial points and ± α corresponds to axial points. The output response was focused on two parameters: the improved organic matter solubilization calculated by soluble chemical oxygen demand (sCOD) and the accumulation of volatile fatty acids (VFA). Solubilization is indicated as the ratio of soluble organic fraction and total biosolids fraction. Higher soluble organic fraction (sCOD) in bioreactors provide a higher amount of readily biodegradable organic fraction for anaerobic microorganisms to increase biomethane production but extremely high sCOD may also delay biomethane production by reducing pH of the reactors (Hallaji et al., 2019). Industrial applications focus on high organic

loading but too high concentrations lead to increased VFA concentrations (decreasing pH) which become inhibitory for the anaerobic digestion process (Chen et al., 2008; Feng et al., 2017). Therefore, for optimization of output response parameters: sCOD (Y_1) and VFA (Y_2), twenty-two experimental runs were augmented with six axial points in duplicates, eight factorial points and one centre point in duplicate. Experimental conditions of CCD were developed using Design-Expert® 11.1.2.0.

The relationship between dependent response variables (sCOD and VFA) and independent variables (applied voltage, exposure time and electrode spacing) was explained by the second-order polynomial model as shown in Eq. (3.5).

$$Y_i = \beta_0 + \sum_i \beta_i X_i + \sum_{i<j} \sum_j \beta_{ij} X_i X_j + \sum_i \beta_{ii} X_i^2 \qquad [3.5]$$

where, Y represents the responses, X represents the independent variables and β represents the regression coefficients (β_0, β_i, β_{ij} and β_{ii} are the intercept, linear, interaction and quadratic terms, respectively). To evaluate the adequacy of generated model and decide the statistical significance of the regression coefficients, analysis of variance (ANOVA) was applied. The significance of all the variables was tested statistically at a level of p = 0.05. Student t-test was conducted to find an interrelation between the independent variables and output responses thereby accepting the null hypothesis since no significant deviation could be found in the p-value. The quality of fit of the polynomial model was expressed by the coefficient of regression (R^2) and adjusted regression (R^2_{adj}), and statistical significance was checked by the Fisher (F) -test in the program with selected p at 95% confidence level. The primary objective of the optimization process was to maximize the Y_1 and Y_2 output response parameters with maximum desirability. The experimental matrix and the influence of the variables was depicted by two-dimensional (2D) contour plots and three-dimensional (3D) interface in Design Expert® 11.1.2.0.

Table 3.3. Levels of independent variables used for EK pretreatment optimization

Variable labels	Coded factors (X_i)	Coded levels				
		-1.681(-α)	**-1**	**0**	**+1**	**+1.681(+α)**
Applied voltage (V)	X_1	33.68	40	60	80	86.32
Exposure time (min)	X_2	4.20	20	70	120	135.80
Electrode spacing (cm)	X_3	6.74	8	12	16	17.26

3.4.2.2 EK pretreatment setup

The EK pretreatment setup (Fig. 3.4) comprised of multiple plastic feed tanks with 10-20 cm diameters and height ranging from 25-35 cm, DC power supplier, tachometer (RPM gauge), two graphite electrodes, flash mixer, ammeter (current regulation in circuit) and multimeter (voltage regulation in circuit). The feed tank was partially filled with PRS and DC was passed through the sample with the help of the electrodes to complete the circuit. The experimental design matrix consisting of twenty-two runs as generated by CCD were conducted at varying applied voltages, duration and electrode spacing and the output responses (sCOD and VFA in mg/L) were input in the software. Two-third of graphite electrodes acted as both anode and cathode were immersed in substrate for each experimental run without touching the base of tank. The insulated flash mixer was rotated at 150 rpm to maintain the homogeneity of suspension throughout the pretreatment process.

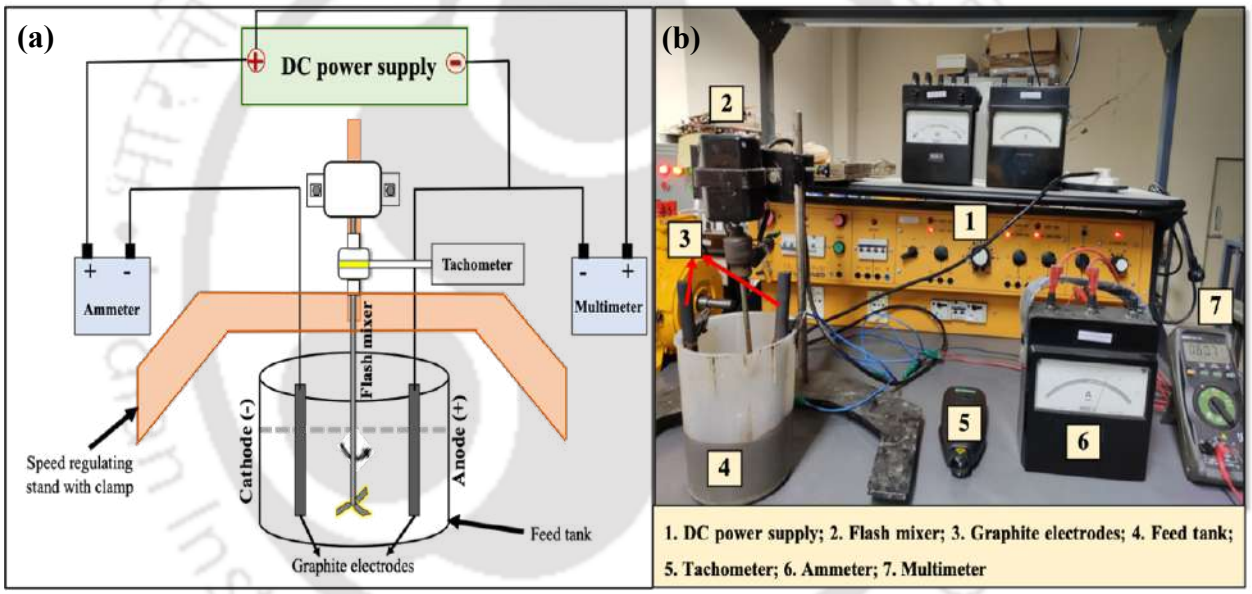

Fig. 3.4. (a) Schematic diagram and (b) experimental framework of the electrokinetic pretreatment

3.4.2.3 Biochemical methane potential batch assay

Upon optimizing the EK pretreatment conditions using CCD, the BMP batch assays were conducted at the optimized pretreatment condition with a motive to prepare the feedstock with improved soluble organic matter content thereby shortening the hydrolysis phase. The BMP test was conducted in graduated 1000 mL borosilicate glass reactor bottles at four different I/S (inoculum and substrate) ratios (0.3, 0.4, 0.5, and 0.7) along with two controls of untreated sludge and inoculum. Based on volatile solids content, the amount of PRS and DS were optimized and

presented in Table 3.4. The 1000 mL reactor bottles were connected to borosilicate glass aspirator bottles of similar capacity which were filled with 1.5 N NaOH with thymol blue as an indicator to engross carbon dioxide and trace gases of ammonia and hydrogen sulphide. Nitrogen gas was expunged into the reactor bottles for 3 min to create an anaerobic condition thereby sealing the reactors with rubber stoppers. The reactors were maintained at mesophilic temperature range and placed in triplicates. Manual mixing was done 2-3 times a day for better homogeneity of the samples. The principle of the liquid displacement method was followed for biogas quantification (Haak et al., 2016). The displaced biogas from each reactor was collected each day and measured using a graduated cylinder. The AD of EK pretreated PRS was conducted for 60 d. The 1L batch study was scaled up to 20L to test large-scale operational conditions for the optimum I/S ratio with a working volume of 14L to evaluate the compositional alterations throughout the digestion period.

Table 3.4. Substrate composition for BMP test assay

I/S ratio	PRS (g)	DS (g)	De-ionized water (g)
0.3	209.93	100	390.07
0.4	174.11	100	422.89
0.5	139.28	100	560.72
0.7	104.48	100	495.52
C_s	100	0	600.00

NB: Total weight for all the ratios is 700g; C_S- Control sludge

3.4.2.4 Energy assessment

Based on the experimental results obtained, it is imperative to determine the scalability and economic sustainability of the electrokinetic (EK) pretreatment on PRS ensuing anaerobic biodegradability. The input energy (Q_i) provided for EK pretreatment is the summation of energy consumption by DC power supply and energy utilized for flash mixing of the substrate as calculated in Eq. (3.6).

$$Q_{in} = P_{EK}t + P_F t = (V_V \cdot I)t + (\mu \cdot G^2 \cdot V_t)t \quad [3.6]$$

where, Q_{in} is the total input energy utilized for EK pretreatment (J), P_{EK} power utilized by DC (J/s), P_F is the power of the flash mixer (Watt), V_V is the voltage used for pretreatment (V), I is the

current utilized in pretreatment (A), t is the time elaPRSed for pretreatment process (s), μ is the viscosity of sludge (Pa·s), G is the velocity gradient (350 s^{-1}) and V_t is the utilized volume of the feed tank (m^3).

The output energy after anaerobic digestion of pretreated PRS was calculated from the highest methane (CH_4) yield obtained during the digestion process and calculated as shown in Eq. (3.7).

$$Q_{out} = \rho\, Y_m \S V \eta \qquad [3.7]$$

where, Q_{out} is the output energy from anaerobic digestion of PRS after pretreatment, ρ is density of pretreated PRS (kg/m^3), Y_m is the maximum methane yield produced during anaerobic digestion of pretreated and untreated PRS respectively (m^3 CH_4/kg VS), § is lower heating value of methane (35,800 kJ/m^3), V is working volume of reactor (m^3), η is energy conversion efficiency (assumed 90%).

Therefore, the energy balance for anaerobic digestion of EK pretreated PRS can be expressed as the difference between total output and total input energy as shown in Eq. (3.8).

$$\Delta Q = Q_{out} - Q_{in} \qquad [3.8]$$

3.4.3 Microbial Pretreatment

The microbial pretreatment was conducted utilizing two different bacterial strains: *Pseudomonas putida* 7525 (Strain I) and *Kosakonia oryziphila* IH3 (Strain II).

(A) Pretreatment with Strain I

3.4.3.1 Bacterial strain inoculation and pretreatment setup

Laccase (Lac) enzyme-producing bacterium *Pseudomonas putida* 7525 used in this study was procured from MTCC (Microbial Type Culture Collection), CSIR-IMTech, Chandigarh, India. The freeze-dried bacterial culture was inoculated in nutrient broth (pH=7.5) and incubated for 48 h under shaking conditions (LabTech Refrigerated shaking incubator, Daihan Labtechasia Pte Ltd, Korea) at 30 ± 0.5 °C and 120 rpm. The growth of the bacterium was in the log phase with 1×10^8 CFU/mL (Fig. 3.5a). Further, the growth of the bacterium was optimized at 1×10^7 and 1×10^9 CFU/mL to optimize the extent of solubilization of PRS. These three different optimized bacterial nutrient-broth cultures were used for PRS pretreatment studies (Kavitha et al., 2014) as shown in Fig. 3.5.

The PRS was inoculated in four conical flasks (500 mL) in duplicates with PRS (working volume = 350 mL) and 10 mL of overnight grown bacterial culture having 10^7, 10^8 and 10^9

CFU/mL and untreated PRS was kept as control (Fig. 3.5b). The *P. putida* strains enhance the sludge breakdown through Lac enzymes secreted by the bacterium. The optimum temperature, pH and shaking speed for the pretreatment of PRS were 35°C, 7.0 and 120 rpm respectively. Incubation of the inoculated and control flasks at 35 ± 0.5 °C and 120 rpm was carried out for 10 d as shown in Fig. 3.5 (c). The samples were centrifuged (5000×g for 25 min) to extract the biomass and suitable quantities of samples were taken each day to analyze sCOD and VFA to evaluate the optimum dosage and duration at which the solubilization would be maximum. The enhanced solubilization would lead to accelerated hydrolysis during the anaerobic digestion of pretreated PRS.

Fig. 3.5. (a) Bacterial inoculum, (b) samples inoculated with bacterial isolates at different dosages, and (c) incubation

3.4.3.2 Enzymatic activity

Upon obtaining the optimum operating conditions from Section 3.4.3.2 for maximum solubilization, the Lac enzymatic activity for the optimum dosage was evaluated using guaiacol oxidation assay for the entire pretreatment duration as explained by Kalra et al. (2013). To quantify the enzymatic activity, the reddish-brown color obtained due to oxidation of guaiacol by Lac was

measured at 450 nm. The reaction solution included guaiacol (2 mM), sodium acetate buffer (10 mM), and crude enzyme. The reaction solutions were incubated at 30°C for 15 min duration in triplicates, and the enzymatic activity was calculated against a blank reagent at 450 nm (ε = 0.6740 μM/cm) using a UV-Vis spectrophotometer. The activity of the enzyme was articulated as IU/mL, where 1 IU is the quantity of enzyme needed to oxidize 1 μmol guaiacol/min.

3.4.3.3 Anaerobic biodegradability test assay

Upon optimizing the bacterial pretreatment conditions, the biochemical methane potential (BMP) batch assay tests were conducted at the optimized pretreatment condition to prepare the feedstock with improved soluble organic matter content. The anaerobic biodegradability of the hydrolyzed PRS was assessed in 1L Erlenmeyer glass bottles utilized as anaerobic reactors with a working volume of 700 mL. The 1L BMP test was conducted for five different inoculum and pretreated substrate ratios (I/S) (0.3, 0.4, 0.6, 0.7, 1) at optimum pretreatment conditions (dosage and duration) along with a control of untreated sludge. The quantities fed for each mixing ratio and control are tabulated in Table 3.5, based on VS content. The anaerobic reactors were then setup and operated as per Section 3.3.1. The anaerobic digestion was conducted for 50 d. The 1L batch study was scaled up to 20L to test large-scale operational conditions for the optimum I/S ratio with a working volume of 14L to evaluate the compositional alterations throughout the digestion period.

Table 3.5. Substrate composition for 1L BMP test assay

I/S ratio	PRS (g)	DS (g)	De-ionized water (g)
0.3	209.93	100	390.07
0.4	174.20	100	422.89
0.5	139.36	100	560.72
0.7	104.52	100	495.52
1	69.68	100	530.32
Control	100	0	600.00

NB: Total weight for all the ratios is 700g

(B) Pretreatment with Strain II

3.4.3.4 Bacterial strain and pretreatment setup

A novel lignin peroxidase (LiP) enzyme-producing bacterial strain identified as *Kosakonia oryziphila* strain IH3 (Accession no. MZ605201) was earlier isolated in the laboratory of Indian Institute of Technology Guwahati, India and utilized for the pretreatment study. The culture's glycerol stock was streaked on nutrient agar plate containing (g/L); beef extract, 1.0; yeast extract, 2.0; peptone, 5.0; NaCl, 5.0; agar powder, 15; pH=7.5 and incubated for 2 d in an incubator at 30± 0.5 °C, and bacterial colonies were inoculated from the plate into 50 mL nutrient-broth and incubated for 1 d under shaking conditions (LabTech Refrigerated Incubator shaker, Daihan Labtechasia Pte Ltd, Korea) at 30± 0.5 °C and 120 rpm. The log phase bacterial growth with 1×10^8 CFU/mL was optimized at 1×10^7 and 1×10^9 CFU/mL to estimate PRS solubilization. This nutrient-broth-grown bacterial culture was utilized for the pretreatment study. PRS was incubated in conical flasks (duplicates) with 10 mL of overnight-grown-bacterial culture having 10^7, 10^8 and 10^9 CFU/mL and untreated PRS (control) for 6 d at 30°C and120 rpm. Samples were collected every day and centrifuged to analyze soluble chemical oxygen demand (sCOD) and volatile fatty acids (VFA) to estimate the optimum dosage and duration for maximum solubilization.

3.4.3.5 Enzymatic activity

In a UV-Vis spectrophotometer (Cary 60 UV-Vis Spectrophotometer, Agilent) at 310 nm wavelength, LiP enzymatic activity was evaluated (at optimum dosage condition) in centrifuged culture supernatants after H_2O_2-dependent oxidation of veratryl alcohol to veratraldehyde. The enzymatic activity was measured as IU/mL, and one-unit LiP activity equals the quantity of enzyme necessary to oxidize 1 mmol of veratryl alcohol converted to veratraldehyde per mL per minute. All tests were carried out in triplicate and data was reported as mean±SD.

3.4.3.6 Experimental design of anaerobic biodegradability assay using CCD-RSM

CCD-RSM was applied to design the optimization study of anaerobic biodegradability of bacterially pretreated PRS and statistically analyze the relationship between independent parameters affecting the output responses. In this study, CCD-RSM was applied to examine the combined effects of substrate/inoculum (S/I) ratios and pH on the biogas yield. A five level and three factorial CCD was formulated for optimization. Two independent variables selected for this study were S/I (X_1) and pH (X_2) coded at five different levels: −1 (low level), 0 (central), +1 (high level), and two outer points corresponding to 'η' where, $\alpha = 2^{k(1/4)}$ (k = 2, η = ±1.414) (Table 3.6). The developed regression model followed the equations corresponding to levels as: $x_1 = (X_1 - 2.5)$

and $x_2 = [(X_2-7)/0.5]$ (Yılmaz and Şahan, 2020). ±η corresponded to axial points and ±1 corresponded to factorial points. The output response targeted cumulative biogas yield (mL/gVS_{added}) till 50 d of digestion period. For optimization of output response parameter, thirteen experimental runs were expanded with four factorial points, four axial points and five centre points. The experimental array was constructed in Design-Expert® 11.1.2.0. The output response (biogas) was correlated by the independent variables (S/I and pH) using second-order polynomial equation as per Eq. (3.5). To evaluate the adequacy of generated model and decide the statistical significance of the regression coefficients, analysis of variance (ANOVA) was applied. The significance of all the variables was tested statistically at a level of p = 0.05. Student t-test was conducted to find an interrelation between the independent variables and output responses thereby accepting the null hypothesis since no significant deviation could be found in the p-value. The quality of fit of the polynomial model was expressed by the coefficient of regression (R^2) and adjusted regression (R^2_{adj}), and statistical significance was checked by the Fisher (F) -test in the program with selected p at 95% confidence level. The primary objective of the optimization process was to maximize the output response parameter with maximum desirability. The experimental matrix and the influence of the variables was depicted by two-dimensional (2D) contour plots and three-dimensional (3D) interface in Design Expert® 11.1.2.0.

Table 3.6. Levels of independent variables during optimization

Variable labels	Coded factors (X_i)	Coded levels				
		-1.414(-η)	**-1**	**0**	**+1**	**+1.414(+η)**
S/I	X_1	1.085	1.5	2.5	3.5	3.914
pH	X_2	6.292	6.5	7	7.5	7.707

3.4.3.7 Anaerobic biodegradability batch assay setup

The experimental matrix developed by CCD-RSM consisting of 13 experimental runs was placed in duplicates alongwith control sludge and inoculum to frame the 1L BMP batch assay. For every run order, 1L Erlenmeyer glass bottles were utilized as anaerobic reactors and fed with DS and bacterially pretreated PRS at optimum pretreatment conditions (Table 3.7). The pH of each reactor as per the design matrix was maintained by sodium bicarbonate and dilute sulfuric acid. Thereafter, sufficient amount of deionized water was added to the reactors to maintain the uniformity of the working volume (700 mL) in each reactor. The anaerobic reactors were then setup as per Section 3.4.1.4. The 1L batch study was scaled up to 20L (14L working volume) to conduct

the conformity test and also to evaluate the PRS compositional alterations throughout the digestion period at a larger scale.

Table 3.7. Experimental design matrix showing substrate composition for BMP assay

Run order	S/I ratio	pH	PRS* (g)	DS (g)	De-ionized water (g)
1	1.50	7.50	102.30	100	497.70
2	3.91	7.00	266.66	100	333.34
3	2.50	7.71	170.50	100	429.50
4	2.50	7.00	170.50	100	429.50
5	3.50	6.50	238.70	100	361.30
6	1.09	7.00	74.338	100	525.66
7	2.50	6.29	170.50	100	429.50
8	3.50	7.50	238.70	100	361.30
9	2.50	7.00	170.50	100	429.50
10	2.50	7.00	170.50	100	429.50
11	2.50	7.00	170.50	100	429.50
12	1.50	6.50	102.30	100	497.70
13	2.50	7.00	170.50	100	429.50
Experimental	Control	-	100.00	0	600.00

*Amounts calculated based on VS content

3.5 PHASE III- COMBINATION STUDY

The combination study was performed in two phases. In phase I, the nitrogen-rich PRS was co-digested with YW, a carbon-rich putrescible lignocellulosic organic waste of residential sources of petrochemical refineries to optimize the nutrient balance and moisture content for effective microbial proliferation and feedstock biodegradation. In phase II, the co-digestion process was further intensified ensuing different types of pretreatment to evaluate the extent of solubilization of the feedstock. Batch anaerobic biodegradability assays were thereby conducted at optimum pretreatment conditions to evaluate the biogas enhancement against untreated co-digestion.

3.5.1 Co-digestion study

3.5.1.1 Experimental design for optimization of co-digestion of PRS and YW

For optimization of the co-digestion study, central composite design response surface methodology (CCD-RSM) was applied to design the experimental matrix and statistically analyze

the relationship between process parameters affecting the output response. In this study, CCD-RSM evaluated the combined interactive effect of C/N ratio and pH on the biogas yield. For optimization of the independent parameters (C/N and pH), CCD with two factors at five levels was selected. Each independent parameter (X_1 = C/N ratio and X_2= pH) was coded at five levels : −1 (low level), 0 (central), +1 (high level), and two outer points corresponding to 'α' where, $\alpha = 2^{(p/4)}$ (p = 2, α = ±1.414) as shown in Table 3.8. Preliminary experimentations led to the determination of the ranges at -1 and +1 levels for each variable. ±1 and ± α corresponded to factorial and axial points respectively. 13 experimental runs with five replications at central design point alongwith four axial and four factorial points were augmented for the optimization of the output response targeting cumulative biogas yield (mL CH_4/gVS_{added}) till 50 d of digestion period. The design matrix was developed using Design-Expert® 11.1.2.0. (Table 3.7). The relationship between independent response variables (X) and dependent output response (Z) was expressed by the second-order polynomial equation [Eq. (3.5)]. The variability of the regression model was checked using analysis of variance (ANOVA) and the statistical significance was checked using Fisher-test (F-test) with 95% confidence (p-value). For optimization, the prime objective was to maximize biogas yield with utmost desirability within the selected range of independent variables. The regression model and the influence of independent variables were illustrated by a two-dimensional (2D) contour plot and three-dimensional (3D) interface.

Table 3.8. Levels of independent variables used for optimization of biogas production

Variable labels	Coded factors (X_i)	Coded levels				
		-1.414(-α)	**-1**	**0**	**+1**	**+1.414(+α)**
C/N	X_1	21.89	25	32.5	40	43.11
pH	X_2	5.86	6.2	7	7.8	8.13

3.5.1.2 Anaerobic biodegradability assay formulated using CCD-RSM

The design matrix generated using CCD-RSM consisting of thirteen experimental runs was evaluated for biogas production using 1L BMP assay. For every run order conducted in duplicate, suitable amount of feedstock mixture consisting of substrate (PRS) and co-substrate (YW) was fed into 1L Erlenmeyer glass reagent bottles acting as anaerobic reactors. The design mix to be fed into each reactor for every experimental run order was calculated using the Eq. (3.9) (Ghaleb et al. 2021).

$$C/N\,(mix) = \frac{\sum_{i=1}^{n}\,[x_i\,\{C_i\,(100 - m_i)\}]}{\sum_{i=1}^{n}\,[x_i\,\{N_i\,(100 - m_i)\}]} \qquad [3.9]$$

where, $^{C}/_{N}\,(mix)$ is the C/N ratio of the feedstock mixture; x_i = the wet weight of materials (substrate and co-substrate (s) in g or kg); C_i is the carbon content of materials (%); N_i is the nitrogen content of materials (%); m_i is the moisture content of materials (%). Since in this study, single co-substrate (YW) was utilized, the amount of substrate (PRS) was kept constant (50g) and accordingly the required amount of co-substrate (YW) was calculated using Eq. (3.9) for every run order (Table 3.9). The working volume was 700 mL in each reactor. pH inside the reactors was maintained using either dil. sulphuric acid (H_2SO_4) or sodium bicarbonate (Na_2CO_3). Anaerobic condition was created through N_2 gas purging. Thereafter, the reagent bottles were affixed with 1L aspirator bottles consisting of 1.5N NaOH and thymol blue as an alkali indicator using transparent silicon gas collection pipes. The setup was maintained at mesophilic temperature conditions. Biogas was collected each day and the accumulated biogas was then evaluated for every run order by the end of 50 d of digestion period. Upon obtaining the optimum conditions, the 1L batch study was scaled up to 20L (14L working volume) capacity to conduct the conformity test and evaluate the utilization of organic fraction due to the co-digestion of PRS with YW.

Table 3.9. Experimental design matrix showing compositions of PRS and YW in BMP assay

Run order	C/N	pH	PRS (g)	YW (g)	DS (g)	De-ionized water (g)
1	25.00	6.20	50	4.06	100	545.94
2	32.50	8.13	50	14.25	100	535.75
3	32.50	7.00	50	14.25	100	535.75
4	32.50	7.00	50	14.25	100	535.75
5	21.89	7.00	50	1.63	100	548.37
6	32.50	7.00	50	14.25	100	535.75
7	40.00	6.20	50	46.75	100	503.25
8	32.50	7.00	50	14.25	100	535.75
9	32.50	7.00	50	14.25	100	535.75
10	32.50	5.86	50	14.25	100	535.75
11	25.00	7.80	50	4.06	100	545.94
12	43.11	7.00	50	98.50	100	451.50
13	40.00	7.80	50	46.75	100	503.25
Experimental	C*	-	50	0	100	550.00

*Control (monodigestion)

3.5.2 Electrokinetically enhanced co-digestion study

3.5.2.1 Optimization of electrokinetic pretreatment using CCD-RSM

For optimization of electrokinetic (EK) pretreatment on the solubilization of PRS mixed with YW at optimum co-digestion condition, CCD-RSM was selected as described by Design-Expert® 13.0 to model the interactive effects of independent parameters: applied voltage (X_1) and exposure period (X_2) on the response of output parameters: sCOD (soluble chemical oxygen demand) (Y_1) and VFA (volatile fatty acids) (Y_2). CCD was coded with two factors at five levels: -1 (low), 0 (medium), +1 (high), and two boundary levels corresponding to 'k' where, $k = 2^{(p/4)}$ ($p = 2$, $k = \pm 1.414$) as shown in Table 3.10. Preliminary investigations and literature review led to variation of applied voltage and exposure period over the ranges (30-70) V and (10-90) min respectively with corresponding central values of 50V and 50 min. The design matrix generated thirteen experimental runs. An empirical model was generated using each output response correlating the experimental data sets using a second-order polynomial equation (Eq. 3.5) In order to define an interaction between the process parameters and the output responses, ANOVA (Analysis of variance) was applied. The probability value (p-value) at 95% confidence interval evaluated the significance of model terms. Design Expert® 13.0 visually depicted the impact of independent variables through the utilization of two-dimensional (2D) contour plots and three-dimensional (3D) interface plots.

Table 3.10. Coded levels of independent variables used for the optimization of pretreatment

Variable labels	Coded factors (X_i)	Coded levels				
		-1.414(-k)	-1	0	+1	+1.414(+k)
Voltage (V)	X_1	21.7157	30	50	70	78.2843
Exposure time (min)	X_2	-6.56	10	50	90	106.56

3.5.2.2 Electrokinetic pretreatment framework

The EK pretreatment framework consisted of a cylindrical plastic feed tank (diameter = 10 cm, height = 25 cm), a DC power source, a tachometer to gauge the RPM, two graphite electrodes acting as a cathode and an anode, a flash mixer, an ammeter for regulating the current, and a multimeter for regulating the voltage in the circuit (Fig. 3.4). The feedstock container was partially filled with PRS and YW (as explained in Section 2.3.1), and the electrodes were used to complete the circuit by passing DC through the sample. The experimental design matrix, generated through CCD-RSM, facilitated the systematic examination of output responses, namely sCOD and VFA

(measured in mg/L). These investigations were carried out by subjecting the design matrix to varying applied voltages and exposure durations. For each experimental run, about two-thirds of the graphite electrodes (cathode and anode) were immersed in the feedstock container without nudging the bottom of the container. To ensure the maintenance of a homogeneous suspension throughout the pretreatment process, the insulated flash mixer was operated consistently at 120 rpm.

3.5.2.3 Anaerobic digestibility assay

In order to ascertain the biomethane potential generated due to EK pretreatment on co-digestion of PRS and YW at optimum conditions, 1L BMP batch assays were conducted at different inoculum (DS) and EK pretreated feedstock ratios (I/F) (0.3, 0.4, 0.5, 0.7) and control (untreated feedstock) for 50 d. The feedstock (PSYW) is PRS mixed with YW at C/N =32.5 and pH=7.0 and the digestion process for all mixing ratios was conducted as mentioned in Section 3.3.1. The quantities of pretreated feedstock and DS fed into the reactors at different mixing ratios based on VS content is shown in Table 3.11. Upon obtaining the most appropriate mixing ratio providing maximum biogas, the batch study was scaled upto 20L capacity (14L working volume) in order to ascertain the pollutant degradation. The reactors were setup for three conditions in two replicates: (a) pretreated co-digestion, (b) untreated co-digestion and (c) untreated mono-digestion and were run for 60 d at mesophilic temperature conditions. The energy assessment was conducted as per section 3.4.2.4.

Table 3.11. Pretreated feedstock (PSYW) and inoculum (DS) compositions

I/F ratio	PSYW (g)	DS (g)	De-ionized water (g)
0.3	68.5	100.0	531.5
0.4	57.1	100.0	542.9
0.5	45.7	100.0	554.3
0.7	34.3	100.0	565.7
Control*	50.0	100.0	550.0

NB: Total weight for all the ratios is 700g; *Untreated PSYW

3.5.3 Microbially enhanced co-digestion study

3.5.3.1 Bacterial strains and pretreatment setup

Lignin peroxidase (LiP) enzyme-producing bacterial strain identified as *Bacillus subtilis* IH-1 (Accession no. MZ618640), and laccase (Lac) enzyme-producing bacterium identified as *Bacillus*

velezensis IH-2 (Accession no. MZ605121) were earlier isolated from the PRS in the laboratory of IIT Guwahati, India and utilized for the pretreatment study.

For *Bacillus subtilis* IH-1 strain, the glycerol stock of the bacterial culture was streaked onto a nutrient agar plate maintaining a pH of 7.5, (consisting of beef extract = 1.0 g/L, yeast extract = 2.0 g/L, peptone = 5.0 g/L, NaCl = 5.0 g/L, and agar powder =15 g/L) and incubated at 30±0.5 °C at 120 rpm for 2 d. 50 mL of nutrient-broth utilized for the inoculation of the bacterial colonies were also incubated at 30±0.5°C and 120 rpm for 1 d. The log phase bacterial growth was observed to be 1×10^8 CFU/mL which was further optimized at 1×10^7 and 1×10^9 CFU/mL to evaluate the extent of solubilization of feedstock (PRS mixed with YW at optimum co-digestion conditions). For the pretreatment study, 10 mL of overnight-grown bacterial culture admixed with the feedstock for each dosage was incubated for 10 d at 30°C and 120 rpm as shown in Fig. 1. Samplings were done every day to evaluate the most appropriate bacterial dose and pretreatment duration for maximal solubilization in terms of volatile fatty acids and soluble chemical oxygen demand.

For *Bacillus velezensis* IH-2 strain, the bacterial culture was inoculated in conical flasks containing MSM by inoculating one loop of glycerol stored culture (Haq et al., 2022). The MSM broth was utilized to inoculate the overnight-grown bacterial culture having an optical density (OD-600nm) of 1.0, and incubated for a day under shaking conditions (LabTech Refrigerated Incubator shaker, Daihan Labtech asia Pte Ltd, Korea) at 120 rpm and 35±0.5°C. The growth of the bacterium was in the log phase with 1×10^9 CFU/mL. Further, the growth of the bacterium was optimized at 1×10^8 and 1×10^7 CFU/mL to optimize the extent of solubilization of PRS.

The nutrient-broth-grown bacterial cultures were utilized for the pretreatment study. PRS mixed with YW at optimum conditions from Section 3.5.1 was incubated in conical flasks (duplicates) with 10 mL of overnight-grown-bacterial culture having 10^7, 10^8 and 10^9 CFU/mL and untreated PRS (control) for 10 d at 30°C and 120 rpm. Samples were collected every day and centrifuged to analyze soluble chemical oxygen demand (sCOD) and volatile fatty acids (VFA) to estimate the optimum dosage and duration providing maximum solubilization. The strain providing maximum solubilization (sCOD and VFA) was further utilized for anaerobic biodegradability batch assay at optimum pretreatment conditions pertaining to that particular strain.

3.5.3.2 Enzymatic activities

- **Lignin peroxidase (LiP)**

The lignin peroxidase (LiP) was evaluated by the oxidation of veratryl alcohol (VA) to veratraldehyde and the enzymatic characteristics were assessed using VA and H_2O_2 as substrates.

For all the bacterial dosages, the LiP activities in centrifuged culture supernatants were determined using a UV-Vis spectrophotometer (Cary 60 UV-Vis Spectrophotometer, Agilent) at a wavelength of 310 nm after H_2O_2-dependent oxidation of VA to veratraldehyde. The activity of LiP was quantified in International Units per mL (IU/mL), with one unit defined as the amount of enzyme necessary to oxidize 1 mmol of VA to veratraldehyde per mL of solution per minute under standard assay conditions. Each enzymatic activity was assessed in triplicate and presented as mean±SD.

- **Laccase (Lac)**

The Laccase (Lac) enzymatic activity was measured using the guaiacol oxidation assay for all the dosages for the whole 10 d of pretreatment. Crude laccase, 2 mM guaiacol and 0.1 M sodium acetate buffer at pH 5.0, consisted of the reaction mixture which was incubated at 30°C for 15 min in triplicates. 1 mL of distilled water was utilized as blank. The reddish-brown colour produced by Lac due to guaiacol oxidation was observed using a UV-Vis spectrophotometer in comparison to a blank reagent at the wavelength of 450 nm to determine the enzyme activity (ε =0.674 μM/cm) (Kuppusamy et al., 2017). The Lac activity was expressed as International Units (IU) per mL, where 1 IU represents the amount of enzyme necessary to oxidize 1 μmol guaiacol per min.

3.5.3.3 Anaerobic biodegradability batch assay setup

Upon optimizing the pretreatment conditions based on maximum solubilization, the sludge or feedstock was assessed for 1L BMP batch assay at optimum pretreatment conditions and was conducted as Section. 3.4.2.3 at five different inoculum and pretreated feedstock (I/F) ratios (0.3, 0.4, 0.5, 0.7 and 1.0) alongwith one control (untreated) in duplicate. The quantities of pretreated feedstock and DS (inoculum) to be fed into each reactor was evaluated based on VS content and presented in Table 3.12. The reactors were run for 50 d in mesophilic temperature conditions. Upon optimizing the I/F ratio giving maximum accumulated biogas by the end of the digestion period, the 1L batch assay was scaled upto 20L capacity to ascertain the changes in toxic pollutant compositions throughout the digestion period in a larger scale.

Table 3.12. Pretreated feedstock (PSYW) and inoculum (DS) compositions for BMP test

I/F ratio	PSYW (g)	DS (g)	De-ionized water (g)
0.3	35.52	100	564.48
0.4	29.60	100	570.40
0.5	23.68	100	576.32
0.7	17.76	100	582.24
1.0	11.84	100	588.16

3.6 PHASE IV- OPERATION OF LAB-SCALE ANAEROBIC BIPHASED BAFFLED REACTOR (ABBR)

3.6.1 Drafting and fabrication of ABBR

A 20 L ABBR with 14 L working volume was constructed with stainless steel anaerobic for biodegradation of PRS as shown in Fig. 3.6(c). The design of ABBR was based on a two-phased floating drum type technology consisting of horizontal baffles. The ABBR is divided into two phases: phase 1, responsible for fermentation by the action of acidogenic bacteria and acetogenic bacteria, and phase 2, responsible for methanogenesis by the action of methanogenic bacteria. The horizontal baffle configuration in phase 1 leads to improved retention times, facilitating hydrolysis, acidogenesis, and acetogenesis (Fig. 3.6a). Acetogenesis and methanogenesis take place in phase 2. This arrangement ensures better microbial proliferation for optimal biogas generation. During the digestion process, the intermediate products generated in phase 1 are directed to the bottom of phase 2 through a separator. Phase 2 contains a sludge bed consisting of a higher microbial consortium, while the headspace is utilized to store the produced biogas. Previous literature highlighted issues with acidification and limited methane production in single-stage reactors (Demirel and Yenigün, 2002). In the two-stage reactor, the separation of hydrolysis and acidogenesis from acetogenesis and methanogenesis restricts the synergistic work of microbial consortia (Wang et al., 2016). The proposed design in this study not only attempted to address the problems of excess acidification and methane inhibition in single-stage reactors, but also the restriction of microbial synergism in dual-stage reactors (Costello et al., 1991; Lafitte-Trouqué and Forster, 2000; Schievano et al., 2012; Wang et al., 2016; Baldi et al., 2019). This innovative design resolves both problems, making it an economically viable solution for organic solid waste treatment and energy recovery. The utilization of a two-phase reactor with baffle walls provides agitation, sufficient contact time, harnessing the synergistic potential of different microbial groups, contributing to an efficient treatment of organic wastes.

The 20 L ABBR consisted of one inlet, one outlet, gas outlet and two sample collection ports (Fig. 3.6c). It was fabricated at the Mechanical Engineering Workshop, IIT Guwahati, Assam, India, as per the draft shown in Fig. 3.6 (a) and (b). Solid works was used for preparing the sketches, and 1.5 mm thick stainless steel sheets were used for fabrication, 2 inch brass ball valves were used at outlet and 2 inch stainless steel ball valve was used for gas collection pipe. Spot welding was done at the edges of phase separation wall at the centre of the reactor. The gas outlet was affixed with 5 L borosilicate glass aspirator bottle containing 1.5 N NaOH with thymol blue as an indicator to engross carbon dioxide and trace gases of ammonia and hydrogen sulphide. Methane-enriched

biogas was measured each day using the principle of liquid displacement method. The amount of NaOH displaced each day determines the amount of biogas produced, which was quantified using a graduated measuring cylinder.

3.6.2 Operation of ABBR

The ABBR was firstly acclimatized with 5 kg of DS as inoculum and kept as it is for 20 d. Thereafter the ABBR was operated on a fill and draw mode with daily feeding, continuously for 200 d in two stages. In stage I, the ABBR was operated with untreated PRS for 100 d. In stage II, ABBR was fed with electrokinetically pretreated PRS at 60V, 83.5 min and electrode spacing of 11.6 cm (obtained from Section 3.4.2) for next 100 d.

During stage I, following 30 d of acclimatization, the ABBR was initially fed with untreated PRS at an OLR of 0.85 kg COD m^{-3} d^{-1} for 40 d, which was further increased stepwise (1.15 and 1.63 kg COD m^{-3} d^{-1}) and maintained for 30 d for each OLR. The HRT was estimated to vary from 23-12 d during operation of ABBR at different OLRs with untreated PRS. During stage II, the ABBR was initially fed with EK pretreated PRS at an OLR of 0.8 kg COD m^{-3} d^{-1} for 30 d, which was increased step-wise (1.2, 1.5 and 1.9 kg COD m^{-3} d^{-1}) till the end of 100 d. The HRT was estimated to vary from 17-7 d during operation of the reactor at different OLRs with pretreated PRS. Throughout both stages, samples were collected every five days for physico-chemical analysis to assess variations in pollutants and characterize the biogas composition. The daily biogas production was recorded, and the biogas composition was analyzed using Gas Chromatography (GC, Dhruva, Chromatograph and Instruments Company, India) at five-day intervals until the end of the digestion period.

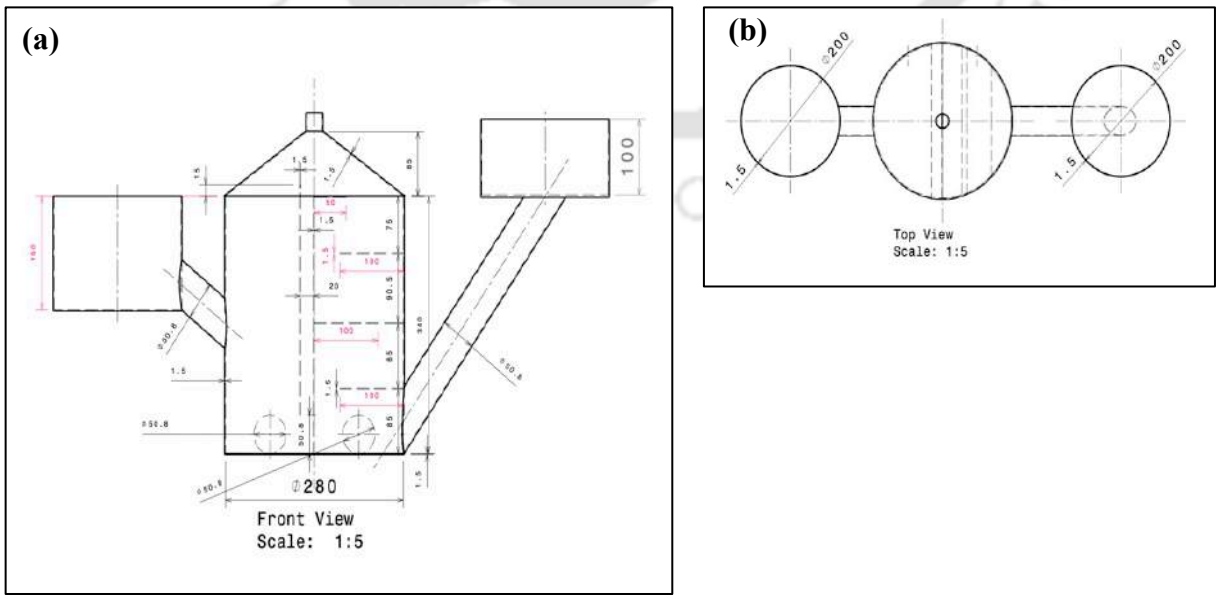

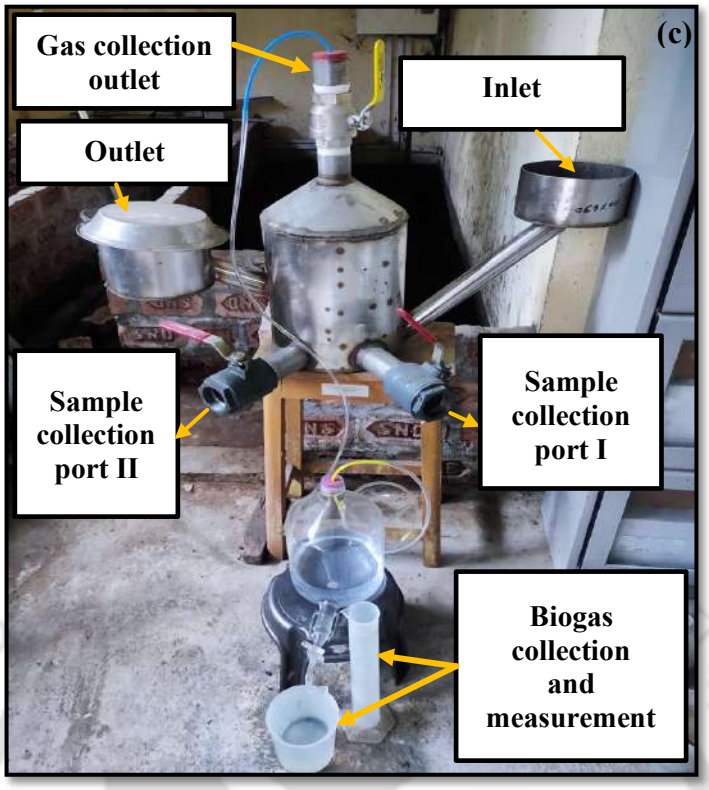

Fig. 3.6. Drafting of (a) side view, (b) top view, and (c) pictorial representation of ABBR

3.7 ANALYTICAL METHODS

Process parameters that signify performance, buffering capacity and degradability of the substrate within the reactor were analyzed. They included, total solids (TS), moisture content (MC) and volatile solids (VS) (APHA. 2012). pH value of the sample was measured by mixing substrate with deionized water in the ratio 1:10 (w/v) and shaking for 2 h at 100 rpm in horizontal shaker. Portable pH meter was used for determining the pH of the sample. The sample to be analysed for sCOD was centrifuged and filtered with ordinary filter paper to remove suspensions. The filtrate was further filtered via 0.45-µm membrane filter and the supernatant was used to prepare suitable dilutions. Closed reflux titrimetric method was then used for determining the sCOD of the samples (Standard Methods 5220 C) (APHA, 2012). The VFA was analyzed by pH filtration and short distillation method by DiLallo and Albertson (1961). Soxhlet extraction method was employed using n-hexane as extractant to quantify oil and grease (Standard Methods 5520 E) (APHA, 2012). For estimation of total petroleum hydrocarbon (TPH), 10g of sample was mixed with 100 mL of dichloromethane (DCM) and extracted for at least 30 min using a separatory funnel until a clear extract could be achieved. To the recovered portion, 3.0 g of silica gel was added for removal of polar materials and then dried over a Na_2SO_4 column (Adeniji et al., 2017). The petroleum hydrocarbons were then recovered and estimated after evaporation of organics-solvent mixture

using a rotary evaporator at 45 °C under 20 mm Hg partial vacuum for 2 h. The weight after evaporation was taken, and this residual weight was reported as total petroleum hydrocarbons (TPH) in g/kg. Total phenol was estimated using direct photometric method using 4-amino antipyrine in presence of potassium ferricyanide solution at a pH of 7.9 ± 0.1 to form a colored antipyrine dye whose absorbance was measured at 500 nm in a spectrophotometer (APHA, 2012). The lignin content (acid soluble and insoluble lignin) was determined by the National Renewable Energy Laboratory (NREL) protocol (Kontogianni et al., 2019). Acid insoluble lignin content was determined by gravimetric technique. Acid soluble lignin was determined by UV spectrophotometer through colorimetric technique at 205 nm with the hydrolysate obtained after filtration of cooled insoluble lignin and 4% H_2SO_4 solution was set as a reference blank. For cellulose analysis, 3 mL of acetic/nitric reagent was added to 0.5 g of PRS sample and hydrated in water bath and was centrifuged. After cooling, supernatant was discarded and residue was infused with 67% H_2SO_4. Further, anthrone reagent was added to diluted sample and boiled for 10 min. Finally, cellulose content was measured through colorimetric technique at 603 nm by using spectrophotometer and anthrone reagent was set as reference blank (Updegraff, 1969). Hemicellulose content was evaluated by subtracting the acid detergent fibre (ADF) from the neutral detergent fibre (NDF) as mentioned by Goering and Van (1975).

3.8 INSTRUMENTAL CHARACTERIZATION

Field Emission Scanning Electron Microscopy (FESEM) micrographs were used to discern the change in the physical structure of the substrate before and after pretreatment. The variation in surface elemental composition of feedstocks was determined using FESEM conjunct with Energy Dispersive X-ray spectroscopy (EDX) (Sigma, Zeiss) after double-coating with gold. Double gold plating (Au) was applied in conductive sludge samples to build up a charge and avert further degradation during the FESEM examination. Electron High Tension (EHT) of 3.00 kV and different magnifications were used for standard comparison of sludge morphology before and after pretreatment. The presence of organic functional groups was analyzed and compared using Fourier transform infrared spectroscopy (FTIR) before and after pretreatment. 1 mg of dried sample was blended with 200 mg of potassium bromide (KBr) in a mortar and compressed into transparent discs for 3 min at 10 MPa. The FTIR spectra of 16 scans were then recorded from 4000 to 400 cm^{-1} at a resolution of 4 cm^{-1} to obtain a single infrared spectrum. The elemental composition of a sample was evaluated using a CHNS analyser (Euro EA 3000, Euro Vector, Italy). For evaluation of total organic carbon (TOC), the sample was centrifuged and filtered using a Whatman Filter paper. 15-20 ml of the filtrate was then analysed for TOC in presence of zero air gas and under

subjection to a high furnace temperature (600°-750°C). The analysis was done via Shimadzu TOC Analyser. The results were recorded as triplicates and every injection utilized 5 ml of the sample.

The organic pollutant conversion was analyzed using GC-MS (Gas Chromatography coupled to Mass Spectrometry). The metabolites of samples were extracted using dichloromethane (DCM). For each extraction, the separated organic layer was collected, filtered (Whatman filter no. 54) over anhydrous Na_2SO_4, and vacuum evaporated. The residues of the samples were then dissolved in acetonitrile (ACN) and expunged with N_2 gas. The major organic compounds contained in the samples thereafter were analyzed by direct aqueous-injection gas-chromatography coupled to spectrometric mass selective detector (PE Autosystem XL gas chromatograph interfaced with a Turbomass mass) using a capillary column PE-5MS (20 m × 0.18 mm internal diameter, 0.18 µm film thickness) in which 1 µL of the silylated aliquot of each sample was injected in the injector port of the GC–MS (GC/MSTQ8040, Shimadzu, Japan). The specific column was initially maintained at 50°C for 5 min, then heated to 300°C at 10°C/min, and finally maintained for 5 min as holding time. The flow rate of He (Helium) used as the carrier gas was 1mL/min. In full-scan mode, electron ionization (EI) mass spectra were estimated for a range of m/z values (30–550) at 70 eV. The metabolites were identified by comparing the spectra of the analyzed samples with library search (NIST).

3.9 PHYTOTOXICITY ASSESSMENT

The phytotoxicity was evaluated in the seeds of *V. radiata* L. germinated on the digestate of samples after AD process and compared with that of the untreated PRS sample using the modified test procedure by Matthews and Hastings (1987). The test seeds of *V. radiata* L. were prepared by completely submerging in 0.1% w/v of $HgCl_2$ {mercury (II) chloride} solution for 10 min for surface sterilization and washed with deionized water after 10 min to remove the traces of $HgCl_2$. Healthy seeds were identified and transferred to petridishes for seed germination evaluation. For the phytotoxicity study of untreated sludge, 100g of PRS was mixed with 200 mL of deionized water and agitated for 20 h to homogenize the PRS sample. After AD, 100g of digestate of pretreated PRS was directly mechanically agitated for 20 h. After agitation, the samples were filtered using 0.45µm pore-sized membrane, thereby using the filtrate for the toxicity tests. Different v/v dilutions of 50%, 75% and 100% samples (digestate and untreated) were used to prepare the test solutions using deionized water. Petridishes were moistened with respective solutions and tap water (used as control). The petridishes were placed in a growth chamber at 28°C in the dark for 48 h and the number of seeds germinated after 48 h were noted. Germination index

(GI) (%) was used as an indicator of phytotoxicity assessment test in the study and evaluated as shown in Eq. (3.10) (Priac et al., 2017; Siles-Castellano et al., 2020).

$$GI(\%) = \frac{(L_d * G_d)}{(L_c * G_c)} * 100 \quad [3.15]$$

where, L_d and L_c are the root lengths of germinated seeds in digestate and control; G_d and G_s are the germination rates in digestate and control. Germination rate (G) is the ratio of number of germinated seeds in sample by the number of total seeds expressed as percentage. The biomass and seedling growth were analyzed after 3-5 d of incubation with the light facility of 16 h dark period and 8 h light period.

3.10 INSTRUMENTS USED

Different instruments used for the analysis of the samples are shown in Table 3.13.

Table 3.13. Various instruments and their brand names that were utilized during study

Parameter tested	Instrument	Model/Manufacturer
pH	μ pH system 361	132, Systronics. India
COD	COD Digester	Wealtec Corp., Model No. HB-1
Weight	Weighing Balance	RADWAG Wagi Elektroniczne
VS	Muffle Furnace	DASS & CO.
Drying	Hot Air Oven	Testing Instrument Mfg. Pvt. Co. Ltd.
Sample preservation	Refrigerator	TEKSOL Corporation
Mixer and Grinder	Philips	HL7756/00
Oil and grease	Soxhlet apparatus	Borosil
TPH	Soxhlet apparatus	Borosil

Chapter 4

INOCULUM STUDY

This chapter deals with the viability of anaerobic digestion of petroleum refinery sludge with two different inoculations of an animal manure source (undigested residue and anaerobically well-acclimated digested sludge) at different mixing ratios. The prima facie intention was to evaluate the suitable mode of inoculation for anaerobic digestion with petroleum refinery sludge.

4.1 INITIAL CHARACTERIZATION OF SUBSTRATE AND INOCULUMS

To investigate the feasibility of any substrate for the AD process, a comprehensive physical and chemical characterization of the substrate as well as the inoculum is obligatory since their unique features determine the providence of the AD process. Table 4.1 summarizes the initial characterization of PRS and inoculums (UR and DS). Initial moisture content (MC) of PRS was 87.5% with 75% of VS illustrating high organic matter content. The substrate and inoculums in this study had a wide range of VS/TS content along with sCOD and VFA suggesting its suitability for AD. The initial nearly neutral pH of PRS and the inoculums also support AD process. The initial characterization values of PRS were in accordance with the studies conducted various researcher (Kriipsalu et al., 2008; Liang et al., 2019).

Table 4.1. Initial characterization of petroleum refinery sludge and inocula

Parameters	**Units**	**PRS[a]**	**UR[a]**	**DS[a]**
pH	-	7.03 ± 0.3	7.03 ± 0.62	7.8 ±0.46
Moisture content (MC)	%	87.55 ± 2.32	82.35 ± 1.4	86.43 ± 1.87
Total solids (TS)	%	12.45 ± 2.32	17.65 ± 1.8	13.57 ± 1.87
Volatile solids (VS)	% TS	75.02 ± 5.73	82.04 ± 0.5	44.949 ± 1.06
sCOD	mg/L	1024 ± 144.5	2200 ± 173.5	1600 ±160.42
VFA	mg/L	350 ± 5.41	400 ± 5.5	380 ± 7.45
O&G	% dry solids	25.29 ± 5.3	BDL[c]	BDL[c]
TPH	g/kg	162.5 ± 90.59	BDL[c]	BDL[c]

All values are mean ± standard deviation from triplicates,[b]Not Reported, [c]Below Detectable Limit

4.2 ANAEROBIC BIODEGRADABILITY ASSAY

AD of PRS is challenging since it depends on the concentration of toxicants which become inhibitory for the methane-producing bacteria, and the presence of recalcitrant compounds (Kriipsalu et al., 2008). The recalcitrant nature of hydrocarbons is attributed to unfavourable environmental conditions and lesser application of microbes utilizing hydrocarbons under anaerobic conditions. Therefore, providing a favourable microbial inoculation for AD of PRS is necessary since it will not only increase microbial diversity but also improve the biodegradation efficiency with improved solubilization (Wang et al., 2016). Inoculums are desired to be homogenous, sieved and preincubated, having a wide microbial variety ensuring an adequate level of hydrolytic and methanogenic activity. Anaerobic biodegradation of a substrate can be directly proportioned with the rate of methane production from the substrate in the presence of the seed environment. Therefore, to determine the methane potential of PRS, BMP test assays were carried out with both types of inocula (UR and DS) at five different mixing ratios of inoculum and sludge (UR/PRS or DS/PRS) of 0.3, 0.4, 0.5, 0.7 and 1 for 70 d. Based on the extent of biogas production, solubilization and organic matter degradation, the most efficient inoculum was eventually evaluated to be suitable for biodegradation of PRS.

4.3 COMPARATIVE STUDY ON ANAEROBIC BIODEGRADATION OF PRS

4.3.1 Biogas production

Anaerobic biodegradation of a substrate can be directly proportioned with the rate of biogas production from the substrate in the presence of the seed environment. When PRS was anaerobically digested with UR as inoculum, the maximum biogas production was observed on 40^{th} d for mixing ratio, UR:PRS = 0.4 (Fig. 4.1a). The cumulative biogas production was also highest for mixing ratio UR:PRS = 0.4 followed by 0.5, 0.7, 0.3 and 1 respectively as shown in Fig. 4.2(a). While PRS was digested with DS as inoculum source, the highest biogas yield was observed on 36^{th} d for DS:PRS = 0.5 (Fig. 4.1b). Also, the cumulative biogas production order for all the mixing ratios of DS and PRS was observed to be 0.5> 0.3> 0.4> 0.7> 1 as shown in Fig. 4.2(b). Interestingly, the cumulative biogas production from control UR was 2.7-fold higher than that produced by control DS. This might be reasoned as UR when used as an inoculum source had substantial organic matter content to be solubilized (as seen in Table 4.1), which itself went through the anaerobic digestion process along with the substrate despite providing a microbial/seed environment. The behavior of UR was majorly observed as an unfavourable inoculum source for PRS because the net biogas yields obtained from the digestion of PRS and UR were much lower

than that obtained from the digestion of PRS and DS (the net maximum cumulative biogas production of UR:PRS = 0.4 was 1344 mL whereas the same for DS:PRS =0.5 was 4134 mL by the end of the 70 d of digestion). The cumulative biogas production curve for all the ratios of PRS and UR showed prolonged lag phases which could be attributed to the fact that the microbial environment created by UR for digestion with PRS might be responsible for producing inhibitory substances which prevented the biogas production from PRS compared to PRS digestion with DS as inoculum source (De Vrieze et al., 2015; Wojcieszak et al., 2017). Instead, Haak et al. (2016) explained that the microbes enduring on petrochemical refinery waste show Monod kinetic growth with long lag phases which prevent the attainment of optimum methane production from such waste. Based on daily and cumulative biogas production, the DS from an operational anaerobic digester was observed to be a better inoculum source.

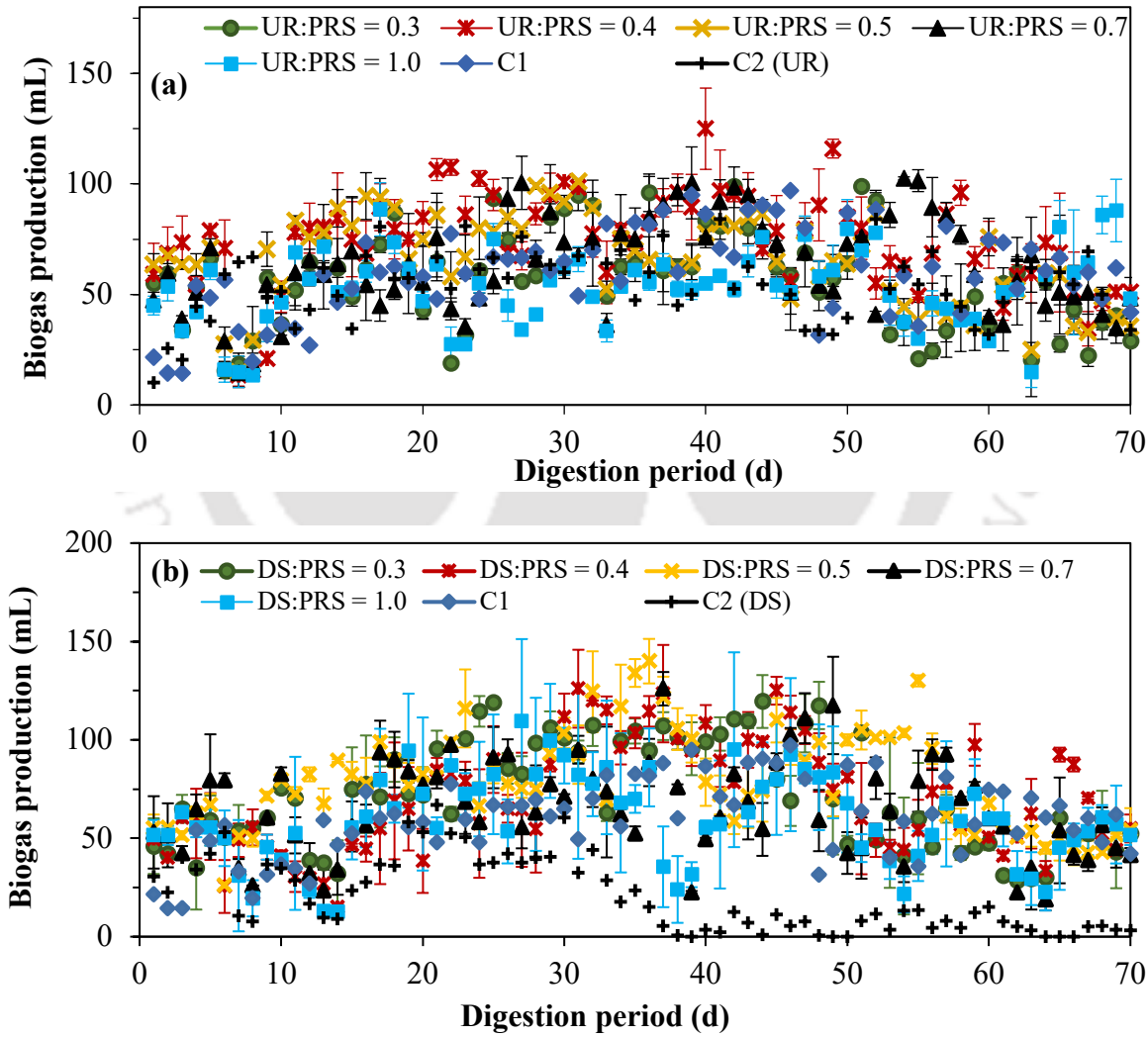

Fig. 4.1. Daily biogas production when PRS is anaerobically digested with (a) UR (b) DS

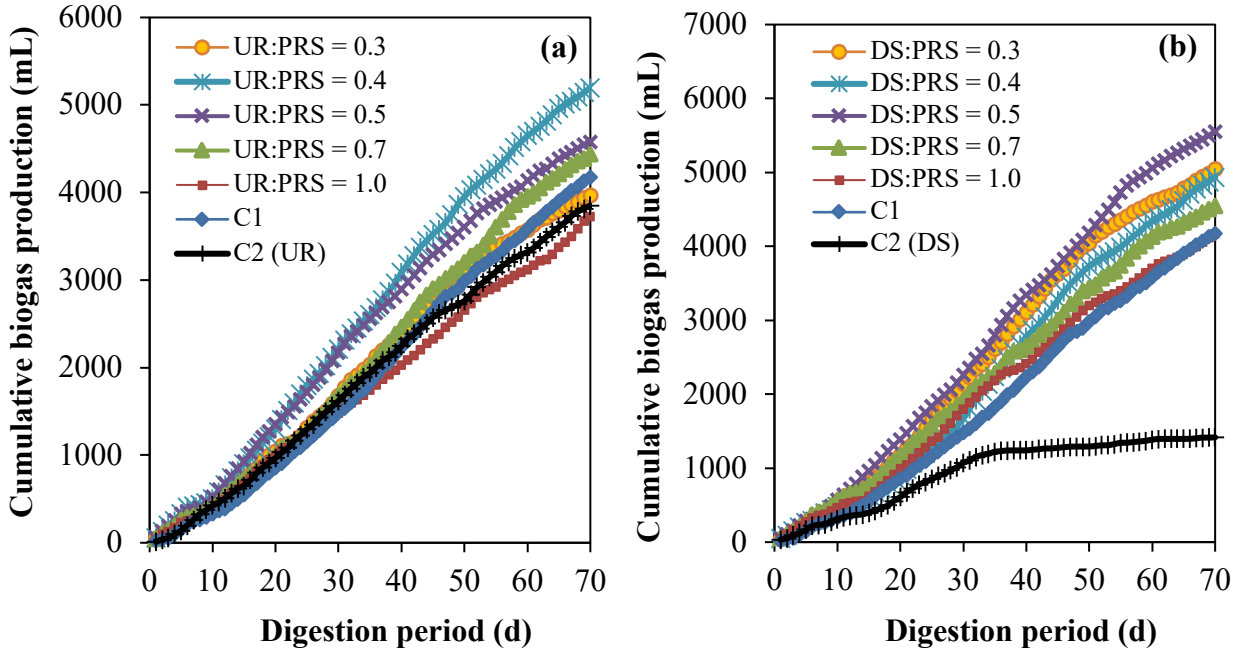

Fig. 4.2. Cumulative biogas production when PRS is anaerobically digested with (a) UR (b) DS

4.3.2 Effect of inocula on the solubilization of PRS

The efficacy of solubilization and the extent of hydrolysis of any sludge can be gauged by the measurement of sCOD. This parameter indicates the extent of biogas production since the amount of readily available biodegradable organic content increases with the increase in sCOD concentration, thereby increasing the biogas production from any substrate (Hallaji et al., 2019; Wang et al., 2016). Upon digestion of PRS with UR, the highest solubilization was attained at 30 d for UR:PRS=0.4 and observed to be 2540 mg/L but the actual solubilization {after deduction of sCOD produced by control inoculum, C2(UR)} was evaluated to be 650 mg/L as shown in Fig. 4.3(a). When PRS was digested with DS, the actual maximum sCOD was evaluated to be 950 mg/L at 30 d for DS:PRS = 0.4 as shown in Fig. 4.3(b) which was about 46% higher than that of UR:PRS=0.4. The biogas production also elevated after the attainment of maximum solubilization i.e., after 30 d for both the inocula since the production of biogas is directly related to the improvement in sCOD (Marsolek et al., 2013). In Fig. 4.3(b) at 50 d, the actual sCOD again increased to 670 mg/L for DS:PRS =0.5. Consequently, the biogas production also increased for DS:PRS=0.5 after 50 d (Fig. S1(b)). Therefore, the trend in the solubilization curves for both the inocula nearly correlates with the respective biogas production curves throughout the digestion period but the variation in the trendline of sCOD curve can be attributed to the order of microbial attack susceptibility varies for petroleum hydrocarbons. Das and Chandran (2011) explained the order of microbial attack influence on petroleum hydrocarbons as n-alkanes>branched alkanes>

small aromatics> cyclic alkanes>polycyclic aromatics. The initial increase in sCOD from 0th d to 30th d was due to solubilization of lighter-weighted aliphatics and a second peak obtained at 40th d could be attributed to the solubilization of heavier-weighted cyclic alkanes and polyaromatics. High molecular weighted hydrocarbons are recalcitrant and cannot be degraded without any pretreatment, though their percentage degradation efficiency varies with the type of pretreatment applied (Brown et al., 2017).

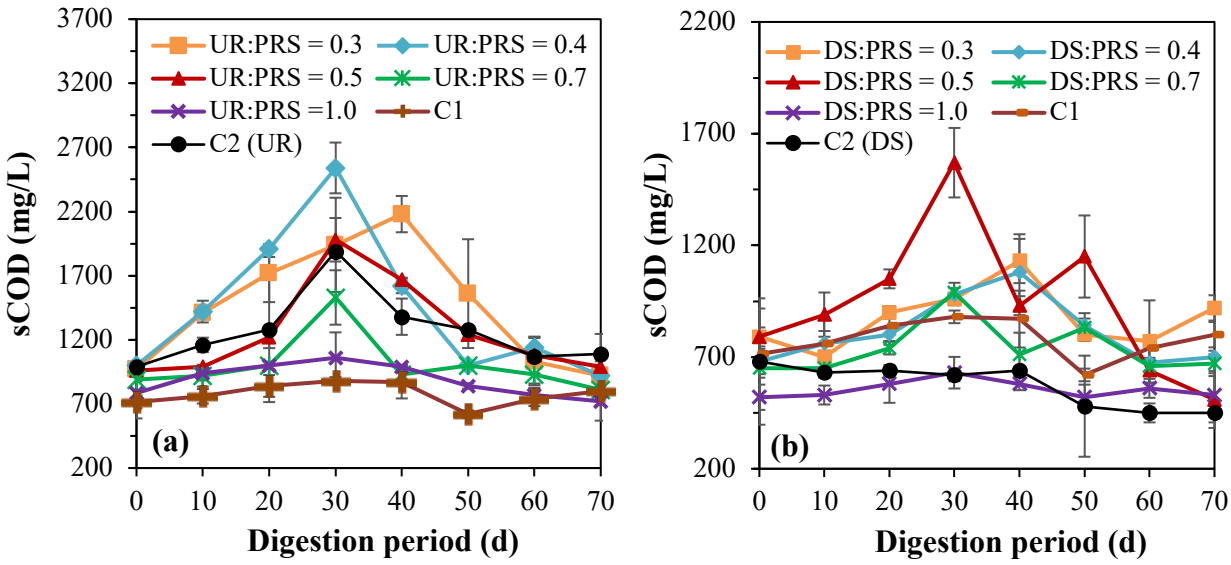

Fig. 4.3. Variation of sCOD when PRS is anaerobically digested with (a) UR (b) DS

4.3.3 Effect of inocula on VFA accumulation

Fig. 4.4 (a) and Fig. 4.4 (b) show the variation in the accumulation of VFA when PRS was digested with UR and DS respectively. The extent of acidification of a substrate can be realized with the accumulation of VFA which would facilitate biogas production. The maximum VFA accumulation was observed to be at 30 d for UR:PRS = 0.4 (480 mg/L) and DS:PRS = 0.5 (440 mg/L). The trend of VFA concentration curve for both the inocula varied for all the mixing ratios. The highest accumulations for all the mixing ratios were attained at different periods which suggested that the varying ratios do influence the degree of acidification for the same sludge suggesting the fermentation rates to be different for all the ratios. The increase in VFA concentrations from 0 to 30 d for DS:PRS= 0.4 indicated the activation of hydrolytic, acidogenic and syntropic acetogenic bacteria, and the ceasing of VFA thereafter indicated the activation of methanogenic archaea converting acetate to methane and carbon dioxide (Lee et al., 2015). The mixing ratios, UR:PRS= 1 and DS:PRS = 1 showed poor VFA accumulations compared to other ratios and therefore the methane yields were also observed to be lower for mixing ratio 1. Wang et al. (2016) reported the maximum VFA accumulation upon digestion of petroleum refinery waste

with municipal wastewater treatment sludge as inoculum in a two-phase anaerobic reactor to be 486.4 mg/L at mesophilic temperature condition and HRT = 4 d which correlates with this batch study showing the VFA concentrations were being obtained at a longer digestion period.

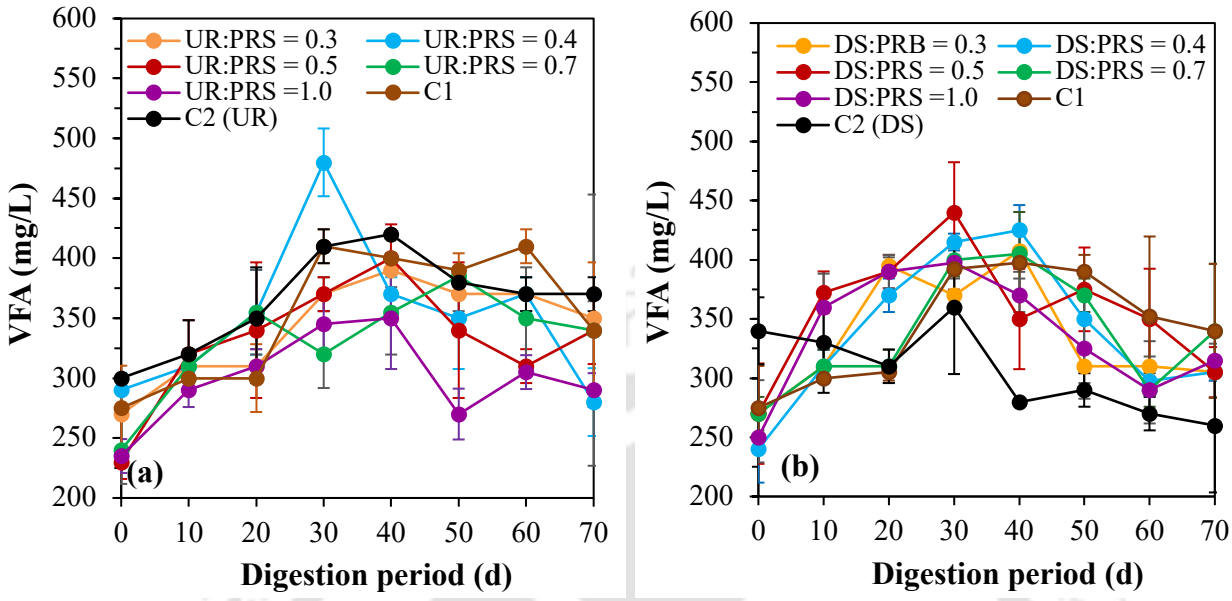

Fig. 4.4. Variation of VFA when PRS is anaerobically digested with (a) UR (b) DS

4.3.4 Effect of inocula on VS degradation

Fig. 4.5 shows the comparative VS degradation percentage when PRS was digested with UR and DS as inocula at different mixing ratios. The ratios showing the highest solubilization for UR and DS showed maximum sludge stabilization, but the digestion of PRS with DS showed a higher VS degradation percentage with the highest being 10.78% for DS:PRS = 0.5 compared to that of UR:PRS = 0.4 (9.12%). Based upon the methane production, solubilization and organic removal percentages, the PRS was observed to have associated better with the microbial environment provided by DS from an already operational steady anaerobic digester but the hydrolysis phase was observed to be lengthy. The rate of methane production was uneven suggesting the degradation to be complex necessitating the requirement of pretreatment.

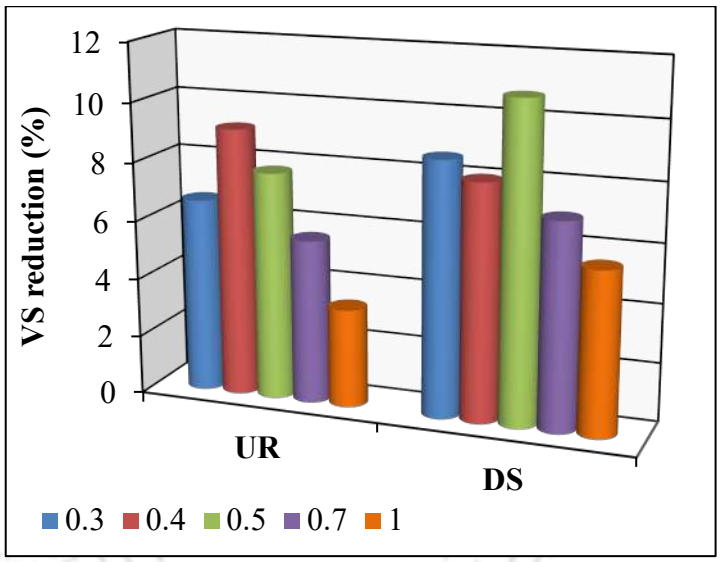

Fig. 4.5. VS degradation when PRS is anaerobically digested with UR and DS

4.4 16S METAGENOME SEQUENCING OF THE EFFICIENT INOCULUM

This study was conducted to focus on the identification of different bacterial and archaeal communities present in the most efficient inoculum for evaluating the anaerobic degradation of PRS in pretreatment and co-digestion studies. Since, the anaerobic biodegradability assay of PRS with DS as inoculum showed better organic matter degradation and higher biogas production, therefore, the DS was analyzed by 16S metagenome sequence method.

4.4.1 Taxonomic distribution

The pie charts below illustrate the distribution of taxonomic domains at phyla, class and order levels for the annotations. Each slice indicates the percentage of reads with predicted ribosomal RNA genes annotated to the indicated taxonomic level.

4.4.1.1 Taxonomic hits distribution at phylum level

The relative microbial abundance of the inoculation introduced into an anaerobic digester, has a significant impact on the performance and stability of the digestion process. The composition and diversity of microorganisms in the inoculum can influence the breakdown of organic matter, biogas production, and overall process efficiency (Liu et al., 2017). The relative microbial abundance present in the DS at the phylum level is shown in Fig. 4.6. The predominant phyla observed in the DS were *Bacteroidetes* (28.5%), *Proteobacteria* (24.6%), *Firmicutes* (16.6%), *Actinobacteria* (9.6%), *Spirochaetes* (5.4%) and *Chloroflexi* (3%) comprising more than 85% of the total reads. *Firmicutes* and *Proteobacteria* are considered majorly to be facultative anaerobes, while members of the *Bacteroidetes* and *Actinobacteria* are strictly anaerobes and therefore, have the ability to

survive in fermentative and obligate stage of any anaerobic reactor (Malele et al., 2018). *Proteobacteria* and *Bacteroidetes* are responsible for the degradation of organic fraction of a substrate whereas, *Chloroflexi* reportedly engages in the fermentation of alkanes under anaerobic and sulphate-reducing conditions (Lee et al., 2022).

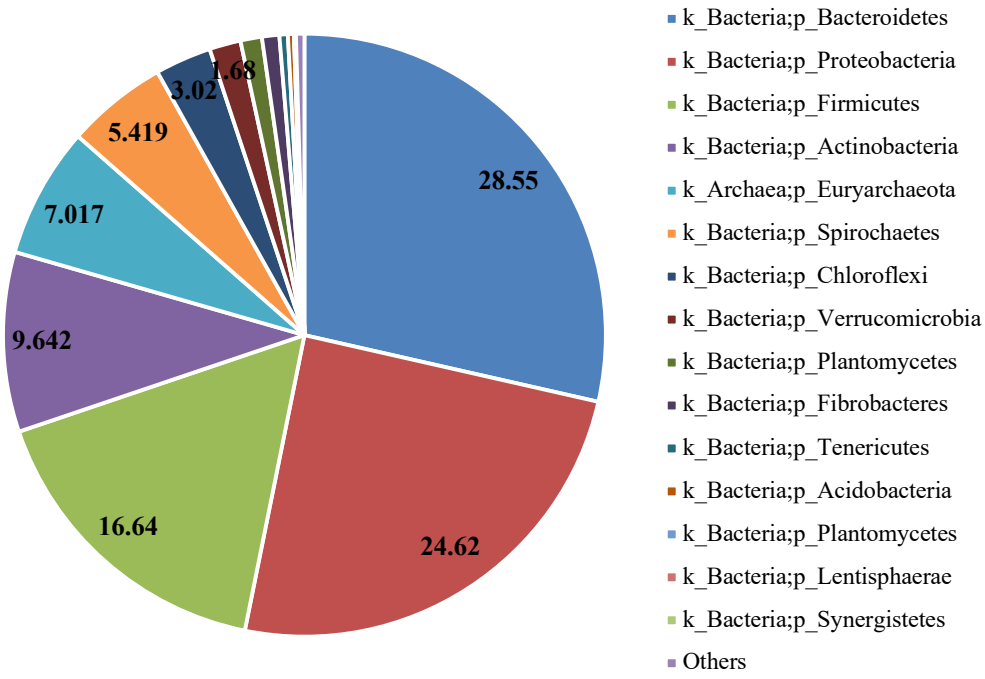

Fig. 4.6. Taxonomic hit distribution of DS at phylum level

4.4.1.2 Taxonomic hits distribution at class level

Alphaproteobacteria (9.6%), *Betaproteobacteria* (14.7%), *Gammaproteobacteria* (4.9%) and *Deltaproteobacteria* (6.2%) were the dominant bacterial class of the phylum group of *Proteobacteria* with each one of them exhibiting hydrocarbon-degrading properties by controlling the cycle of organic (C and N) and inorganic compounds (Fig. 4.6). Members of the *Betaproteobacteria* class has the potential to anaerobically degrade PAH compounds, especially under nitrate-reducing conditions as reported by Sierra-Garcia et al. (2014). *Deltaproteobacteria* is also well-known to be involved in anaerobic hydrocarbon degradation (Roy et al., 2018). Their presence in various biogas reactors including industrial-scale had been reported in various studies (De Francisci al., 2015; Sun et al., 2017). The abundant classes in *Bacteroidetes* were observed to be *Bacteroidia* (19.5%), *Flavobacteriia* (0.9%), and *Cytophagia* (0.8%), and the dominant classes in *Firmicutes* were *Clostridia* (11.3%) and *Bacilli* (1.9%). Some other classes with high abundance were *Spirochaetes* (5.8%), *Actinobacteria* (8.6%), and *Anaerolineae* (4%).

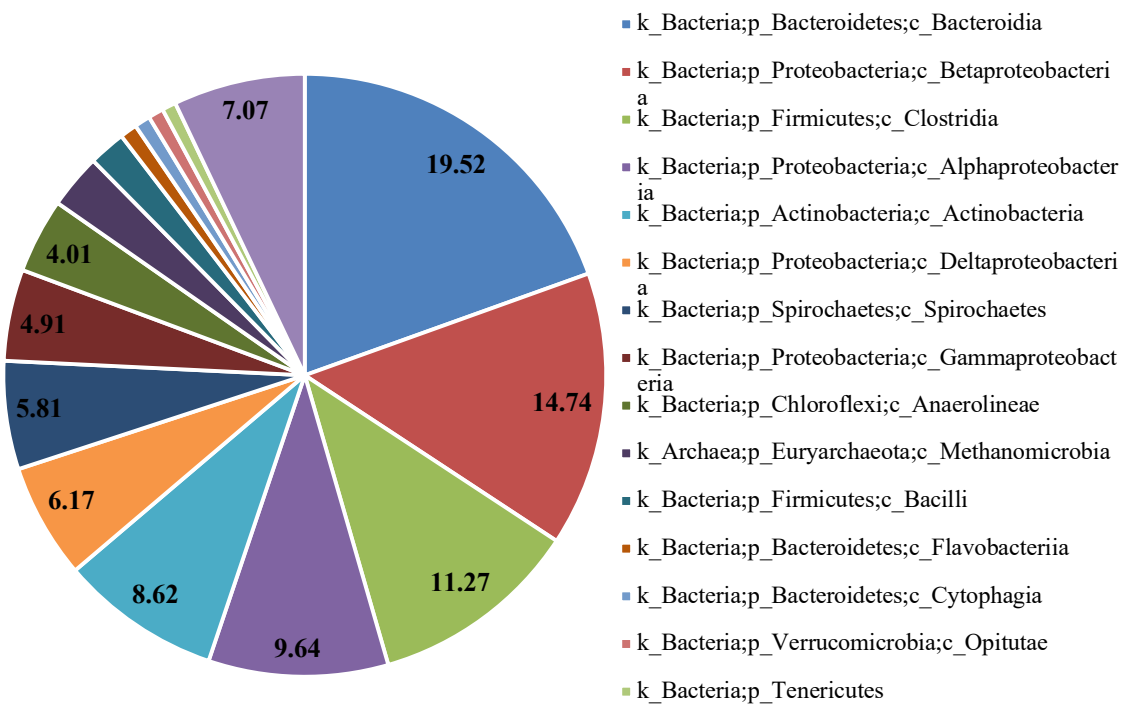

Fig. 4.7. Taxonomic hit distribution of DS at class level

4.4.1.3 Taxonomic hits distribution at order level

Taxonomic hits distribution at order level shows predominance of *Bacteroidales* (18.5%), *Clostridiales* (12.7%), *Burkholderiales (*9.3%), and *Rhizobiales* (8.6%) as represented in the Fig. 4.8. The predominance of the bacterial communities reportedly represented a significant fraction of the microbial communities inside an anaerobic digester (Treu et al., 2019). Some other taxonomic hit at order level showing predominance were *Actinomycetales* (7.6%), *Anaerolineales* (6.2%), *Xanthomonadales* (5.8%), and *Rhodobacterales* (4.9%).

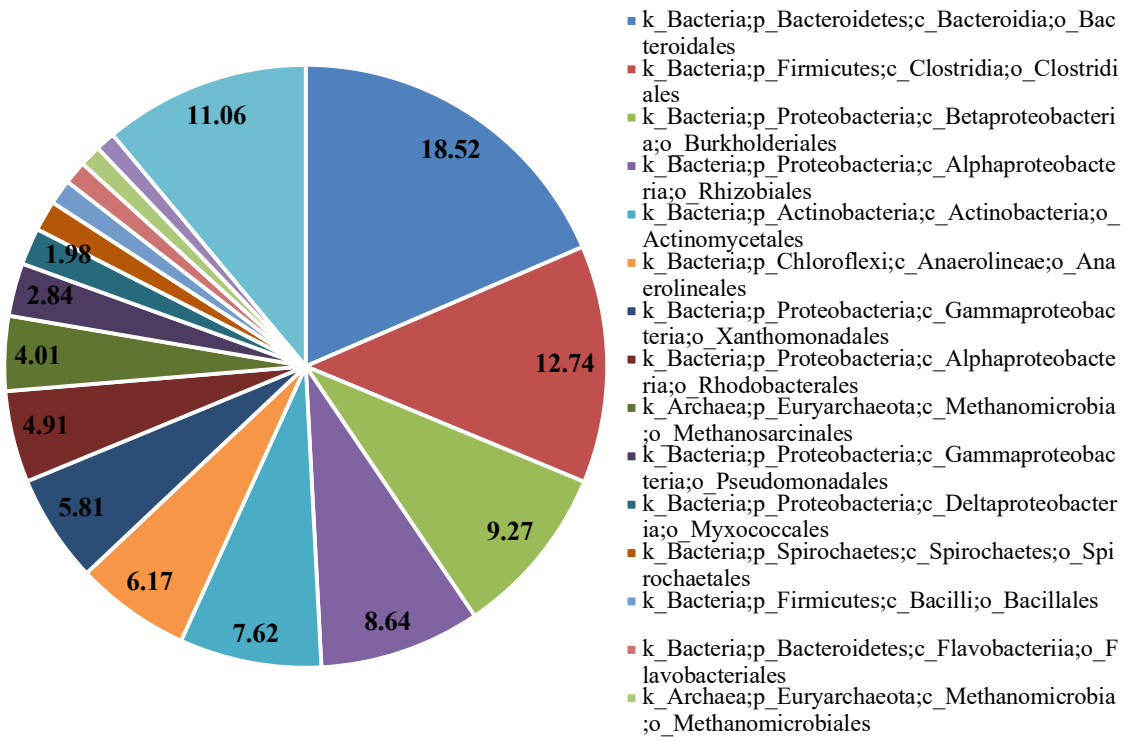

Fig. 4.8. Taxonomic hit distribution of DS at order level

4.5 CONCLUSION

The findings of this chapter confirm significant differences between the two types of inocula. PRS when inoculated with DS demonstrated superior biogas production (**3-fold higher**) compared to inoculation with UR within 70 d of digestion. This difference can be attributed to the higher effective biogas yield achieved by DS, while UR performed poorly to create an optimal environment for the biodegradation of PRS. Inoculation with DS exhibited better performance, showcasing higher adaptability, better solubilization (**46% higher**) thereby, achieving the highest reduction in VS (**19% higher**). Also, the microbial composition of DS showed significant predominance of *Proteobacteria, Bacteroidetes* and *Firmicutes* at phylum level. At the order level, *Bacteroidales* and *Clostridiales* were found to be enriched in the DS, emphasizing their crucial role in the microbial consortium for AD. Nevertheless, the relatively low organic matter degradation and biogas production from AD of PRS indicated limited biodegradability. Therefore, it is imperative to conduct comprehensive studies on pretreatment and co-digestion methods, which are extensively discussed in chapter 5 and chapter 6 of this study.

Chapter 5

PRETREATMENT STUDY

This chapter deals with the influence of different types of pretreatment techniques, i.e. thermal, electrokinetic, and microbial on the solubilization of PRS. This chapter further deals with the enhancement in biogas yields followed by hydrocarbon degradation due to these applied pretreatments.

5.1 THERMAL PRETREATMENT

Different modes of heat are applied to PRS to find out the most suitable mode of heat as pretreatment with the most efficient inoculum. Morphological study of the substrate and energy assessment of recovered energy after pretreatment is carried out to govern the economic viability of the pretreatment used. Additionally, phytotoxicity assessment of PRS (before and after biogas production) is investigated on mung bean (*Vigna radiata* L.) for the safety of the environment.

5.1.1 Optimization of different modes of thermal pretreatment on PRS

5.1.1.1 Dry heat

Fig. 5.1 (a) and (b) show the effect of temperature and exposure time respectively, on the solubilization and VFA accumulation of PRS due to the application of dry heat. During the temperature study, the variation of temperature between 70°C and 160°C resulted in maximum solubilization of 2380 mg/L at 140°C which increased by 2.3 times of the control/untreated sludge. The maximum VFA was also observed at 140°C which was about 1.3 times that of the control sample. PRS was exposed to each temperature for 50 min to investigate the effect of temperature variation through dry heat application. Application of 140°C for 50 min modified the PRS chemical characteristics by fragmentation of intermolecular bonds aiding the release of soluble organic dimers and monomers (Appels et al., 2010). The temperature range for pretreatment was chosen between 70-140°C since thermal treatment beyond 200°C leads to pyrolysis of hydrocarbons present in petroleum sludge and therefore temperature range below 200°C was considered suitable for pretreatment (Wang et al., 2007). In this study, application of dry heat at temperatures greater than 140°C resulted in fumes leading to ash production indicating destruction of organic fraction of the substrate and evaporation of short-chain fatty acids. Thermal pretreatment at temperature ranges of 170-190°C was reported to enhance solubilization of sludge but its biodegradability gets reduced due to Maillard reactions forming melanoidins at those temperatures which were highly recalcitrant (Dwyer et al., 2008; Zhang et al., 2020). The trend of both VFA and sCOD curves was

similar. The sCOD increased from 70°C to 80°C and dropped at 90°C, which again further increased till 140°C, achieving the peak value, only to drop at 110°C. These intermediate decreases in sCOD were because of elevated vaporization of VFA (Yeshanew et al., 2016). Effective thermal pretreatment can be seen up to a certain temperature, beyond which certain inhibitory compounds are formed which decreases the biodegradability of a substrate (Carrere et al., 2010). Also, the thermal decomposition pattern in hydrocarbons ranges from lower-weighted hydrocarbons such as aliphatics to heavier-weighted hydrocarbons such as polycyclic aromatics (Das and Chandran, 2011). Initial temperatures led to fragmentation of easily available organic carbons (aliphatics) which successively got fragmented to higher molecular weighted hydrocarbons with an increase in temperature (Gojgic-Cvijovic et al., 2012). The temporal study conducted at 140°C for a range of time from 30-180 min led to the maximum solubilization of 2850 mg/L at 60 min. The maximum sCOD and VFA increased by 178.32% and 53.6% that of untreated sludge respectively at 60 min optimizing the operating conditions as 140°C for 60 min. The improved solubilization shall lead to improved hydrolysis of PRS thereby increasing the methane yield.

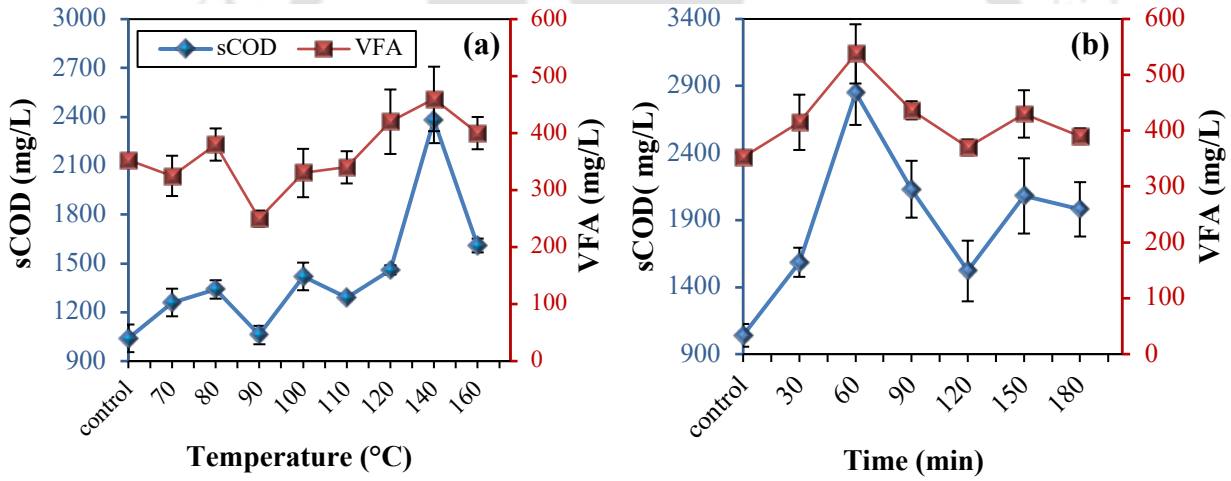

Fig. 5.1. Optimization of dry heat application (a) Temperature study (b) Temporal study

5.1.1.2 Moist heat

(i) Pressurized moist heat

Table 5.1 shows the effect of pressurized moist heat application on PRS. During pressurized moist heat application through an autoclave on PRS, the temperature was varied from 80 to 120°C at 10°C intervals and each temperature was maintained for 30 min. The pressure was kept under 3 bar to prevent formation of recalcitrant compounds and improved toxicity (Wahidunnabi and Eskicioglu, 2014). The sCOD increased from 80°C to 100°C attaining the maximum value of 1190 mg/L at 100°C after which the sCOD kept decreasing till 120°C. During the pretreatment from 80-

100°C, the external pressure superseded the internal resistance of the sludge structure fragmenting the sludge particulate matter thereby liberating intracellular substances (Ennouri et al., 2016). The VFA also increased similarly to sCOD and achieved the maximum value of 380 mg/L at 100°C after which it decreased since temperature higher than 100°C led to a reduction in soluble organic content due to vaporization of VFAs. During pretreatment, the particulate organic compounds were liquidized and became soluble thereby increasing VFA concentrations due to hydrolysis of dissolved organic compounds into simpler volatile compounds (Lie et al., 2012). The optimum temperature of 100°C for pressurized moist heat application was evident from the temperature study. The exposure time was then varied from 20-80 min at the optimum temperature of 100°C. At 60 min, the COD solubilization was observed to be maximum and was about 102% higher compared to control (untreated) which was much higher than Ennouri et al. (2016), who obtained maximum VS solubilization (about 70%) of industrial sludge through autoclave pretreatment at 120°C. The maximum VFA for this study was also obtained at 60 min exposure duration which was 1.12 times higher than that of control PRS. Zhou et al. (2015) used the application of thermal pretreatment through an autoclave to improve the biodegradability of petrochemical sludge at operating conditions of 130°C for 20 min and out of other pretreatments (ultrasound, alkaline pretreatment) used, thermal pretreatment using autoclave was reported to have produced maximum methane production from petrochemical sludge due to improved solubilization and sludge dewaterability.

Table 5.1. Temperature and temporal study to optimize moist heat application on PRS

Pressurized moist heat						Agitated open moist heat					
Temperature study			Temporal study			Temperature study			Temporal study		
Temp	sCOD[a] (mg/L)	VFA[a] (mg/L)	Time (min)	sCOD[a] (mg/L)	VFA[a] (mg/L)	Temp	sCOD[a] (mg/L)	VFA[a] (mg/L)	Time (min)	sCOD[a] (mg/L)	VFA[a] (mg/L)
80°C	950 ± 42.43	310 ± 14.14	20	1040 ± 85.62	345.5 ± 28.09	60°C	990 ± 14.14	390 ± 10.05	30	1150 ± 113.13	426.25 ± 26.51
90°C	1080 ± 56.57	330 ± 25.02	40	1580 ± 95.05	390 ± 30.23	70°C	1160 ± 56.57	430 ± 42.45	60	1290 ± 102.38	495 ± 35.35
100°C	1190±12 7.28	380 ± 28.28	60	2070 ± 180.06	395 ± 36.58	80°C	1360 ± 88.02	470 ± 14.14	90	1380 ± 105.09	331.25 ± 44.19
110°C	1090 ± 50.41	310 ± 14.14	80	1368 ± 95.42	295 ± 23.06	90°C	1180 ± 70.71	430 ± 12.03	120	1600 ± 125.73	332.5 ± 10.61
120°C	1035 ± 77.79	290 ± 14.45	--	--	--	100°C	1020± 83.62	390± 22.18	150	1200 ± 97.62	290 ± 14.14

[a]Mean ± standard deviation from triplicates

(ii) Agitated open moist heat

During temperature variation from 60-100°C, the maximum sCOD and VFA were obtained as 1360 mg/L and 470 mg/L respectively at 80°C as shown in Table 5.1. If compared with the temperature study of moist heat under pressure (< 3 bar), moist heat without pressure was better in improving the solubilization but at a lower temperature. This can be attributed to the fact that continuous agitation of sludge during the pretreatment period led to better homogenization of sludge which in turn improved its solubilization at lower temperatures. A control studied at 80°C for 40 min exposure period without agitation resulted in sCOD and VFA concentrations of 1100±32.56 mg/L and 415±10.168 mg/L respectively, which proved that continuous agitation led to better homogenization of PRS and improved solubilization (since sCOD and VFA concentrations were increased by 23.6% and 13.25% respectively at 80°C due to agitation). Agitation at elevated temperatures improved solubilization due to breakdown of soluble organics present in the sludge through positive shear force effect, promoting effectual contact between the sludge particulates (Yang et al., 2018). Rubal et al. (2012) reported that heating and agitating primary sludge from municipal wastewater treatment plant in a fermenter apparatus improved soluble COD in the range of 8-10% at different solids retention times. The trend in sCOD and VFA variation from the temporal study were dissimilar as maximum sCOD of 1600 mg/L was exhibited at 120 min but maximum VFA of 495 mg/L was attained at 60 min which might be because of increased vaporization of VFAs due to the agitation of sludge for a longer duration. Another control was maintained at 80°C for 120 min without agitation which was evaluated to be 20% lower sCOD (1280±42.18 mg/L) and 15.33% lower VFA (281.5±5.14 mg/L) compared to that obtained with agitation at the same operating condition. The sCOD obtained from optimum operating conditions (80°C, 120 min) was about 1.5 times higher than the control sludge.

5.1.1.3 Microwave irradiation

The microwave irradiation applies microwave energy to penetrate any substrate with the electromagnetic field through molecular interaction providing heat with greater efficiencies and therefore, this method is useful for the fragmentation of heavier to lighter hydrocarbons through a quick temperature increase thereby improving the dewaterability of that hydrocarbon-rich substrate (Hu et al., 2013; Johnson and Affam, 2018). Microwave irradiation on PRS was applied through variation of temperature from 100-250°C, each temperature being exposed for 2 min as shown in Table 5.2. From the temperature study, the sCOD was observed to vary in direct proportion with VFA. The

maximum sCOD and VFA increased from 100-160°C where they attained peak values of 1248 mg/L and 380 mg/L respectively. The increase in sCOD and VFA can be attributed to the fact that the application of microwave leads to the dissolution of bound organic matter releasing intracellular organic content. The electromagnetic waves polarize side-chain macromolecules of PRS through rapid oscillation and the microwave energy gets converted to heat by internal resistance to rotation, activating bond disorientation and decomposition in hydrocarbons (Bozkurt and Apul, 2020). The increase in temperature beyond 160°C led to decrease in both sCOD and VFA concentrations. This was because elevated temperatures (160-180 °C) cause polymerization of low molecular-weighted compounds forming recalcitrant components through caramelization process thereby decreasing the organic content (Toreci et al., 2010; Bozkurt and Apul, 2020). The temporal study conducted at 160°C for a temperature range from 3-20 min, exhibited the highest solubilization of 1950 mg/L at 3 min which was about 1.8 times higher than that of the control PRS. The maximum VFA was obtained similarly at 3 min and was about 1.12 times that of control PRS. Microwave energy application in different types of sludge has been proven to be better than any other conventional heating process (Carrere et al., 2010; Hu et al., 2013). The temperature and temporal optimization study improved PRS solubilization through sludge denaturation at a very short duration.

Table 5.2. Temperature and temporal study to optimize the application of microwave irradiation on PRS

Temperature study			**Temporal study**		
Temperature	**sCOD[a] (mg/L)**	**VFA[a] (mg/L)**	**Time (min)**	**sCOD[a] (mg/L)**	**VFA[a] (mg/L)**
100°C	960 ± 42.41	300 ± 20.21	3	1950 ± 212.14	392.5 ± 12.87
140°C	960 ± 60.54	280 ± 25.06	5	990 ± 95.62	310 ± 20.64
160°C	1248 ± 90.61	380 ± 18.62	10	1610 ± 122.61	310 ± 14.14
180°C	1000 ± 81.86	360 ± 22.28	15	1150 ± 102.64	340 ± 20.08
200°C	980 ± 50.06	320 ± 13.69	20	960 ± 85.62	355 ± 18.85
220°C	860 ± 48.07	300 ± 32 81	--	--	--
250°C	860 ± 56.42	280 ± 21.24	--	--	--

[a] Mean ± standard deviation from triplicates

5.1.2 Morphological and chemical characterization

The physical morphology of PRS before pretreatment (Fig. 5.2a) showed numerous overlapping solid uneven layers with voids. The irregularly shaped solid particles depicted a conglomeration of nodules surrounded by some finer particles. After thermal pretreatment, the solid nodules were observed to transform into a bed of round and tubular-shaped finer particles (Fig. 5.2b). The edges were mostly irregular presenting a hollow amorphous structure of PRS after pretreatment. The FTIR spectra before and after thermal pretreatment of PRS are shown in Fig. 5.2(c). The absorbance at 3156 cm^{-1}indicates O-H stretch corresponding to the hydroxyl group and water. The sharp peaks obtained at 2925 and 2854 cm^{-1} indicate symmetric and asymmetric C-H aliphatic stretch respectively (Ennouri et al., 2016). After pretreatment, the asymmetric C-H stretch was observed to be completely fragmented and vanished. The short-broadened peak was observed at 1640 cm^{-1} indicates C=C stretch corresponding to alkenes and aromatic rings while the sharp peaks observed in the range 1404-1458 cm^{-1} indicate C-H stretch for methyl group. The declining absorbance pattern after pretreatment signified intramolecular and intermolecular changes in PRS. The decreased intensity at 1034cm^{-1} indicated a significant reduction in C-O stretch of primary alcohols while the absorbances in the range 500-800 cm^{-1} correspond to phenyl group of PRS which showed slight changes in the intensity after pretreatment (Rajasekar et al., 2005).

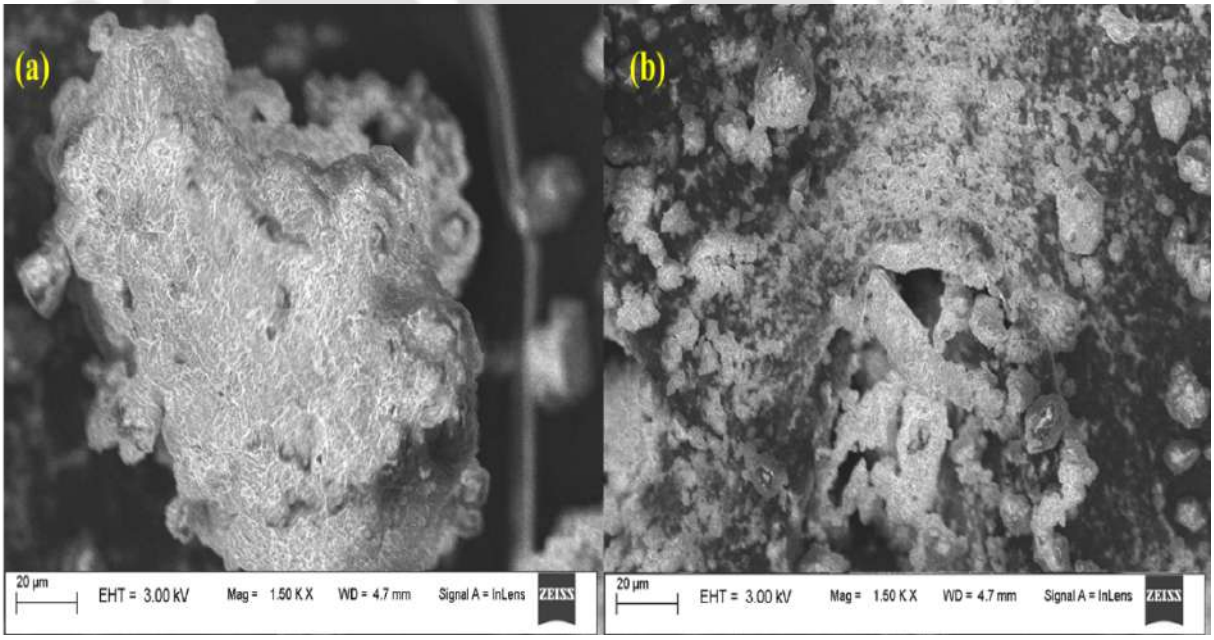

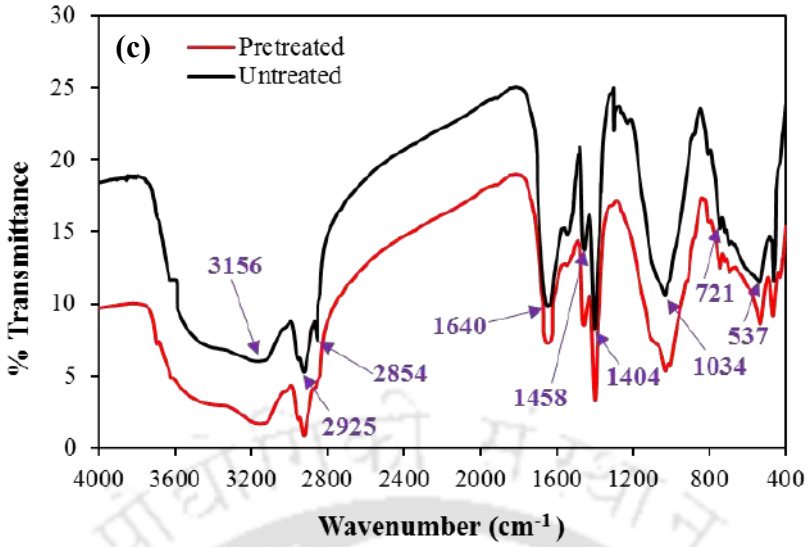

Fig. 5.2. FESEM micrographs of PRS (a) before, (b) after dry heat pretreatment, and (c) FTIR spectra of PRS before and after dry heat thermal pretreatment

5.1.3 Effect of thermal pretreatment on anaerobic biodegradability of PRS

The daily biogas production curve before and after pretreatment through dry heat application at different inoculum and sludge ratios (DS:PRS) is shown in Fig. 5.3(a). The peak daily biogas production was observed to be 223 mL/gVS_{added} at 31 d. for DS:PRS=0.5. This highest daily biogas production due to dry heat pretreatment was found to be 66.42% higher and was achieved 4 d earlier compared to control or untreated digestion of PRS. The daily biogas production curve clearly showed improved hydrolysis since biogas production from PRS was increased during the initial period of digestion after pretreatment for all the ratios. This was due to the breakage of chemical bonds present in the sludge converting insoluble particulate COD to soluble organic COD thereby increasing the biogas yield (Aboulfoth et al., 2015).

Fig. 5.3(b) shows the cumulative biogas production curve of PRS with and without pretreatment. Pretreatment through dry heat application was observed to produce maximum cumulative biogas of 6928 mL/g VS_{added} for DS:PRS =0.5, which was about 24.8% higher than the untreated PRS (5551 mL/gVS_{added}). The improved solubilization of PRS through dry heat application was readily accessible by the hydrolytic and fermentative bacteria which guided the PRS digestion process towards its faster utilization by methanogenic bacteria (Borges and Chernicharo, 2009; Zhang et al., 2020). The undesirable performance of untreated PRS was due to the presence of refractory organic compounds (polyaromatic, heterocyclic compounds) and certain percentages of these were reported to be toxic to

methane-producing bacteria (Haak et al., 2016). Therefore, a longer lag phase for untreated PRS was quite visible from the cumulative production curve. Reduced lag phase, sludge viscosity with improved sludge handling through thermal pretreatment have already been reported (Carrere et al., 2010). Wang et al. (2016) reported thermal pretreatment (dry heat) to be the most effective pretreatment (compared to ultrasonication, alkaline and combined ultrasonic-thermal) for improved solubilization of petrochemical sludge. The cumulative biogas production for all mixing ratios followed the order: 0.5>0.7>0.4>0.3>Control.

During this study, pH values remained in the range of 6.3-7.4 for all the mixing ratios, and there was no sudden drop of pH below 6.3 suggesting sufficient buffering capacity of the reactors throughout the digestion period. The optimum pH is desired to be in the range of 6.8-7.2 to prevent reactor failure from excess acidification and poor buffering capacity (Cioabla et al., 2012). Also, the maximum organic matter removal percentage after pretreatment was evaluated to be 48.712% for DS:PRS=0.5, which was 4.52 times that of the untreated PRS (Fig. 5.3c). Wang et al. (2016) reported VS removal efficiency of 53.1% from a continuous reactor through dry heat thermal pretreatment (using muffle furnace) of waste activated sludge from an oil refinery which is close to the result obtained in this batch reactor study and has a scope of improved efficiency in a continuous reactor study. The VS degradation order of various mixing ratios followed the order: 0.5>0.7>0.4>0.3>Control which corroborated the order of biogas production potential for different mixing ratios suggesting a direct co-relationship between them. Thermal pretreatment leads to W/O demulsification due to increased temperature of emulsions leading to the reduction of viscosity, thereby stimulating settlement of water droplets in emulsion. This leads to fragmentation of heavier hydrocarbons into lighter hydrocarbons making easy access for anaerobic microbial consortium resulting in enhanced biodegradability of PRS (Shie et al., 2004).

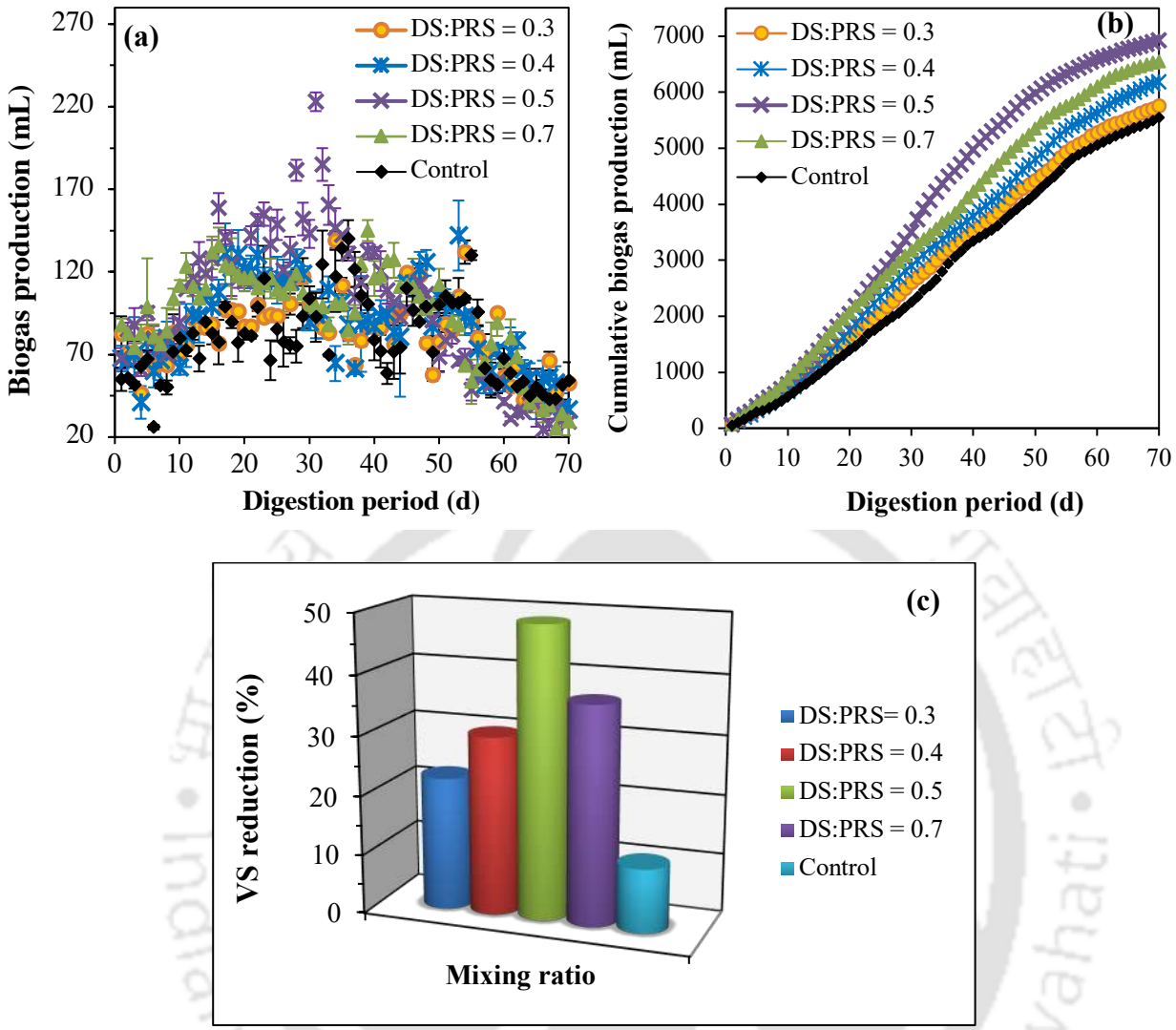

Fig. 5.3. Variation of (a) daily biogas, (b) cumulative biogas, and (c) VS degradation during anaerobic digestion of thermally pretreated PRS

5.1.4 Energy assessment study

Evaluation of economic feasibility is imperative to justify the thermal pretreatment used for the improvement of anaerobic biodegradability of PRS. The energy demand for the pretreatment process should not exceed the amount of energies recovered in the form of methane and heat. Upon evaluation of dry heat application as pretreatment at optimum operating conditions (140°C, 60 min) on PRS, a net positive energy, Q_T = 21826.0352 kJ was obtained (Q_B = 21821.96 kJ, Q_H = 97.6752 kJ and Q_U = 57.6 kJ). This signified that dry heat application as thermal pretreatment of PRS is a feasible process

with satisfactory energy recovery efficiencies making it a sustainable strategy for utilization of petroleum refinery wastes.

5.1.5 Scaled up batch study

The 1 L BMP study was scaled up to 20 L capacity with 14 L working volume for DS:PRS =0.5 to evaluate the alterations in the composition of the pollutants in larger-scale.

5.1.5.1 Biogas yield

Anaerobic biodegradation of a substrate can be proportioned directly with the rate of biogas production from the substrate in the presence of the seeding environment. In Fig. 5.4(a), the peak daily biogas production from thermally pretreated PRS at optimum operating conditions (140°C and 60 min) in presence of DS as seeding environment was obtained on 33rd d which was about 11.2 folds higher than that of the untreated PRS till 60 d of digestion period. The shortening of hydrolysis phase after thermal pretreatment could be ascertained from the fact that the peak daily biogas was obtained 4 d earlier compared to anaerobic biodegradation of untreated PRS. Application of 140°C for 60 min modified the chemical characteristics of PRS by fragmentation of intermolecular bonds aiding the release of soluble organic dimers and monomers (Appels et al., 2010). The cumulative biogas production after 60 d of digestion resulted in 40.12% increment after thermal pretreatment as compared to untreated (Fig. 5.4b). The lower biogas production from untreated PRS might be attributed to the presence of refractory organic compounds (polyaromatic, heterocyclic compounds) reported to be toxic to methane-producing bacteria (Haak et al., 2016). Therefore, a longer lag phase for untreated PRS was quite visible from the cumulative production curve. Reduced lag phase, sludge viscosity with improved sludge handling through thermal pretreatment have already been reported by Carrere et al. (2010). Wang et al. (2016) reported thermal pretreatment to be the most effective pretreatment (compared to ultrasonication, alkaline and combined ultrasonic-thermal) for improved biogas production due to maximum increment in solubilization of petrochemical refinery sludge.

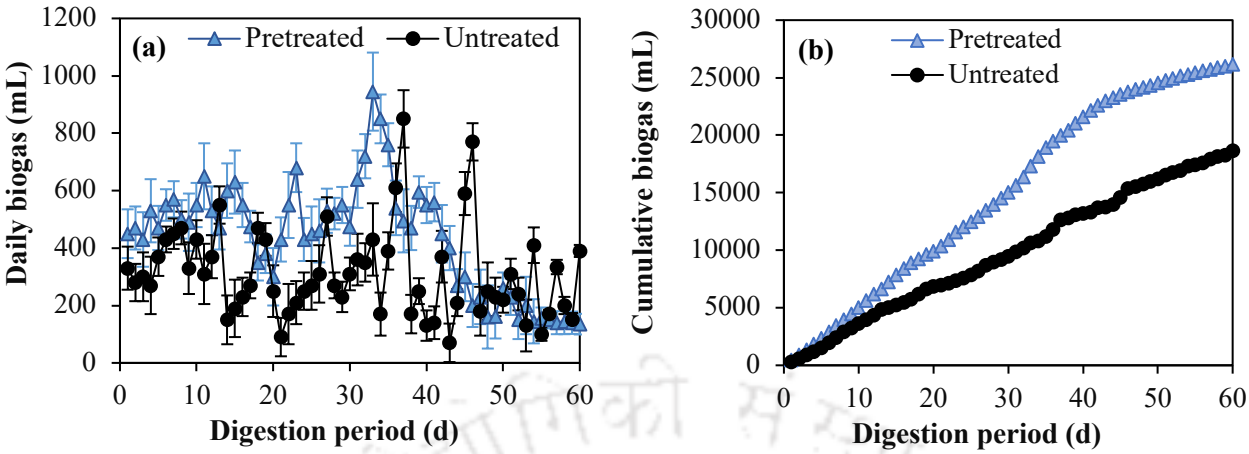

Fig. 5.4. Daily and cumulative biogas production of thermally pretreated PRS at optimum conditions

5.1.5.2 Pollutant degradation (TPH, O&G and total phenol)

During anaerobic degradation of petroleum hydrocarbons, the hydrogen-degrading microorganisms reduce hydrocarbon equivalents to molecular hydrogen (H_2) which is converted to CO_2 and CH_4 by the methanogenic archaea. In Fig. 5.5(a), a decreasing trendline was observed for the total petroleum hydrocarbon (TPH) content of the pretreated PRS with 38.8% removal by the end of digestion period of 60d. The TPH removal could be attributed to two types of hydrocarbons mostly susceptible to microbial attack: aliphatic (including alicyclic) and aromatic hydrocarbons. The aliphatics include saturated (alkanes) and unsaturated (alkenes and alkynes) hydrocarbons which get activated in anaerobic condition through carboxylation yielding C-odd n-alkanes to C-even fatty acids through a series of reactions facilitating the fermentation process (Holliger and Zehnder, 1996). This activates glutaryl-CoA dehydrogenase or acetyl-CoA acyltransferase enzyme catalyzing the final step of fatty acid through β-oxidation to acetyl-CoA and CO_2 entering the tricarboxylic acid (TCA) cycle. The aliphatic hydrocarbons might also follow a fumerate addition pathway by glycyl radical enzymes undergoing decarboxylation following β-oxidation thereby entering the TCA cycle (Sierra-Garcia et al., 2014). The aromatics might follow fumerate addition pathway or hydroxylation or carboxylation to form a common intermetiate (benzoyl-CoA) which subsequently leads to reductive dearomatization of aromatic ring following hydrolytic ring cleavage due to activation of ring cleavge hydrolase thereby enetering the TCA cycle (Widdel and Rabus, 2001). The rate of degradation of petroleum hydrocarbons decreases with time, obtaining an apparent plateau due to recalcitrant compounds

exhibiting a slow-degradation tendency. The TPH degradation of only 17% in control (untreated) PRS could be due to the activity of sulfate-reducing, nitrogen-fixing and methanogenic consortium already present in PRS as reported by Roy et al. (2018).

The oil and grease (O&G) trendline during the AD process steadily decreased resulting in 56% removal by the end of the digestion period after thermal pretreatment [Fig. 5.5(b)]. During AD, decomposition of long-chain hydrocarbons to shorter ones lead to viscosity reduction facilitating oil degradation (Ke et al., 2019). The O&G removal was enhanced by 3.6 times due to pretreatment compared to control (untreated). Petroleum hydrocarbons are utilized by microbes through direct adherence to macro-oil droplets and aggregation with emulsified oil (Ward et al., 2003). During their hydrocarbon accession, bioemulsifiers or biosurfactants are produced leading to the demulsification of PRS. The similarity in O&G removal and TPH trendline might be related to emulsification of hydrocarbons by these bioemulsifiers stimulating TPH degradation (Ke et al., 2021).

Total phenol decremented from 680 mg/L to 243 mg/L within 60 d of AD [Fig. 5.5(c)]. Phenol degradation in anaerobic condition was due to the activation of phenol-degrading microbes (Sierra-Garcia et al., 2014). During AD, mineralization of phenols proceeds via 4-hydroxybenzoate into the benzoyl-CoA pathway to form cyclohex-1-ene carboxyl- CoA, which then undergoes ring cleavage and β-oxidation to form acetate with the help of acidogens and acetogens (Levén et al., 2012). The methanogens thereby convert the acetate to produce biogas (CH_4 and CO_2). Total phenol removal of 64% obtained in this study at mesophilic temperature range led to 2.7 folds improvement in phenol removal compared to that of control (untreated) indicating great potential for phenol degradation during AD of thermally pretreated PRS.

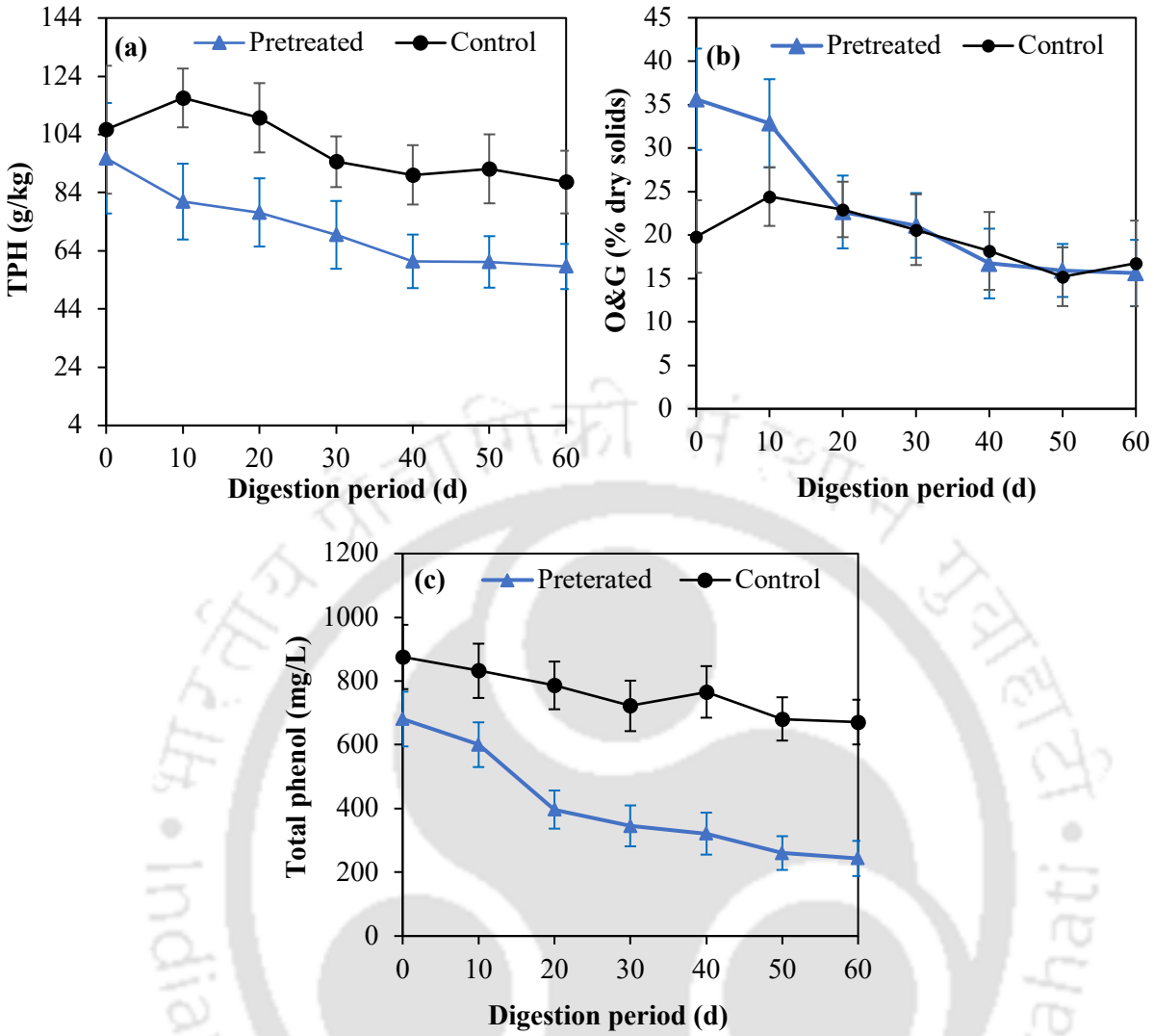

Fig. 5.5. Variation in (a) TPH, (b) O&G, and (c) total phenol throughout the digestion period

5.1.5.3 Phytotoxicity evaluation of batch digestate

The cumulative study of physical and chemical analysis with toxicity test is favourable for the estimation of the quality of sludge samples before being discharged into the environment. Hence, PRS samples (before and after methane generation) were assessed for their phytotoxicity. The phytotoxicity test using *V. radiata* L. (mung bean) on the germination of seed and sprout length has been contemplated as a suitable method for sludge, wastewater or chemical toxicity study (Wang and Keturi, 1990). Phytotoxicity examination using seed germination test is sensitive as it could be easily inhibited by any kind of toxic substance existing in the environment. This study evaluates the phytotoxicity of different concentrations of PRS samples using mung bean seed germination tests for a duration of 48 h. The seed germination inhibition in mung bean for different concentrations of PRS samples is given

in Table 5.3. There was no inhibition in seed germination in control (tap water). The seed germination inhibition was observed upto 25% of sludge extracts. At 25% concentration of both sludge samples, the inhibition of seed germination was negligible. 30% and 40% germination inhibitions were found at the untreated sludge extract of 50% and 75% dilution respectively which gradually decreased (10%) when seeds were exposed to a treated sludge sample of the 75% dilution only. At 100% PRS dilution of untreated sample, 50% seed germination inhibition was observed while after digestion the percentage of seed germination increased upto 80%.

The effect of PRS samples on the growth of mung bean seeding following 5 d is evident in Table 5.3 and Fig. 5.6. The highest root growth of early seedling of mung bean (4.16±0.33 cm) was observed at 25% concentration of untreated PRS sample whereas, in digested samples, the root length of the mung bean was increased at the same concentration of sludge extract (6.30±0.50 cm). As the concentration of sludge extract increased a significant inhibition of root length was observed in both PRS samples (Table 5). The significant reduction of shoot length (4.06±0.41cm) was observed at 100% extract of untreated PRS sample while the reduction value decreased (5.16±0.32 cm) in digested PRS sample of the same concentration in comparison to control. On the other hand, the reduction in biomass of mung bean seedling was 35.7% which was gradually decreased (20.5%) when exposed to treated 100% dilution of PRS extract sample. The significant reduction in seed germination, shoot length, root length and biomass of mung bean grown in PRS extract might be correlated with the utilization of soluble COD and organic TPH after the AD process. This observation corroborates the results obtained from different studies on crop plants (Cokkizgin, 2012; Sangeetha and Thangadurai, 2014; Haq et al., 2016). Seed germination inhibition at higher digestate extract might be the consequence of a disturbed osmoregulatory system due to the presence of high organic content causing toxicity and osmotic stress in plants (Oliveira, 2012; Kasoobi, 2017). Remarkable reduction in root and shoot length, and biomass of the plant signify the bioconversion of phenolics, hydrocarbons and other organic pollutants present in industrial sludge (Haq et al., 2016).

Table 5.3. Effect of different concentration of untreated PRS samples and digestate on seed germination, shoot length, root length and biomass of early seedling of mung bean

Sludge (%)	GR (%)	Shoot length (cm)	Root length (cm)	Biomass (gm)
Control	100±0.42	9.12±0.73	7.08±0.57	1.12±0.09
Before				
25	90±0.29	7.42±0.59	4.16±0.33*	0.97±0.08
50	70±0.42*	7.20±0.58	3.70±0.30*	0.95±0.08
75	70±0.39*	4.95±0.54*	2.76±0.22*	0.85±0.07
100	50±0.41*	4.06±0.41*	2.02±0.16*	0.72±0.07
After				
25	100±0.39	8.92±0.71	6.30±0.50	1.02±0.09
50	100±0.35	7.73±0.62	5.67±0.45*	0.99±0.08
75	90±0.26	6.80±0.40*	2.99±0.22*	0.92±0.07
100	80±0.45*	5.16±0.32*	2.76±0.12*	0.89±0.07

Values are mean ± standard deviation from triplicates

*p <0.05, significant when compared to control using ANOVA

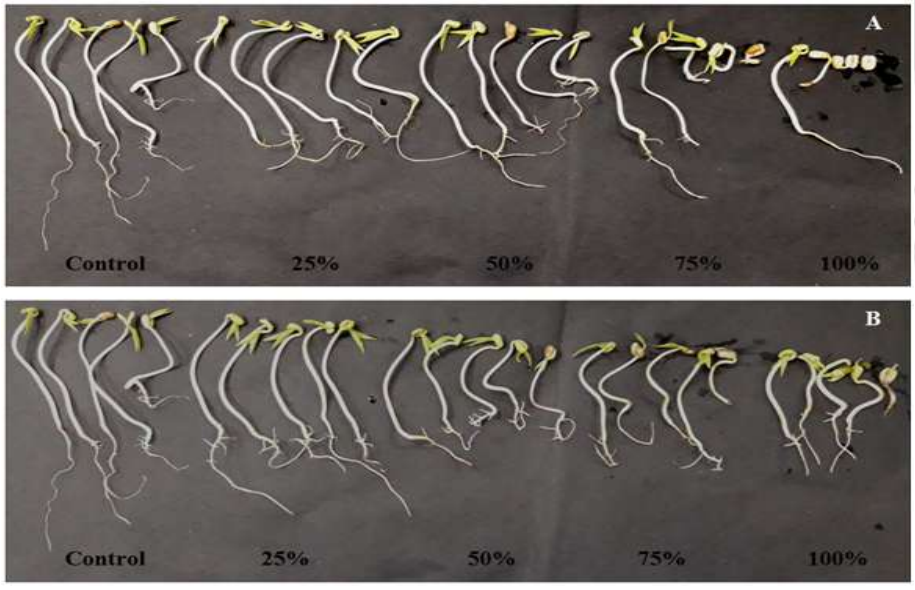

Fig. 5.6. Effect of different concentrations of PRS (A) before and (B) after anerobic digestion on early seedling growth of mung bean (*Vigna radiata* L.)

5.2 ELECTROKINETIC PRETREATMENT

5.2.1 Interpretation of design model for electrokinetic pretreatment study

The formulated design matrix with experimental and predicted results is shown in Table 5.4. The interactive effect of the independent variables (X_1, X_2 and X_3) on output responses were fitted to second-order polynomial equations for both the responses in coded and uncoded forms. For the output response of solubilization (sCOD), the ratio of maximum and minimum valued responses (max/min) was 3.52. The model suggests a mandatory transformation for max/min> 10 but for max/min< 3, power transformation has little effect. In this model, the ratio is between 3 and 10 and therefore, a square-root power transformation was opted for optimization of sCOD. The regression model for sCOD (mg/L) in terms of actual and coded factors was obtained as Eqs. (5.1) and (5.2) respectively.

$$\sqrt{\text{sCOD}} = -5.22 - 0.065\,X_1 + 0.572\,X_2 + 6.72\,X_3 + 0.0028\,X_1X_2 - 0.0215\,X_1X_3 - 0.0052\,X_2X_3 + 0.000726\,X_1^2 - 0.00381\,X_2^2 - 0.2029\,X_3^2 \quad [5.1]$$

or,

$$\sqrt{\text{sCOD}} = 58.18 - 0.7918\,X_1 + 7.14\,X_2 + 0.7942\,X_3 + 2.81\,X_1X_2 - 1.72\,X_1X_3 - 1.05\,X_2X_3 + 0.2906\,X_1^2 - 9.55\,X_2^2 - 3.25\,X_3^2 \quad [5.2]$$

To analyze the output response of VFA, max/min=1.529 which is less than 3, did not necessitate the application of power transformation and the regression model for VFA (mg/L) in terms of actual and coded factors was thereby obtained as Eq. (5.3) and (5.4) respectively.

$$\text{VFA} = -63.058 + 5.112\,X_1 + 9.56\,X_2 + 56.36\,X_3 + 0.012\,X_1X_2 + 0.085\,X_1X_3 + 0.034\,X_2X_3 - 0.0715\,X_1^2 - 0.0709\,X_2^2 - 3.142\,X_3^2 \quad [5.3]$$

or,

$$\text{VFA} = 672.64 - 32.32\,X_1 + 38.24\,X_2 - 46.03\,X_3 + 11.88\,X_1X_2 + 6.88\,X_1X_3 + 6.88\,X_2X_3 - 28.64\,X_1^2 - 177.30\,X_2^2 - 50.29\,X_3^2 \quad [5.4]$$

Upon solving either of the equations for output responses (sCOD and VFA), the optimum value for each independent variable was established for optimizing both the output responses for anaerobic digestion of pretreated PRS.

Table 5.4 Design matrix by CCD-RSM with experimental and predicted outputs

Run order	Applied voltage (V)	Exposure time (min)	Electrode spacing(cm)	sCOD (mg/L)		VFA (mg/L)	
	X_1	X_2	X_3	Experimental	Predicted	Experimental	Predicted
1	60	70	12	3499.91	3384.91	674.00	672.64
2	86.3215	70	12	3211.49	3322.37	585.00	580.51
3	40	20	16	2199.61	2087.58	380.00	362.58
4	60	4.1963	12	1020.16	1039.42	305.00	315.21
5	60	70	17.2643	2860.11	2872.96	520.00	524.96
6	33.6785	70	12	3591.6	3567.67	660.00	665.57
7	80	20	8	1380.12	1211.74	385.00	380.01
8	80	120	16	3019.5	2794.18	400.00	401.93
9	40	120	8	2599.98	2433.45	520.00	521.12
10	60	70	12	3499.91	3384.91	674.00	672.64
11	80	20	16	1160.08	1228.5	290.00	287.95
12	86.3215	70	12	3211.49	3322.37	585.00	580.51
13	33.6785	70	12	3591.6	3567.67	660.00	665.57
14	40	20	8	1380.12	1488.42	485.00	482.14
15	60	70	17.2643	2860.11	2872.96	520.00	524.96
16	80	120	8	3165.19	3226.24	450.00	466.49
17	40	120	16	2560.36	2731.11	425.00	429.06
18	60	70	6.7357	2586.74	2653.28	650.00	646.12
19	60	135.804	12	2557.32	2604.06	425.00	415.86
20	60	135.804	12	2557.32	2604.06	425.00	415.86
21	60	4.1963	12	1020.16	1039.42	305.00	315.21
22	60	70	6.7357	2586.74	2653.28	650.00	646.12

5.2.2 Statistical significance and fitting of the model

5.2.2.1 Effect on soluble chemical oxygen demand

To evaluate the significance and adequacy of the mathematical model, analysis of variance (ANOVA) was applied. ANOVA is a statistical tool applied to determine any significant difference among the group of parameters and checks the impact of the group of factors by comparing their means (Zuo et al., 2020). The result of the ANOVA for quadratic model of sCOD using square-root power transformation is shown in Table 5.5. The model F-value was 91.96 suggesting the model was significant with only 0.01% chance of this large value occurring due to noise. The regression model analysis suggested that linear term (X_2), quadratic terms (X_1X_2 and X_1X_3) and interactive terms (X_2^2 and X_3^2) were significant model terms (p-value<0.05). Degrees of freedom (DF) of lack of fit was 5 (greater than 3) and DF of pure error was 7 (greater than 5) suggesting a valid lack of fit test. The coefficient of variance (C.V.) was 2.94 which was very low suggesting higher reliability and accuracy of the experimental data points (Behera et al., 2018) The R^2 value of 0.9857 advocated that the regression model could explain 98.57% variability in the dependent output response suggesting high significance of the regression model (Granato and de Araújo Calado, 2014). The R-squared value > 0.75 indicates a substantially good fit of the model. The predicted R^2 of 0.8857 was in reasonable agreement with the adjusted R^2 of 0.9750 (since $R^2_{adj} - R^2_{pred} < 0.2$). Adequate precision of 27.921 measured the signal to noise ratio which was desired to be less than 4. This model indicated an adequate signal and therefore, could be used to navigate the design space.

Table 5.5 ANOVA for response surface quadratic model of sCOD

Source	Sum of squares	DF[g]	Mean Square	F-value[h]	p-value[i]
Model	1764.34	9	196.04	91.96	< 0.0001
X_1 (Voltage)	9.36	1	9.36	4.39	0.0580
X_2 (Time)	760.86	1	760.86	356.90	< 0.0001
X_3 (Electrode spacing)	9.42	1	9.42	4.42	0.0574
$X_1 X_2$	63.12	1	63.12	29.61	0.0001
$X_1 X_3$	23.65	1	23.65	11.09	0.0060
$X_2 X_3$	8.74	1	8.74	4.10	0.0657
X_1^2	0.7346	1	0.7346	0.3446	0.5681
X_2^2	793.62	1	793.62	372.27	< 0.0001
X_3^2	91.76	1	91.76	43.04	< 0.0001
Residual	25.58	12	2.13		
Lack of Fit	25.58	5	5.12		
Pure Error	0.00	7	0.00		

SD[j]	Mean	R^2	R^2_{adj}	R^2_{pred}	Adequate precision	C.V[k]
1.46	49.69	0.9857	0.9750	0.8857	27.92	2.94

[g] Degrees of freedom; [h] Fishers (F) test; [i] Probability value (< 0.05 is significant and > 0.1 is not significant); [j] standard deviation; [k] co-efficient of variation

5.2.2.2 Effect on volatile fatty acids

The result of the ANOVA for quadratic model of VFA is shown in Table 5.6. The model F-value of 388.92 expressed the model was significant. In this regression model for VFA analysis, X_1, X_2, X_3, $X_1 X_2$, X_1^2, X_2^2 and X_3^2 were significant model terms (p-value< 0.05). The LOF sum of squares was similar to the residual error implying non-significant LOF relative to the pure error, which was desirable for the model to fit. The low C.V value of 2.00 implied a greater degree of accuracy and credibility of the experimentation data points. The R^2 value of 0.9966 implied more than 99.66% of the variance was attributable to the variables in VFA production. The predicted R^2 (0.9790) was in reasonable agreement with adjusted R^2 (0.9940) with adequate precision of 57.179 and these analyses proved the high degree of reliability of the response model.

Table 5.6 ANOVA for response surface quadratic model of VFA

Source	Sum of squares	DF	Mean Square	F-value	p-value
Model	3.485E+05	9	38727.66	388.92	< 0.0001
X_1 (Voltage)	15589.32	1	15589.32	156.55	< 0.0001
X_2 (Time)	21829.73	1	21829.73	219.22	< 0.0001
X_3 (Electrode spacing)	31632.43	1	31632.43	317.66	< 0.0001
$X_1 X_2$	1128.13	1	1128.13	11.33	0.0056
$X_1 X_3$	378.13	1	378.13	3.80	0.0751
$X_2 X_3$	378.13	1	378.13	3.80	0.075
X_1^2	7133.26	1	7133.26	71.63	< 0.0001
X_2^2	2.735E+05	1	2.735E+05	2746.14	< 0.0001
X_3^2	21996.99	1	21996.99	220.90	< 0.0001
Residual	1194.94	12	99.58		
LOF[1]	1194.94	5	238.99		
Pure Error	0.0000	7	0.0000		

SD	Mean	R^2	R^2_{adj}	R^2_{pred}	Adequate precision	C.V
9.98	498.77	0.9966	0.9940	0.9790	57.179	2.00

[1] Lack of Fit; p-value<0.05 is significant and p-value >0.1 is insignificant

5.2.3 Combined interactive effect of independent variables on sCOD

A three-dimensional response surface and two-dimensional contour plot were generated to discern the interactive effect of independent variables keeping one variable constant at the central level. Fig 5.7 shows the interactive effect of applied voltage, exposure time and electrode spacing on solubilization of PRS. Solubilization of any organic substrate can be quantified by total suspended solids (TSS), total dissolved solids (TDS), TS and soluble COD but due to the recalcitrant and oily nature of PRS depicting a low concentration of soluble COD (Table 1), sCOD is taken as an indicator of solubilization of this substrate (Haak et al., 2016; Siddique et al., 2017). In Fig. 5.7(a), the sCOD concentration increased with the increase in applied voltage and time until it reached an optimum value of 3594.76 mg/L, only to decline thereafter (voltage >76.14 V and time> 99.52 min). The increase in sCOD concentration can be attributed to the fact that the application of DC in PRS increases the

conductivity leading to an increase in sCOD due to conversion of complex double or triple-bonded hydrocarbons and low molecular-weighted polyaromatics to a soluble organic fraction (Niqui-Arroyo and Ortega-Calvo, 2010). The number of protons released from the sludge electrolyte just counterbalanced the number of electrons supplied by DC power supply at 76.14V for 99.52 min (central electrode spacing) and therefore, till that operating condition, the sCOD increased upto 3.21 times of the untreated PRS. But the decrease in solubilization thereafter might be due to an increase in resistance which led to an increase in ohmic heating thereby restricting the flow of electrons (Kaur and Singh, 2016). At the central level of electrode spacing, when 80V was applied constantly for 20 min duration, the sCOD was obtained to be minimum (1457 mg/L). At higher voltages, the electrical resistance in PRS is higher and ohmic heating is faster which might have reduced the rate of increase in solubilization (Conrardy et al., 2016). For example, in this study, at an electric potential of 6.67 V/cm, the temperature of the electrolyte increased by 15°C in 20 min whereas at a lower electric potential of 3.33V/cm for 20 min resulted in only 7°C rise in temperature. The effect of voltage and time (X_1X_2) is highly significant in deciding the output response of sCOD due to the low p-value ($p<0.0001$). The voltage to be varied between 40V and 80V was incorporated in the RSM model due to great efficiencies observed in sludge dehydration (56-63%), solids removal (5-14%) and hydrocarbon removal (40-54%) in previous studies (Elektorowicz et al., 2006; Yang et al., 2005).

In Fig. 5.7(b), the interactive effect of voltage and electrode spacing on sCOD was observed at the central level of exposure time (70 min). At any given constant voltage, the sCOD increased with an increase in electrode spacing up to an optimum value and decreased thereafter with any subsequent increase in electrode spacing. Both maximum and minimum interactive effects on sCOD were recorded for 40 V but at different electrode spacings of 13.5 cm (3570.16 mg/L) and 8 cm (2862.5 mg/L) respectively. The maximum and minimum effect increased the output response (sCOD) by 3.2 and 2.55 times that of untreated sludge respectively but the maximum interactive effect had a desirability of 99.3% which was much higher compared to that of minimum interactive effect (23%). This suggests higher credibility of the maximum optimum output condition (40V, 13.5 cm electrode spacing). Higher electrode spacing increases resistance due to less flow of electrons and this might be the reason that at 40V, with 5.5 cm increase (8 cm to 13.5 cm) in electrode distance, the percentage increase in sCOD was only 24.5% (Gidudu and Chirwa, 2020). The electric potential of 2.9V/cm (40V, 13.5cm) should also exhibit a higher O/W demulsification rate compared to that of 5V/cm (40V, 8 cm) since demulsification of oily sludge is higher at lower potential gradients. (Yang et al., 2005). The rate of change of sCOD with varying applied voltages and electrode spacings at central level of exposure

time was not very profound as compared to other corresponding independent parameters but the experimental data points advocated a high degree of reliability due to the low p-value (p=0.006) of X_1X_3 which was highly significant for the response model.

Fig. 5.7(c) represents the interactive effect of electrode spacing and exposure duration at central level of voltage. The sCOD increased with increase in electrode spacing and exposure duration up to an optimum value (3542.67 mg/L), at an operating condition of 60 V at 12.26 cm for 88.5 min, and decreased thereafter with any subsequent alteration of electrode distance (>12.26 cm) and time (>88.5 min). For a particular electrode potential, electrokinetic treatment increases soluble organic matter accumulation (in terms of COD) and water removal efficiency with an increased exposure time (Yuan and Weng, 2003). Change in pollutant dynamics of PRS due to application of EK treatment is due to electroosmotic flow driven by the electric field produced by the applied DC voltage in the sludge electrolyte. But when a specific potential gradient is applied beyond the optimum condition, the number of protons released by the sludge electrolyte becomes insufficient to neutralize the number of additional electrons being applied to the system by DC power supply (Kargi et al., 2010). Therefore, after achieving an optimum condition, the evaporation of volatile acids leads to a decrease in solubilization of PRS thereby decreasing sCOD concentration. Also, the heavier-weighted hydrocarbons (polyaromatics) which are difficult to solubilize due to their recalcitrant nature might have required higher applied voltage or exposure time which would have further improved the solubilization (Yuan and Weng, 2003). But the goal of this study was to improve solubilization to a percentage where the consortia of anaerobic microorganisms will be able to easily degrade the substrate (PRS) due to hydrolysis stage abridgment, thereby augmenting the biogas production, cogitating a sustainable amount of power investment in the pretreatment process.

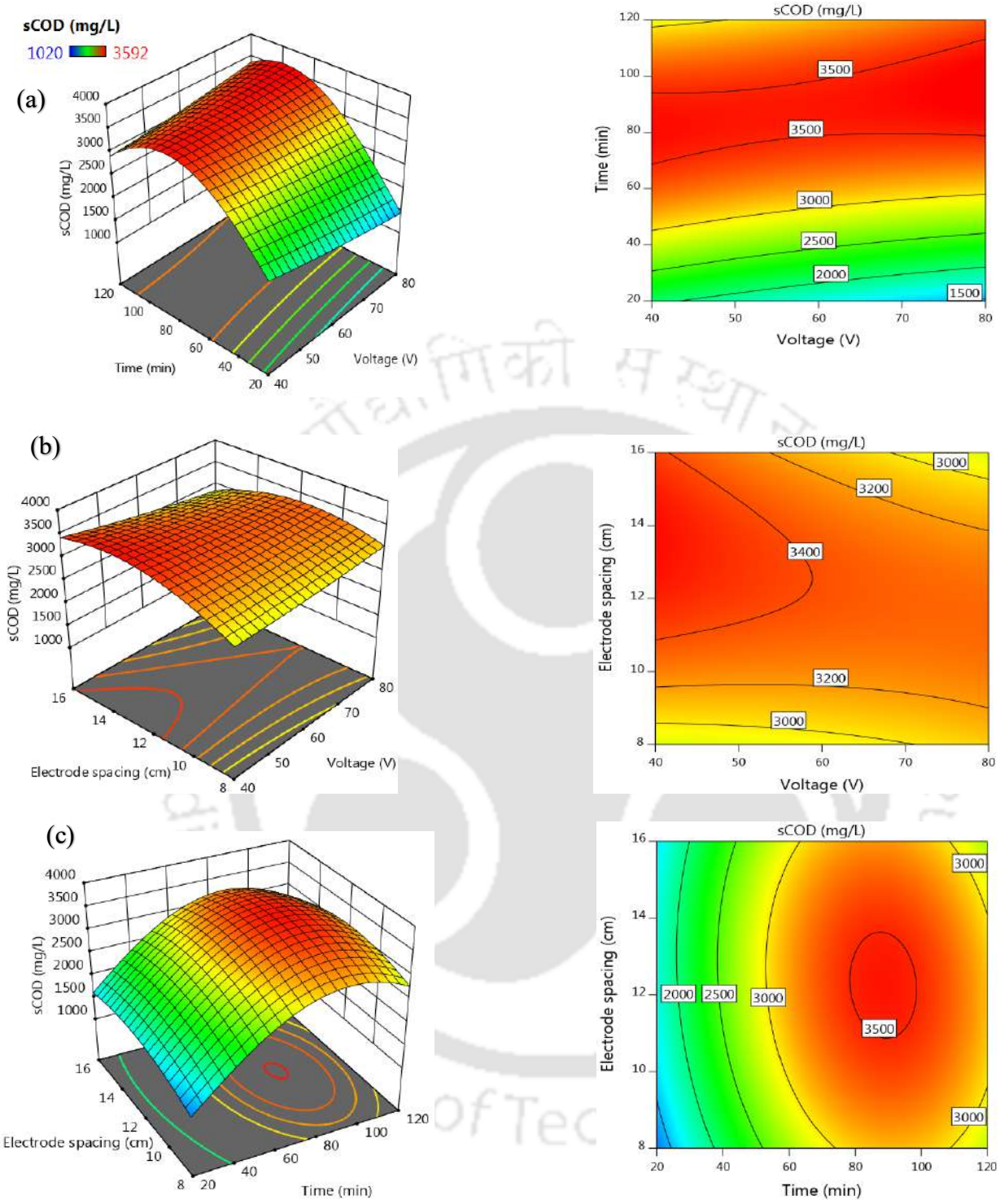

Fig. 5.7. Response surface (3D) and contour plots (2D) of different variable interaction on soluble chemical oxygen demand (a) interactive effect of voltage and time (b) interactive effect of voltage and electrode spacing (c) interactive effect of electrode spacing and time

5.2.4 Combined interactive effect of independent variables on VFA

Fig. 5.8 shows the interactive effect of applied voltage, exposure time and electrode spacing on volatile fatty acids (VFA) content of PRS. Quantitative analysis of VFA is decisive to bioenergy production since it is essential for the maintenance of the metabolism of microbial community inside an anaerobic reactor (Zhou et al., 2018). In Fig. 5.8(a), applied voltage and exposure time were varied at central level of electrode spacing. The VFA increased with the increasing exposure period achieving the maximum output response (682.45 mg/L) at an applied voltage of 52.15 V for 75.53 min and decreased thereafter with any subsequent alteration in operating conditions. The maximum VFA increased by 2.73 times that of the untreated PRS which might be attributed to the breakage of unsaturated hydrocarbons since they are more reactive compared to saturated hydrocarbons. For example, alkenes are hydrocarbons consisting of carbon-carbon double bond (C=C) which are relatively more reactive than the C-C bond of alkanes. The double bond of an alkene consists of one sigma (σ) and one pi (π) bond. This π -bond is weaker and acts as a nucleophile facilitating the addition of electrophiles in presence of an electric field provided by DC supply. This ultimately leads to the formation of short-chain fatty acids (VFA) due to improved sludge dewaterability in presence of an electric field (Yang et al., 2005; Zeng et al., 2019). A study conducted by Yang et al. (2005) was reported to have increased pH with the applied DC supply in oily sludge where they hypothesized the reason behind as long-chain fatty acid (carboxylic acid) dissociation into negatively charged fatty acid $RCOO^-$ radicals and H^+ ions where $RCOO^-$ would combine with metal ions (Na^+, K^+) present in the sludge to form the fatty acid salt and H^+ and OH^- would combine to form water increasing sludge dewaterability which can be advocated by this study which sees an improvement in the VFA (short-chain fatty acids) concentrations due to the applied electric field. Also, as the processing time of the pretreatment process increments, the hike in VFA production is proportional to the available electrical energy supplied with increasing voltage for solubilization of complex organic substrate (Gidudu and Chirwa, 2020). This eventually improves the bioaccessibility of contaminant hydrocarbons (Niqui-Arroyo and Ortega-Calvo, 2010). When the voltage is increased beyond optimum (>52.15 V), the number of protons being released from the substrate became insufficient to equalize the enormous number of electrons being released by DC supply thereby decreasing VFAs and solubilization (Yu et al., 2014; Gidudu and Chirwa, 2020). Also, the extra negatively charged dissociated long-chain fatty acid radicals ($RCOO^-$) not reacting with the scanty metal ions, might have migrated back to the anode by electrostatic forces and recombined with H^+ ions leading to decrease in VFA (Yang et al. (2005).

The interactive model of voltage and time variation is highly significant ($p<0.05$) and therefore, the results are extremely credible.

The variation of electrode spacing and voltage at central level of exposure time was observed in Fig. 5.8(b). The increase in applied voltage and electrode spacing increased VFA till 51.4 V and 10.2 cm electrode spacing and decreased subsequently (>51.4 V and >10.2 cm spacing). The minimum output response (522 mg/L) was obtained at 80V and 16 cm electrode spacing. Higher voltage might enhance the electroosmosis and electrophoresis but higher electrode spacing sedates the decontamination process (Gidudu and Chirwa, 2020).

Fig. 5.8(c) shows the interactive effect of electrode spacing and exposure period on VFA concentration at central level of voltage (60V). The VFA concentration increased with increase in electrode spacing and exposure time achieving the peak value (676.5 mg/L) at an electrode distance of 9 cm exposed for a duration of 66.2 min. The significant hike in VFA was observed after 66.2 min duration of pretreatment as compositional changes in sludge (e.g., dewaterability, solubilization, evaporation of fatty acids) were more profound at higher processing time of EK pretreatment (Yuan and Weng, 2003; Guo et al., 2011). The VFA was found the least at an electrode spacing of 16 cm and duration of 20 min. Clearly, the EK pretreatment duration is the most crucial parameter in VFA concentration monitoring. Different types of VFA have different actions on the archaeal and bacterial community of an anaerobic digester and therefore, optimum VFA levels are conditional on the type of digester and feedstock (Franke-Whittle et al., 2014). In this study, all the analyses advocated that the regression model was significant and the optimization results obtained by CCD-RSM for VFA optimization were reliable and admissible.

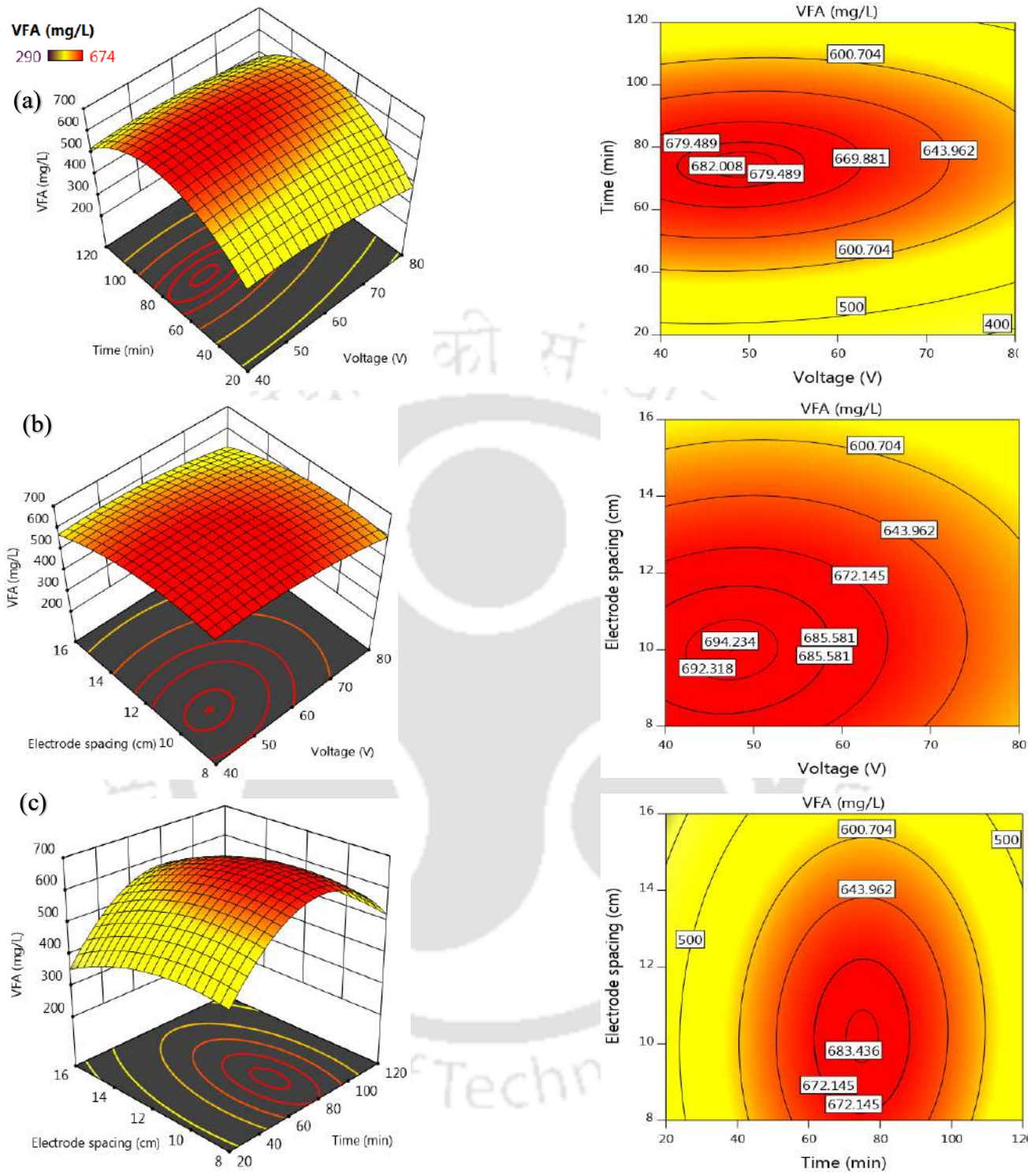

Fig. 5.8. Response surface (3D) and contour plots (2D) of different variable interaction on volatile fatty acids (a) interactive effect of voltage and time (b) interactive effect of voltage and electrode spacing (c) interactive effect of electrode spacing and time

5.2.5 Validation of the model

In order to check the conformity of the optimization model, the sCOD and VFA analyses for EK pretreatment were performed at the optimum condition (voltage: 60V, exposure time: 83.5 min and electrode spacing: 11.6 cm) with a desirability of 99.3% for maximizing solubilization and VFA concentrations. The validation experiment resulted in sCOD and VFA values (Table 5.7) within the standard deviation of the predicted values of sCOD (3519.82 ± 203.27mg/L) and VFA (674±9.97 mg/L) obtained from the model. The sCOD and VFA incremented by 230% and 172% compared to control which were comparable with the study of Lee and Rittmann (2011), who obtained 220% improvement in sCOD after application of high-voltage pulsed electric current as pretreatment to waste activated sludge (WAS).

Table 5.7. Compositional analysis before and after pretreatment of PRS

Pretreatment	sCOD (mg/L)	VFA (mg/L)
Before	1120 ± 86.56	250 ± 8.41
After*	3700 ± 176.58	680 ± 5.72

All values are mean ± SD; *Pretreatment (60V, 83.5 min, 11.6 spacing)

5.2.6 FTIR

The FTIR spectra before and after electrokinetic pretreatment of PRS are shown in Fig. 5.9. The absorbances at 3302 cm^{-1} and 2121.05 cm^{-1} indicated O-H stretch corresponding to the hydroxyl group and water, and symmetric/asymmetric C-H aliphatic stretch respectively (Ennouri et al., 2016). After pretreatment, their declining absorbances signified intramolecular and intermolecular changes in PRS. The declining absorbance of the sharp peak at 1642.43 cm^{-1} after pretreatment of PRS signified fragmentation of -C=C- stretch corresponding to alkenes and aromatic rings confirming our stated hypothesis in VFA accumulation after pretreatment, whereas the short-broadened peak observed at 1412.33 cm^{-1} indicated reduction of C-H stretch for methyl group. The newly formed sharp peak at 1016.33 cm^{-1} after pretreatment indicated a significant fragmentation of C-O stretch of primary alcohols from PRS while the absorbance at 612.28 cm^{-1} corresponded to phenyl group of PRS which showed a significant reduction in the intensity after pretreatment suggesting the molecular level alteration in PRS due to electrokinetic pretreatment (Rajasekar et al., 2005).

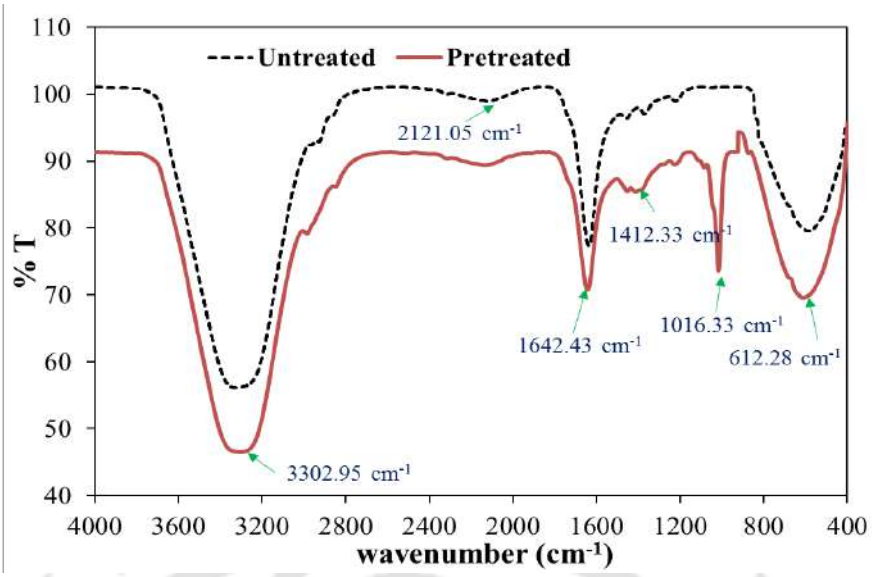

Fig. 5.9. FTIR spectra before and after electrokinetic pretreatment of PRS at optimized operating conditions from RSM

5.2.7 BMP test assay after electrokinetic pretreatment of PRS

Fig. 5.10 shows the anaerobic degradation of different inoculum:sludge (DS:PRS) ratios of electrokinetic pretreated PRS at optimum operating conditions obtained from the regression model by RSM. The increment in sCOD and accrual of VFA concentrations due to EK pretreatment expedited the hydrolysis stage augmenting biogas from PRS. The highest biogas yield was observed on the 25th d for DS:PRS = 0.4 which was 57.3% higher than that of the untreated (control) sludge as shown in Fig. 5.10(a). The maximum cumulative biogas yield from Fig. 5.10(b) was also observed for ratio DS:PRS = 0.4 resulting in 66.7% increase compared to that of the control, which was much higher than that obtained in other studies utilizing WAS as substrate (Westerholm et al., 2016; Lee and Rittmann, 2011). The cumulative biogas production followed the order of DS:PRS ratios as: 0.4> 0.3> 0.7>0.5 resulting in subsequent increases of 66.7%, 49.5%, 33.69% and 30.08% of biogas compared to untreated respectively. Salerno et al. (2009) applied pulsed electric field as pretreatment to WAS which increased biogas potential by 100% due to improvement in solubilization in terms of sCOD. In this study, the subsequent improvement in daily biogas from 10th to 40th d of digestion could be attributed to the microbial attack susceptibility to PRS which varies in the order: n-alkanes> branched alkanes> small aromatics> cyclic alkanes> polycyclic aromatics (Das and Chandran, 2011). The intensified sCOD of PRS after pretreatment was readily accessed by the hydrolytic and fermentative bacteria to produce VFA and organic acids which could be advocated by the reduction in pH during the first 30 d of digestion as seen in Fig. 5.10(c) (Lee and Rittmann, 2011). pH affects the AD process

in terms of hydrolysis rate, microbial community dominance created by the seeding environment, biogas production and inhibition by recalcitrant components. The lowering of pH in the range of 6.795-6.88 for all mixing ratios except control depicted degradation through enzymatic reactions, and further improvement in pH (6.88-7.53) from 30th to 60th d hinted the predominance of methanogenic activity with sufficient buffering capacity during that period. The optimum pH should be in the range of 6.8-7.2 to prevent reactor failure from excess acidification and poor buffering capacity (Cioabla et al., 2012). The control sludge showed poor degradation and delayed fermentative activity due to the lowering of pH after 40 d of digestion period which could also be observed from its VS (organic matter) removal percentage of only 7.84% as shown in Fig. 5.10(d) by the end of 60 d. The organic matter removal was measured in terms of VS reduction percentage and observed to be the maximum for DS:PRS = 0.4 owing to the fact that this ratio provided highest biogas too. By 60th d, the VS degradation followed the order: 0.4>0.3>0.5>0.7. Though the biogas yield from ratios 0.5 and 0.7 were almost similar but VS degradation of ratio 0.5 was 24.3% higher than ratio 0.7. This might be attributed as underutilization of added VS in ratio 0.7 or production of some inhibitory substances (such as H_2S or NH_3) or insufficient acclimatization of the reactor. In contrast to that, there might be an underestimation of biogas yield from ratio 0.5 due to leakage of gas from the batch anaerobic reactor as well. The possibility of leakage can arise during sample collection for analysis when the rubber stoppers were not resealed properly (Haak et al., 2016). The VS removal of about 63% from this study was higher compared to the study of Lee and Rittmann (2011) reporting volatile suspended solids removal efficiency of less than 30% after 20 d of solids retention time for AD of pulsed electrically pretreated WAS and Westerholm et al. (2016) reporting 49% VS removal after 72 d of anaerobic digestion (phase I) of electrokinetic pretreated WAS.

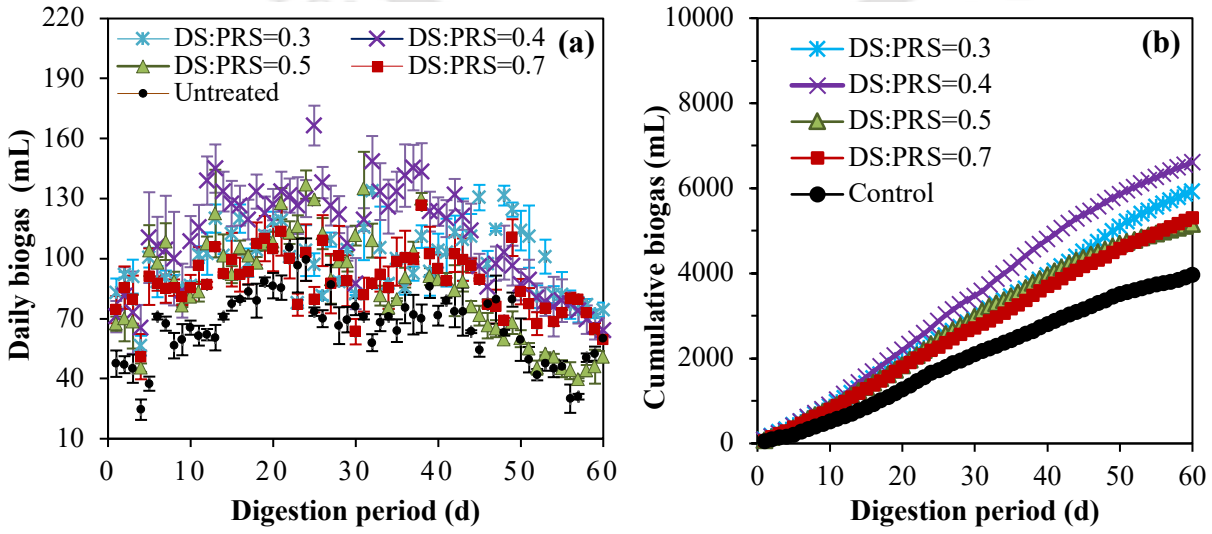

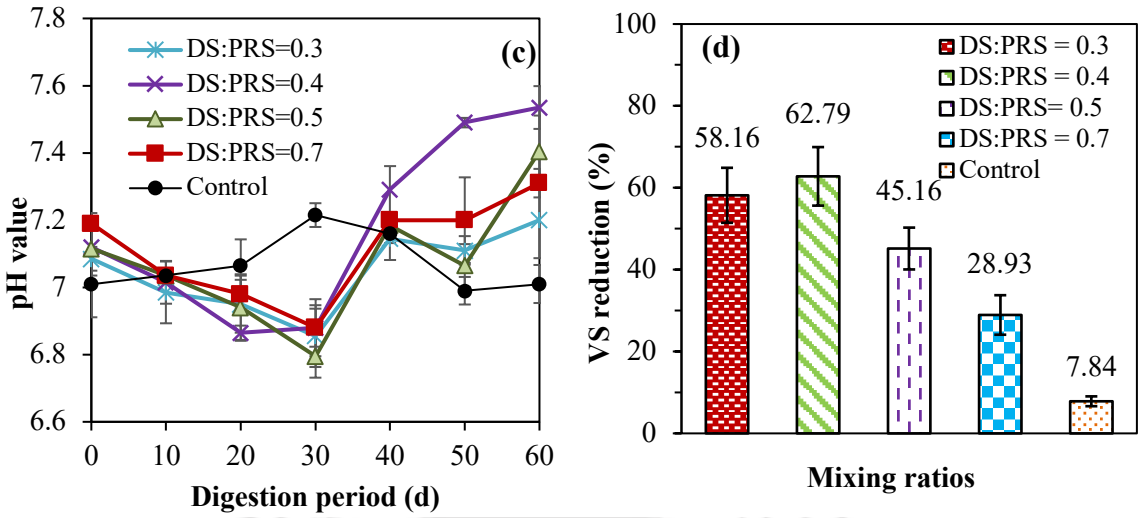

Fig. 5.10. Variation in (a) daily biogas, (b) cumulative biogas (c) pH and (d) VS reduction during digestion of EK pretreated PRS

5.2.8 Energy assessment

The energy assessment is imperative to justify the economic viability of the pretreatment used for PRS with an aim to ameliorate its biodegradability. The energy demand for the pretreatment process should not exceed the amount of energies recovered in the form of biogas. Electrokinetic pretreatment of PRS at optimum operating conditions (applied voltage: 60V; exposure duration: 83.5 min; electrode spacing: 11.6 cm) resulted in a net positive energy, ΔQ = 3508.23 kJ (where Q_{in} = 322.06 kJ and Q_{out} = 3830.346 kJ). This signified the feasibility of the pretreatment process with satisfactory energy recovery efficiencies making it a sustainable strategy for the utilization of petroleum refinery wastes.

5.2.9 Phytotoxicity assessment

In order to evaluate the quality of digestate to be discharged into the environment after the AD process, toxicity test is conducted. It also gives an estimate of the quality of sludge samples before being discharged into the environment. In this study, the different mixing ratios of PRS samples after the AD were assessed for their phytotoxicity using *V. radiata* L. on the germination of seed. PRS when disposed in reclaimed lands or soils, has the potential to deteriorate their physical-biochemical properties restricting plant productivity and growth due to decrease in soil enzymes and microbial abundance. PRS can cause restriction of essential nutrients, oxygen, water and even cause groundwater contamination (Haider et al., 2021). The impact of PRS toxicity could be well observed through *V. radiata* L. seed germination inhibition percentages at different dilutions (50%, 75% and 100%) impacting the root, shoot and seedling biomass growth of plants (Table 5.8).

Table 5.8. Effect of different concentrations of untreated and EK pretreated PRS samples on seed germination, shoot length, root length and biomass of early seedling of *V. radiata* L.

Sludge	Dilution ratio (%)	Germination (%)	Shoot length (cm)	Root length (cm)	Biomass (gm)
Control	-	100±0.32	10.04±0.73	8.17±0.57	1.06±0.09
Untreated	50	73.33±0.57*	7.24±0.23	5.80±0.28*	0.82±0.03
	75	63.33±0.53*	5.14±0.54*	3.24±0.17*	0.71±0.04
	100	46.67±0.57*	3.90±0.51*	1.73±0.26*	0.64±0.04
DS:PRS=0.3	50	93.33±0.31*	7.84±0.64*	6.02±0.53	0.94±0.02
	75	90±0.28*	6.84±0.51*	4.89±0.48*	0.87±0.04
	100	83.33±0.44*	4.88±0.38	2.73±0.12*	0.72±0.03
DS:PRS=0.4	50	100±0.27*	8.92±0.72	6.82±0.44*	0.97±0.05
	75	96.67±0.31*	7.84±0.37*	5.89±0.38*	0.91±0.07
	100	90±0.62*	6.28±0.64*	3.89±0.31*	0.88±0.04
DS:PRS=0.5	50	96.67±0.15*	8.18±0.61*	6.91±0.48*	0.95±0.02
	75	93.33±0.31*	7.06±0.52	5.94±0.37*	0.9±0.04
	100	90±0.39	5.61±0.34*	2.94±0.29	0.88±0.06
DS:PRS=0.7	50	100±0.34*	9.06±0.81*	7.02±0.55	0.97±0.03
	75	96.67±0.16*	8.12±0.59*	5.68±0.41*	0.92±0.02
	100	93.33±0.38*	5.79±0.42*	3.24±0.45*	0.90±0.05

Values are mean ± standard deviation from triplicates

*p <0.05, significant when compared to control using Analysis of variance (ANOVA)

The rate of germination was observed to be 73%, 63% and 46.7% for the untreated extract of PRS at dilutions of 50%, 75% and 100% respectively. As a result, the germination index (GI) was evaluated and plotted as shown in Fig. 5.11. GI is an indicator of both the germination rate and root length of plants since the roots are not only responsible for the translocation of soluble toxic components to the plants through shoots, but also change the composition, water holding capacity and mineralogical

components of soil (Merkl et al., 2005). Polar, non-ionizable and water-soluble hydrocarbon compounds are transported by the roots of germinated plants to their shoots leading to the bioaccumulation of the polyaromatic hydrocarbons (PAHs) in plants. Even the constituents of PRS bind to the soil particles and trap pore water increasing the mobility of hydrocarbon compounds to the subsurface layers of soils (Dettenmaier et al., 2009; Haider et al., 2021).

After the AD of pretreated PRS, the rates of germination increased (Table 5.8). For 50% digestate dilution extract, the GI order of DS:PRS ratios was: 0.7 ≈ 0.4>0.5>0.3. For 75% dilution, the order was 0.4>0.7 = 0.5>0.3 and for 100% dilutions, the order was: 0.7>0.4>0.5>0.3. The mixing ratio 0.4 showed maximum biogas yield and organic matter removal and therefore, its digestate showed maximum germination rate and GI for dilutions 50% and 75% digestate extract, suggesting the activation of microbial flux in the process environment was optimum at that mixing ratio to utilize the organic fraction of the substrate to the maximum leading to reduced inhibition. The reduction of immiscibility of PRS emulsions due to EK pretreatment led to enhancement of soluble organic carbon fraction thereby steering the AD process compared to that of the untreated PRS (Elektorowicz et al., 2006; Gill et al., 2014; Gidudu and Chirwa, 2020). The least GI of mixing ratio 0.3 may be attributed to the underutilization of intracellular organic content till 60 d of digestion period requiring a higher digestion period. Also, there might be toxic inhibition on the anaerobic microbial community for ratio 0.3. The biomass growth was sufficiently improved after the AD process for all the mixing ratios (maximum biomass growth observed for DS:PRS=0.4) due to the reduction of petroleum hydrocarbon content leading to decreased phytotoxicity. The phytotoxicity and increased germination inhibition in untreated PRS could be attributed to the oxidative stress induction due to the high concentration of aliphatic and aromatic hydrocarbon content (Merkl et al., 2005; Haider et al., 2021). The substantial improvement in shoot, root and seedling growth (Table 5.8) for all the mixing ratios (DS:PRS) signified the alteration of the organic hydrocarbon and phenolic pollutants during the AD process leading to decreased toxicity.

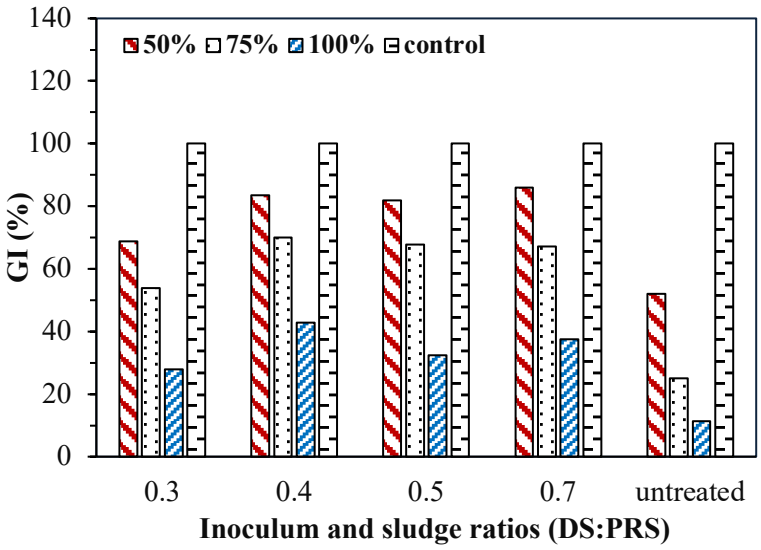

Fig. 5.11. Variation of germination index (%) of *V. radiata* L. for all inoculum and substrate (DS:PRS) ratios after the anaerobic digestion process

5.2.10 Scaled-up batch study of electrokinetic pretreated PRS

5.2.10.1 Biogas yield

In Fig. 5.12(a), the peak daily biogas production from EK pretreated PRS at optimum operating conditions (60V, 83.5 min, 11.6 cm spacing) in presence of DS as seeding environment was obtained on 20th d which was about 32% higher and achieved 17 d earlier compared to untreated PRS within 60 d of digestion period. This attributed the accelerated hydrolysis phase dut to the applied EK pretreatment at optimum conditions. The cumulative biogas production after 60 d of digestion resulted in 61% increment after EK pretreatment as compared to untreated (Fig. 5.12b). The diminished biogas production observed in untreated PRS could be plausibly attributed to the presence of refractory organic compounds, including PAH and heterocyclic compounds (Haak et al., 2016; Roy et al., 2016). These specific compounds have been extensively reported in the literature to exhibit toxicity towards methane-producing bacteria, impeding their metabolic activity (Haak et al., 2016). Consequently, the untreated PRS displayed a prolonged lag phase, as observed from the cumulative biogas production curve. The existence of these refractory organic compounds in PRS serves as a hindrance, inhibiting the efficient breakdown and conversion of organic matter into biogas. Therefore, EK pretreatment targeting the removal or transformation of these toxic compounds prove to be an be indispensable strategy to enhance the biogas production potential of PRS.

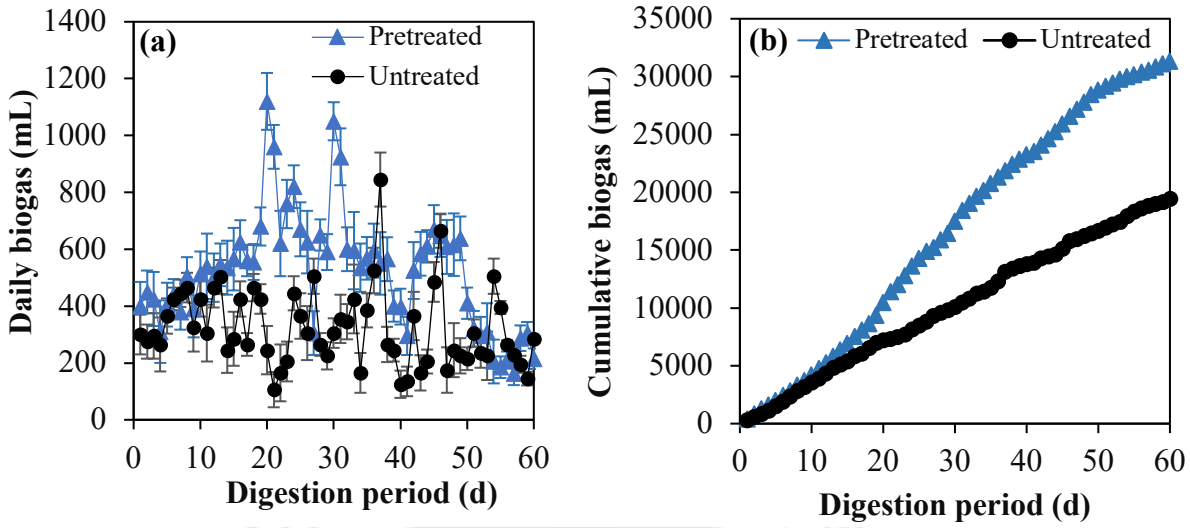

Fig. 5.12. Daily and cumulative biogas production of EK pretreated PRS at optimum conditions

5.2.10.2 Pollutant variation (TPH, O&G and total phenol)

During anaerobic degradation of petroleum hydrocarbons, the hydrogen-degrading microorganisms reduce hydrocarbon equivalents to molecular hydrogen (H_2) which is converted to CO_2 and CH_4 by the methanogenic archaea. In Fig. 5.13(a), a decreasing trendline was observed for the total petroleum hydrocarbon (TPH) content of the pretreated PRS with 57.4% removal by the end of digestion period of 60d. The TPH degradation of only 17% in untreated PRS could be due to the activity of sulfate-reducing, nitrogen-fixing and methanogenic consortium already present in PRS as reported by Roy et al. (2018). Microbial degradation of TPH involves two main types of hydrocarbons: aliphatic and aromatic. Aliphatic hydrocarbons undergo carboxylation, leading to the conversion of n-alkanes into fatty acids through fermentation. Enzymes like glutaryl-CoA dehydrogenase and acetyl-CoA acyltransferase play a crucial role in this process. Aliphatics can also follow a fumarate addition pathway or undergo β-oxidation, entering the tricarboxylic acid (TCA) cycle. Aromatic hydrocarbons can undergo fumarate addition, hydroxylation, or carboxylation, forming a common intermediate called benzoyl-CoA. The intermediate is then subjected to reductive dearomatization and hydrolytic ring cleavage, eventually entering the TCA cycle (Sierra-Garcia et al., 2014). Elektorowicz and Habibi (2005) reported 43% removal of light hydrocarbon content when the EK process was applied to remediate oily sludge.

The oil and grease (O&G) trendline during the AD process steadily decreased resulting in 72.44% removal by the end of the digestion period after EK pretreatment [Fig. 5.13(b)]. EK pretreatment leads

to the transportation of oil and grease (hydrophobic neutral molecules) within the organic substrate due to the electroosmotic (EO) flow created by the DC power supply. Under the influence of an electric field, the oil transport is due to the momentum transfers from EO flow of water occurring in pore surfaces which increases the permeability of PRS due to capillary enlargement by colloidal displacement (Ghazanfari et al., 2012). Also, PRS consists of emulsifying agents such as water-in-oil (W/O), organic acids, asphaltenes, resins and minerals which occur as a film on the surface of dispersed droplets of water. The finer particles get adsorbed at the surface fencing droplet coalescence (Elektorowicz and Habibi, 2005). This separation of solids from W/O emulsion improves the water droplet coalescence through the separation of water and oil (near cathode), thereby increasing the O&G removal and sludge dewaterability (Yuan and Weng, 2003; Glendinning et al., 2007). Yang et al. (2005) in their study reported efficient oil and grease removal for electrokinetic treatment conducted at 60 V and 22 cm electrode spacing and reported at voltages lower than 60V, the O&G removal was negligible. The O&G removal due to AD was enhanced by 4.6-folds due to EK pretreatment compared to untreated.

Total phenol decremented from 225.4 mg/L to 62.2 mg/L within 60 d of AD [Fig. 5.13(c)]. Total phenol removal of 72.43% obtained in this study at mesophilic temperature range led to 2.8 times improvement in phenol removal compared to untreated PRS indicating great potential for phenol degradation during AD of EK pretreated PRS.

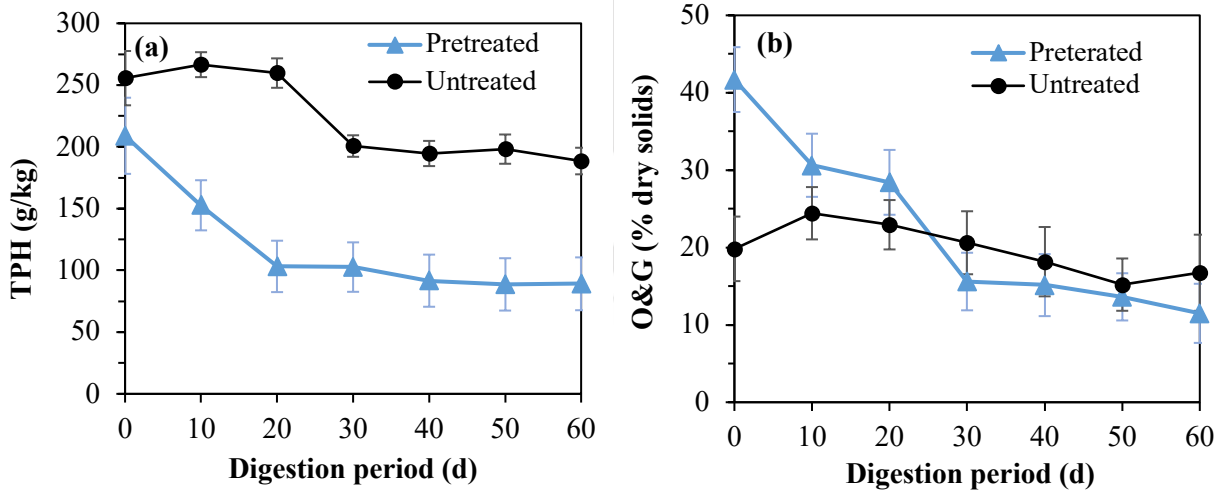

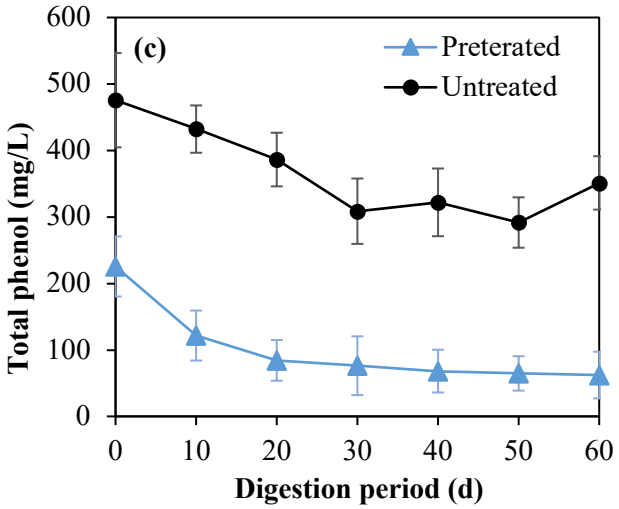

Fig. 5.13. Variation of (a) total petroleum hydrocarbon content, (b) oil and grease and (c) total phenol throughout the digestion period of EK pretreated PRS

5.3 MICROBIAL PRETREATMENT

(A) Pretreatment with Strain I (*Pseudomonas putida*)

5.3.1. Effect of *P. putida* strain on solubilization of PRS

P. putida strain has the potential to utilize PRS as a carbon substrate for population multiplication thereby degrading the hydrocarbon constituents. The extent of degradation depends on the enzymatic activity involved in the microbial species proliferation, which modifies the chemical characteristics of sludge through fragmentation of intermolecular bonds aiding the release of soluble organic dimers and monomers. This leads to improvement in the solubilization and biodegradation of sludge (Ward et al., 2003; Cerqueira et al., 2011). In this study, the effect of bacterial pretreatment using *P. putida* strain on solubilization of PRS was quantified by measuring soluble COD and volatile fatty acid (VFA) concentrations at three different dosages (10^7, 10^8 and 10^9 CFU/mL) (Fig. 5.14). PRS is rich in microbial diversity as reported by Roy et al. (2018b) and therefore, a control was kept as a reference to indicate the solubilization alteration in PRS due to the utilization of *P. puitda*. In Fig. 5.14 (a) and (b), the sCOD and VFA increased with the increment in pretreatment duration (incubation) for all the dosages till the optimum value and decreased thereafter with further increment in pretreatment duration. The maximum sCOD (7680 mg/L) and VFA (775.5 mg/L) were obtained on the 6^{th} d of incubation at a dosage of 10^8 CFU/mL. The maximum sCOD and VFA for dosage 10^8 CFU/mL were 3.49 and 2.22 times that of the untreated PRS. The incremented sCOD obtained in this study was 2.37 times higher than that obtained by Merrylin et al. (2013) who performed biological pretreatment of

municipal sewage sludge using *Bacillus licheniformis* strain. The initial increment in sCOD till the optimum value could be attributed to the oxidative process involved behind the intracellular attack of organic hydrocarbon present in PRS by a group of enzymes (oxygenases and peroxidases) catalyzing the incorporation of molecular oxygen (O_2) into the organic compounds (Cerqueira et al., 2011). These organic compounds get converted into intermediates of the central intermediary metabolism through peripheral degradation pathways during the process {e.g., tricarboxylic acid (TCA) cycle}. The biosynthesis of intermediates of the TCA cycle leads to an increase in biomass growth thereby improving the solubilization (Tuhuloula et al., 2019). The decrease in sCOD after the attainment of the peak value (6^{th} d) was due to the reduction in bacterial population due to the depletion in available organic carbon (food) leading to their endogenous decay. The peak sCOD obtained in this study for dosage 10^8 CFU/mL was 2.29 times higher as obtained by Kavitha et al. (2014), who utilized two *Bacillus* strains for pretreatment of waste activated sludge but their maximum sCOD was obtained 102 h earlier in comparison to this study. Pretreatment duration is one of the pivotal factors in bacterial pretreatment since the percentage of organic matter solubilization increases with an increment in pretreatment duration till the enzymatic activity intensification from the utilized microbial strain (single strain or composite strain), beyond which the solubilization ceases (Ferdeș et al., 2020). The order of solubilization at different dosages was: 10^8 CFU/mL> 10^9 CFU/mL> 10^7 CFU/mL. When PRS was pretreated with *P. putida* dosage of 10^9 CFU/mL, the maximum sCOD (5600 mg/L) and VFA (655.5 mg/L) increased by 2.54 and 1.87 times respectively that of the untreated. The maximum sCOD and VFA obtained for 10^9 CFU/mL were 27.08% and 15.47% lower than those obtained for dosage 10^8 CFU/mL. The rate of increase in solubilization can be lower at higher dosage of bacterial colonies due to extracellular enzymatic activity inhibition delaying the hydrolysis process (Kavitha et al., 2014; Ferdeș et al., 2020). The sCOD and VFA trend lines were similar for all the dosages. Initially, bacteria started consumption of the easily available soluble organic hydrocarbons (such as, aliphatic and long-chain hydrocarbons, unsaturated hydrocarbons) which when ceased, the bacteria secreted exoenzymes to solubilize the particulate organic fraction leading to bacterial growth thereby augmenting the sCOD and VFA concentrations till the particulate organic fraction availability. For pretreatment at a dosage of 10^7 CFU/mL, sCOD and VFA incremented by 2.53 and 1.38 times of untreated respectively which were lower than both the dosages. Although the growth of *P. putida* is fast and resistant to extreme conditions, these bacteria are utterly sensitive to high concentrations of hydrocarbon contaminants and are susceptible to oxygen and nutrients limitations. The gram-negative nature of *P. putida* delays and inhibits the biodegradation activity at higher concentrations of pollutants or lower dosages of bacteria utilized for sludge solubilization (Tuhuloula et al., 2019).The decrease in solubilization after 5^{th} and

6th d for dosages 10^9 CFU/mL and 10^7 CFU/mL respectively was due to the active enigmatic growth of the bacterial population on solubilized lysates of PRS (Kavitha et al., 2014). Therefore, the optimum dosage and duration of pretreatment were observed to be 10^8 CFU/mL for 6 d which maximized sCOD to be utilized for enhanced digestibility of PRS and the subsequent improved VFA shall ameliorate the hydrolysis of the complex substrate.

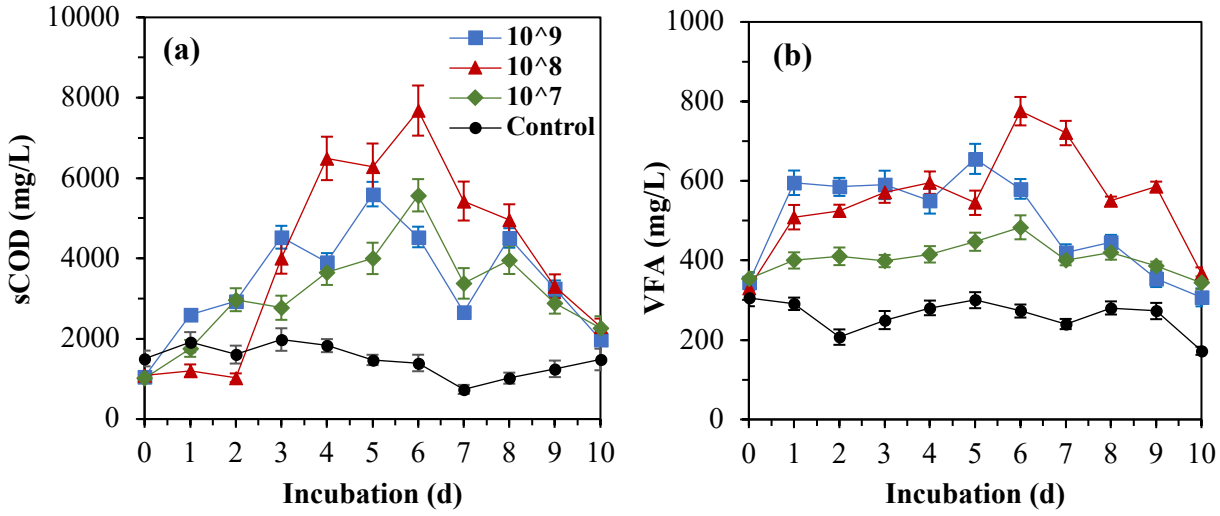

Fig. 5.14. Variation of (a) sCOD and (b) VFA during *P. putida* pretreatment

5.3.2. Effect of enzymatic activity due to *P. putida* pretreatment at optimum condition

The improved solubilization of PRS through bacterial pretreatment can be arbitrated by a specific enzymatic system. In this study, the effect of the enzymatic system throughout the pretreatment duration (10 d) was observed at the optimum dosage of 10^8 CFU/mL. Biodegradation of petroleum hydrocarbons depends on the intricacy of the chemical structure, type and position in group substitution and the adaptation level of the specific enzyme system (Verma et al., 2016; Tuhuloula et al., 2019). Laccases are multicopper blue oxidoreductase enzymes having the potential to oxidize phenolic as well as non-phenolic hydrocarbon compounds by converting O_2 molecule to water (H_2O) on coexistent four-electron reduction. Laccase enzymes are widely distributed as monomeric, dimeric and tetrameric glycoproteins characterized by some higher plants, fungi and bacteria, and its activity has been widely reported in *Pseudomonas* sp. (Verma et al., 2016; Bhandari et al., 2021). The laccase enzyme gradually accelerated from 1.64 to 18.84 IU/mL during the initial 6 d of incubation advocating the augmentation in solubilization during that period. The increase in enzymatic activity could be attributed to the catalytic potential of laccase affecting the oxidation of nonphenolic hydrocarbons and phenolic compounds having multiple functional groups by the formation of two H_2O molecules with

concomitant electron loss of a single O_2 molecule (Bhandari et al., 2021). The peak laccase activity of 18.84 IU/mL on 6th d commended the maximum sCOD and VFA obtained on 6th d suggesting maximum enhancement in the synthesis and breakdown of organic and aromatic hydrocarbon compounds present in PRS. Verma et al. (2016) obtained 25.12 IU/mL of laccase activity for the wild strain of *P. putida* LUA15.1. The enzymatic activity decreased after 6th d which could be attributed to the slowdown of laccase-catalyzed reaction due to the presence of recalcitrant compounds (high-molecular weighted) having higher redox potential or lower diffusion of PRS into active pockets making them extremely difficult to oxidize or degrade (Chauhan et al., 2017). The easily degradable hydrocarbon constituents were exhausted by the microbial population through secretion of extracellular laccase enzymes till 6th d resulting in maximum solubilization which decreased subsequently till 10th d (3.23 IU/mL) due to ceasing laccase enzymatic activity advocating a direct co-relation of solubilization due to bacterial pretreatment with the specific enzymatic system involved behind the bacterial species.

5.3.3. Chemical characteristics after *P. putida* pretreatment at optimum condition

The identification of the distribution of organic functional groups in untreated and pretreated PRS was done by Fourier Transform Infrared Spectroscopy (FTIR). The FTIR spectra before and after *P. putida* pretreatment of PRS are shown in Fig. 5.15. The flattening of peak intensity at the absorbance of 3330.27 cm^{-1} corresponding to –OH stretch signified degradation of alcohols and carboxylic acid functional groups of PRS due to *P. putida* pretreatment (Ennouri et al., 2016). This led to increment in short-chain fatty acid concentrations thereby improving the solubilization of petroleum hydrocarbons due to pretreatment. The increased peak intensity at 2121.05 cm^{-1} was related to improved symmetric/asymmetric C-H aliphatic stretching vibrations of total petroleum hydrocarbon (TPH) content due to bacterial pretreatment which resulted from the fragmentation of heavy molecular weighted petroleum hydrocarbons to lighter ones (Sun et al., 2020). The declining absorbance of the sharp peak at 1633.26 cm^{-1} after pretreatment signified dissociation of -C=C- and -C=O- stretches corresponding to alkenes, carboxylates and aromatic rings which also affirmed the VFA accumulation due to pretreatment (Ennouri et al., 2016). An immensely intensified peak at 1103.82 cm^{-1} was newly formed after pretreatment which indicated dissociation of TPH into C-H stretch corresponding to methyl group. The fragmentation of phenyl group stretch at absorbance 587.10 cm^{-1} of untreated PRS into multiple short peaks within the range of absorbance of 400-800 cm^{-1} after pretreatment signified the phenolic group dissociation into short-chain unsaturated or saturated hydrocarbons (Kumar et al., 2014). This illustrated that *P. putida* attacked not only the saturated and unsaturated structures but also

fragmented the fatty, branched and aromatic structures of hydrocarbons during pretreatment suggesting the molecular level decomposition of PRS resulting in improved solubilization.

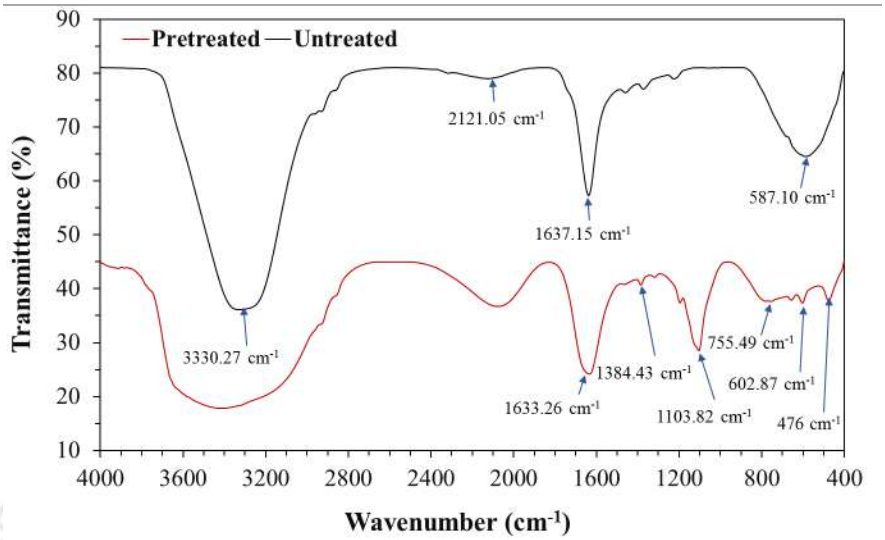

Fig. 5.15. FTIR spectra before and after bacterial pretreatment of PRS at optimized operating condition

5.3.4. BMP assay after *P. putida* pretreatment

Fig. 5.16 shows the anaerobic biodegradability of different inoculum:sludge (DS:PRS) ratios of pretreated PRS at optimum conditions. The enhancement in sCOD and accrual of VFA concentrations due to *P. putida* pretreatment expedited the hydrolysis stage boosting biogas from PRS. From Fig. 5.16(a), the highest daily biogas production was observed on 23rd d for mixing ratio DS:PRS = 0.5 which was 87.5 % higher than control (untreated) PRS. During the initial digestion period, the leisurely rate of increase in biogas was due to the lag phase observed during acclimatization of the substrate with the inoculum inside the anaerobic reactors. After 3-4 d, the biogas production augmented with the subsequent increase in digestion period. This was due to the cleavage of chemical bonds dissipating the organic fraction into soluble phase to be utilized by the microbial consortium for biogas production (Kavitha et al., 2014). From Fig. 5.16(b), the cumulative biogas production was observed to be maximum for DS:PRS = 0.5 resulting in 62.27% improvement compared to control by the end of 50 d of digestion which was higher than Merrylin et al. (2013) who conducted pretreatment of non-flocculated municipal sewage sludge with *Bacillus licheniformis* strain and reported 57% biogas enhancement. The obtained results were also higher than many bacterial pretreatment studies conducted on lignocellulosic substrates with *Bacillus licheniformis* sp., *Bacillus subtilis* sp., *Lactobacillus deiliehii* sp. and *Pseudomonas* sp. as mentioned by Ferdeș et al. (2020). The cumulative

biogas for all the mixing ratios followed the order: 0.5> 0.4> 0.3> 0.7> 1.0. Control (untreated) PRS performed unenviably due to the presence of refractory organic compounds (polyaromatic or heterocyclic compounds) which were reported to be toxic to methane-producing bacteria (Haak et al., 2016). The control, therefore, showed poor degradation ability as observed from VS reduction of 18.6% by the end of 50 d of digestion as shown in Fig. 5.16(c). The maximum VS degradation was observed for DS:PRS=0.5 (66.67%) followed by ratios 0.4 (58.9%), 0.7 (51.48%), 0.3 (50.92%) and 1 (48.93%) respectively, and the obtained result was higher than that estimated by Merrylin et al. (2013), indicating optimum utilization of PRS due to *P. putida* pretreatment in this study.

The variation in pH during AD of pretreated PRS is shown in Fig. 5.16(d). The intensified sCOD of PRS after pretreatment was readily accessed by the hydrolytic and fermentative bacteria to produce VFA and organic acids which could be advocated by the reduction in pH during the first 25 d of digestion (Wang et al., 2016). Initially, the pH of the substrate ranged from 7.085 to 7.19 for all mixing ratios and dropped in the range of 6.69-6.88 within 21 d of digestion suggesting the formation of acidic compounds through depolymerization of PRS by enzymes produced by the microbial population. The further rise in pH after 21 d till the range of 7.26-7.56 for all mixing ratios indicated the activation of methanogenic bacteria for accrual production of biogas from PRS. The operational pH should be in the range of 6.6-7.6 to prevent reactor failure from excess acidification and poor buffering capacity (Wang et al., 2016). The rapid hydrolysis resulting in improved organic matter removal and enhanced biogas production from batch BMP assay advocated the efficient biodegradation of PRS due to *P. putida* pretreatment.

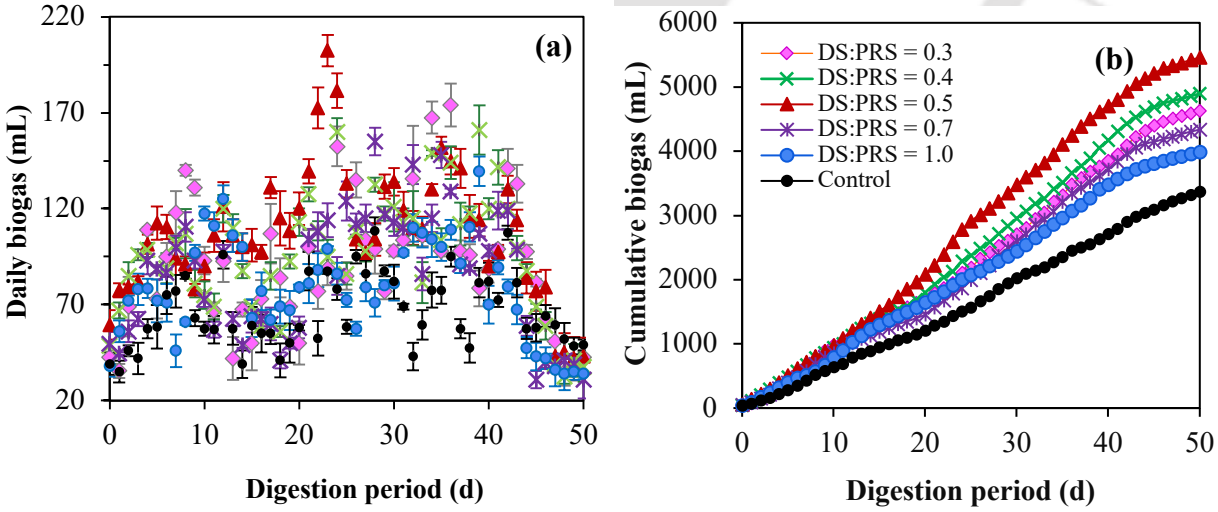

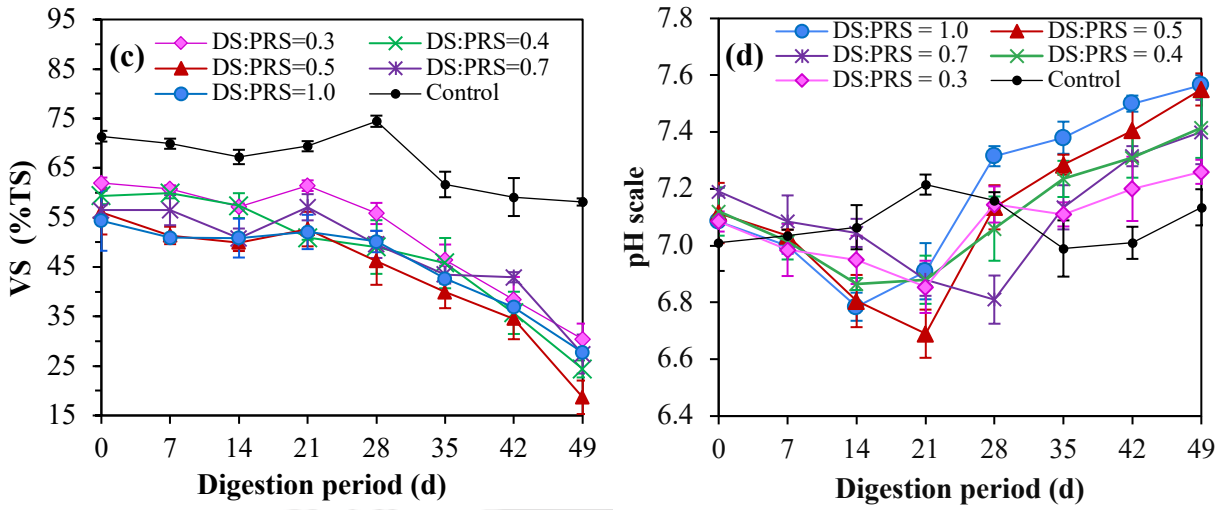

Fig. 5.16. Variation in (a) daily biogas, (b) cumulative biogas, (c) VS degradation, and (d) pH during AD of *P. putida* pretreated PRS at optimum condition

5.3.5. Scaled-up batch study of *P. putida* pretreated PRS

The biogas production and analytical investigation of 1L BMP batch assay illustrated definite results, therefore, the batch assay was scaled up to 20L in order to examine the pollutant biodegradation and variation in biogas enhancement to clearly depict the feasibility of the digestion process at a larger scale. The 20L batch assay was conducted in triplicates with the most appropriate mixing ratio of DS:PRS=0.5 (maximum cumulative biogas obtained from 1L BMP study) maintaining the working volume of 14L. A control consisting of untreated sludge was kept as a reference.

5.3.5.1 Biogas yield

The daily biogas yield from *P. putida* pretreated PRS at mixing ratio DS:PRS = 0.5 was compared with that of untreated PRS in the scale-up study as shown in Fig. 5.17 (a). The maximum daily biogas production was obtained on 29th d of AD after pretreatment which was 30.58% higher compared to untreated. The accelerated hydrolysis could be evident from the fact that the peak biogas was obtained 8 d earlier after *P. putida* pretreatment. The cumulative biogas production was enhanced by 54.61% after pretreatment as compared to untreated {Fig. 5.17(b)}. The percentage enhancement is 7.8% lower in comparison to the 1L batch study (62.3%). Weiland (2006) explained that the biogas production is lower when the feedstock volume increases in batch reactors which could be attributed to the difference in the homogeneity of the feedstock and inoculum, the amount of VS content fed to the reactor, the increased accumulation of inhibitory compounds or the higher quantities of recalcitrant components in complex feedstock such as PRS. The change in process dynamics due to microbial pretreatment

could be well observed from the augmented biogas yield. The enhanced biogas denoted the solubilization of a surplus quantity of soluble organic hydrocarbon compounds made available by *P. putida* (at optimum conditions) due to their unique enzymatic structure (Singh et al., 2010; Tuhuloula et al., 2019). The variation of organic carbon solubilization during the AD process could be observed in Fig. 5.17(c). The improvement in total organic carbon (TOC) solubilization from 317.3 mg/L to 555.3 mg/L from 0^{th} to 14^{th} d was due to the oxidation of organic fraction of hydrocarbon (TOC) by hydrolytic and fermentative microorganisms resulting in the accumulation of volatile fatty acids responsible for lowering of pH as shown in Fig. 5.17(d). The accumulated VFAs are converted to acetate through the action of acetogenic bacteria (Wang et al., 2016). The increase in pH after 28^{th} d could be due to lowering of VFA concentrations due to conversion of acetate to hydrogen (H_2), and the decrease in TOC after 28^{th} d could be attributed to the oxidation of organic carbon to carbon dioxide (CO_2) resulting in subsequent conversion of H_2 and CO_2 to biogas by the methanogenic consortium. This could be responsible for peak biogas generation from pretreated PRS after 28^{th} d. In the untreated PRS due to the presence of recalcitrant hydrocarbon compounds, the activity of the microorganisms was slow resulting in lower biogas yield (Haak et al., 2016; Janajreh et al., 2020). The suitable culture condition and the effective strain (*P. putida*) made the pretreatment process efficient by abridging the hydrolysis phase almost by a week thereby enhancing biogas production which was observed to be higher compared to various other bacterial strains as mentioned by Ferdeș et al. (2020).

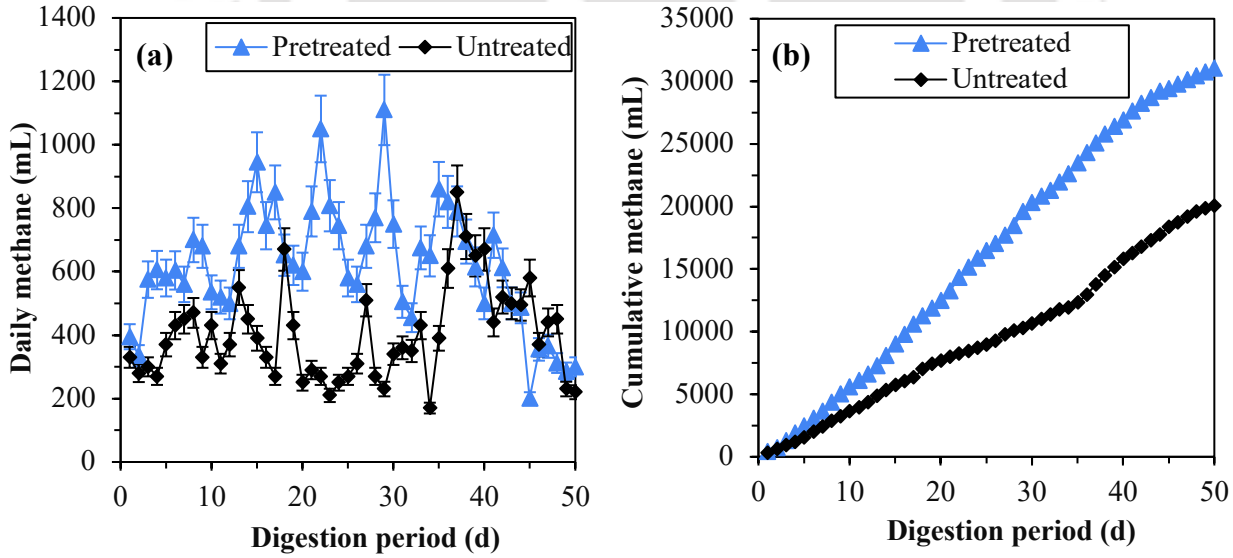

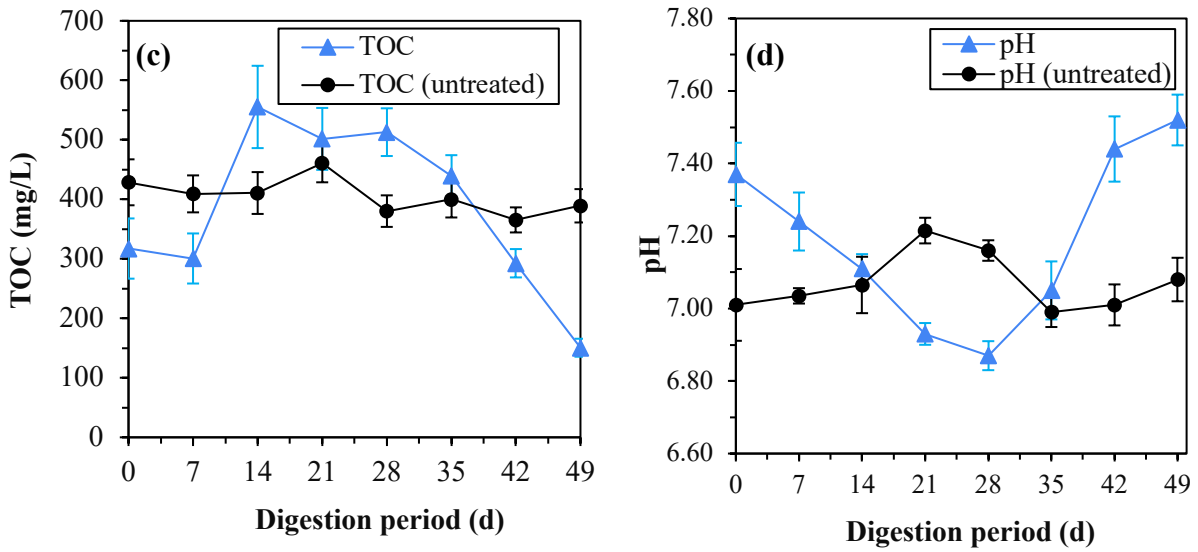

Fig. 5.17. (a) Daily biogas yield, (b) cumulative biogas yield, (c) TOC and (d) pH variation during scale-up batch study

5.3.5.2 Biodegradation of pollutants (TPH, O&G and phenols)

Anaerobic degradation of petroleum hydrocarbons in the absence of any exogenous electron acceptors occurs via their disproportionation to biogas (CH_4) and carbon dioxide (CO_2). The AD process initially utilizes the hydrogen-degrading microorganisms to reduce hydrocarbon equivalents by the formation of molecular hydrogen (H_2). The methanogenic consortium thereby converts H_2 and CO_2 to CH_4. The thermodynamic feasibility of the digestion process is supervised by the combined action of hydrogen-degrading microorganisms and methanogenic consortium (Heider and Schühle, 2013). In this study, a decreasing trendline was observed for the total petroleum hydrocarbon (TPH) content of the pretreated PRS throughout the digestion period {Fig. 5.18(a)}. The TPH reduction after pretreatment was observed to be 57.07% by the end of 49 d of digestion period out of which, 40.57% degradation was observed within the first 14 d of digestion period. The percentage TPH reduction was relatively constant from 14-35d of digestion period. Two types of hydrocarbons mostly susceptible to microbial attack are aliphatic (including alicyclic) and aromatic hydrocarbons, but follow a preference order as: aliphatics> aromatics (Cerqueira et al., 2011). The aliphatics include saturated (alkanes) and unsaturated (alkenes and alkynes) hydrocarbons among which the alkenes and alkynes are significantly more reactive than alkanes due to the nature of the respective carbon-carbon (C–C) multiple bonds (double or triple bonds). During the first 14 d of digestion period, the microbial population consumed the easily degradable unsaturated aliphatics and the reduced rate of TPH reduction after 14 d of digestion might be attributed to the relatively lesser reactive potential of alkanes due to strong and

localized aliphatic (C–C) bond or inability of anaerobic microorganisms to activate any reactive functional group (Bian et al., 2015). The rate of degradation of petroleum hydrocarbons decreases with time, obtaining an apparent plateau due to recalcitrant compounds exhibiting a slow-degradation tendency (Hu et al., 2013). The gradual decrement in TPH content of 26.95% (69.87 g/kg to 51.029 g/kg) from 35-49 d of digestion could be attributed to the degradation of alicyclic hydrocarbons consisting of non-aromatic ring structures. There might also be the dissociation of low molecular weighted aromatic structures containing one or more aromatic rings, but mostly these are infused to highly complex structures (Heider and Schühle, 2013). The TPH degradation of 29.18% in control (untreated) PRS after 49 d of digestion could be ascertained due to the activity of sulfate-reducing, nitrogen-fixing and methanogenic archaea already present in PRS as reported by Roy et al. (2018b) from functional biomarker gene analysis but since these are indigenous microbial consortia, therefore, their lower degradation ability was evident. Ke et al. (2021) performed bioremediation of oily sludge using four exogenous bacterial strains (*Luteimonas huabeiensis, Chelatococcus daeguensis*, *Pseudomonas aeruginosa*, *Bacillus subtilis*) and reported maximum TPH removal of 55.4% by *Pseudomonas aeruginosa* strain at 35°C which is in close accordance with this study (57.07% TPH removal), but the mixed culture of those bacterial strains improved TPH removal by only 8.7%. The complex bacterial consortium is equipped with comprehensive enzymatic abilities from mixed bacterial populations increasing the rate of hydrocarbon degradation but the type and activity of bacterial strains including the biodegradation duration are keys to maximize degradation efficiency. Gojgic-Cvijovic et al. (2012) reported 82% TPH removal from petroleum sludge after 84d of bioremediation conducted by a bacterial consortium of *Pseudomonas*, *Bacillus*, *Micromonospora* and *Achromobacter* species. In this study, the enhancement in TPH degradation from 29.18% (control) to 57.07% after bacterial pretreatment with *Pseudomonas putida* strain could be attributed to the action of laccase catalysis activity at optimum operating conditions {22.84 IU/mL} through reduction of an oxygen molecule to H_2O accompanied by oxidation of one electron from the aromatic hydrocarbon which ultimately got converted to quinones (Chauhan et al., 2017; Bhandari et al., 2021). Also, laccase catalysis could be involved in non-aromatic compound oxidation through the presence of natural mediators such as phenol as reported by Johannes and Majcherczyk (2000). These mediators get oxidized by laccase and form highly active cation radicals to oxidize nonaromatic compounds. In this way, the generated bacterial laccase due to pretreatment got utilized during anaerobic digestion through decomposition of high molecular weighted compounds to lower ones facilitating 95.58% higher hydrocarbon degradation of pretreated PRS compared to untreated.

The O&G removal during the AD process is shown in Fig. 5.18(a). The O&G steadily decremented during the anaerobic digestion process with observed removal of 62.98% by the end of the digestion period after bacterial pretreatment. The O&G removal was improved by 134.82% due to *P. putida* pretreatment compared to control (untreated). In the AD process, oil degradation occurs through long-chain hydrocarbon decomposition to shorter ones, resulting in viscosity reduction (Ke et al., 2019). Microbial consortium accesses hydrocarbon through direct microbial adherence to macro oil droplets and agglomeration with emulsified or pseudo solubilized oil (Ward et al., 2003). Microorganisms feed onto hydrocarbons as sole carbon sources and during the process bioemulsifiers or biosurfactants are produced leading to demulsification of PRS. The O&G reduction of 25% (56.79 to 42.57 % dry solids) during the first 7 d could be attributed to the action of bioemulsifiers during the fermentation process facilitating extracellular degradation of PRS (Gojgic-Cvijovic et al., 2012; Ke et al., 2019). The subsequent reduction of O&G after the fermentation process could be attributed to demulsification due to biosufactant production. The O&G removal trend line was similar to the TPH reduction trend line since these bioemulsifiers enable emulsification of petroleum hydrocarbons stimulating TPH degradation (Ke et al., 2021).

Fig. 5.18(b) shows the degradation of phenol throughout the anaerobic digestion process of pretreated PRS. The phenol was reduced from 198.71 mg/L on 0^{th} d to 15.94 mg/L by the end of the 49^{th} d of the anaerobic digestion process resulting in 91.97% of phenol removal which was 27.74% higher than the study conducted by Khan et al. (2019). The rate of anaerobic degradation of phenol increases with time due to the activation of phenol-degrading microbes (Xu et al., 2020). Out of the total 91.97% phenol removal, 77.13% removal was accomplished within the first 7 d of digestion period and the rest removal was accomplished in the remaining 42 d of digestion. During anaerobic digestion, mineralization of phenols proceeds via 4-hydroxybenzoate into the benzoyl-CoA pathway to form cyclohex-1-ene carboxyl- CoA, which then undergoes ring cleavage and β-oxidation to form acetate with the help of fermentative and acetogenic bacterial consortium (Levén et al., 2012). The methanogenic bacteria then convert the acetate to produce CH_4 and CO_2 thereby converting phenol into biogas. The benzoyl-CoA or benzoate acts as the central intermediate of the anaerobic degradation pathway of phenol (Heider and Schühle, 2013). Levén et al. (2012) reported that the phenol degradation pathway is also dependant upon temperature since at mesophilic temperature range (maintained in this study), benzoic acid acted as an intermediate for simultaneous turnover of benzoate resulting in incremented phenol degradation compared to thermophilic temperature range. This could be due to the reversible capacity of temperature-sensitive enzymes such as phenol carboxylase and 4-

hydroxybenzoate decarboxylase depicting the inability to get activated at thermophilic temperature range. Total phenol removal of 91.97% obtained in this study at mesophilic temperature range was 27.74% higher than the study conducted by Khan et al. (2019). The improvement in phenol removal by 175.6% compared to control (untreated) indicated great potential for phenol degradation due to laccase catalysis activity at optimum operating conditions in pretreated PRS (Bhandari et al., 2021).

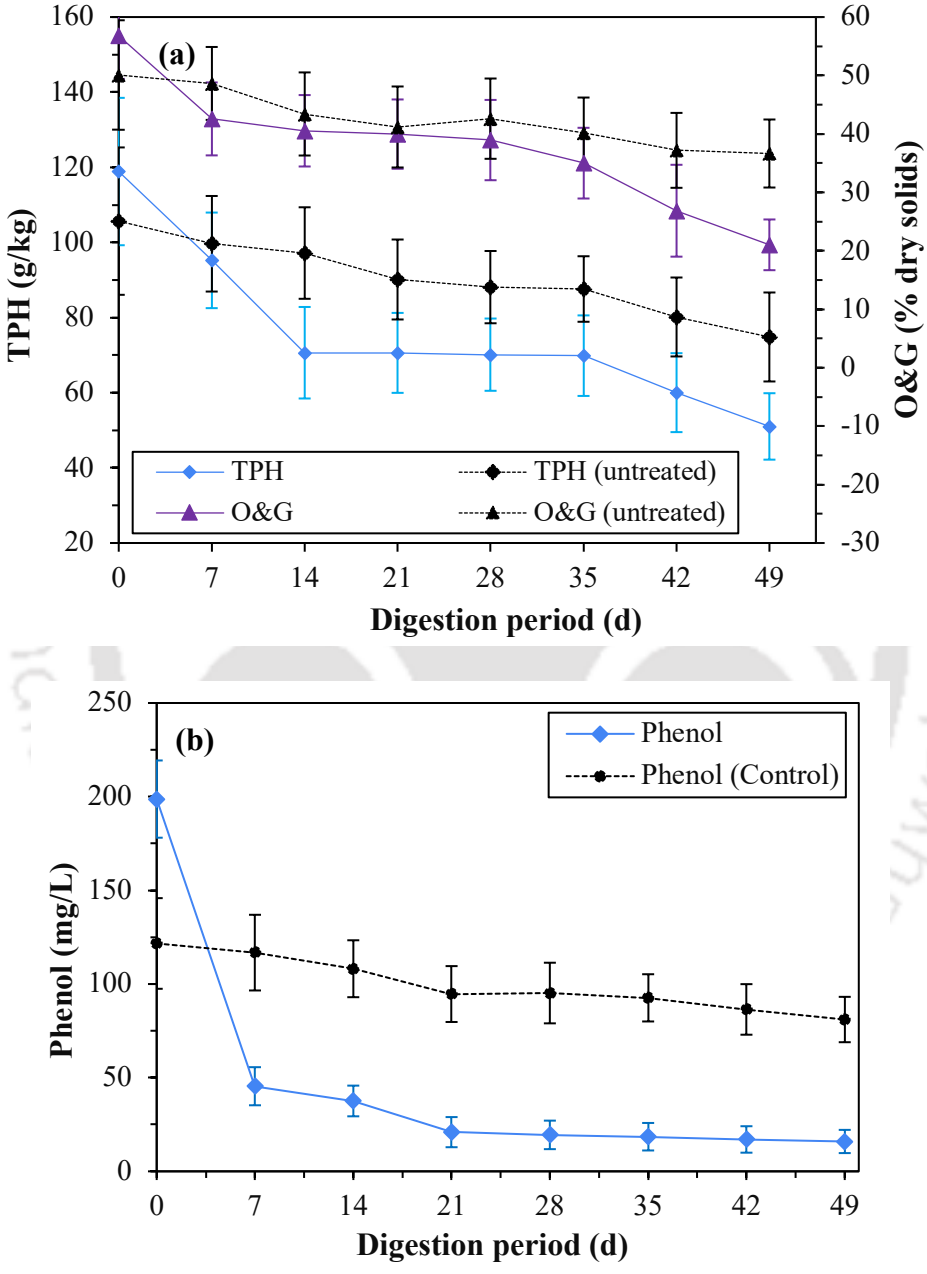

Fig. 5.18. Variation in (a) total petroleum hydrocarbon (b) oil and grease and (c) total phenols throughout the digestion period

(B) Pretreatment with Strain II (*Kosakonia oryziphila*)

5.3.6 Effect of *Kosakonia oryziphila* strain IH3 on PRS solubilization

Potential bacterial species incorporate petroleum hydrocarbons as carbon sources for their energy and reproduction through the conversion of heavy-weighted hydrocarbon compounds to lower masses responsible for the facilitation of the fermentation process. This fermentation ensues through synthesis of microbial extracellular enzymes capable of dissociating the recalcitrant polymers of the substrate steering solubilization and biodegradation of the substrate (Das and Chandran, 2011). *Kosakonia oryziphila* is a gram-negative, non-spore-forming and rod-shaped bacteria having the potential to solubilize organic substrate in both aerobic and anaerobic condition since it has been characterized as a facultative anaerobe (Hardoim et al., 2013; Li et al., 2016). Aerobic environmental conditions mostly result in quick and paramount degradation of majority of hydrocarbon pollutants (Das and Chandran, 2011). Fig. 5.19. shows the effect of bacterial pretreatment using *K. oryziphila* on solubilization of PRS through the estimation of sCOD and VFA concentrations at three different dosages of 10^7, 10^8 and 10^9 CFU/mL incubated for a duration of 6 d. Roy et al. (2018b) reported the abundant microbial diversity present in PRS due to which a control (untreated) was incubated as a reference to advocate the actual augmentation in solubilization due to *K. oryziphila* strain. In Fig. 5.19(a) and (b), both sCOD and VFA concentrations for dosage 10^8 CFU/mL increased with increase in pretreatment duration till 4^{th}d achieving the maximum values, thereafter leading to a subsequent decrease in both the concentrations. The maximum sCOD incremented by 3.64 times that of the control on 4^{th} d of incubation. The initial increment in sCOD could be attributed to the enzymatic key reaction catalyzed by peroxidases and oxygenases through consolidation of molecular oxygen (O_2) in order to commence the intracellular attack on the organic fraction of PRS. The hydrocarbons follow step-by-step peripheral degradation pathways into the intermediates of the central intermediary metabolism {tricarboxylic acid (TCA) cycle} and their biosynthesis result in increase in biomass growth thereby improving the sCOD (Das and Chandran, 2011). The maximum VFA concentration for dosage 10^8 CFU/mL was incremented by 1.64 times that of the control on 4^{th} d of incubation. The enzymes involved in the metabolic pathways of alkanes (monooxygenases) or aromatics (both mono and dioxygenases) incorporate hydroxyl groups derived from molecular O_2 into the subsequent aliphatic chain or aromatic ring respectively. This leads to the conversion of formed alcohols from aliphatic hydrocarbon chain to the corresponding carboxylic acids or short chain fatty acids leading to increment in VFA concentration (Fathepure, 2014). Even the generated phenolic compounds through ring hydroxylation of aromatics are responsible for oxidative ring cleavage ultimately leading to the

formation of fatty acids. The decrease in sCOD and VFA after the attainment of the peak values on 4th d could be attributed to the ceasing of bacterial growth due to the depletion in available organic carbon leading to their endogenous decay. At 10^9 CFU/mL dosage, the maximum sCOD and VFA also incremented with the increase in incubation period and were obtained a day earlier compared to the dosage of 10^8 CFU/mL, but the values were 38.5% and 12.4% lower respectively compared to that of 10^8 CFU/mL. This might be because the attainment of optimal solubilization for a substrate during microbial pretreatment depends on a variety of factors: dosage, treatment duration, and nutrient accessibility as reported by Ferdeș et al. (2020), and at dosages of bacterial colonies higher than optimum decrease the solubilization due to inhibition in extracellular enzymatic activity thereby, impeding the hydrolysis process. The sCOD and VFA for 10^9 dosage CFU/mL decreased thereafter till the end of the incubation period with a slight increase in sCOD on 5th d which could be attributed to the fact that at higher dosages of bacterial colonies the bacteria secrete exoenzymes after the cessation of the easily available soluble organics to further solubilize the particulate organic fraction. The maximum sCOD and VFA at dosage of 10^7 CFU/mL were incremented by 2.22 and 1.14 times that of the untreated on 3rd d of incubation but were lower than that of the other two dosages. Gram-negative bacterial strains might delay or inhibit the degradation activity at higher pollutant concentrations or lower dosages of bacterial colonies utilized for PRS solubilization (Hardoim et al., 2013; Li et al., 2016; Tuhuloula et al., 2019). Different dosages of *K. oryziphila* for PRS solubilization follows the order: 10^8 CFU/mL>10^9 CFU/mL>10^7 CFU/mL. The peak solubilization values obtained in this study were higher than microbial pretreatment studies conducted on waste activated sludge from municipal wastewater treatment plant, or different lignocellulosic substrates as reported by Kavitha et al. (2014) and Ferdeș et al. (2020). The optimal dosage and duration of pretreatment were observed to be 10^8 CFU/mL and 4 d which maximized sCOD to be utilized for improved digestibility of PRS and the subsequent increment in VFA shall accelerate the hydrolysis of the complex substrate.

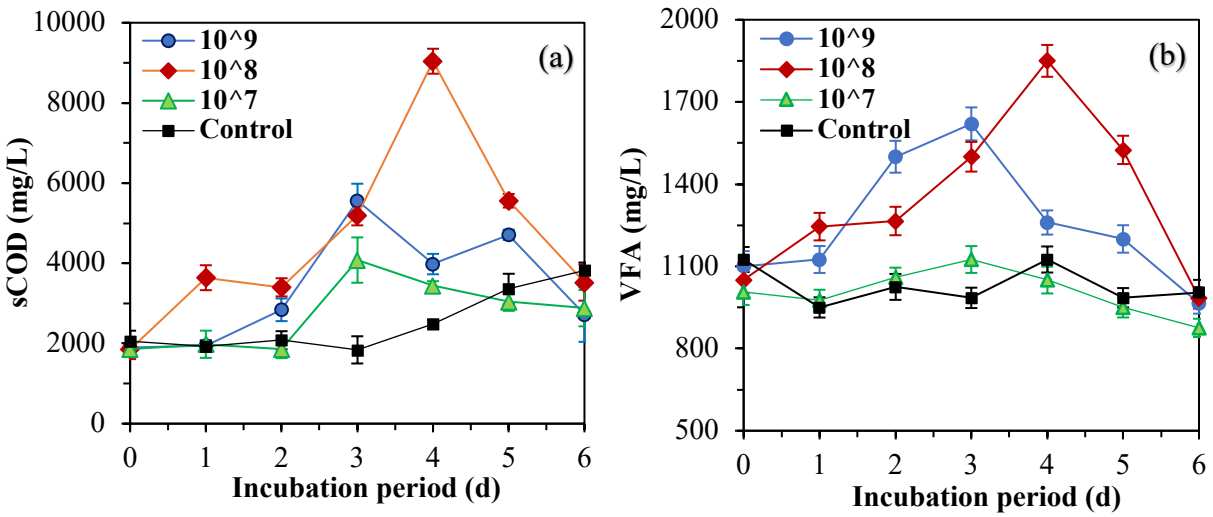

Fig. 5.19. Variation of (a) soluble chemical oxygen demand and (b) volatile fatty acids concentration during bacterial pretreatment of PRS

5.3.7 Effect of enzymatic activity due to *K. oryziphila* pretreatment on PRS

Microbial degradation of petroleum hydrocarbons depends on the complexity of the chemical structures, type and position in group substitution and the adaptation level of discrete enzymatic system and therefore, the enhancement in solubilization of PRS due to *K. oryziphila* pretreatment can be adjudged by a specific enzymatic system (Tuhuloula et al., 2019). In this study, the effect of LiP was examined for the optimum dosage (10^8 CFU/mL) throughout the pretreatment duration. Lee et al. (2015) reportedly proved that one of the major enzymes in the lignin system such as, LiP has the ability to degrade petroleum aromatic hydrocarbons. LiPs belonging to the family of oxidoreductase, are heme-containing enzymes secreted mainly by some bacteria and fungi which degrade the aromatic pollutants via an oxidative process. In this study, the LiP activity increased from 0^{th} d (4.16 IU/mL) till 4^{th} d, achieving the maximum activity of 20.52 IU/mL only to decrease thereafter with any further increase in incubation period. The peak LiP activity on 4^{th} d commended the attainment of maximum sCOD and VFA on that particular day suggesting utmost utilization of organic hydrocarbons. In the presence of H_2O_2 as a cosubstrate and veratryl alcohol as a mediator, LiP has the ability to degrade phenolic compounds present in PRS (Karigar and Rao, 2011). The initial improvement in enzymatic activity can be hypothesized as microbial LiP attack on organic fraction of aromatic pollutants through single-electron oxidation to generate free cation radicals which undergo a series of chemical reactions such as, hydroxylation or cleavage of C–C bond resulting in the formation of hydrophilic compounds thereby converting the insoluble hydrocarbon fraction to soluble form which improves the solubilization of PRS (Kumar and Chandra, 2020). The decrease in LiP activity from 4^{th} d (20.52

IU/mL) to 6th d (16.94 IU/mL) could be attributed to the decay of the free cation radical which are again dependent on the groups of aromatic rings. It might also be related to the fact that the easily degradable hydrocarbon constituents were exhausted by the microbes through LiP secretion till 4th d after which the recalcitrant compounds led to reduction in LiP reaction velocity thereby decreasing its catalytic activity (Lee et al., 2015). The enzymatic activity variation suggested a direct co-relation of solubilization due to bacterial pretreatment with the specific enzymatic system involved behind the bacterial species.

5.3.8 FTIR at optimal pretreatment conditions due to *K. oryziphila* pretreatment

The organic functional groups identified in untreated and pretreated PRS at optimal dosage and incubation through FTIR revealed flattened –OH stretch signifying degradation of alcohols and carboxylic acid functional groups of PRS which comprehended the increment in short-chain fatty acid concentrations thereby improving the solubilization of PRS. Microbial pretreatment led to degradation of symmetric and asymmetric C-H aliphatic stretch through fragmentation of heavy molecular weighted hydrocarbons to lighter ones. Also, -C=C- and -C=O- stretches corresponding to alkenes, carboxylates and aromatic rings were also dissociated affirming the VFA accumulation due to pretreatment (Ennouri et al., 2016). Intensified fragmentation of TPH into C-H stretch corresponding to methyl group including dissociation of phenyl group stretch into short-chain unsaturated or saturated hydrocarbon content (Kumar et al., 2014) advocated decomposition of saturated, unsaturated, branched and aromatic hydrocarbons due to pretreatment.

5.3.9 Interpretation of design model for anaerobic biodegradability of *K. oryziphila* pretreated PRS

The experimental and predicted results of the developed design matrix is exhibited in Table 5.9. The experimental data incorporating the response analysis indicated the combined interactive effect of the independent parameters (X_1 = S/I and X_2 = pH) on output response (Y = biogas yield) by fitiing into second-order equations in coded and uncoded (actual) forms. The regression model for biogas yield (mL/g-VS_{added}) in terms of coded and actual factors are indicated in Eqs. (5.5) and (5.6) respectively.

$$Y_{coded} = 103.86\,X_1 + 375.00\,X_2 + 171.88\,X_1X_2 - 541.12\,X_1^2 - 271.75\,X_2^2 - 4991.00 \quad [5.5]$$

$$Y_{actual} = 403.23\,X_1 + 15108.62\,X_2 + 343.75\,X_1X_2 - 541.12\,X_1^2 - 1087\,X_2^2 - 51148.03 \quad [5.6]$$

Upon solving any of the above equations for biogas yield, the optimal value for every independent parameter was generated for maximizing the output response with utmost desirability for *K. oryziphila* pretreated PRS.

5.3.9.1 Statistical significance and fitting of the model

ANOVA mathematically evaluated the quadratic regression model towards its significance and reliability in order to examine any significant difference among the variables and responses. ANOVA for quadratic model of biogas yield revealed the model F-value = 127.06 and p-value <0.0001 indicating substantial contribution against the output response at 95% confidence level ($p<0.05$) thereby, advocating high significance relative to the pure error of the regression model (Table 5.10). The non-linear regression equation revealed that linear terms (X_1 and X_2), quadratic term (X_1X_2) and interactive terms (X_1^2 and X_2^2) were all significant with p-value <0.05. Low coefficient of variance of 1.69 suggested high reliability of the experimental data (Yılmaz and Şahan, 2020). The R^2 value was observed to be 0.9774 advocating the model could explain 97.74% of the response variability advocating high significance of the model. R^2 values in the range of 0.75-1.0 signifies good statistical models with best of fit (Behera et al., 2018). The R^2_{pred} of 0.9225 was in close agreement with the R^2_{adj} of 0.9813 (since $R^2_{adj} - R^2_{pred} < 0.2$). Adequate precision of 24.376 < 4.0 estimated the desired signal to noise ratio suggesting an adequate signal to be used to navigate the design space. Fig. 5.20 (a) indicated that the model was highly credible for achieving augmented biogas yield with least irregularity. Fig. 5.20(b) shows that there was no anomaly in this experimentation and the model was successful for obtaining the output response. The scattered points in the residual vs predicted plot {Fig. 5.20 (c)} suggested no definite pattern which validated the reliability of the generated model (Lai et al., 2014).

Table 5.9 Experimental and predicted values of the design matrix developed by CCD-RSM

Run order	Coded factors		Actual factors		Biogas	
	X_1	X_2	S/I	pH	Experimental*	Predicted
1	-1	+1	1.50	7.50	4157.50	4277.39
2	+1.414	0	3.91	7.00	4062.50	4055.63
3	0	+1.414	2.50	7.71	5080.00	4977.83
4	0	0	2.50	7.00	4991.00	4991.00
5	+1	-1	3.50	6.50	3750.00	3735.11
6	-1.414	0	1.09	7.00	3860.00	3761.87
7	0	-1.414	2.50	6.29	3920.00	3917.17
8	+1	+1	3.50	7.50	4773.50	4828.86
9	0	0	2.50	7.00	4991.00	4991.00
10	0	0	2.50	7.00	4991.00	4991.00
11	0	0	2.50	7.00	4991.00	4991.00
12	-1	-1	1.50	6.50	3821.50	3871.14
13	0	0	2.50	7.00	4991.00	4991.00
Control (C1)[a]					3286.00	-
Control (C2)[b]					1091.00	-

*The cumulative biogas yields are effectual values reported after subtracting the cumulative biogas from C2 by the end of digestion; [a]C1- Untreated PRS, [b]C2- Inoculum

Table 5.10. ANOVA for response surface quadratic model of biogas yield

Source	Sum of squares	DF[c]	Mean Square	F-value[a]	p-value[b]
Model	3.653E+06	5	7.306E+05	127.06	< 0.0001
X_1 (S/I)	86294.83	1	86294.83	15.01	0.0061
X_2 (pH)	1.125E+06	1	1.125E+06	195.66	< 0.0001
$X_1 X_2$	1.182E+05	1	1.182E+05	20.55	0.0027

X_1^2	2.037E+06	1	2.037E+06	354.28	< 0.0001
X_2^2	5.137E+05	1	5.137E+05	89.35	< 0.0001
Residual	40247.62	7	5749.66		
Lack of Fit	40247.62	3	13415.87		
Pure Error	0.0000	4	0.0000		

SD[d]	**Mean**	**R^2**	**R^2_{adj}**	**R^2_{pred}**	**Adequate precision**	**C.V[e]**
75.83	4490.77	0.9891	0.9813	0.9225	24.376	1.69

[a] Fishers-test; [b] Probability value (< 0.05 implies significant and >0.1 insignificant); [c] Degrees of freedom; [d] standard deviation; [e] co-efficient of variation

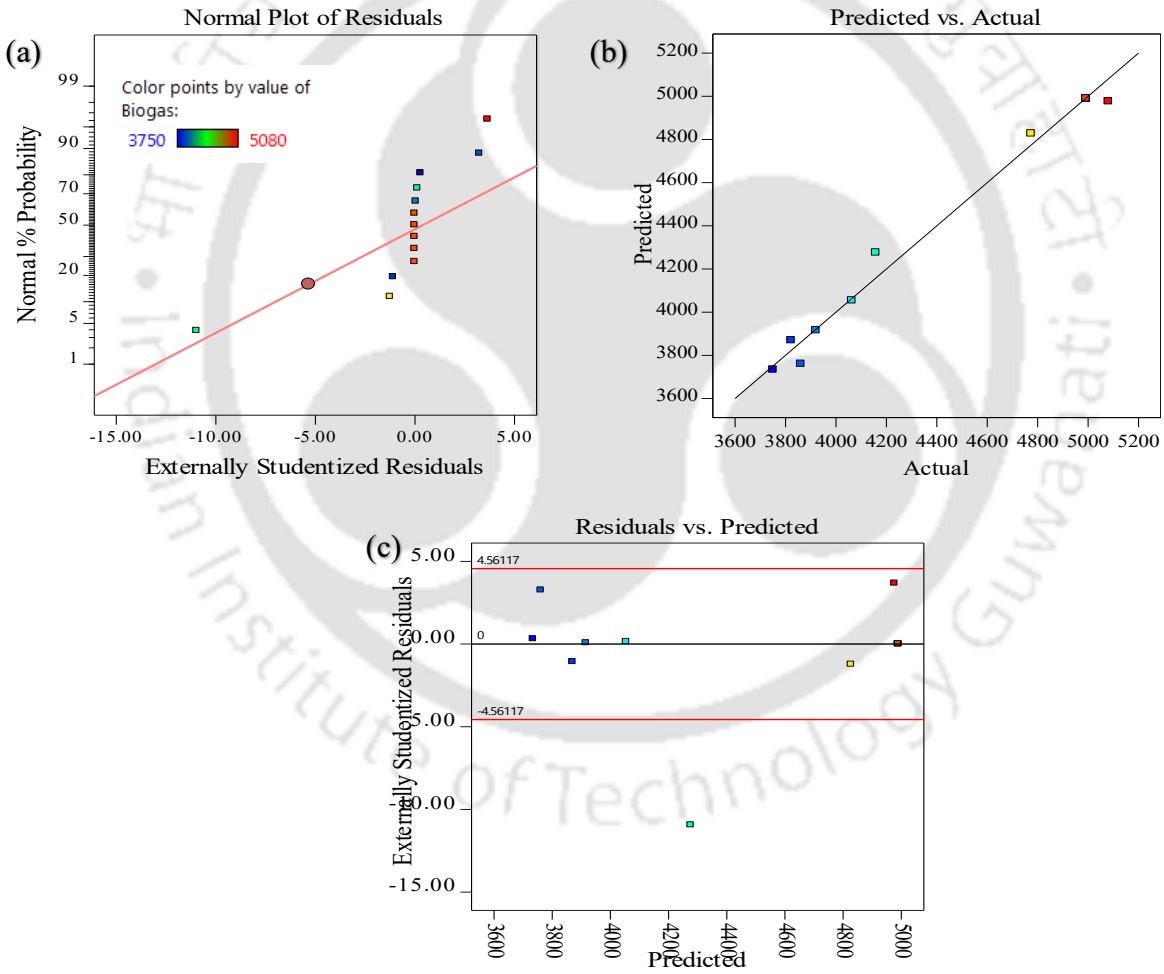

Fig. 5.20. (a) Predicted vs actual cumulative biogas plot, (b) normal plot of residuals and (c) residuals vs predicted plot of independent variables on biogas yield

5.3.9.2 Interactive effect of S/I and pH on biogas yield

Fig. 5.21(a) and (b) show a 3D interface plot and 2D contour plot respectively to perceive the interactional outcome of independent parameters. The significant interaction ($p = 0.0027<0.05$) for the combined effect of S/I ratio and pH on biogas yield revealed a stable control on the AD process establishing a direct co-relation with the performance of the anaerobic reactor. In Fig. 5.21(a), the biogas yield was observed to have incremented with the increase in S/I ratio and pH till an optimum value only to have decremented thereafter with any further increase in S/I ratio (>2.697) by the end of 50 d of digestion period. Siddique et al. (2016) in their study on petrochemical wastewater reported highest accumulated methane yield at substrate (food) and inoculum (microorganism) ratio of 2.0 at mesophilic temperature range which is near to the value obtained in this study. The decrease in biogas yield after achieving the peak value (5143 mL) might be attributed to the fact that at higher S/I ratios there might be inhibition caused due to inadequate methanogenic activity at higher pollutant concentrations of complex substrate (Pellera and Gidarakos, 2016). An appropriate inoculum consists of copious amounts of active microbes having the potential to convert the organic matter to biogas and the S/I ratio is essential for the rate of degradation of recalcitrant substrate (such as PRS) since it governs not only the biogas composition, digestion period and reactor stability, but also enhances the microbial activity inside a digester (Siddique et al., 2016). The optimum S/I ratio differs with the type of substrate since it depends upon the production of VFA and ammonium from the hydrolysis of complex matter controlling the buffering capacity of digester (Kameswari et al., 2012; Pellera and Gidarakos, 2016). The minimum biogas yield (3735.11 mL) was observed at S/I=3.5 and pH=6.5. In order to prevent excess acidification, the pH in intended to be in the range of 6.8-7.2, since, methanogenic microbial consortium might face inhibition beyond this range. pH< 6.5 favors the activity of hydrolytic and acidogenic bacterial community delaying the methanogenic activity resulting in lower methane yield. This might be the reason behind observing lower biogas yields at lower pH values {Fig. 5.20(b)}. The individual variation of pH did not have a profound effect on the biogas generation, but the interactive terms for S/I (X_1^2) and pH (X_2^2) were highly significant ($p < 0.0001$) indicating a synergistic effect of S/I and pH on the biogas generation of *K. oryziphila* pretreated PRS. The maximum cumulative biogas from pretreated PRS at optimum conditions (S/I=2.697 and pH =7.382) was 56.51% higher than that of the untreated (control C1) during 50 d of digestion which was comparable with the study conducted by Merrylin et al. (2013) reporting 57% biogas enhancement after pretreatment of non-flocculated municipal sewage sludge with *Bacillus licheniformis* strain.

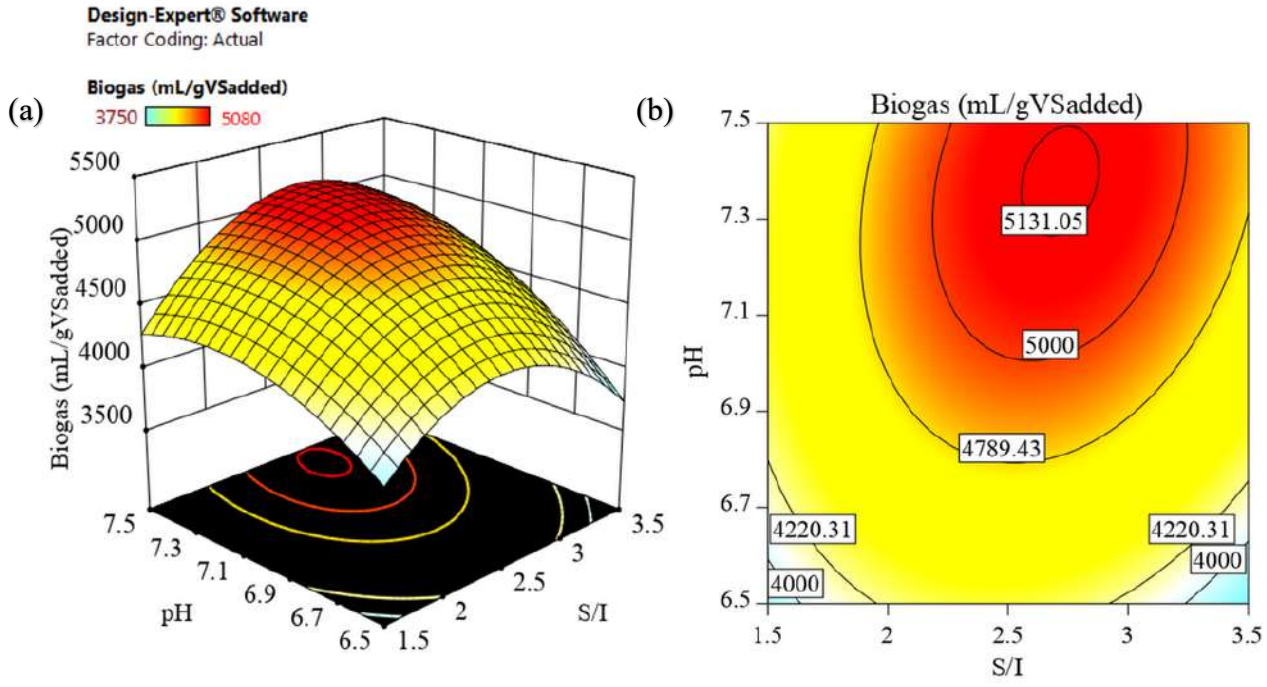

Fig. 5.21. (a) 3D response surface plot and (b) 2D contour plot of S/I and pH on biogas yield

5.3.9.3 Validation of the regression model

The veracity of the optimization model was examined for maximum cumulative biogas production, a conformity test was conducted at optimal conditions generated by the model (S/I=2.697 and pH =7.382) with 100% desirability. The conformity test was conducted in a scaled-up batch reactor of 20 L capacity in triplicates (14 L working volume) to not only validate the biogas enhancement (keeping a control of untreated PRS of similar capacity) obtained from 1 L batch assay designed by CCD-RSM, but also to examine the pollutant biodegradation during the digestion process at a larger scale.

(i) Biogas yield

Fig. 5.22(a) shows the peak daily biogas yield from *K. oryziphila* pretreated PRS, to be 25.88% higher and achieved 13 d earlier as compared to untreated (control). The cumulative biogas production was augmented by 50.21% after pretreatment as compared to untreated {Fig. 5.22(b)} indicating accelerated hydrolysis due to bacterial pretreatment. This percentage enhancement is in close accordance with that of the predicted enhancement from 1 L batch assay (56.51%) and the 6.3% lower percentage could be attributed to the fact that when substrate volume increases in batch reactors, higher quantities of recalcitrant compounds are present which disturb the homogeneity of the substrate and inoculum due to accumulation of inhibitory compounds (Weiland, 2006). The unique enzymatic

structure of *K. oryziphila* enhanced solubilization of a surplus quantity of soluble organic hydrocarbon compounds enhancing the biogas yield (Tuhuloula et al., 2019; Kumar and Chandra, 2020).

The organic carbon solubilization during the AD process could be observed in Fig. 5.22(c). The increment in TOC solubilization from 1206 mg/L to 1818.4 mg/L from 0th to 21st d could be attributed to oxidation of organic hydrocarbon by hydrolytic and fermentative bacteria resulting in the production of VFAs. The accumulated VFAs are converted to acetate through the action of acetogenic bacteria (Wang et al., 2016). The decrease in TOC after 21st d might be due to the oxidation of organic carbon to CO_2 resulting in subsequent conversion of H_2 and CO_2 to methane by the action of methanogenic bacteria. This advocated the observed peak biogas generation from pretreated PRS after 21st d. In untreated PRS, the activity of the microorganisms was slow due to high toxicant concnetration resulting in lower biogas yield and poor organics solubilization (Haak et al., 2016). This is also evident from poor VS degradation (21.75%) of untreated sludge whereas preterated PRS resulted in 72.44% VS degradation (Merrylin et al., 2013; Kavitha et al., 2014; Wang et a., 2016) {Fig. 5.22(d)}. The suitable culture condition and *K. oryziphila* strain proved to be effective in accelerating the hydrolysis thereby augmenting the biogas yield compared to other bacterial strains as explained by Ferdeș et al. (2020) in recalcitrant substrates.

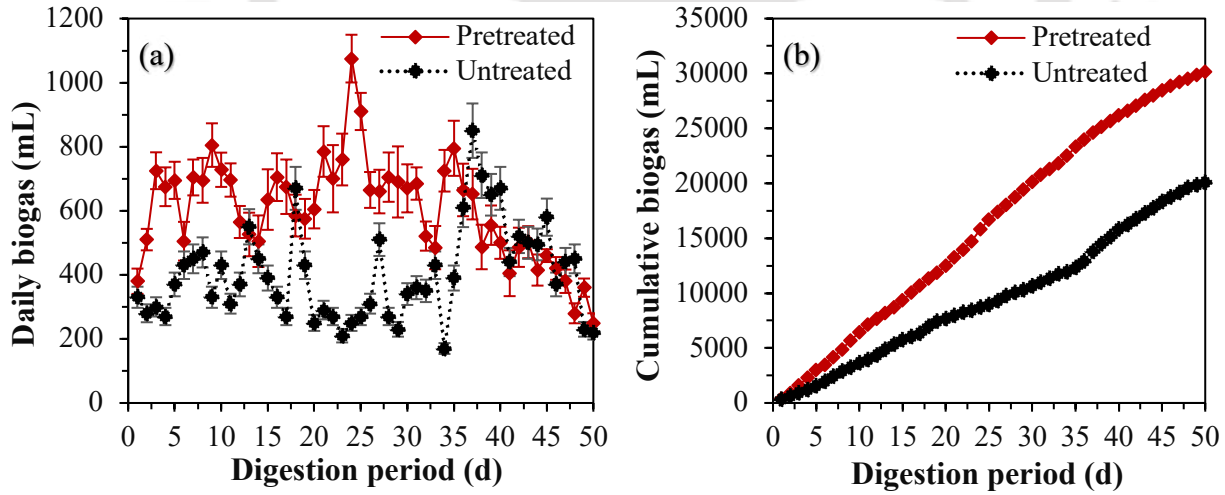

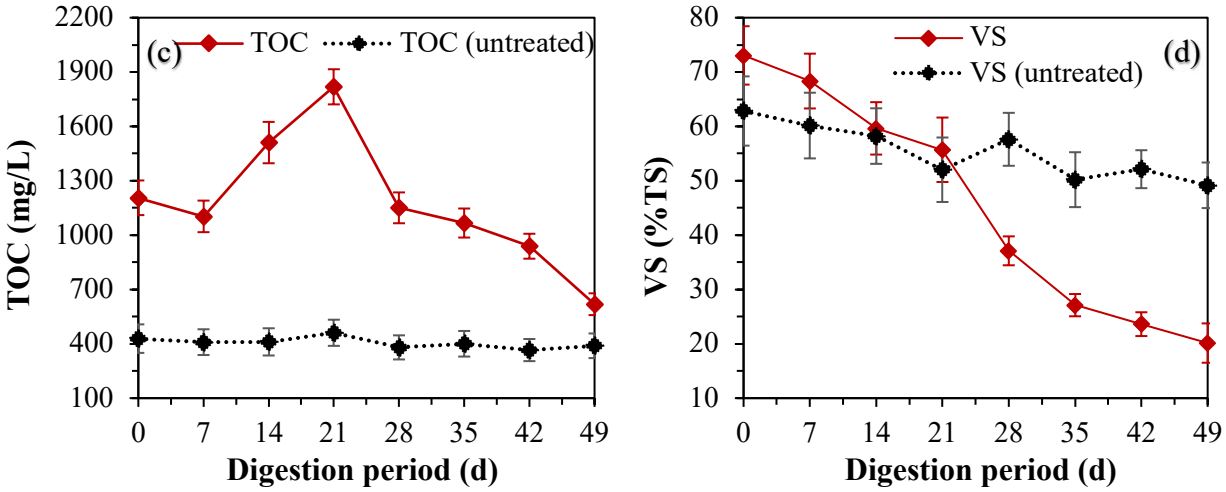

Fig. 5.22. (a) Daily biogas, (b) cumulative biogas, (c) TOC and (d) VS degradation variation during scale-up batch study

(ii) TPH, O&G and phenol biodegradation

During anaerobic degradation of petroleum hydrocarbons, the hydrogen-degrading microorganisms reduce hydrocarbon equivalents to molecular hydrogen (H_2) which is converted to CO_2 and CH_4 by the methanogenic archaea. In Fig. 5.23, a decreasing trendline was observed for the total petroleum hydrocarbon (TPH) content of the pretreated PRS with 56.16% removal by the end of digestion period. The TPH removal could be attributed to two types of hydrocarbons mostly susceptible to microbial attack: aliphatic (including alicyclic) and aromatic hydrocarbons. The aliphatics include saturated (alkanes) and unsaturated (alkenes and alkynes) hydrocarbons which get activated in anaerobic condition through carboxylation yielding C-odd n-alkanes to C-even fatty acids through a series of reactions facilitating the fermentation process (Holliger and Zehnder, 1996). This activates glutaryl-CoA dehydrogenase or acetyl-CoA acyltransferase enzyme catalyzing the final step of fatty acid through β-oxidation to acetyl-CoA and CO_2 entering the tricarboxylic acid (TCA) cycle. The aliphatic hydrocarbons might also follow a fumerate addition pathway by glycyl radical enzymes undergoing decarboxylation following β-oxidation thereby entering the TCA cycle (Sierra-Garcia et al., 2014). The aromatics might follow fumerate addition pathway or hydroxylation or carboxylation to form a common intermetiate (benzoyl-CoA) which subsequently leads to reductive dearomatization of aromatic ring following hydrolytic ring cleavage due to activation of ring cleavge hydrolase thereby enetering the TCA cycle (Widdel and Rabus, 2001). The rate of degradation of petroleum hydrocarbons decreases with time, obtaining an apparent plateau due to recalcitrant compounds exhibiting a slow-degradation tendency. Almost constant TPH degradation (59.49 g/kg to 57.15 g/kg)

from 28-48 d could be associated with inhibition posed by highly complex structures (Widdel and Rabus, 2001). The TPH degradation of only 19.8% in control (untreated) PRS could be due to the activity of sulfate-reducing, nitrogen-fixing and methanogenic consortium already present in PRS as reported by Roy et al. (2018b). Grishchenkov et al. (2000) reported 15-18% TPH degradation (including alkanes and few PAHs) within 50 d under anaerobic condition using two strains of *Pseudomonas* sp. and one strain of *Brevibacillus* sp. Ke et al. (2021) reported TPH removal of 55.4% by *Pseudomonas aeruginosa* strain at 35°C which is in close accordance with this study. The O&G trendline during the AD process steadily decreased resulting in 62.46% removal by the end of the digestion period after bacterial pretreatment (Fig. 5.23). During AD, decomposition of long-chain hydrocarbons to shorter ones lead to viscosity reduction facilitating oil degradation (Ke et al., 2019). The O&G removal was enhanced by 132.97% due to pretreatment compared to control (untreated). Petroleum hydrocarbons are utilized by microbes through direct adherence to macro-oil droplets and aggregation with emulsified oil (Ward et al., 2003). During their hydrocarbon accession, bioemulsifiers or biosurfactants are produced leading to the demulsification of PRS. The similarity in O&G removal and TPH trendline might be related to emulsification of hydrocarbons by these bioemulsifiers stimulating TPH degradation (Ke et al., 2021). Total phenol decremented from 94.57 mg/L to 10.94 mg/L within 50 d of AD (Fig. 5.23). Phenol degradation in anaerobic condition was due to the activation of phenol-degrading microbes (Sierra-Garcia et al., 2014). During AD, mineralization of phenols proceeds via 4-hydroxybenzoate into the benzoyl-CoA pathway to form cyclohex-1-ene carboxyl- CoA, which then undergoes ring cleavage and β-oxidation to form acetate with the help of acidogens and acetogens (Levén et al., 2012). The methanogens thereby convert the acetate to produce biogas (CH_4 and CO_2). Total phenol removal of 88.43% obtained in this study at mesophilic temperature range was 22.81% higher than the study conducted by Khan et al. (2019) which could be attributed to reversible nature of temperature-sensitive enzymes (phenol carboxylase and 4-hydroxybenzoate decarboxylase) not getting activated at thermophilic temperature range (Levén et al., 2012). The improvement in phenol removal by 3.29 times that of control (untreated) indicated great potential for phenol degradation due to LiP catalysis activity unlocking the phenyl group during AD of pretreated PRS (Ferdes, et al., 2020).

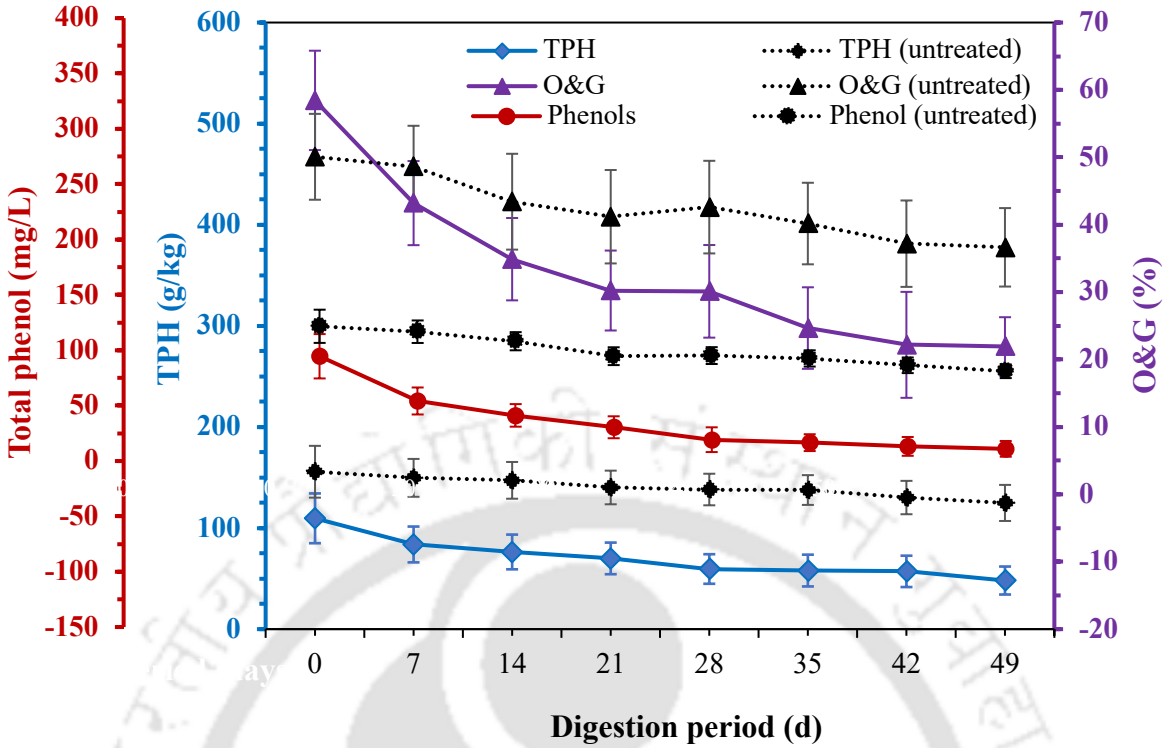

Fig. 5.23. TPH, O&G and total phenol degradation throughout the anaerobic digestion process

5.3.10 Phytotoxicity assessment

Phytotoxicity assessment was conducted to determine the digestate quality to be disposed into the surrounding habitat after the digestion process. In this study, the digestate of scaled-up batch assay after the digestion process was examined for phytotoxicity using mung bean (*V. radiata* L.) on seed germination inhibition. If PRS is disposed in reclamation grounds or soils, then it has the prospective to diminish the physico-chemical properties of the soils inhibiting the flourishment of plants due to inhibition in microbial abundance and enzymes present in soil. PRS can limit essential nutrients, water and oxygen to soil (Hu et al., 2013). The phytotoxicity could be noticed through mung bean seed germination inhibition percentages at 50%, 75% and 100% dilutions effecting the seedling biomass growth of plant including their root and shoot length (Table 5.11). Rates of germination of digestate sample after the AD process was observed to have incremented by 16.66%, 17.39% and 19.04% at 50%, 75% and 100% sample dilution extract respectively compared to untreated PRS. Fig. 5.24 shows the germination index (GI) considered as an index of both the rate of seed germination and length of roots of plants. Consideration of root length is vital in phytotoxicity estimation since roots are responsible for migration and accumulation of soluble toxic components (polar, water-soluble and non-ionizable hydrocarbons) to the plants through shoots (Merkl et al., 2005). After the digestion of

pretreated PRS, the GI of digestate incremented by 57.47%, 49.158%, 51.66% at 50%, 75% and 100% sample dilution extract respectively compared to untreated PRS indicating improved microbial flux activity after the AD due to reduction in immiscibility of PRS emulsions. Haider et al. (2021) explained that the elevated inhibition in germination of untreated PRS could be related to the inductive oxidative stress due to the presence of elevated PAH concentrations. The significant amelioration in root length, shoot length and biomass growth indicated transformation of organic fraction of hydrocarbon and phenolic pollutants due to anaerobic digestion thereby abating toxicity.

Table 5.11. Outcome of untreated and pretreated PRS samples on seed germination, shoot length, root length and seedling biomass growth of *V. radiata* L.

Sludge	Dilution ratio (%)	Germination (%)	Shoot length (cm)	Root length (cm)	Biomass (gm)
Control	-	100±0.32	9.57 ± 0.52	5.86 ± 0.142	0.92±0.07
Untreated	50	76.67±0.57*	7.34±0.21*	4.82±0.28*	0.58±0.03
	75	73.33±0.53*	5.92±0.54	4.18±0.12*	0.42±0.04
	100	70.00±0.57*	4.21±0.48*	1.35±0.34*	0.34±0.04
Digestate	50	96.67±0.31*	8.19±0.52*	6.22±0.53	0.87±0.02
	75	90±0.28*	6.24±0.41*	5.08±0.48*	0.82±0.04
	100	83.33±0.44*	4.96±0.42	1.72±0.21*	0.71±0.03

All values are expressed as mean ± SD from triple repetitions

* p-value <0.05; significant in comparison with control using ANOVA

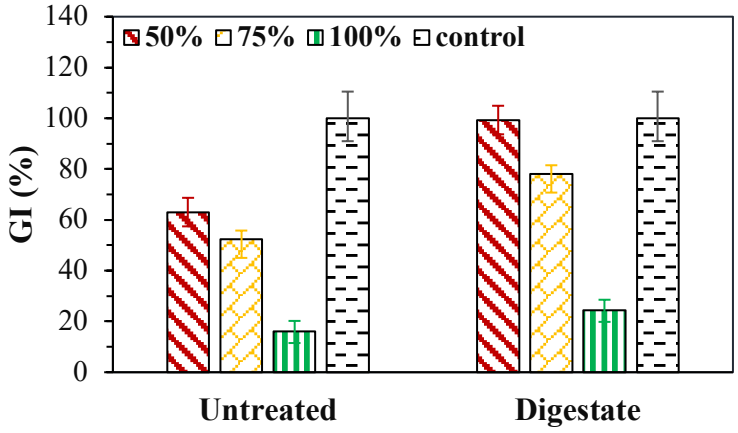

Fig. 5.24. Germination index (%) variation of mung bean before and after the anaerobic digestion of microbially pretreated PRS

5.4. COMPARATIVE CONCLUSION

Through the comprehensive pretreatment studies encompassing thermal, electrokinetic, and microbial approaches, it became apparent that optimization of electrokinetic pretreatment enhanced maximal solubilization of PRS (3.3-fold). Moreover, upon conducting anaerobic biodegradability assessments, it was evident that electrokinetically pretreated PRS under optimum conditions yielded the highest augmentation of biogas (Table 5.12). Concurrently, the removal of O&G demonstrated pronounced efficiency during the anaerobic digestion of electrokinetically pretreated PRS. However, the overall removal of TPH appeared to be comparable between electrokinetic and microbial (*Pseudomonas putida*) pretreatments. Notably, the highest removal of total phenol was observed through microbial pretreatment utilizing *Pseudomonas putida* strain. This could be attributed to the involvement of laccase enzymes, facilitated by *Pseudomonas* species during the degradation process of PRS, which exhibits a notable affinity for oxidizing phenolic hydrocarbon compounds, resulting in higher percentage of phenol removal. Furthermore, the phytotoxicity assay conducted on the digestate demonstrated a notable decrease in seed inhibition, accompanied by increased seedling growth and biomass of *Vigna radiata* L. (mung bean), suggesting reduced toxicity across all types of pretreatments.

Table 5.12. Comparative analysis of the pretreatment study

Type of pretreatment	**Optimum conditions**	**Biogas enhancement (%)**	**TPH removal (%)**	**O&G removal (%)**	**Total phenol removal (%)**
Thermal (dry heat)	140ºC, 60 min	40.1	38.8	56.1	64.3
Electrokinetic	60V, 83.5 min, 11.6 cm electrode spacing	61.1	57.3	71.5	72.4
Microbial (*P. putida*)	10^8 CFU/mL, 6 d	54.6	57.1	63	91.7
Microbial (*K. oryziphila*)	10^8 CFU/mL, 4 d	50.2	56.2	62.5	88.4

Chapter 6

COMBINATION STUDY

This chapter focuses on enhancing the anaerobic biodegradability of PRS through two stages. Stage 1 involves optimizing co-digestion of PRS with suitable co-substrate, while Stage 2 explores different pretreatment techniques (electrokinetic and microbial) combined with co-digestion to maximize biogas production.

6.1 CO-DIGESTION STUDY

6.1.1 Diagnostic evaluation and statistical analysis of the model

The experimental and predicted values of the design matrix developed by CCD-RSM for the co-digestion of PRS with YW is shown in Table 6.1. The experimental results incorporating the response surface analysis indicated the combined interactive effect of the chosen independent parameters (X_1= C/N ratio and X_2= pH) on the dependant output response (biogas yield) in coded and uncoded (actual) forms by fitting into second-order polynomial equations. The developed regression model in terms of coded and actual factors are represented in Eqs. (6.1) and (6.2) respectively.

$$Z_{coded} = 246.79\,X_1 + 382.92\,X_2 - 233.75\,X_1X_2 - 852.56\,X_1^2 - 698.56\,X_2^2 + 4043.00 \quad [6.1]$$

$$Z_{actual} = 1290.79\,X_1 + 17025.85\,X_2 - 38.96\,X_1X_2 - 15.16\,X_1^2 - 1091.50\,X_2^2 - 78732.90 \quad [6.2]$$

Either of the Eqs. (6.1) or (6.2) was solved to obtain the optimum values of C/N ratio and pH maximizing the biogas yield with utmost desirability percentage according to the developed model. The statistical significance and adequacy of the quadratic regression model was evaluated using analysis of variance (ANOVA). The model F-value = 79.3 and p-value <0.0001 indicated significant contribution again the 95% confidence level ($p<0.05$) suggesting sufficient adequacy relative to the pure error (Table 6.2). The linear terms (X_1 and X_2), quadratic term (X_1X_2) and interactive terms (X_1^2 and X_2^2) were also significant with p-value <0.05. A low C.V. value of 4.98 suggested high reliability of the experimental data points. The R^2 value of 0.9827 advocated that the quadratic model could explain 98.27% of the response variability suggesting high significance of the model. The close agreement of R^2_{pred} and R^2_{adj} ($R^2_{adj} - R^2_{pred} < 0.2$) indicated high degree of accuracy of the model,

and adequate precision of 23.11 resulted in adequate signal to navigate the design space. Fig. 6.1(a) showed high credibility for obtaining the augmented biogas yield with least incongruity, and Fig. 6.1(b) showed no irregularity in the experimental data points. Also, no definite pattern could be derived from the scattered points of the residual vs predicted plot [Fig. 6.1(c)] and therefore, the developed quadratic regression model was observed to be adequately reliable (Yılmaz and Şahan, 2020).

Table 6.1. Experimental design matrix showing experimental and predicted values

Run order	Coded factors		Actual factors		Biogas	
	X_1	X_2	C/N	pH	Experimental[a]	Predicted
1	-1	-1	25.00	6.20	1680.00	1628.41
2	0	+1.414	32.50	8.13	2990.00	3187.40
3	0	0	32.50	7.00	4043.00	4043.00
4	0	0	32.50	7.00	4043.00	4043.00
5	-1.414	0	21.89	7.00	1905.00	1988.85
6	0	0	32.50	7.00	4043.00	4043.00
7	+1	-1	40.00	6.20	2709.00	2589.50
8	0	0	32.50	7.00	4043.00	4043.00
9	0	0	32.50	7.00	4043.00	4043.00
10	0	-1.414	32.50	5.86	2038.00	2104.35
11	-1	+1	25.00	7.80	3006.00	2861.75
12	+1.414	0	43.11	7.00	2507.00	2686.90
13	+1	+1	40.00	7.80	3100.00	2887.84
Experimental (C[b])					2923.00	-

[a]Cumulative biogas yields by the end of digestion period; [b]C- Cumulative biogas yield due to monodigestion of PRS

Table 6.2. ANOVA for quadratic regression model of biogas yield

Source	Sum of squares	DF[a]	Mean Square	F-value[b]	p-value[c]
Model	9.377E+06	5	1.875E+06	79.31	< 0.0001
X_1 (C/N)	4.873E+05	1	4.873E+05	20.61	0.0027
X_2 (pH)	1.173E+06	1	1.173E+06	49.61	0.0002
$X_1 X_2$	2.186E+05	1	2.186E+05	9.24	0.0188
X_1^2	5.056E+06	1	5.056E+06	213.83	< 0.0001
X_2^2	3.395E+06	1	3.395E+06	143.56	< 0.0001
Residual	1.655E+05	7	23646.61		
Lack of Fit	1.655E+05	3	55175.43		
Pure Error	0.0000	4	0.0000		

SD[d]	Mean	R^2	R^2_{adj}	R^2_{pred}	Adequate precision	C.V[e]
153.77	3088.46	0.9827	0.9703	0.8766	23.11	4.98

[a]Degrees of freedom; [b]Fishers-test; [c]Probability value (< 0.05 implies significant and >0.1 insignificant); [d] standard deviation; [e] co-efficient of variation

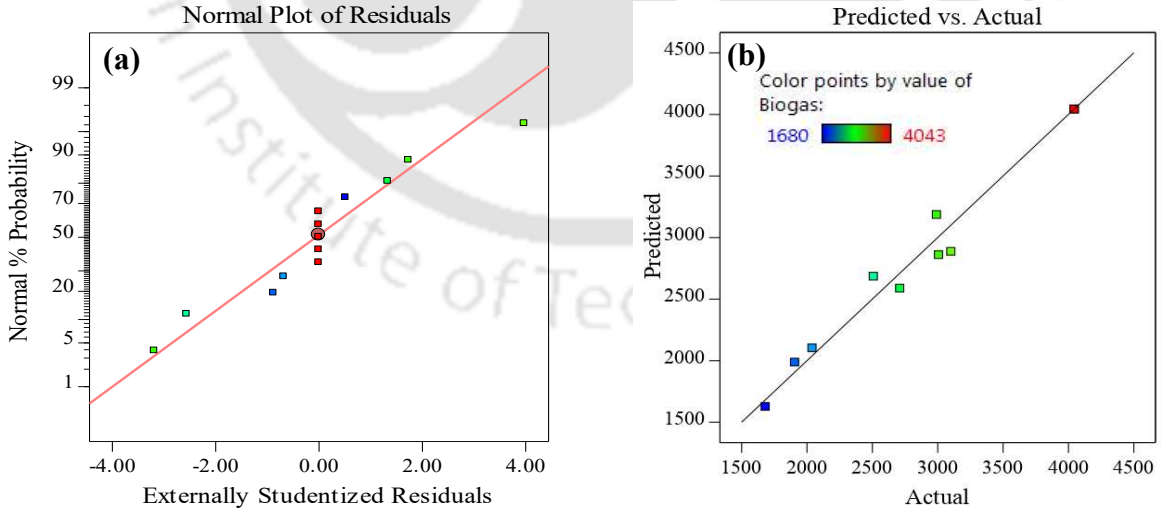

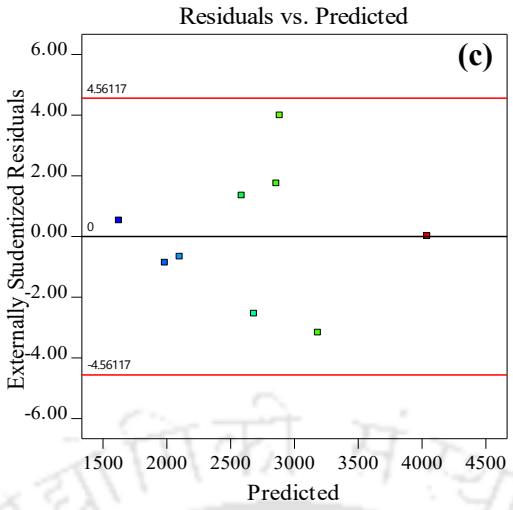

Fig. 6.1. (a) Predicted vs actual cumulative biogas plot, (b) normal plot of residuals and (c) residuals vs predicted plot of biogas yield

6.1.2 Interactive effect of C/N and pH on biogas yield

Fig. 6.2(a) and (b) show the 3D response surface plot and 2D contour plot respectively indicating the interactive outcome of independent variables, C/N ratio and pH on the dependent response of biogas yield due to the co-digestion of PRS with YW. The consolidated effect of C/N and pH on the biogas yield established a significant interaction ($p = 0.0188 < 0.05$) indicating a direct correlation of the independent variables with the performance of the anaerobic co-digestion (AnCoD) process. In Fig. 6.2(a), the cumulative biogas production increased with the combined increase in C/N ratio and pH till an optimum value of 4.043 L was obtained. Upon achieving the optimum value, the biogas production gradually decreased with any further alteration in the C/N ratio (>32.5) and pH (>7.0). Carbon, a basic energy source for the anaerobic microbial consortium, and nitrogen, an essential nutrient for their metabolism through organic matter synthesis, when become limiting factors, hampers the nutrient balance required for efficient degradation of a substrate due to inefficient metabolism depicted by the microorganisms affecting the methane generation potential (Dioha et al., 2013). C/N ratio, as desired to be in the range of 20-35, when higher, leads to rapid consumption of N by microorganisms limiting the growth and functioning of microbial cells due to N scarcity, thereby, lowering biogas production. This might be the reason behind observing reduced biogas (2.87 L) at C/N=40 and pH = 7.8 by the end of 50 d of digestion period. pH not only influences the accumulation of VFAs but also the chemical equilibria of ammonia (NH_3) and hydrogen sulphide (H_2S) acting as common inhibitors during the AD process. For an efficient biogas production, pH is desired to be in

the range of 6.8-7.2. At higher pH values in nitrogen-rich substrates such as PRS, free ammonia predominates over ammonium ion (NH_4^+) acting as major inhibitor in the digestion process (Zhang et al., 2018). At lower pH values, the activity of hydrolytic and acetogenic bacteria predominates over the methanogenic bacteria inhibiting the methanogenesis process resulting in lower biogas production which might be attributed to the reason behind obtaining reduced biogas yield (1.68 L) at pH = 6.2 and C/N =25 by the end of 50 d of AnCoD process. Also, low C/N ratio of 25 might have led to increased accumulation of total ammonia nitrogen (inhibitor) thereby diminishing the biogas yield (Zeshan and Visvanathan, 2012). Co-digestion of nitrogen-rich PRS with carbon-rich YW not only compensated the nutrient imbalance in terms of C/N ratio but also diluted the inhibitory or toxic compounds thereby enhancing the biogas yield by 38.3% at optimum conditions (C/N =32.5 and pH =7.0) compared to monodigestion of PRS by the end of 50 d of AnCoD period. This is in close agreement with Lee et al. (2022), who reported about 40% increment in methane production when secondary sludge of petroleum refinery was co-digested with food waste and swine manure upon C/N ratio optimization.

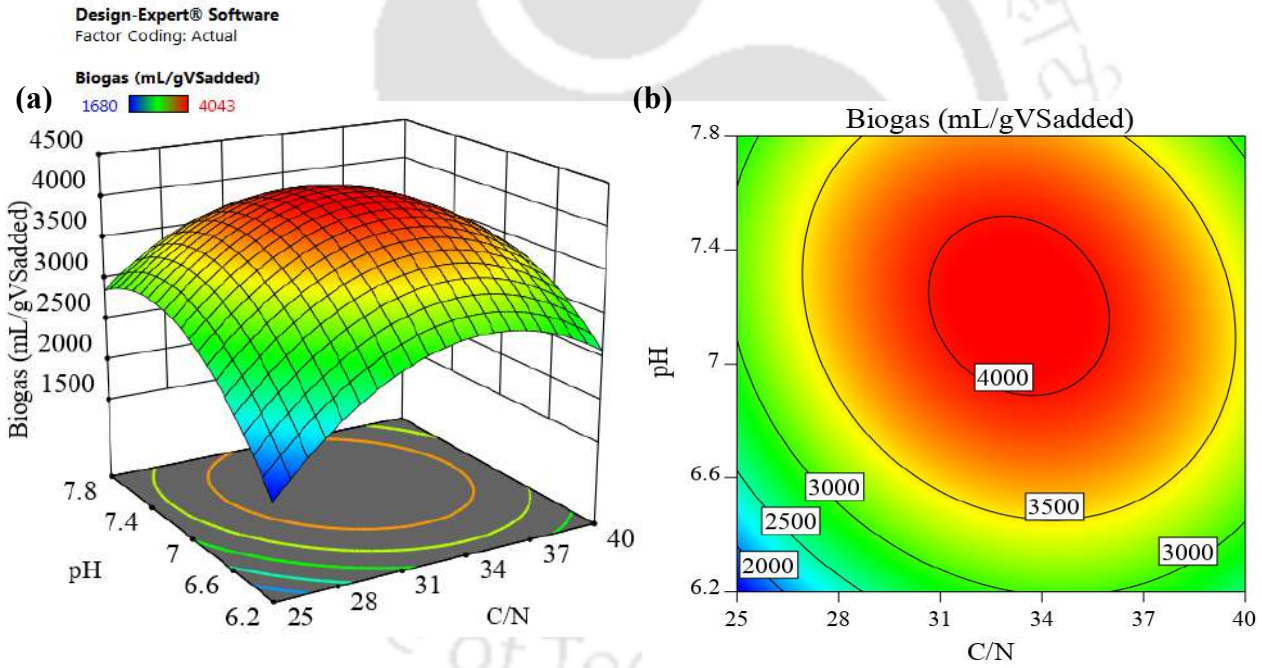

Fig. 6.2. (a) Interface (3D) plot and (b) contour (2D) plot showing the interactive effect of C/N and pH on biogas yield

6.1.3 Regression model validation

To validate the optimization model, a conformity experiment was run at optimum condition generated by the regression model (C/N=32.5, pH=7.0) for obtaining maximum cumulative biogas yield with 100% desirability. The experiment was conducted in a scaled-up batch study (20 L capacity,

14 L working volume) in duplicate to validate the biogas enhancement compared to monodigestion of PRS (control) in a larger-scale as shown in Fig. 6.3. The peak daily biogas was observed on 26th d of co-digestion period which was 7d earlier compared to the monodigestion (Fig. 6.3a). The cumulative biogas was augmented by 40.14% compared to that of monodigestion which was in close agreement with the predicted optimum value conferred by the regression model (Fig. 6.3b). Castro et al. (2022) performed co-digestion of petroleum refinery activated sludge with food waste and reported about 109.6% biogas increment compared to monodigestion which is 2.86 folds higher than the biogas enhancement achieved in the present study. This might be reasoned as the presence of readily available soluble organic fraction in the co-substrate (food waste) being utilized in their study. Though the augmented hydrolysis due to the balance of C/N and pH led to biogas enhancement but the limited digestibility of the co-substrate utilized in this study, YW, due to its lignocellulosic content posing a recalcitrant nature has been reported in various studies which necessitated pretreatments such as, application of thermal or hydrothermal techniques for improving solubilization followed by biogas augmentation as reported by Li et al. (2014). Ghaleb et al. (2021) co-digested biological sludge from petroleum refinery with mechanically and thermo-chemically pretreated highly lignocellulosic sugarcane bagasse to obtain 3.45 folds biogas enhancement for C/N=30 against C/N=22.6, which becomes an energy-intensive process. Application of an economically feasible, energy-saving pretreatment to intensify the biodegradability with improved digestibility facilitated the combination study.

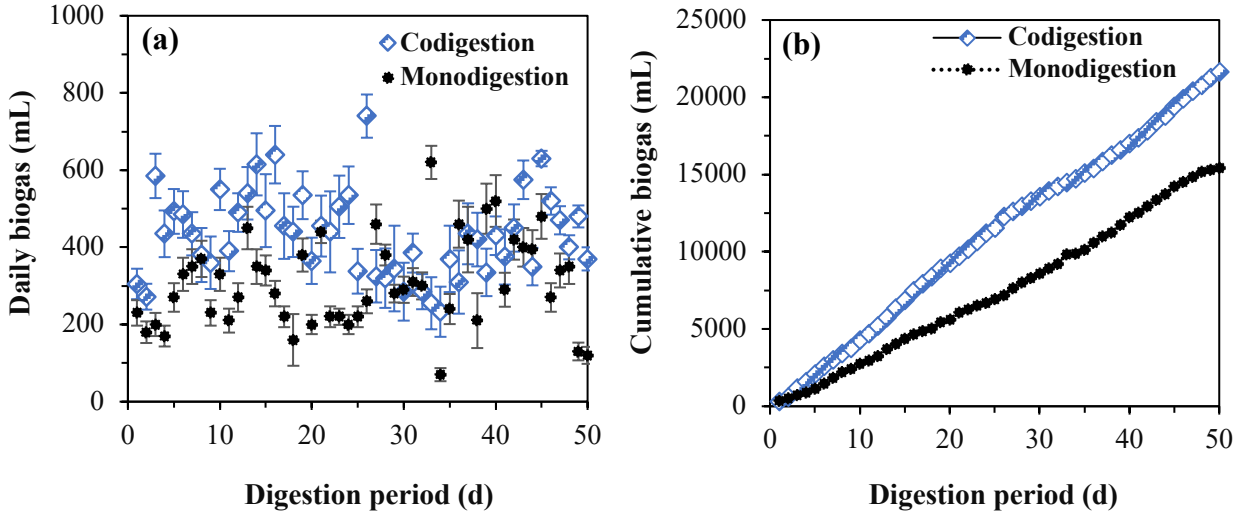

Fig. 6.3. (a) Daily biogas and (b) cumulative biogas production during the validation study of the regression model

6.2 ELECTROKINETICALLY ENHANCED CO-DIGESTION STUDY

6.2.1 Optimization of electrokinetic pretreatment process using CCD-RSM

The applied voltage supplied by DC power and the duration for which it is being applied are considered independent factors for the optimization of the electrokinetic (EK) pretreatment for enhanced co-digestion of PRS and YW. The pretreatment was conducted on the feedstock, PSYW (PRS mixed with YW as per Section 6.1.). Table 6.3 shows the experimental matrix exhibiting the experimental and predicted values of 11 run orders depicted by CCD-RSM on the response of dependent variables (sCOD and VFA concentrations). The relationship between independent parameters (X_1 = applied voltage; X_2 = exposure time) and model responses (Y_1 = sCOD; Y_2 = VFA) was fitted to a second-order quadratic polynomial equation which is represented in both coded and actual factors for both the responses in Eqs. (6.3), (6.4), (6.5) and (6.6).

When sCOD as output response,

$$sCOD_{coded} = 541.72\ X_1 + 785.84\ X_2 - 833.33\ X_1X_2 - 598.43\ X_1^2 - 1731.52\ X_2^2 + 6680.17 \quad [6.3]$$

$$sCOD_{actual} = 228.78\ X_1 + 179.95\ X_2 - 1.04\ X_1X_2 - 1.49\ X_1^2 - 1.08\ X_2^2 - 4706.27 \quad [6.4]$$

When VFA as output response,

$$VFA_{coded} = 33.19\ X_1 + 26.42\ X_2 - 52.36\ X_1X_2 - 83.05\ X_1^2 - 117.9\ X_2^2 + 800.09 \quad [6.5]$$

$$VFA_{actual} = 25.69\ X_1 + 11.30\ X_2 - 0.06\ X_1X_2 - 0.21\ X_1^2 - 0.07\ X_2^2 - 182.82 \quad [6.6]$$

Upon solving any of the aforementioned equations to derive the values of output responses, the corresponding optimal values for applied voltage and exposure time are generated. These optimal values play a pivotal role in maximizing the output responses with utmost desirability. ANOVA exhibited that the models for both the output responses (sCOD and VFA) were statistically good since the probability for the regression was considerably significant at a 95% confidence level ($p < 0.05$) (Table 6.4). As the table shows, applied voltage and exposure time were significant model variables for both sCOD and VFA with p-values <0.0001, indicating the regression model for both responses to

be highly credible. Also, the linear terms (X_1 and X_2), interaction term (X_1X_2), and quadratic terms (X_1^2 and X_2^2) were observed to be significant for both the output responses. The model F-values for sCOD and VFA were 53.55 and 40.98 respectively, implying the models were significant. Any model with a determination coefficient (R^2) between 0.75 and 0.90 could be considered to have a high correlation (Feng et al., 2017). R^2 values for response models of sCOD and VFA were 0.9745 and 0.9670 advocating the regression models of sCOD and VFA could respectively explain 97.45% and 96.7% of the response variability suggesting their high significance, and close correlation between the independent factors and each output response variable. The predicted R^2 for sCOD (0.8450) and VFA (0.7989) were in close agreement with their respective adjusted fitness coefficients (R^2_{adj}) since, $R^2_{adj} - R^2_{pred} < 0.2$. Adequate precision was applied to estimate the signal-to-noise ratio, with a preferable ratio greater than 4. The signal-to-noise ratio of 22.61 for sCOD and 18.20 for VFA, therefore, indicated adequate signals for navigating a design space corresponding to the output response. Low coefficient of variances (C.V.) for both sCOD (5.41) and VFA (3.69) advocated enhanced reliability and precision of experimentation (Abd et al., 2023). Fig. 6.4 shows the predicted vs actual plots of sCOD and VFA illustrating that the model responses were nearly parallel to their respective parity lines, thereby indicating the absence of any anomaly in the experimentations suggesting high credibility of the regression models of both the responses.

Table 6.3. Experimental and predicted outputs for the CCD-RSM matrix

Run order	Voltage (V)	Time (min)	sCOD (mg/L)		VFA (mg/L)	
	X_1	X_2	Experimental	Predicted	Experimental	Predicted
1	50.00	50.00	6740.45	6680.17	805.12	800.09
2	50.00	50.00	6740.45	6680.17	805.12	800.09
3	70.00	10.00	5258.57	4939.43	689.58	658.29
4	70.00	90.00	4832.32	4844.44	610.12	606.39
5	50.00	50.00	6740.45	6680.17	805.12	800.09
6	50.00	50.00	6740.45	6680.17	805.12	800.09
7	50.00	106.57	4370.69	4328.47	605.10	601.65
8	30.00	10.00	2460.65	2189.33	505.12	487.17
9	21.71	50.00	4621.42	4717.20	585.65	587.06
10	50.00	10.00	3560.00	4162.81	605.52	655.77
11	50.00	50.00	6740.45	6680.17	805.12	800.09
12	78.28	50.00	6086.00	6249.41	660.67	680.94
13	30.00	90.00	5367.73	5427.67	635.12	644.73
Experimental (Untreated PSYW)			2380.00	-	700.00	-

Table 6.4 Analysis of variance for response surface model of sCOD and VFA

Response 1: sCOD						
Source	**Sum of squares**	**DF[a]**	**Mean Square**	**F-value[b]**	**p-value[c]**	
Model	2.3×10^7	5	4.6×10^6	53.55	< 0.0001	
X_1 (Voltage)	2.3×10^6	1	2.3×10^6	27.46	0.0012	
X_2 (Exposure time)	4.0×10^6	1	4.0×10^6	46.89	0.0002	
$X_1 X_2$	2.8×10^6	1	2.8×10^6	32.49	0.0007	
X_1^2	2.5×10^6	1	2.5×10^6	29.55	0.0010	
X_2^2	1.4×10^6	1	1.4×10^7	170.20	< 0.0001	
Residual	5.9×10^5	7	85487.7			
Lack of Fit	5.9×10^5	3	1.9×10^5			
Pure Error	0.0000	4	0.0000			
SD[d]	**Mean**	**R^2**	**R^2_{adj}**	**R^2_{pred}**	**Adequate precision**	**C.V[e]**
292.38	5404.59	0.9745	0.9563	0.8450	22.61	5.41
Response 2: VFA						
Source	**Sum of squares**	**DF**	**Mean Square**	**F-value**	**p-value**	
Model	1.3×10^5	5	26254.6	40.98	< 0.0001	
X_1 (Voltage)	8814.9	1	8814.9	13.76	0.0076	
X_2 (Exposure time)	4529.5	1	4529.5	7.07	0.0325	
$X_1 X_2$	10968.4	1	10968.4	17.12	0.0044	
X_1^2	48656.1	1	48656.1	75.95	< 0.0001	
X_2^2	67463.4	1	67463.4	105.31	< 0.0001	
Residual	4484.5	7	640.6			
Lack of Fit	4484.5	3	1494.8			
Pure Error	0.0000	4	0.0000			
SD	**Mean**	**R^2**	**R^2_{adj}**	**R^2_{pred}**	**Adequate precision**	**C.V**
25.31	686.34	0.9670	0.9434	0.7989	18.20	3.69

[a]Degrees of freedom; [b]Fisher's-(F) test; [c]Probability value; [d]standard deviation; [e]co-efficient of variation

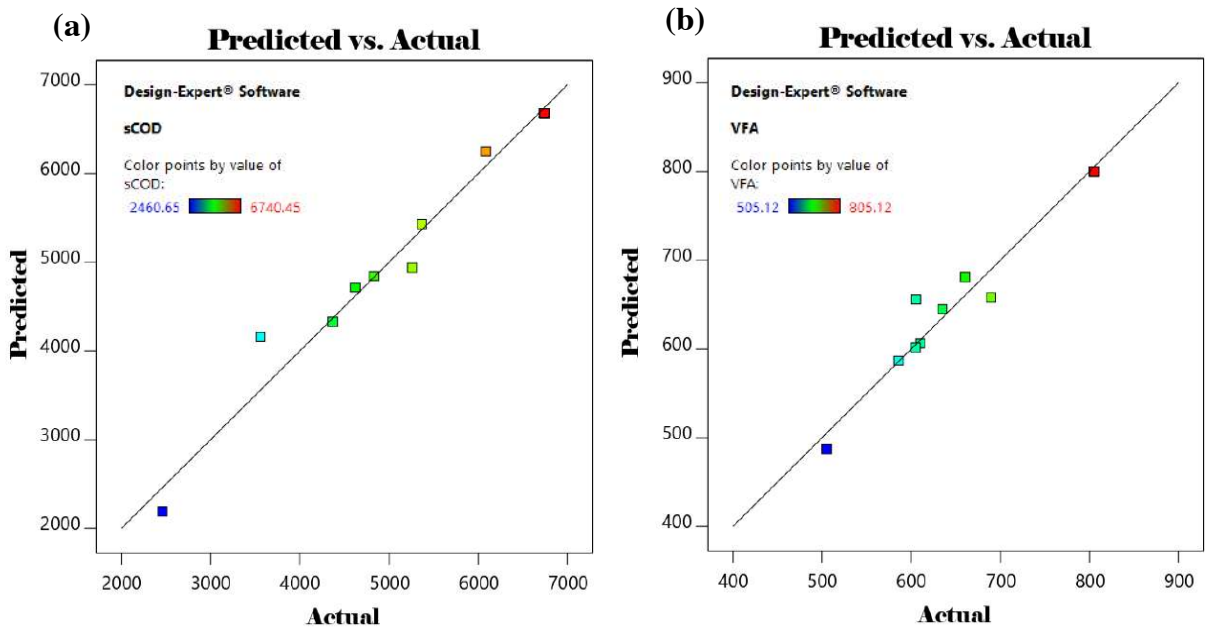

Fig. 6.4. Predicted vs actual plots of output responses, (a) sCOD and (b) VFA

6.2.2 Interaction effects using CCD-RSM

6.2.2.1 Interaction effects of independent parameters on sCOD

Fig. 6.5 exhibits the interactive impact of applied voltage through a DC power supply and its corresponding exposure duration on the enhanced solubilization of PSYW (a mixture of PRS and YW under optimal conditions) as a result of EK pretreatment. Assessing the solubilization of organic substrates can be accomplished through various indicators, including total suspended solids (TSS), total dissolved solids (TDS), total solids (TS), and soluble COD (sCOD). However, given the oily nature of the substrate (PRS) and the high recalcitrance of the lignocellulosic co-substrate (YW), sCOD is utilized as an indicator of solubilization in this study, as suggested by Salerno et al. (2009). As illustrated in Fig. 6.5(a), the sCOD steadily increased with a simultaneous rise in applied voltage and exposure duration, reaching an optimal value of 6746.85 mg/L. However, any further alterations in the independent parameters (i.e., voltage > 51.5V and time > 64.9 min) resulted in a subsequent decline in sCOD. The commencing increment in sCOD could be attributed to the conversion of insoluble heavy-molecular-weighted hydrocarbon compounds present in PRS to lighter soluble fractions, facilitated by the electric field generated by the DC voltage (Saini et al., 2020; Gidudu and Chirwa, 2020). This might also be due to the disruption of the cell membrane of the YW leading to the release of the intracellular organic fraction thereby, converting the complex organic macromolecules to smaller ones resulting in improved soluble fractions (Cai et al., 2022). At the optimized parameters of 51.5 V and 64.9 min, a striking 2.83-fold increase in

soluble COD (sCOD) was achieved compared to the untreated feedstock (PSYW). This significant enhancement was a result of the equilibrium between the number of electrons released by the DC power supply and the number of protons released from the feedstock electrolyte. However, as the applied voltage surpassed this optimum, a decline in sCOD ensued. This reduction can be attributed to the escalating electrical resistance caused by the increased current flow at higher voltages, leading to a rise in temperature due to the Joule effect, as elucidated by Daneshmand et al. (2012). Additionally, Kaur and Singh (2016) observed that higher voltages induce ohmic heating, restricting the flow of electrons and further contributing to the decrease in sCOD. Notably, the sCOD reached its minimum value (2422.3 mg/L) when exposed to 31V for 10.7 min between the graphite electrodes. During the EK process, the decontamination mechanism involves the movement of the organics (solid phase) to the anode due to electrophoresis, and water and oil (liquid phase) towards the cathode due to electroosmosis resulting in the dissociation of colloidal aggregates in the sludge matrix under the influence of the created electric field at a particular DC voltage. The extent of separation depends upon a lot of factors such as electric potential, voltage gradient, electrical conductivity, and pH (Gill et al., 2014). Therefore, at applied voltages or exposure periods lower than the optimum, the percentage organic fraction of solids in soluble form diminishes, resulting in reduced solubilization. Due to the low p-value (p=0.0007), the combined interaction of applied voltage and exposure time (X_1X_2) in this study was highly significant in advocating the credibility of the regression model for determining the output response of sCOD.

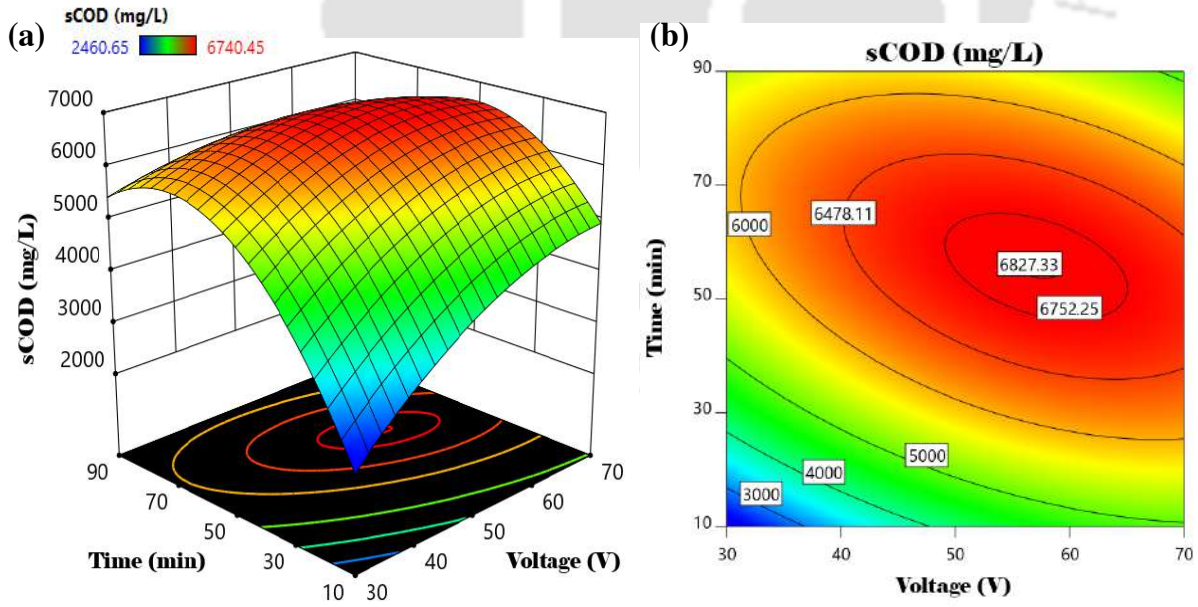

Fig. 6.5. (a) 3D interaction plot and (b) 2D contour plot of the effects of applied voltage and time on soluble chemical oxygen demand

6.2.2.2 Interaction effects of independent parameters on VFA

Fig. 6.6 shows the combined interaction of applied voltage and exposure time on the total VFA concentrations. The VFA accumulation in the feedstock increased as both independent parameters were simultaneously elevated, reaching a peak value of 804 mg/L. This optimal value was attained when an applied voltage of 53.5V was employed for 52.8 min. However, any subsequent alterations in the operating conditions resulted in a decrease in VFA concentrations. The variation in VFA concentrations might be attributed to the transportation of electrolysis ions [hydroxide (H^+) and hydroxyl (OH^-)] at the electrodes leading to the electro-dewatering of feedstock (Citeau et al., 2011). As a consequence, long-chain fatty acids in the feedstock (PSYW) undergo dissociation, transforming into negatively charged short-chain fatty acid ($RCOO^-$) radicals along with an increase in H^+ ions. These factors contribute to the initial rise in VFA concentrations under the influence of the electric field generated by the applied DC voltage (Fig. 6.6a). The dissociated fatty acid radicals might combine with metal ions present in the feedstock to form fatty acids salts (surface-active agents) enhancing the solid-stabilized emulsion displacement into the aqueous phase by altering the surface electric charges as a result of adsorption and interfacial tension (Yang et al., 2005). Also, with the increase in the exposure period of the applied voltages, VFA production rises in proportion to the electrical energy supplied for solubilizing organic feedstock (Gidudu and Chirwa, 2020). The peak VFA at 53.5V exposed for 52.8 min resulted in 1.65 folds increment against that of untreated PSYW. The increase in applied voltage beyond the optimal threshold of 53.5V caused a shortage of protons released from the feedstock, rendering them inadequate to counterbalance the surplus of electrons liberated by the DC power supply. This electrochemical imbalance consequently resulted in a decline in VFAs and solubilization beyond the optimal conditions. The increment in VFAs accumulation with a concurrent increase in soluble COD was in accordance with the thermal hydrolysis pretreatment study conducted by Zhang et al. (2019) showcasing increment in total VFAs yield in both mesophilic and thermophilic temperature conditions. The interactive model of this study was observed to be highly significant ($p<0.0044$) and therefore, the results of the regression model were extremely reliable.

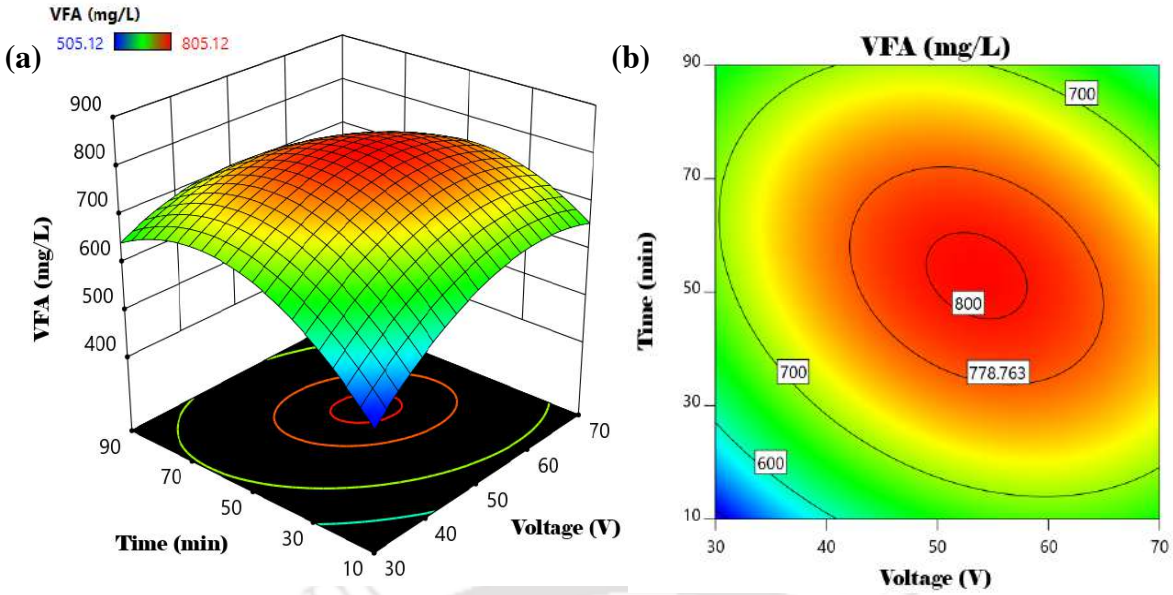

Fig. 6.6. (a) 3D interaction plot and (b) 2D contour plot of the effects of applied voltage and time on volatile fatty acids

6.2.3 Model validation

To validate the accuracy of the optimization model, a comprehensive investigation was carried out to assess the impact of EK pretreatment on the solubilization of the feedstock (PSYW) by examining the sCOD and VFA concentrations at the established optimal conditions. These optimal conditions, characterized by an applied voltage of 53.5V and an exposure duration of 53 min, demonstrated a remarkable 99.8% desirability, signifying the attainment of maximal solubilization and VFA accumulations. The experimental validation of the optimization model was carried out, resulting in sCOD and VFA concentrations of 6480 ± 608.94 mg/L and 820 ± 25.62 mg/L, respectively. Remarkably, these observed values fell well within the range of the predicted concentrations obtained through the application of CCD-RSM (sCOD = 6794.32 ± 328.5 mg/L; VFA = 804 ± 18.84 mg/L). The convergence between the experimental and predicted values provides compelling evidence supporting the reliability, and accuracy of the optimization model. The sCOD increment by 189.3% against untreated feedstock was comparable with the EK pretreatment study conducted by Westerholm et al. (2016) on thickened waste-activated sludge, which reportedly obtained soluble COD enhancement in the range of (180-450%). In this study, the percentage increase in sCOD was 3.8 times higher than the increase observed in the ozone pretreatment study conducted by Champagne and Anderson (2015) on anaerobic co-digestion of municipal wastewater treatment sludge and fat, oil, and grease (FOG). However, the percentage increase in VFA was higher in the other study compared to this one, which may be ascribed to a larger portion of organic compounds that underwent metabolic processing via anaerobic

fermentation yielding fatty acid intermediates. This phenomenon is likely attributable to the substrate composition of the former study, which was less intricate in comparison to the feedstock (PSYW) employed in the present study (Wang et al., 2016). The increment in solubilization of intricate compounds of PSYW due to EK pretreatment would be readily metabolized by the microorganisms for improved biodegradability in conjunction with biogas enhancement.

6.2.4 Morphological and chemical characteristics

The variation in outer surface morphology and relative abundance of elements present in PSYW due to EK pretreatment (53.5 V; 53 min) at optimum co-digestion conditions were investigated by FESEM-EDX and shown in Fig. 6.7 (a-d). The SEM images revealed a compact and rigid structure with few irregular solid and porous granules of the untreated PSYW (Fig. 6.7a). After the EK pretreatment, the structure got deconstructed and truncated with few distorted bundles illustrating porous microstructures with strong linkages suggesting molecular level bond dissociation and depolymerization of the feedstock (Fig. 6.7b). The elemental composition of the feedstock exhibited the dominance of carbon (61.5%) and oxygen (33%) since the feedstock consisted of hydrocarbons and lignocellulose, majorly comprising of C, H, and O (Fig. 6.7c and d). EK pretreatment resulted in increased dewaterability due to the separation of colloidal particles and fine solids from water-oil (W/O) emulsion due to the creation of electric field (Hu et al., 2013). This facilitated the water droplet coalescence in the continuous oil phase leading to electrocoagulation and solid-water-oil phase separation enhancing the solubilization of organic carbon, attributing the increase in C content (65%) after the pretreatment (Glendinning et al., 2007). The decrease in O content from 33% to 29.3% could be ascribed to the decomposition of oxygenated bonds and the liberation of hydrocarbon compounds with lower molecular weights that encompass H and O constituents (Yang et al., 2005).

The variation in functional groups due to EK pretreatment has been represented by the FTIR spectra (Fig. 6.7e). The spectra of PSYW samples showed similar absorption peaks but with different intensities due to EK pretreatment. The reduced absorption peak in the range of 3650-3130 cm^{-1}, indicated the dissociation of hydroxyl (−OH) functional groups existing in free form, intramolecular or intermolecular association representing the hydrogen vibrations of alcoholic groups (Singh and Kumar, 2020). Also, it exhibited dissociation of phenol or carboxyl groups (−COOH) representing the N−H vibrations of amide groups. The reduced transmittance in the waveband range of 2990-2800 cm^{-1} indicated the decomposition of aliphatic ($-CH_3$, $-CH_2$) functional groups. The absorption peak at 1609 cm^{-1} exhibited decomposition of C=C of aromatic rings, C=O stretching in carbonyl and carboxy functional groups of lignin, and C–O stretching and

linkage in guaiacol aromatic methoxy groups prevalent in the polymeric lignin structure of PSYW (Chourasia et al., 2021). Reduced absorption peaks at 1456 cm^{-1} within bands of 1500-1380 cm^{-1} corresponded dissociation of methyl ($-CH_3$) and methylene ($=CH_2$) functional groups while the intensified decrease at 1028 cm^{-1} signified degraded stretching vibrations of the C−OH group of alcohols, ethers, or esters. The peak around 750 cm^{-1} was ascribed to the bending mode of out-of-plane C−H. The last band at 560 cm^{-1} was reduced bending vibration of C−C=O due to aldehydes and ketonic groups of PRS as explained by Singh and Kumar (2020) in their physico-chemical characterization study of petroleum sludge from ETPs.

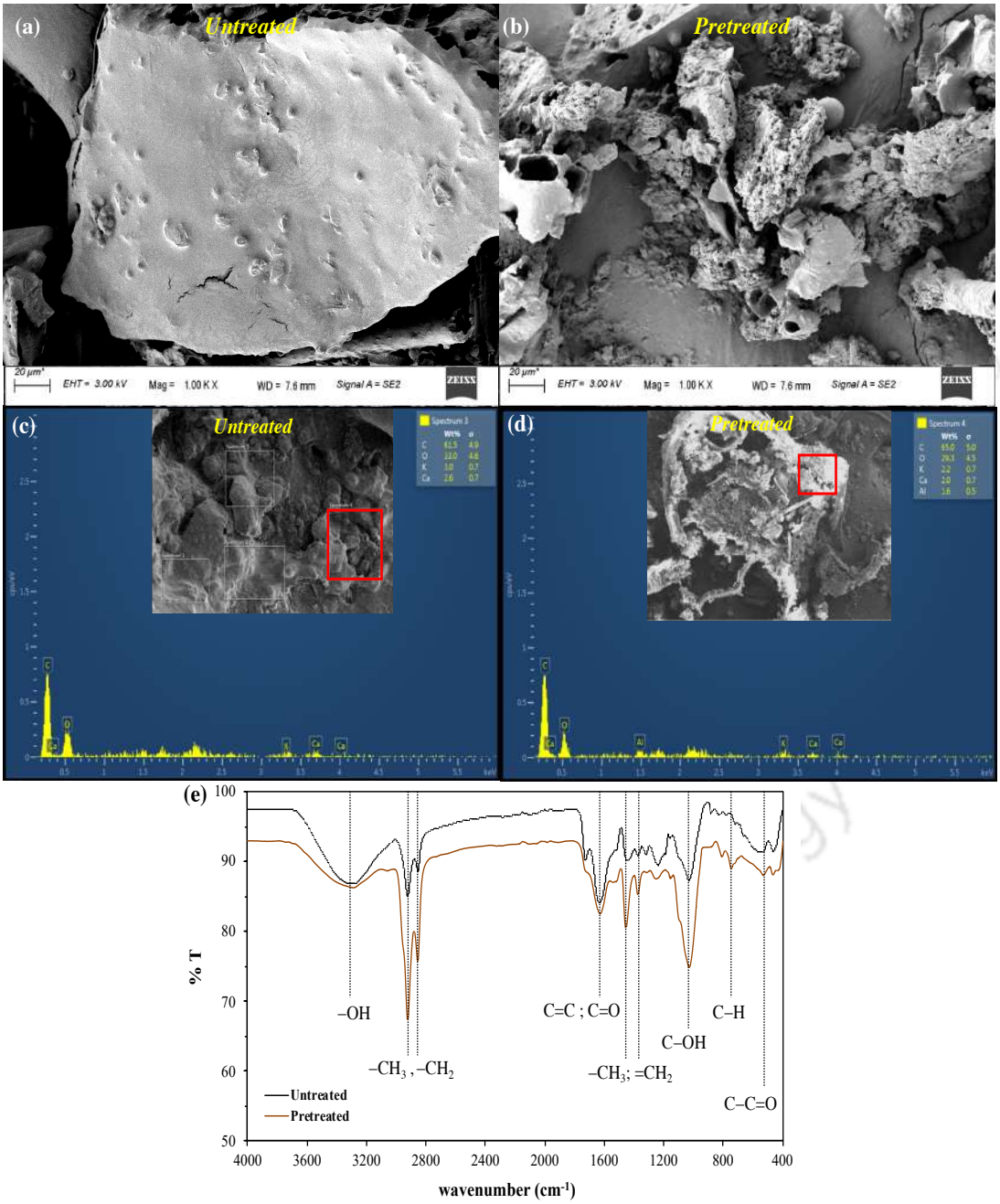

Fig. 6.7. FESEM spectra (a) before and (b) after pretreatment, SEM-EDX spectra (c) before and (c) after pretreatment, (e) FTIR spectra before and after EK pretreatment

6.2.5 Batch assay of anaerobic biodegradability

The extent of anaerobic biodegradability due to EK pretreated co-digestion of PRS and YW at optimum conditions has been illustrated in Fig. 6.8. The variation in daily biogas production for different inoculum/feedstock (PSYW or PRS mixed with YW at C/N=32.5, pH=7.0) ratios (I/F) is shown in Fig. 6.8 (a). For all the mixing ratios, biogas production gradually increased during the first 10 d of the digestion period. The maximum daily biogas was observed on 16^{th} d for I/F=0.4 which was about 62% higher and obtained 11 d earlier compared to that of control (untreated PSYW). This might be attributed to the microbial decomposition of insoluble complex hydrocarbon compounds being solubilized and hydrolyzed into simpler fractions (such as long chain fatty acids, and alcohols) under the influence of extracellular enzymes, being acted upon by the hydrolytic bacteria. This is a rate-limiting step, and therefore, explains the initial variation in the biogas generation at different I/F ratios (Zhen et al., 2017). The I/F ratio observing maximal biogas production could have attained balanced microbial proliferation for the utmost utilization of the organic content. The hydrolyzed compounds are thereby converted to short-chain VFAs and minor by-products (ammonia, hydrogen, and carbon dioxide) by the action of fermentative bacteria. The acetogenic bacteria thereafter act upon the VFAs to convert to H_2 and acetate, which is metabolized by the methanogenic archaea (majorly acetoclastic methanogenesis, minorly hydrogenotrophic methanogenesis) to convert to methane and carbon dioxide attributing to the generation of biogas (Wang et al., 2016; Cai et al., 2022). The cumulative biogas production due to EK pretreated co-digestion was observed to be maximum for I/F= 0.4, which was 55.8% higher compared to untreated co-digestion of PSYW (Fig. 6.8b). EK pretreatment led to the dewatering and removal of not only the soluble ions and neutral organics but also the insoluble organics in the porous feedstock media (Yang et al., 2005; Saini et al., 2020). The resulting improved solubilization led to the enhancement in biogas production by the end of 50d as also observed by Lee and Rittmann (2011) in their focused pulsed pre-treatment study for the improvement in anaerobic digestibility of waste-activated sludge. Different I/F ratios followed the order of cumulative biogas production as: 0.4>0.5>0.3>0.7.

In the presence of a direct current power supply, the induced electroosmotic flow causes the movement of water, resulting in an enhanced permeability of the substrate through capillary enlargement caused by the displacement of colloidal particles. This leads to the electro-demulsification of oil-in-water (O/W), followed by the electro-coagulation of the separated solid phase. Consequently, the solubility of the organic hydrocarbon fraction significantly improves, as corroborated by studies conducted by Elektorowicz et al. (2006) and Conrardy et al. (2016). These soluble hydrocarbon fractions were thereby employed by the anaerobic microbial consortium for

improved biodegradability as accredited from the extent of percentage VS degradation during EK pretreated co-digestion of PSYW (Fig. 6.8c). The maximum VS removal (69%) was observed for I/F= 0.4 followed by ratios 0.5, 0.3 and 0.7, which co-related with the maximal biogas production by the end of 50 d of digestion (Fig. 6.8b). These observed values were higher than that of the pilot-scale anaerobic digestion study conducted by Westerholm et al. (2016) on electrokinetically pretreated waste activated sludge.

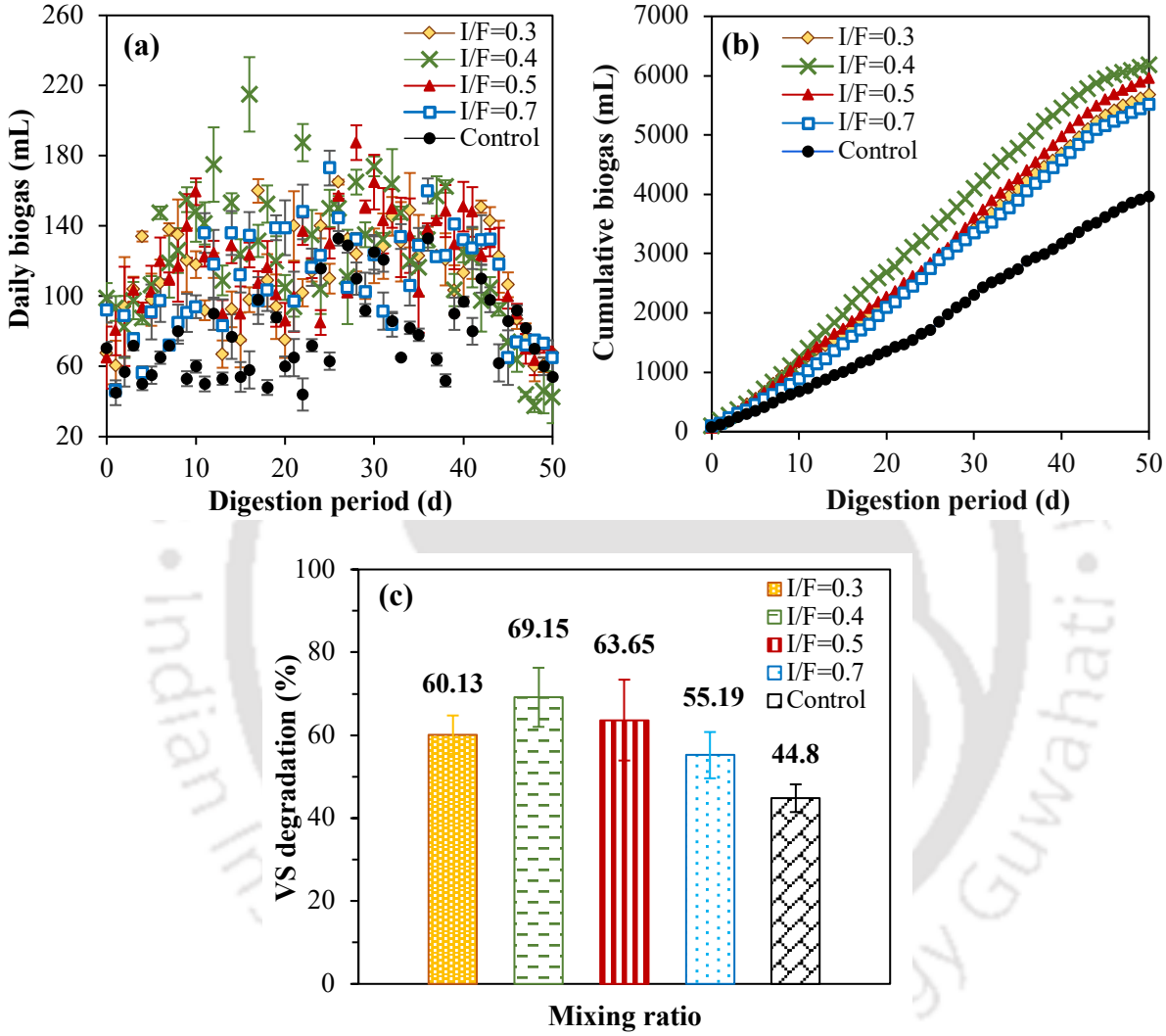

Fig. 6.8. Variation in (a) daily biogas, (b) cumulative biogas, and (c) volatile solids degradation for all the mixing ratios of EK pretreated co-digestion of PRS and YW

6.2.6 Energy Assessment

Conducting an energy assessment holds paramount importance in substantiating the economic feasibility of the employed pretreatment methodology, which aims to enhance the biodegradability of the complex substrate (PRS) as well as the co-substrate (YW). It is essential to ensure that the energy requirements associated with the pretreatment process do not surpass the energy quantities

recuperated in the form of methane. Through the implementation of EK pretreatment during the anaerobic co-digestion of PRS and YW, under meticulously determined optimal conditions (applied voltage: 53.5V; exposure duration: 53 min), a net surplus of energy, ΔE = 6872.43 kJ (where E_{in} = 193.42 kJ and E_{out} = 7065.85 kJ), was achieved. This consequently highlighted the effectiveness and feasibility of the pretreatment technique, which exhibited commendable energy recovery efficiencies establishing itself as a sustainable and prudent approach for the utilization and management of petroleum refinery wastes.

6.2.7 Scaled-up batch study

6.2.7.1 Biogas augmentation

When the 1L EK pretreated anaerobic biodegradability assay was scaled upto 20 L capacity at I/F=0.4, the peak daily biogas production was achieved on 17th d which was about 69% higher and obtained 9 d earlier when compared to the untreated co-digestion of PRS and YW (Fig. 6.9a). The monodigestion of PRS led to a broad hydrolysis phase due to the complex intricate hydrocarbon composition, delaying the microbial activity thereby resulting in scanty biogas production. This was evident from the reduced peak biogas being obtained 11 d later compared to EK pretreated co-digestion. The cumulative biogas production due to EK pretreated co-digestion was 40.5% higher than the untreated co-digestion of PRS and YW, and 84.2% higher than the monodigestion of PRS by the end of 60 d of the digestion period (Fig. 6.9b). The percentage enhancement in biogas due to EK pretreated co-digestion of PRS and YW was about 6% higher than the thermochemical pretreatment study conducted by Champagne and Anderson (2015) for biogas enhancement from the anaerobic co-digestion of municipal wastewater treatment sludge and fat, oil and grease (FOG). Also, Habashi et al. (2016) in their hydrodynamic cavitation pretreated co-digestion study of oily wastewater with waste-activated sludge revealed 30% biogas enhancement which was about 10% higher compared to the results obtained in this study. EK pretreatment conceivably enhanced the efficacy of the co-digestion process, thereby augmenting the energy recovery.

Fig. 6.9(c) shows the variation in total organic carbon (TOC) during the digestion processes. TOC undergoes conversion through a series of biochemical reactions facilitated by a diverse community of microorganisms during the anaerobic digestion process which can be co-related with the rate of increase in biogas production. The TOC of EK pretreated co-digestion increased from 0th d (1206 mg/L) to 20th d (2018.4 mg/L) where it attained the maximal value and gradually decreased thereafter till the end of the digestion period. The initial increase could be attributed to the catalytic action of hydrolytic enzymes secreted by the hydrolytic bacteria for the breakdown of complex organic compounds into simpler soluble forms, thereby increasing the solubility of

organic carbon, making it more accessible for further degradation following acidogenesis, acetogenesis, and finally methanogenesis to convert to biogas (Castro et al., 2022). This can be correlated with the increase in biogas during the initial 20 d of the pretreated co-digestion process (Fig. 6.9a). The peak TOC solubilization due to pretreated co-digestion on 20th d was 2.1 times higher than that obtained during the untreated co-digestion process. The subsequent reduction in TOC can be ascribed to the depletion of the available organic carbon fraction, primarily resulting from its oxidation to CO_2. This oxidation process occurs in conjunction with the release of H_2 originating from VFAs, alcohols, and acetate from the acidogenesis and acetogenesis phases. The ensuing interaction between CO_2 and H_2 leads to the conversion of these compounds into CH_4. A slight increase in TOC values on 40th d could be ascribed to the biological conversion of the particulate organic fraction from the EK pretreatment of the substrate and co-substrate to soluble fraction, increasing the biogas yields as well (Angeriz-Campoy et al., 2018). The inadequate TOC solubilization observed during the monodigestion of PRS could be attributed to the sluggish activity of microorganisms, primarily caused by the elevated concentrations of recalcitrant hydrocarbon fraction (Lee et al., 2022). Combined pretreatment and co-digestion reduces particle size of feedstock and increases the contact between microorganisms and organic matter, thereby promoting the solubilization of organic carbon ensuing enhanced biodegradability (Siddique et al., 2017).

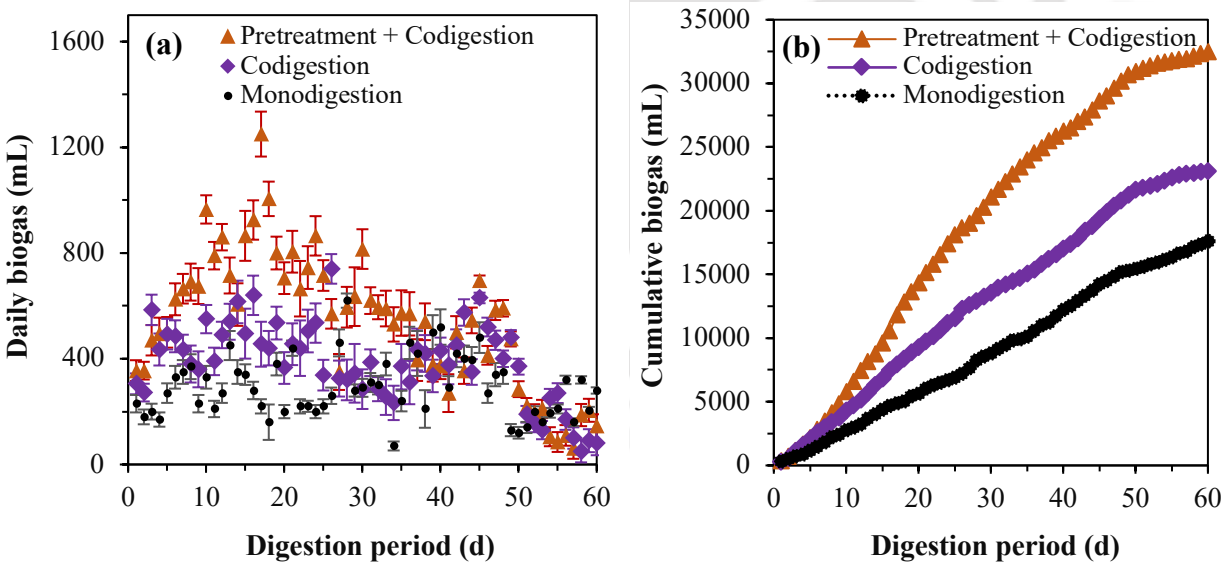

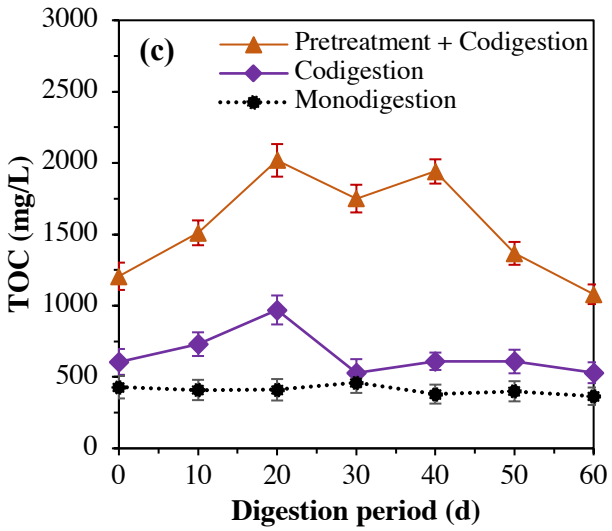

Fig. 6.9. Variation of (a) daily biogas, (b) cumulative biogas and (c) total organic carbon, during the monodigestion, co-digestion, and combined pretreatment and co-digestion processes

6.2.7.2 Pollutant degradation

Anaerobic degradation of petroleum hydrocarbons involves specialized metabolic pathways employed by microorganisms allowing the breakdown and utilization of hydrocarbon compounds in oxygen-limited environments, ultimately resulting in the production of methane and other metabolites. The variation in total petroleum hydrocarbon (TPH) content during the digestion processes has been shown in Fig. 6.10(a). It was observed that the TPH content followed a decreasing trendline throughout the digestion period of 60d. During EK pretreated co-digestion process, the TPH content gradually decreased from 78.2 g/kg (0^{th} d) to 28.2 g/kg (60^{th} d) leading to a removal of 64% which was perceived to be 1.9 folds higher than the untreated co-digestion process. The degradation of petroleum hydrocarbons in anaerobic conditions occurs through different pathways: such as hydrocarbon activation through alkylsuccinate synthases by adding them to fumarate, forming alkylsuccinate intermediates following the breakdown of the activated hydrocarbons into simpler compounds, such as fatty acids, alcohols, and hydrogen, through anaerobic hydrocarbon metabolism. The by-products from hydrocarbon metabolism thereby serve as substrates for methanogenic archaea to be converted to CH_4 as a metabolic end product (Varjani and Upasani, 2017). The reduction in TPH content from 105.7 g/kg (0^{th} d) to 89.6 g/kg (60^{th} d) during the monodigestion of PRS revealed that the percentage TPH removal due to pretreated co-digestion was 4.2 folds higher than the monodigestion. This could be attributed to the heterogenous and multi-phasic intricate composition of the PRS, such as aliphatic hydrocarbon degradation occurs through fumarate addition whereas, aromatic hydrocarbon degradation occurs via diverse

pathways, including fumarate addition, reductive dehalogenation, and other anaerobic aromatic ring cleavage mechanisms (Ward et al., 2003; Haak et al., 2016). Polyaromatic hydrocarbons (PAHs) undergo majorly reductive processes (reductive dehalogenation and anaerobic ring cleavage) performed by specialized microorganisms for their degradation as revealed by Niqui-Arroyo and Ortega-Calvo (2010) in their PAH bioaccessibility study which resulted in 90% PAH content reduction during EK treatment of hydrocarbon polluted soils.

The O&G removals during the digestion processes have been shown in Fig. 6.10(b). PRS is a water-in-oil (W/O) emulsion stabilized by various types of emulsifiers such as asphaltenes, resins, organic acids, and fine solids. These emulsifiers form a film on the surface of water droplets, acting as a barrier against droplet coalescence. However, under the influence of an electric field, the colloidal particles and fine solids separate from the emulsion disrupting this barrier, leading to faster coalescence of water droplets in the oil phase. The separated liquid phase forms an unstable secondary oil-in-water emulsion, undergoing electro-coalescence, resulting in the separation of water and oil phases for microbial degradation (Hu et al., 2013). During EK pretreated co-digestion process, this O&G (emulsion) concentration resulted in 70% removal by the end of 60 d of digestion which was 1.7 folds higher than untreated co-digestion, and 4.2 folds higher than monodigestion of PRS. During the anaerobic digestion process, the microorganisms, having the ability to produce biosurfactants, interact with the oil-water interface and reduce the surface tension between oil and water. This allows the emulsion to disperse into smaller droplets providing a larger surface area for microbial activity, making the oil and grease more accessible for degradation (Varjani and Upasani, 2017). During the pretreated co-digestion process, the microbes even could access the separated oil phase from the secondary oil-in-water emulsion resulting in a higher percentage of O&G degradation.

Fig. 6.10(c) shows the variation in lignocellulosic degradation during the digestion processes. The lignin degradation [acid soluble lignin (ASL) + acid-insoluble lignin (AIL)] for pretreated co-digestion of PRS and YW was 34.3% which was 4.0 folds higher compared to untreated co-digestion. Lignocellulose encompasses the intricate lignin, a complex polymer composed of phenyl propane units, covalently linked to hemicellulose and cellulose. Hemicellulose is a polysaccharide consisting of pentoses, hexoses, deoxy-hexoses, and hexuronic acid, and cellulose is an unbranched biopolymer of glucose monomers (Amin et al., 2017). Lignin, characterized by its intricate aromatic structure, exhibits high recalcitrance, rendering it less susceptible to microbial degradation compared to hemicellulose and cellulose. Due to EK pretreatment, the removal of hemicellulose and cellulose in the co-digestion process were 36.7% and 83% respectively within 60 d, exhibiting 3.8-fold and 2.9-fold enhancements compared to untreated co-digestion and

monodigestion respectively. EK pretreatment disrupted the ring structure of heavily structured aromatic rings of lignin, resulting in truncated lignin fragments. Consequently, hemicellulose and cellulose, consisting of lighter-molecular-weighted compounds, were exposed and became more accessible to microbial activity. During the anaerobic digestion process, these modified lignin fragments underwent demethoxylation, followed by aromatic ring structure cleavage and fermentation, ultimately converting them to acetate, H_2, and CO_2. This metabolic pathway led to 40% biogas augmentation compared to untreated co-digestion of PRS and YW (Fig. 7b) (Khan and Ahring, 2019).

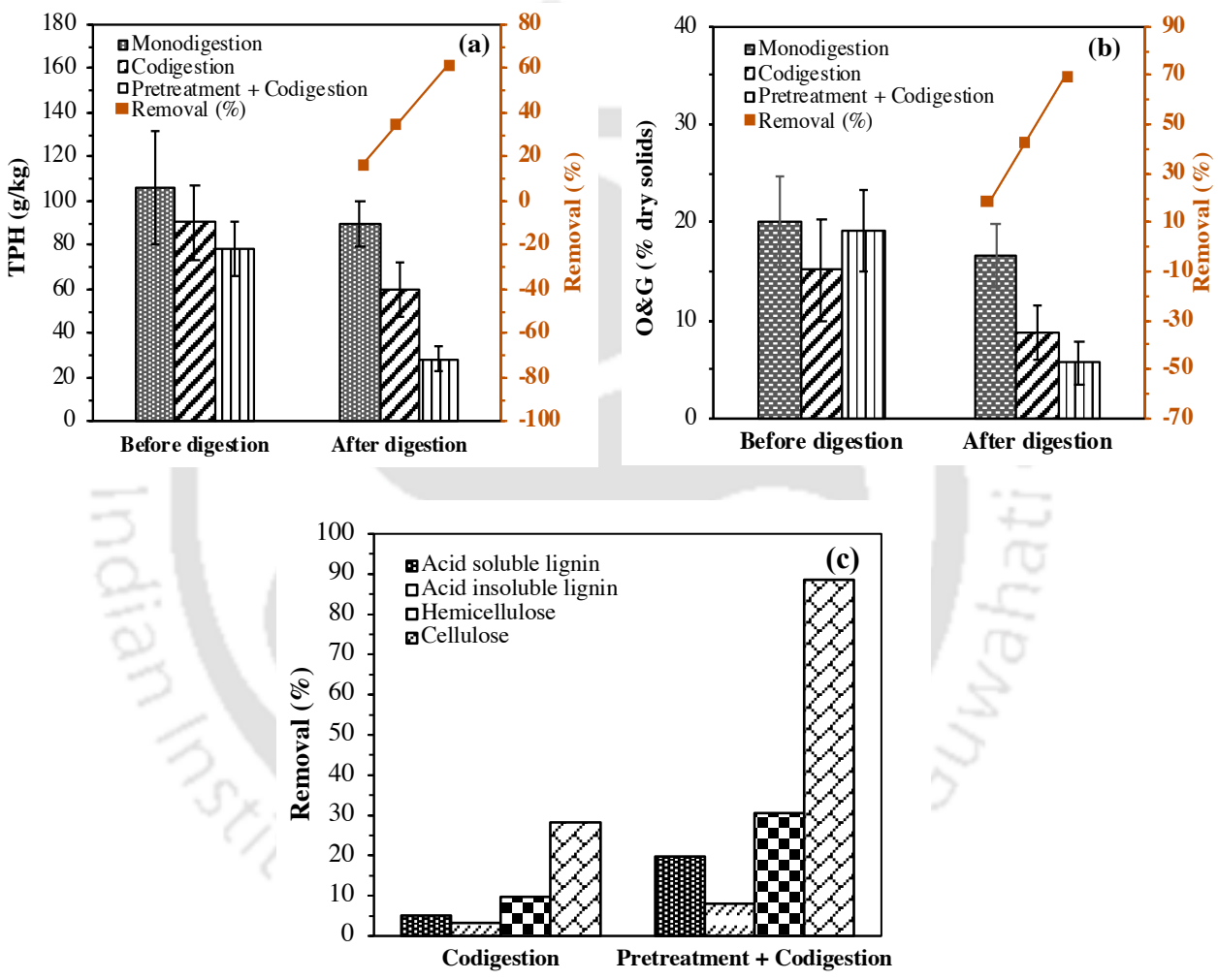

Fig. 6.10. Degradation of (a) TPH, (b) O&G, and (c) lignocellulosic content during the monodigestion, co-digestion, and combined pretreatment and co-digestion of PRS and YW

6.2.7.3 Digestate phytotoxicity

The disposal of PSYW in reclaimed soil possesses the inherent capacity to attenuate the physicochemical attributes of the soil, consequently impeding plant growth through alterations in the microbial community composition and undermining the natural catalytic functionality of soil

enzymes. Hydrocarbon-rich PRS might restrict the availability of essential nutrients, water, and oxygen in soils (Guo et al., 2014). The digestate from EK pretreated co-digestion (PC), untreated co-digestion (UC), and monodigestion (MD) were therefore being assessed for phytotoxicity using *Vigna radiata* L. (black gram), in order to draw a comparative evaluation of their safe disposal into the ecosystem. Digestate phytotoxicity as evaluated through seed germination inhibition at different percentage dilutions (50%, 75% and 100%), resulting in alteration of seedling biomass growth including their root and shoot developments have been indicated in Table 6.5. The rates of germination for the digestate of PC were incremented by 1.08, 1.2, and 1.2 folds corresponding to 50%, 75%, and 100% dilution extracts respectively compared to the digestate of UC. The low germination rates of the digestate of MD could be easily attributed to the toxic intricate hydrocarbon composition of PRS (Haak et al., 2016; Jerez et al., 2021). The germination index (GI) is an indicator of the toxic effects of any substrate through seed germination rate and root length in plants. The root length was observed to decrease with increasing concentrations of dilution extracts for all three digestion processes which could be attributed to the accumulation and migration of the soluble toxic fractions of PRS by the roots though the shoots of plants (Haider et al., 2021).

Fig. 6.11 shows the germination index (GI) calculated by using *V. radiata* L. seeds. It depicted that for the digestate of PC, the GI incremented by 29.8%, 23.2% and 87% for 50%, 75% and 100% dilution extract respectively compared to UC. As per Raj and Antil (2011), if GI>70% for any extract of the sample, then it could be considered as free of phytotoxins. The increase in GI for PC improved the activity of microbial flux through the reduction in the immiscibility of W/O emulsions. Compared to MD, the GI of PC digestate increased by 74.7%, 109.2%, and 170.3% for 50%, 75%, and 100% dilution extracts, respectively. The significant reduction in seed germination, shoot length, root length, and biomass of digestate of MD might be ascribed to the inductive oxidative stress caused by elevated concentrations of PAHs (Niqui-Arroyo and Ortega-Calvo, 2010). The transformation of the organic fraction of PRS and YW through EK pretreated co-digestion resulted in the depletion of toxicity.

Table 6.5. The outcome of digestate samples of EK pretreated co-digestion, untreated co-digestion, and monodigestion on seed germination, shoot length, root length, and seedling biomass growth of *V. radiata* L.

Digestate	Dilution ratio	Germination (%)	Shoot Length (cm)	Root Length (cm)	Biomass (cm)
	Control	100	8.82 ± 0.450	5.02 ± 0.401	0.84 ± 0.08

MD	50	70.00 ± 0.00*	6.85 ± 0.484*	4.62 ± 0.342	0.48 ± 0.04
	75	56.67 ± 0.57	5.45 ± 0.429*	4.05 ± 0.208*	0.38 ± 0.02
	100	50.00 ± 0.00*	4.42 ± 0.438	1.49 ± 0.062*	0.26 ± 0.05
UC	50	86.67 ± 0.57*	7.28 ± 0.507*	5.02 ± 0.622*	0.52 ± 0.04
	75	76.67 ± 1.15	6.05 ± 0.472	5.08 ± 0.410*	0.48 ± 0.04
	100	66.67 ± 0.57*	4.83 ± 0.208*	1.62 ± 0.106	0.30 ± 0.06
PC	50	93.33 ± 0.57*	8.82 ± 0.528*	6.05 ± 0.814*	0.72 ± 0.07
	75	90.00 ± 0.00*	7.75 ± 0.407*	5.33 ± 0.482*	0.65 ± 0.06
	100	80.00 ± 0.00*	5.42 ± 0.318	2.52 ± 0.281*	0.59 ± 0.05

Values are mean ± SD from duplicates; ∗ANOVA established p-value <0.05 as significant with respect to control.

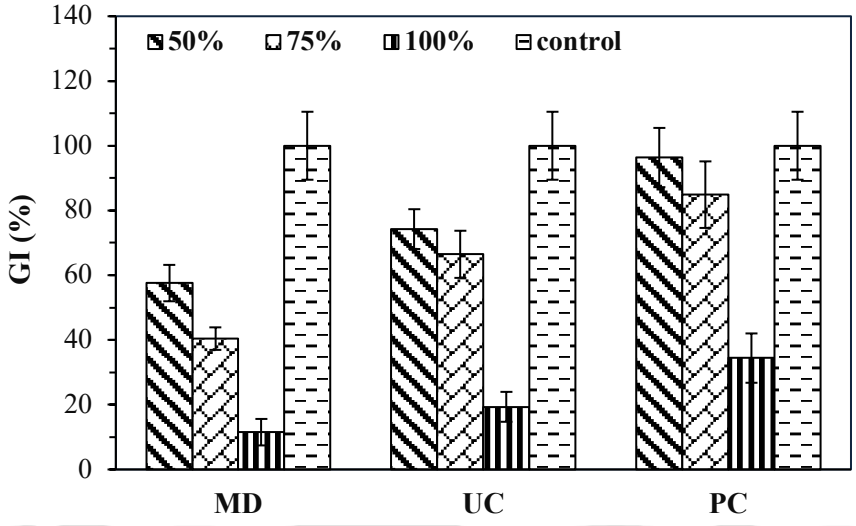

Fig. 6.11. Germination index of seeds of *Vigna radiata* L. incubated in digestate of monodigestion (MD), untreated co-digestion (UC), and EK pretreated co-digestion (PC) of PRS and YW

6.3 MICROBIALLY ENHANCED CO-DIGESTION STUDY

6.3.1 Metagenomics study of petroleum refinery sludge

Based on the National Center for Biotechnology Information (NCBI) taxonomic database, a phylogenetic tree was generated from the taxonomic analysis of metagenomic data which showed that the bacteria domain (99.4%) consisted of the majority of the metagenomic sequences with the remaining sequence consisting of archaea domain, *Euryarcheota* (0.6%) . A certain percentage of sequences remained unclassified. The dominant classified bacterial phyla observed in the PRS were *Proteobacteria* (59.6%), *Bacteroidetes* (10.5%), and *Chloroflexi* (6.2%) (Fig. 6.12a). Roy et al.

(2018) in their study stated that *Proteobacteria* was the most abundant phylum with about 57% relative abundance along-with *Bacteroidetes* and *Chloroflexi* in the bacterial community of the secondary sludge collected from wastewater lagoon of petroleum refinery. *Proteobacteria* and *Bacteroidetes* are responsible for the degradation of organic fraction of a substrate and production of nitrogen (N) compounds whereas, *Chloroflexi* reportedly engages in the fermentation of alkanes under anaerobic and sulphate-reducing conditions (Lee et al. 2022). With a relative abundance of 10.85%, SBR1093 remained unclassified which might be distantly related to any familiar sequence deposited in the NCBI taxonomic database. The presence of *Firmicutes*, *Verrucomicrobia*, *Planctomycetes*, *Gemmatimonadetes* and *Acidobacteria* (constituting about 10% of the total reads) in the PRS was in accordance with the study conducted by Silva et al. (2012) who also observed their presence in varying abundance in the petroleum refinery wastewater generated from their WWTPs. The strictly anaerobic, facultative, fermentative, nitrate-fixing and sulphate-reducing bacteria dominating in the PRS are reportedly efficient hydrocarbon degraders (Xu et al., 2019).

Alphaproteobacteria (22.8%), *Betaproteobacteria* (21.8%), *Gammaproteobacteria* (9.4%) and *Deltaproteobacteria* (5.0%), and *Epsilonproteobacteria* (0.5%) were the dominant bacterial class of the phylum group of *Proteobacteria* with each one of them exhibiting hydrocarbon-degrading properties by controlling the cycle of organic (C and N) and inorganic compounds (Fig. 6.12b). The PAH degrading capacities of these dominant classes of *Proteobacteria* had been reported by Sun et al. (Sun et al., 2010). *Deltaproteobacteria* is well-known to be involved in anaerobic hydrocarbon degradation with their percentage abundance relatively proportional to petroleum hydrocarbon contamination. The presence of aerobic or facultative anaerobic, nitrate reducing-*Alphaproteobacteria* reportedly implicate hydrocarbon metabolizing activities in petroleum-enriched environments (Roy et al., 2018). The abundant classes in *Bacteroidetes* were *Bacteroidia* (8.7%), *Saprospirae* (1.1%), and *Flavobacteriia* (0.6%), and the dominant classes in *Choloroflexi* were *Anaerolinae* (5.7%) and *Thermomicrobia* (0.5%). Some other classes with high abundance were *VHS-B5-50* (10.8%), *Clostridia* (2.1%), *Spartobacteria* (2.1%), *Plantomycetia* (1.9%), *Gemmatimonadetes* (1.6%), *Chloracidobacteria* (1.4%), and *SC72* (1%).

The major classified abundant genera were *Thiobacillus* (12.9%), *Thermomonas* (5.5%), *Bdellovibrio* (4.9%), *Bradyrhizobium* (3.5%), *Longilinea* (3.5%), *Hyphomicrobium* (3.4%), *Parvibaculum* (3.0%), *Alicycliphilus* (2.6%), *HeteroC45_4W* (2.07%), and T78 (1.9%) (Fig. 6.12c). Martin et al. (2012) reported the relative abundance of *Thiobacillus* genera in the degradation of phenanthrene in a PAH-contaminated soil suggesting its hydrocarbon utilizing property.

Phylum

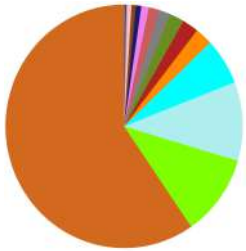

Phylum legend

Legends	Taxonomy	Abundance
	k__Bacteria;p__Proteobacteria	59.57%
	k__Bacteria;p__SBR1093	10.85%
	k__Bacteria;p__Bacteroidetes	10.47%
	k__Bacteria;p__Chloroflexi	6.19%
	k__Bacteria;p__Firmicutes	2.36%
	k__Bacteria;p__Verrucomicrobia	2.2%
	k__Bacteria;p__Planctomycetes	2.0%
	k__Bacteria;p__Gemmatimonadetes	1.56%
	k__Bacteria;p__Acidobacteria	1.43%
	k__Bacteria;p__WS6	1.02%
	k__Bacteria;p__Chlorobi	0.74%
	k__Archaea;p__Euryarchaeota	0.59%
	k__Bacteria;p__Actinobacteria	0.53%
	k__Bacteria;p__Caldiserica	0.19%
	k__Bacteria;p__Synergistetes	0.11%
	k__Bacteria;p__OP1	0.11%
	k__Bacteria;p__Fusobacteria	0.02%
	k__Bacteria;p__Thermotogae	0.01%
	k__Bacteria;p__WPS-2	0.01%
	Others	0.03%

Class

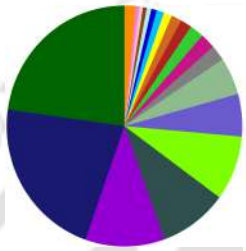

Class legend

Legends	Taxonomy	Abundance
	k__Bacteria;p__Proteobacteria;c__Alphaproteobacteria	22.81%
	k__Bacteria;p__Proteobacteria;c__Betaproteobacteria	21.82%
	k__Bacteria;p__SBR1093;c__VHS-B5-50	10.85%
	k__Bacteria;p__Proteobacteria;c__Gammaproteobacteria	9.44%
	k__Bacteria;p__Bacteroidetes;c__Bacteroidia	8.68%
	k__Bacteria;p__Chloroflexi;c__Anaerolineae	5.72%
	k__Bacteria;p__Proteobacteria;c__Deltaproteobacteria	5.03%
	k__Bacteria;p__Firmicutes;c__Clostridia	2.11%
	k__Bacteria;p__Verrucomicrobia;c__[Spartobacteria]	2.07%
	k__Bacteria;p__Planctomycetes;c__Planctomycetia	1.93%
	k__Bacteria;p__Gemmatimonadetes;c__Gemmatimonadetes	1.56%
	k__Bacteria;p__Acidobacteria;c__[Chloracidobacteria]	1.42%
	k__Bacteria;p__Bacteroidetes;c__[Saprospirae]	1.13%
	k__Bacteria;p__WS6;c__SC72	1.02%
	k__Bacteria;p__Chlorobi;c__Ignavibacteria	0.74%
	k__Bacteria;p__Bacteroidetes;c__Flavobacteriia	0.64%
	k__Bacteria;p__Actinobacteria;c__Actinobacteria	0.52%
	k__Bacteria;p__Proteobacteria;c__Epsilonproteobacteria	0.48%
	k__Bacteria;p__Chloroflexi;c__Thermomicrobia	0.47%
	Others	1.57%

Genus

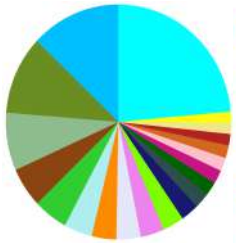

Genus legend

Legends	Taxonomy	Abundance
	k__Bacteria;p__Proteobacteria;c__Betaproteobacteria;o__Hydrogenophilales;f__Hydrogenophilaceae;g__Thiobacillus	12.89%
	k__Bacteria;p__SBR1093;c__VHS-B5-50;o__Unclassified;f__Unclassified;g__Unclassified	10.85%
	k__Bacteria;p__Bacteroidetes;c__Bacteroidia;o__Bacteroidales;f__Porphyromonadaceae;g__Unclassified	7.96%
	k__Bacteria;p__Proteobacteria;c__Gammaproteobacteria;o__Xanthomonadales;f__Xanthomonadaceae;g__Thermomonas	5.49%
	k__Bacteria;p__Proteobacteria;c__Deltaproteobacteria;o__Bdellovibrionales;f__Bdellovibrionaceae;g__Bdellovibrio	4.93%
	k__Bacteria;p__Proteobacteria;c__Betaproteobacteria;o__Burkholderiales;f__Comamonadaceae;g__Unclassified	4.06%
	k__Bacteria;p__Proteobacteria;c__Alphaproteobacteria;o__Rhizobiales;f__Bradyrhizobiaceae;g__Bradyrhizobium	3.53%
	k__Bacteria;p__Chloroflexi;c__Anaerolineae;o__Anaerolineales;f__Anaerolinaceae;g__Longilinea	3.51%
	k__Bacteria;p__Proteobacteria;c__Alphaproteobacteria;o__Rhizobiales;f__Hyphomicrobiaceae;g__Hyphomicrobium	3.39%
	k__Bacteria;p__Proteobacteria;c__Alphaproteobacteria;o__Rhizobiales;f__Hyphomicrobiaceae;g__Parvibaculum	3.05%
	k__Bacteria;p__Proteobacteria;c__Betaproteobacteria;o__Burkholderiales;f__Comamonadaceae;g__Alicycliphilus	2.62%
	k__Bacteria;p__Verrucomicrobia;c__[Spartobacteria];o__[Chthoniobacterales];f__[Chthoniobacteraceae];g__heteroC45_4W	2.07%
	k__Bacteria;p__Chloroflexi;c__Anaerolineae;o__Anaerolineales;f__Anaerolinaceae;g__T78	1.95%
	k__Bacteria;p__Planctomycetes;c__Planctomycetia;o__Gemmatales;f__Isosphaeraceae;g__Unclassified	1.89%
	k__Bacteria;p__Proteobacteria;c__Alphaproteobacteria;o__Sphingomonadales;f__Sphingomonadaceae;g__Unclassified	1.84%
	k__Bacteria;p__Proteobacteria;c__Gammaproteobacteria;o__PYR10d3;f__Unclassified;g__Unclassified	1.77%
	k__Bacteria;p__Gemmatimonadetes;c__Gemmatimonadetes;o__Unclassified;f__Unclassified;g__Unclassified	1.56%
	k__Bacteria;p__Proteobacteria;c__Alphaproteobacteria;o__Rhodospirillales;f__Acetobacteraceae;g__Unclassified	1.54%
	k__Bacteria;p__Proteobacteria;c__Alphaproteobacteria;o__Rhodobacterales;f__Rhodobacteraceae;g__Unclassified	1.53%
	Others	23.58%

Fig. 6.12. (a) Taxonomic hit distribution at phylum level, (b) class level, and (c) genus level displaying the microbial abundance present in the PRS based on 16S rRNA sequence metagenomic data

6.3.2 Optimization of microbial pretreatment

6.3.2.1 Optimization of solubilization due to *B. subtilis* IH-1 pretreatment

Hydrocarbons are selectively metabolized by indigenous bacteria as sole sources of carbon and energy for their growth and reproduction through induction of catalytic enzymes specific to the bacterial species following various pathways for biodegradation. Microbial species proliferation through catalytic enzyme activation modifies the chemical characterization of PRS leading to dissociation of complex insoluble long-chain hydrocarbon compounds to soluble short chain dimers and monomers initiating solubilization of the sludge. *Bacillus subtilis* is an aerobic gram-positive bacterium that can also grow under strict anaerobic conditions when nitrate is utilized as an electron acceptor and therefore, can be regarded as a facultative anaerobe (Hoffmann et al., 1995; Das and Mukherjee, 2007). Biodegradation of majority of hydrocarbon pollutants is faster in aerobic environmental conditions compared to anaerobic conditions (Ward et al., 2003). In this study, the effect of *B. subtilis* pretreatment on the extent of solubilization of PRS mixed with YW at optimal condition (C/N=32.5, pH=7.0) obtained from Section 6.1 (abbreviated as, PSYW) was examined through the variation of sCOD and VFA at three different dosages: 10^7, 10^8 and 10^9 CFU/mL (Fig. 6.13). As observed from the taxonomic analysis of the metagenomics data, PRS has a rich microbial diversity (Fig. 6.12), and therefore, a control was kept as a reference to evaluate the alteration in solubilization of only PRS without incorporation of *B. subtilis* IH1 strain. At a dosage of 10^8 CFU/mL, the sCOD and VFA of PSYW incremented with the increase in incubation period till 5^{th} d and decremented thereafter with further increase in incubation period. The maximum sCOD and VFA for control were observed to be 2695.5 mg/L and 1169.5 mg/L respectively. For dosage 10^8 CFU/mL, the peak sCOD and VFA were 2.2 and 1.4 times higher compared to control. The initial increment in the trendlines could be attributed to intracellular attack by peroxidases and oxygenases due to the incorporation of molecular oxygen (O_2) to result in pre-intermediate compounds {such as, carboxylic acids (short-chain fatty acids) or diols} and their step-by-step biodegradation by peripheral pathways (such as, terminal oxidation, β-oxidation, ω-oxidation) results in the formation of intermediate compounds (pyruvate or acetate) following a central intermediary metabolism (tricarboxylic or TCA cycle). Through the central precursors such as, acetyl CoA, succinate and pyruvate, their biosynthesis results in the growth of cell biomass, thereby improving the sCOD (Das and Chandran, 2011). The lignocellulosic content of PSYW could be dissociated through extracellular depolymerization to aryl and biaryl compounds followed by their mineralization and solubilization of oligomers and monomers utilizing specific catabolic ligninolytic enzymes and pathways {laccase and heme-containing peroxidases such as, lignin

peroxidase (LiP), manganese peroxidase (MnP), versatile peroxidase (VP) and feruloyl esterase (FE)} leading to improved solubilization of the substrate (Wong, 2009). The gradual decrement in sCOD and VFA after 5th d for dosage 10^8 CFU/mL could be attributed to the endogenous decay in bacterial population caused due to the cessation of organic carbon in the available form.

For dosage 10^9 CFU/mL, the sCOD and VFA increased with the increase in pretreatment duration to obtain the maximum values a day earlier compared to the dosage of 10^8 CFU/mL but the values were 13.6% and 6.5% lower respectively compared to the same dosage. This might be attributed to the extracellular enzymatic activity inhibition at higher than optimum dosages of bacterial colonies, delaying the fermentation process, thereby affecting the decomposition of recalcitrant polymers of the substrate (Varjani, 2017; Xu et al., 2019). The slight increase in sCOD and VFA on 6th d might be due to the secretion of exoenzymes by the higher number bacterial colonies striving to further solubilize the particulate organic fraction for their survival after the depletion of available fraction of organic carbon present PSYW.

At dosage 10^7 CFU/mL, the peak sCOD and VFA were 1.5 and 1.1 times higher than the control but were 30.8% and 22.9% lower compared to that of dosage 10^8 CFU/mL which might attributed to the utilization of lesser number of bacterial colonies for improving the solubilization of PSYW (Varjani, 2017). The order of solubilization followed by different dosages of *B. subtilis*: 10^8 CFU/mL > 10^9 CFU/mL > 10^7 CFU/mL. The maximum enhancement in sCOD at 10^8 CFU/mL dosage of *B. subtilis* was 26.4% higher compared to the study conducted by He et al. (2016) who studied *B. licheniformis* anaerobic pretreatment on *Chlorella sp.* biomass for methane augmentation. Also, their maximum enhancement in VFA (41%) obtained at 4% bacterial culture was in agreement with this study. Aerobic metabolic processes are mostly faster and efficient than anaerobic processes for improving the solubilization of complex substrates (Grishchenkov et al., 2000; Wang et al., 2019; Ferdeș et al., 2020).

The degradation of hydrocarbon compounds can be conciliated by a specific enzymatic system followed by the individual bacterial strain subjected to organic decomposition, adaption of polluted environment and the various pathways followed by the enzymatic system for biodegradation. In this study, the effect of lignin peroxidase (LiP) enzyme was examined for different dosages of *B. subtilis* (10^7, 10^8 and 10^9 CFU/mL) throughout the pretreatment duration to corroborate the solubilization of PSYW (Fig. 6.13c). LiP, as secreted by *Bacillus sp.* is a heme-containing extracellular oxidoreductase enzyme having the potential to not only degrade phenolic aromatic compounds but also a wide range of non-phenolic lignin model compounds (Karigar and Rao, 2011). In all the dosages, the LiP activity increased till an optimal value and gradually decreased thereafter till the end of pretreatment duration. The initial increase in the enzymatic activity could

be attributed to the microbial attack due to release of LiP in the presence of H_2O_2 as cosubstrate and VA as mediator resulting in degradation of phenolic compounds and lignin present in PSYW. For dosage 10^8 CFU/mL, the LiP activity was observed to be maximum (16.8 IU/mL) on 5^{th} d of pretreatment which accredited the attainment of maximum sCOD and total VFA on that day. Aromatic hydrocarbon fraction of PSYW could have been attacked by the bacterial species through oxidation of single-electron generating free cation radicals, thereby undergoing a series of chemical reactions (hydroxylation/C–C bond cleavage) to form hydrophilic compounds, which eventually improved the solubilization through the conversion of insoluble organic fractions to soluble forms (Fig. 6.12a). LiP might have also depolymerized the lignin fraction of PSYW through the formation of oxo-Fe (IV) intermediate due to the reaction between H_2O_2 and heme-cofactor following further electron reduction from LiP (Tsegaye et al., 2019). The decrease in LiP activity after attainment of peak values for all the dosages could be attributed to the ceassation of free cation radical based on the aromatic group substitution. The catalytic activity of LiP might have also reduced due to the exhaustion of soluble organic fraction, thereby reducing the reaction velocity of LiP by the remaining recalcitrant fraction (Kavitha et al., 2014). The peak enzymatic activity obtained in this study for dosage 10^8 CFU/mL was 22.6% and 58.5% higher than dosage 10^9 and 10^7 CFU/mL respectively which advocated an interrelationship of the degree of solubilization with the specific enzymatic system followed by the bacterial species during the pretreatment process.

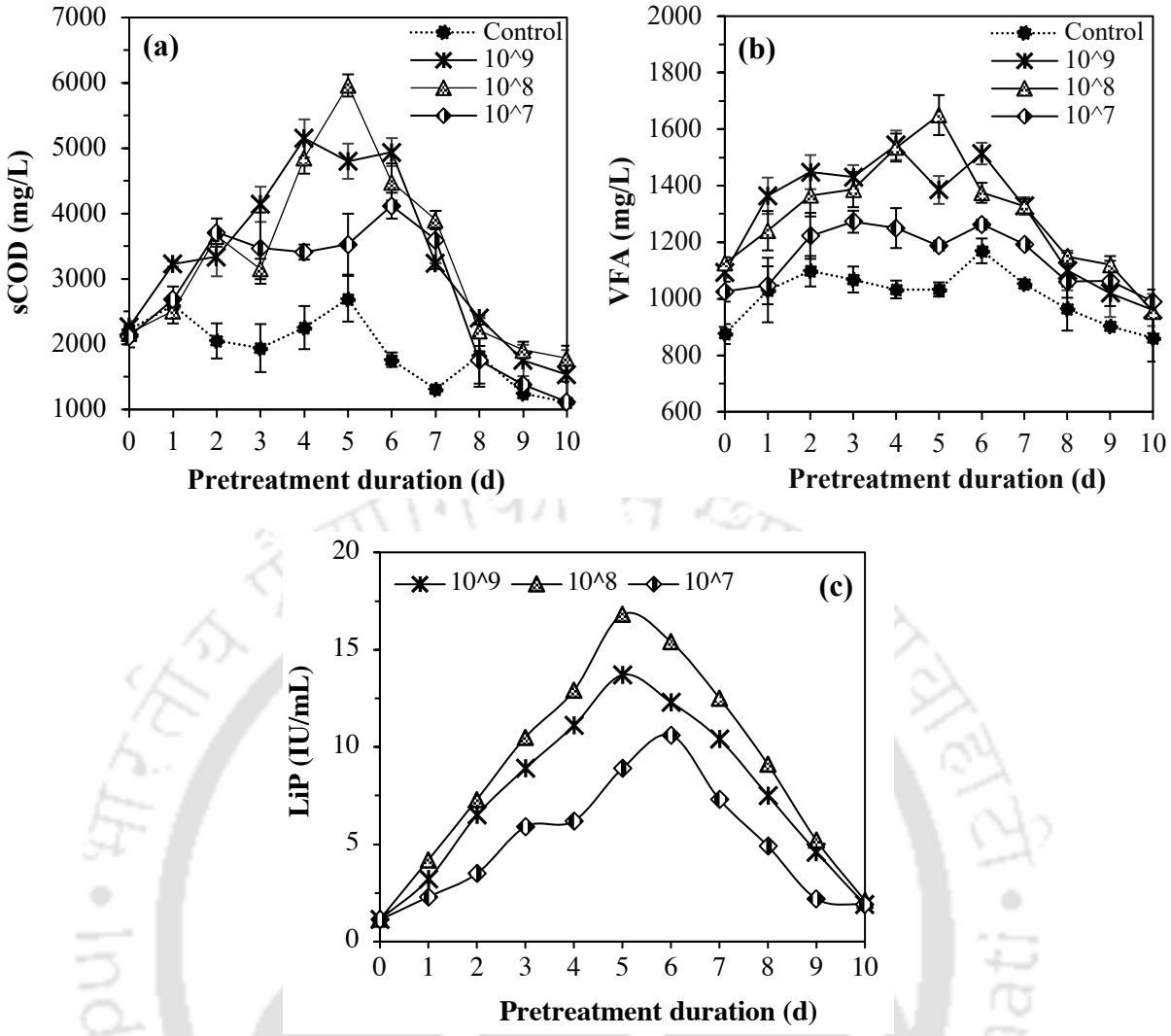

Fig. 6.13. Variation of (a) soluble chemical oxygen demand, (b) total volatile fatty acids and (c) enzymatic activity due to *B. subtilis* pretreatment on PSYW

6.3.2.2 Optimization of solubilization due to *B. velezensis* IH-2 pretreatment

Potential bacterial strains possess the ability to selectively metabolize hydrocarbons by following specific biodegradation pathways in the presence of catalytic enzymes. These enzymes are tailored to the individual bacterial strains, allowing them to efficiently break down heavy-molecular-weight hydrocarbon compounds into lighter fractions, thereby enhancing their solubilization. The extent of solubilization due to *B. velezensis* IH2 pretreatment on PSYW (PRS mixed with YW at C/N=32.5, pH=7.0 as per Section 6.1) was evaluated from the variation in trendline of sCOD and VFA concentrations throughout 10d of pretreatment duration as shown in Fig. 6.17(a) and (b). For all the dosages of *B. velezensis*, sCOD and VFA increased with an increase in the pretreatment duration only to have gradually decreased upon achieving an optimal value (Fig. 6.17a). Although PRS has a diverse range of microorganisms, a control was kept as a benchmark to determine any changes in the solubilization of PSYW without the incorporation of

B. velezensis. For 10^8 CFU/mL of *B. velezensis*, the sCOD was observed to be maximum on 3rd d of pretreatment which was 1.16 and 1.3 folds higher than that observed for 10^9 and 10^7 CFU/mL respectively. For 10^8 CFU/mL, the sCOD incremented from 0th d till 3rd d, when it obtained the maximal value (4723.7 mg/L) and decremented thereafter till the end of the pretreatment duration. The initial rise in sCOD values could be attributed to the intracellular oxidative attack on hydrocarbon compounds due to the catalytic activation of oxygenase and peroxidase enzymes through the integration of molecular oxygen. The hydrocarbons are degraded step-by-step through peripheral degradation pathways resulting in central intermediary intermediates of the tricarboxylic (TCA) cycle. The central precursor metabolites (acetyl-CoA, succinate and pyruvate) synthesize the cell biomass resulting in improved solubilization. The degradation pathways are dependent on the structure and group substitution of the petroleum hydrocarbon compounds, e.g., the methyl group of alkanes is oxidized to form alcohol which then follows dehydrogenation through aldehyde to corresponding carboxylic acid to get metabolized by the β-oxidation pathway of fatty acids (Varjani, 2017). Even cyclic alkanes get dehydrogenated to ketones through conversion to cyclic alcohols during their oxidative process (Das and Chandran, 2011). Also, the oxidative attack on aromatic hydrocarbons (less biodegradable than saturated ones) results in diol formation followed by benzene ring structure cleavage resulting in the formation of dicarboxylic acid (Ward et al., 2003). These corroborated the initial increase in the VFA concentrations to achieve the maximum values for all the bacterial dosages (Fig. 6.17b). The maximal VFA concentration for 10^8 CFU/mL was perceived on 3rd d, and observed to be 1.09 and 1.2 folds higher than that of 10^9 and 10^7 CFU/mL dosages. The subsequent decreasing trendline of VFA concentrations for all the dosages followed a similar trendline as sCOD concentrations which was also reported by Xu et al. (2021) in their microaerobic microbial pretreatment study on anaerobic digestion of lignocellulosic corn stover. The lignocellulosic content of PSYW could have also been dissociated via extracellular depolymerization to aryl and biaryl compounds, followed by mineralization and solubilization of oligomers and monomers using specific catabolic ligninolytic enzymes and pathways [laccase and heme-containing peroxidases such as lignin peroxidase (LiP), manganese peroxidase (MnP), versatile peroxidase (VP) and feruloyl esterase (FE)] leading to improved solubilization (Wong, 2009). The withering of the microbial population and the gradual consumption of the available organic carbon resulting in their endogenous decay by the end of the 10th d could be the cause of the decrease in solubilization in terms of sCOD and VFA for all dosages after the attainment of maximum values.

The order of solubilization due to *B. velezensis* pretreatment on PSYW was: 10^8 CFU/mL >10^9 CFU/mL >10^7 CFU/mL. The diminished peak solubilization in terms of sCOD (14%) and VFA

(8%) as observed for 10^9 CFU/mL compared to 10^8 CFU/mL could be attributed to the delayed hydrolysis rate due to extracellular enzymatic inhibition at bacterial colonies higher than the optimum values as explained by Kavitha et al. (2014). This, in turn, also impedes the activity of biodegradation of bacterial species at higher toxicant concentrations, or lesser than the optimum number of bacterial colonies utilized for the degradation. This corroborated the reduced peaks of sCOD (24%) and VFA (20%) for dosage 10^7 CFU/mL against 10^8 CFU/mL. At optimal dose of 10^8 CFU/mL and pretreatment duration of 3 d, 2.13-fold and 1.7-fold increments in sCOD and VFA respectively were observed compared to control (untreated) PSYW which were in accordance with the biological co-pretreatment study performed by Zhang et al. (2017) on anaerobic co-digestion of food waste and waste activated sludge to obtain 2.3 times increment in sCOD against without co-pretreatment. The improvement in solubilization due to *B. velezensis* pretreatment led to increase in the bioaccessible fraction of organics to be used up by the microbial community for biogas enhancement during the anaerobic digestion process.

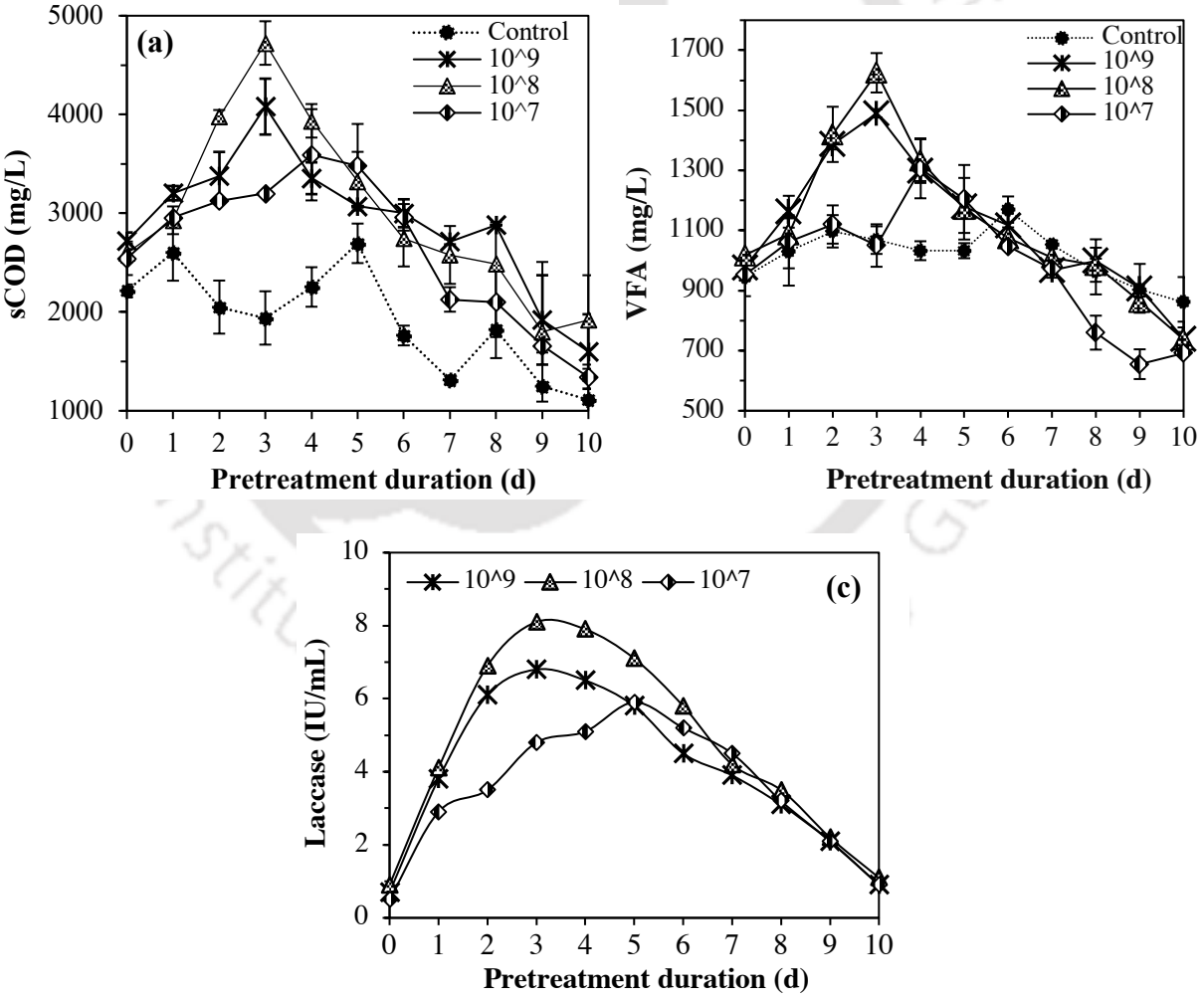

Fig. 6.14. Variation of (a) soluble chemical oxygen demand, (b) total volatile fatty acids and (c) enzymatic activity due to *B. velezensis* pretreatment on PSYW

Bacteria biodegrade pollutants through the development of a catabolic activity responsible for the development of metabolic capabilities by genetic changes, induction of specific enzymes by individual bacterial strains, and their comprehensive enrichment exhibiting the capability of converting those pollutants. The enzymatic variation for *B. velezensis* pretreatment was studied by evaluating laccase (lac) activity throughout the pretreatment duration for all the dosages in order to corroborate the extent of solubilization of PBYW as shown in Fig. 6.17(c). The production of laccase by an aerobic, gram-positive bacterium such as *B. velezensis* had been widely reported (Gangola et al., 2018). Laccase (benzenediol, oxygen oxidoreductases) is one of the groups of enzymes belonging to the family of multicopper oxidase family that is ubiquitous in various fungi and bacteria (Munk et al., 2015). The laccase activity in this study increased with pretreatment duration for all *B. velezensis* dosages to reach a maximum value, then decreased with any additional pretreatment duration extensions (Fig. 6.17c). The reaction mechanism involved behind aromatic petroleum hydrocarbon compounds is the formation of two water molecules on the concurrent loss of an electron by a single oxygen molecule. This extracted electron further triggers the oxidation of a number of benzene ring-containing compounds (Chauhan et al., 2017). Also, laccase has the ability to catalyze lignin polymerization involving catalyzed reactions of the reactive radical intermediates. This occurs due to the initial oxidation of the phenol-hydroxyl groups through catalytic bond cleavage in low-molecular-weighted phenolic lignin model compounds, or inter-unit bond cleavage of lignin substrates in the presence of a lignin mediator system (Munk et al., 2015). In this study, for 10^8 CFU/mL of *B. velezensis*, the peak lac activity was obtained to be 8.1 IU/mL which was 19% and 37.3% higher compared to 10^9 CFU/mL and 10^7 CFU/mL respectively. This could be attributed to the fact that different bacterial species require distinct time for optimum laccase yield. This is even applicable for the quantities of bacterial colonies applied for biodegradation of organic substrate. At lower dosages of bacterial colonies, complex substrates cannot be oxidized directly by laccase due to the lower diffusion of the substrate into the active pockets. At higher dosages, the laccase activity attempting to oxidize the higher-molecular-weighted compounds having higher redox potential again slows down the laccase-catalyzed reaction (Chauhan et al., 2017). The peak lac activity obtained on the 3rd d for 10^8 CFU/mL accredited the maximal sCOD and total VFA obtained on that particular day. A similar trend was observed for optimum solubilization on 3rd d and 4th d for the other two dosages of 10^9 CFU/mL and 10^7 CFU/mL respectively exhibiting an interrelationship between the distinct durations of optimum laccase activity and optimum solubilization of PBYW (Chauhan et al., 2017) (Fig. 6.17a and b). The slowdown of the laccase-catalyzed reaction brought on by recalcitrant compounds having higher redox potential or lower PBYW diffusion into active pockets might be the cause of the decrease in enzymatic activity after reaching the peak values for all dosages (Gangola et al.,

2018). The exhaustion of easily degradable hydrocarbon compounds or simpler modified lignin fragments by the bacterial population might have ceased the catalytic activity of laccase.

6.3.3 Morphological and chemical characteristics at optimum pretreatment conditions

The enhancement in solubilization was observed to be maximum for *B. subtilis* pretreatment in terms of sCOD (2.2 times) and VFA (1.4 times) compared to *B. velezensis* pretreatment on PSYW (Section 6.3.2), and therefore, the *B. subtilis* pretreated feedstock at optimum pretreatment conditions (dosage: 10^8 CFU/mL, 5d) was examined for morphological and chemical characterization studies. The internal microstructure of PSYW due to *B. subtilis* pretreatment was examined using FESEM as shown in Fig. 6.15(a). The morphology of the untreated PSYW depicted a homogeneous rigid structure compacted with few flaky clusters. After the pretreatment, the compact structure metamorphosed into a dissociated structure of abundant round-shaped intragranular pores exhibiting decomposition. Few overhead macropores were also observed in the denatured structure including some flat and flaky portions depicting alteration in molecular conformation due to the pretreatment utilizing *Bacillus* sp. Significant differences in chemical characteristics due to the pretreatment were also observed and illustrated using FTIR spectra (Fig. 6.15b). The flattening of the broad spectrum at 3287 cm^{-1} assigned to bonded and nonbonded –OH and –NH groups exhibited their intramolecular or intermolecular dissociation due to the applied pretreatment. The decremented intensity of absorption peaks at 2922 cm^{-1} and 2854 cm^{-1} corresponding to asymmetric and symmetric aliphatic groups of $–CH_3$ and $–CH_2$ respectively evinced their decomposition (Wang et al., 2022). A small band around 1632 cm^{-1} corresponded to either C=O stretching representing carboxylates, or C=C stretching representing alkenes suggesting their decomposition resulting in improved solubilization (Fig. 6.15a). The absorption peaks at 1375 cm^{-1} corresponded to C–N stretching of aromatics and amides (Ennouri et al., 2016). The reduced peak at 1030 cm^{-1} corresponding to the vibration of C–O stretching exhibited the formation of alcohols, esters and ethers corroborating the increase in VFA concentrations due to the applied pretreatment (Fig. 6.13b). The reduced peaks around 745 cm^{-1} were ascribed to the dissociated C–H stretching corresponding to alkane group. The last band at 532 cm^{-1} corresponded to C−C=O stretching vibrations representing dissociation of aldehydes and ketone groups of PRS and YW. The FTIR spectra due to pretreatment at optimal condition exhibited alteration in chemical characteristics due to the decomposition of aliphatics, phenols, aldehydes, ketones and alcohols leading to improved solubilization.

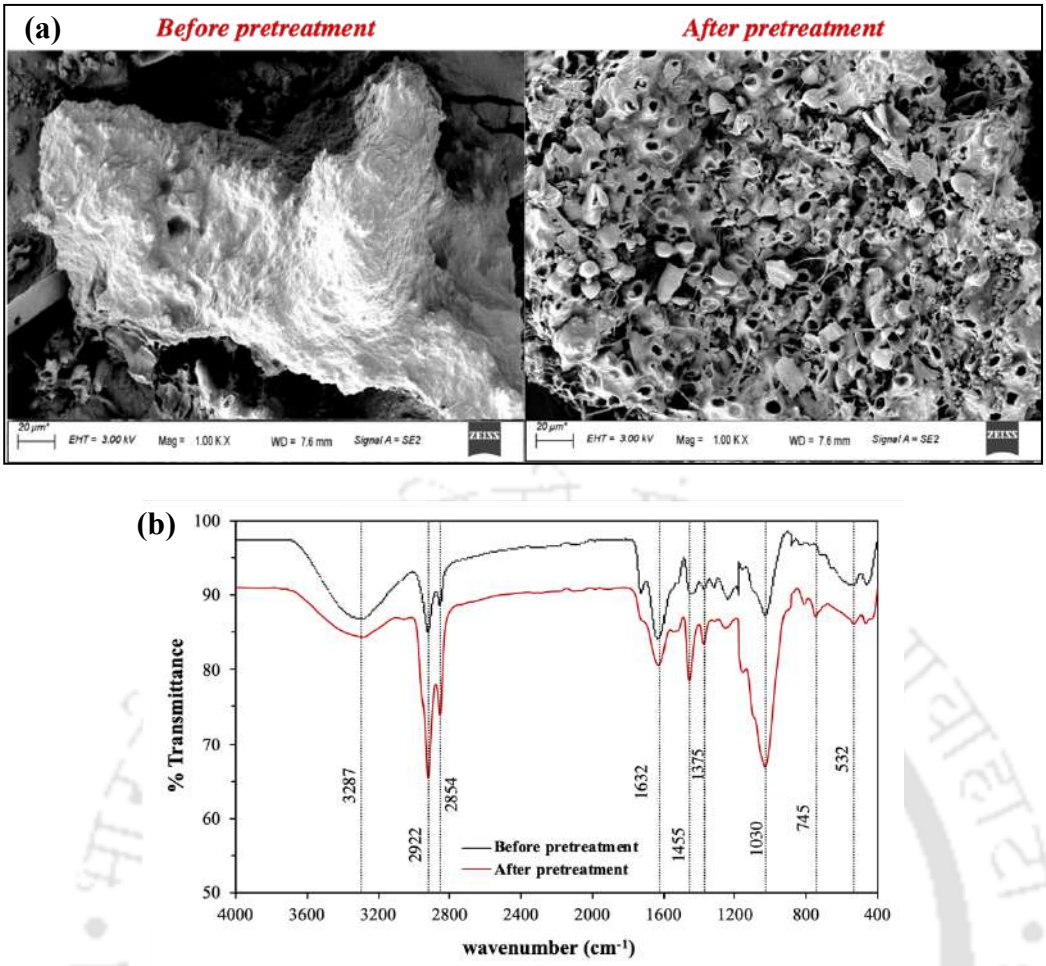

Fig. 6.15. Variation in (a) morphological and (b) chemical characteristics due to *B. subtilis* pretreatment at optimal condition

6.3.4 Anaerobic biodegradability of combined pretreatment and co-digestion of PRS and YW

The improved solubilization due to *B. subtilis* pretreatment at optimum operating conditions was utilized by the hydrolytic and fermentative bacteria to expedite the hydrolysis phase of the anaerobic co-digestion of PRS and YW as observed in Fig. 6.16. Fig. 6.16(a) illustrates the daily biogas yields at different inoculum:feedstock (I/F) ratios of pretreated PSYW at optimal conditions. The maximum daily biogas was observed for I/F = 0.5, which was 47.8% higher and obtained 12d earlier compared to the control (untreated PSYW). Due to the applied pretreatment, the conversion of complex organic compounds of PSYW to soluble monomers and dimers became bio-accessible for the anaerobic microbial consortium to be utilized for enhanced biogas through the secretion of extracellular enzymes. The depolymerization of lignin present in YW to modified lignin fragments due to pretreatment unveiled the easier-to-degrade hemicellulose and cellulose leading to biogas enhancement (Ferdeș et al., 2020). The highest cumulative biogas was also perceived for I/F=0.5 which was 47.6% higher compared to that of control or untreated co-digestion (Fig. 6.16b). This biogas enhancement due to bacterial pretreatment was about 10% higher compared to ultrasonic

pretreatment study conducted on co-digestion of petroleum refinery wastewater with waste activated sludge by Siddique et al. (2017). The cumulative biogas production followed the order: 0.5>0.4>0.3>0.7>0.1. Untreated co-digestion of PSYW (control) unenviably resulted in lower biogas due to the presence of refractory hydrocarbons (polyaromatics or heterocyclics) and recalcitrant lignin polymers proving to be toxic for methanogenic bacteria to be converted to biogas.

Adaptations to aromatic ring structures and double or triple-bonded hydrocarbon compounds at different mixing ratios prove to be wavering for microbes for degradation based on organic matter content. This was observed from the organic matter removal in terms of VS degradation (Fig. 6.16c) (Siddique et al., 2016; Wang et al., 2016). The maximum VS removal of 64.3% was observed to be maximal amongst all other mixing ratios corroborating the reason behind observing peak biogas production for I/F=0.5. The complex intricate structure of both the substrate and co-substrate resulting in VS degradation of 44.8% without any pretreatment was in close accordance with the co-digestion study conducted by Janajreh et al. (2020), who observed 43% VS degradation when 60% petroleum hydrocarbon waste was co-digested with the 40% wastewater treatment sludge. Also, the VS removal in this study due to pretreatment was about 13% higher compared to the study reported by Castro et al. (2022), who observed 52% VS removal after 45 d of co-digestion of petroleum oil refinery waste activated sludge and food waste.

The variation in pH for all mixing ratios during the digestion process is shown in Fig. 6.16(d). The pH values for all mixing ratios were observed to have decremented during the initial 21d of digestion. This could be ascribed as the formation of acidic compounds due to the action of hydrolytic and fermentative bacteria, in order to accumulate VFA through the depolymerization of PSYW. The rise in pH for all the mixing ratios after 21 d, to a range of 7.26–7.56, suggested the activation of methanogenic bacteria for biogas accretion from pretreated PSYW. To avoid reactor failure due to excessive acidification and inadequate buffering, the pH is desired to be within the range of 6.6-7.6 (Castro et al., 2022). The accelerated hydrolysis due to *B. subtilis* pretreatment led to an improvement in organic fraction utilization resulting in biogas augmentation and improved biodegradation when PRS was co-digested with YW.

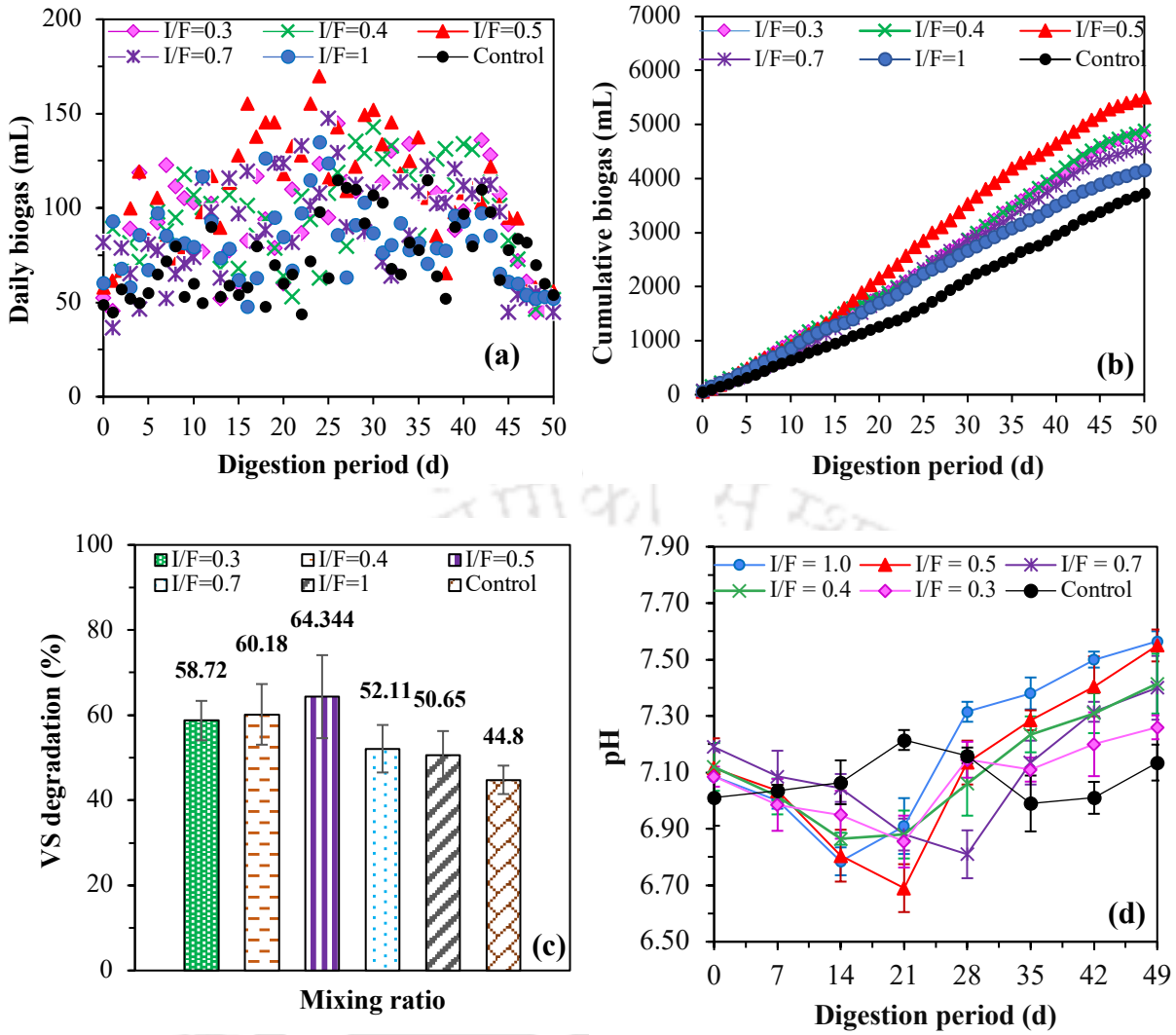

Fig. 6.16. (a) Daily biogas, (b) cumulative biogas, (c) volatile solids degradation and (d) variation in pH during anaerobic digestion of *B. subtilis* pretreated PSYW

6.3.5 Scaled-up batch study

6.3.5.1 Biogas production

From Fig. 6.17(a), the peak daily biogas due to *B. subtilis* pretreatment at optimum conditions (10^8 CFU/mL; 5d) was observed on 20th d which was 37.8% higher and obtained 6 d earlier compared to the untreated co-digestion of PRS and YW. It distinctly showed the accelerated hydrolysis due to the action of fermentative and acetogenic bacteria for utilization of incremented solubilized fraction of the substrate towards biogas enhancement. The mono-digestion was observed to emanate peak biogas on 33rd d of the digestion period. The complex intricate hydrocarbon fraction of PRS consisting of aliphatics, aromatics, polycyclic and polyaromatics was mostly inaccessible or proved recalcitrant leading to delayed hydrolysis by the microbial consortium to convert into biogas (Wang et al., 2016). Haak et al. (2016) reported the impedance

caused during the monodigestion of oil refinery waste without any pretreatment due to the formation of inhibitory toxicants during the digestion process. The cumulative biogas production due to *B. subtilis* pretreatment was incremented by 34.2% compared to untreated co-digestion, and by 75.9% compared to the monodigestion of PRS (Fig. 6.17b). This percentage enhancement was about 10% higher compared to the biological co-pretreatment study of WAS and food waste conducted by Zhang et al. (2017), who reported a 24.6% higher methane yield compared to that without pretreatment. The exhaustion of soluble organics might have led to the ceasing of biogas production after 50 d of digestion (Fig. 6.17a). Slight increase in the biogas production values during 35-45 d of combined pretreatment and co-digestion could be ascribed to the remaining enzymes due to the *B. subtilis* pretreatment further attempting to solubilize the particulate organic fraction for improving the rate of hydrolysis of not only the substrate (PRS) but also the co-substrate (YW) (Kavitha et al., 2014). The efficiency of the combination of anaerobic co-digestion and pretreatment is variable and majorly depends on the nature of co-substrate(s) utilized and the type of pretreatment (Elalami et al., 2019). A comparative study has been tabulated in Table 6.6 for showing biogas enhancements due to application of different types of pretreatments combined with co-digestion of petroleum refinery waste.

The organic matter degradation as evaluated through the reduction in VS was 75.82% for pretreated co-digestion of PRS and YW by the end of 60 d of digestion period. This percentage removal was 1.7 folds and 3.7 folds higher compared to the untreated co-digestion and monodigestion of PRS respectively which was in close accordance with the biological co-pretreatment study conducted by Zhang et al. (2017) on WAS and food waste, reporting 77.2% VS removal within 60 d. The recalcitrant nature of untreated PRS is evident which led to its poor organics removal and low biodegradability during the monodigestion process (Haak et al., 2016). Fig. 6.17(c) shows the variation in total organic carbon (TOC) during the digestion processes. In pretreated co-digestion process, the TOC first incremented from 0^{th} d to 20^{th} d, obtained the maximum value and gradually decremented thereafter till the end of digestion period. The initial increase in TOC could be attributed to the bioconversion of insoluble organic carbon to soluble form, formation of extracellular intermediate metabolites and VFAs accumulation which get converted to acetate during the fermentation and acetogenic phase, resulting in biogas during the methanogenesis phase (Wang et al., 2016). The maximum TOC solubilization (1618 mg/L) obtained on 20^{th} d during the combined pretreatment and co-digestion process was 86% higher compared to the untreated co-digestion. The decrease in TOC values thereafter could be attributed to the exhaustion of the available fraction of organic carbon due to its oxidation to CO_2, which upon combining with H_2 released from fatty acids, alcohols and acetate, got converted to methane.

A marginal increase in TOC values on 40th d could be attributed to the bioconversion of the particulates of the pretreated substrate and co-substrate to soluble substrates attempted by the anaerobic microbial consortium ameliorating the biogas yield as well (Fig. 6.17a). Poor organic carbon solubilization during the monodigestion of PRS could be attributed to the leisurely action of microorganisms predominantly due to the presence of high concentrations of recalcitrant hydrocarbon compounds as reported by Varjani (2017).

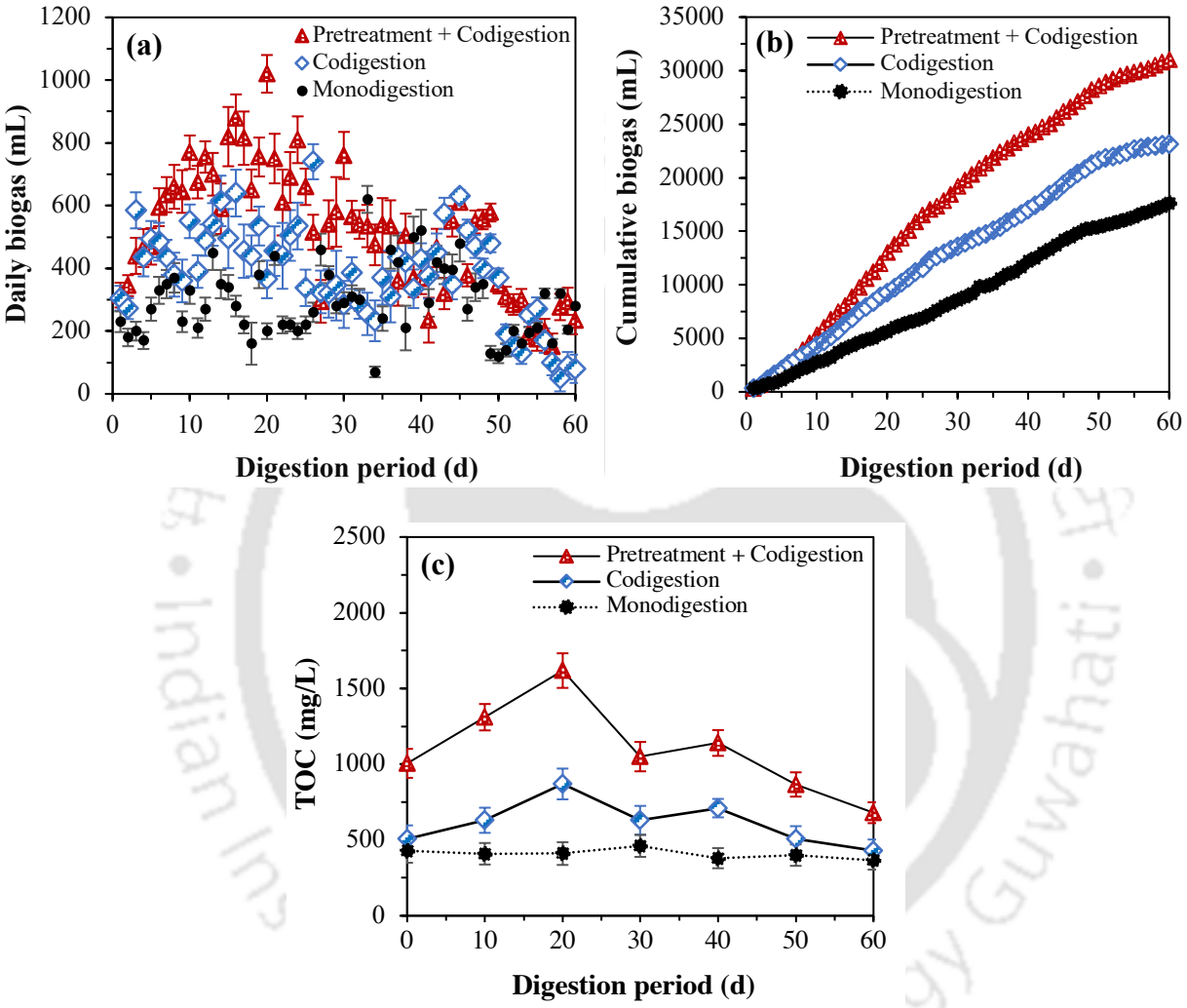

Fig. 6.17. Variation of (a) daily biogas, (b) cumulative biogas and (c) total organic carbon during the mono-digestion (PRS), co-digestion, and combined pretreatment and co-digestion of PRS and YW

6.3.5.2 Hydrocarbon, emulsion and lignin degradation

Fig. 6.18(a) shows the variation in total petroleum hydrocarbon content (TPH) during the digestion processes. Due to pretreated co-digestion, the percentage of TPH removal during the process was 56% within 60 d, being 1.7 folds higher compared to untreated co-digestion (33.67%), and 3.7 folds higher compared to monodigestion (15.12%) of PRS. The petroleum hydrocarbon

degradation through methanogenic enrichment occurs either via proton-reducing acetogenic bacteria converting hydrocarbon compounds to acetate $(CH_3COO)^-$ and H_2; methanogenic archaea (*Methanosaeta*) forming CH_4 and CO_2 from $(CH_3COO)^-$ during acetoclastic methanogenesis; or another group of methanogenic archaea (*Methanoculleus* and *Metanospirillum*) converting CO_2 and H_2 to CH_4 during hydrogenotrophic methanogenesis (Mbadinga et al., 2011). Even the modified lignin fragments formed due to the action of LiP-enzyme producing *B. subtilis* pretreatment through lignin depolymerization of YW ultimately appended to the biomethane augmentation (Khan and Ahring, 2019). The percentage of TPH removal due to untreated co-digestion was 54.9% higher than monodigestion which could be attributed to the incorporation of nutrient balance through C/N ratio optimization leading to the optimal proliferation of microbes thereby diluting the toxic compounds (Janajreh et al., 2020).

From Fig. 6.18(b), it could be illustrated that the oil and grease (O&G) removal due to pretreated co-digestion was 1.4 and 3.5 folds higher compared to untreated co-digestion and monodigestion respectively. The O&G degradation commences when the insoluble macro oil pollutants directly adhere to the microbial cell wall. The microbes produce a wide range of biosurfactants during hydrocarbon accretion, which either stay attached to the cell wall or are released as extracellular molecules. These biosurfactants effectively demulsify O/W emulsions by lowering the interfacial tension of the emulsions, reducing their viscosity (Varjani and Upasani, 2017).

The lignin degradation (ASL+AIL) for pretreated co-digestion of PRS and YW was observed to be 27.7% which was 3.3 folds higher against untreated co-digestion within 60 d of digestion (Fig. 6.18c). Lignocellulosic content due to mono-digestion of PRS was below detectable limits. The hemicellulose and cellulose removals from pretreated co-digestion were 30.6% and 88.5% respectively which were 3.2 and 3.1 folds higher compared to untreated co-digestion. The *B. subtilis* strain produced oxidoreductase LiP enzyme for depolymerization of lignin fraction through oxidative reactions, producing active radicals with high redox potential. This resulted in the formation of lignin fragments, and exposure of hemicellulose and cellulose (lighter-molecular-weighted compounds) which became more bioavailable for microbes for anaerobic decomposition (Ferdeș, et al., 2020; Khan and Ahring, 2019).

Table 6.6. Combined pretreatment and co-digestion of petroleum refinery wastewater/sludge with different types of co-substrates

Substrate	Co-substrate(s)	Type of pretreatment	Time	Biogas/methane enhancement	Reference
Petroleum refinery wastewater	Beef and dairy cattle manure	Peroxide oxidation for substrate (30% H_2O_2, 1.0 mM Fe^{3+}) Thermal for co-substrates (100-140°C)	60 d	50% against untreated co-digestion	Siddique et al. (2014)
Petroleum refinery wastewater	WAS	Thermal (microwave) (175 °C, 30 min, 2000kPa)	31 d	53% against untreated co-digestion	Siddique et al. (2017)
Petroleum refinery wastewater	WAS	Ultrasonic (20 kHz, 60% amp, P= 350 W)	31 d	25% against untreated co-digestion	Siddique et al. (2017)
Petroleum refinery biosludge	Sugarcane bagasse	Thermo-chemical {Thermal: (100 °C, 150 rpm); Chemical: (1% NaOH, 60 min)}	33 d	3.4 folds against lowest biogas condition • *Highest*: {C/N = 30, $VS_{cosubstrate}$/ $VS_{inoculum}$ = 0.18} • *Lowest:* {C/N = 22.6, $VS_{cosubstrate}$/ $VS_{inoculum}$ = 0.09}	Ghaleb et al. (2021)
Petroleum refinery biosludge	Yard waste	Biological (*B. subtilis*) (10^8 CFU/mL, 5 d)	60 d	• 76% against mono-digestion • 34% against untreated co-digestion	This study

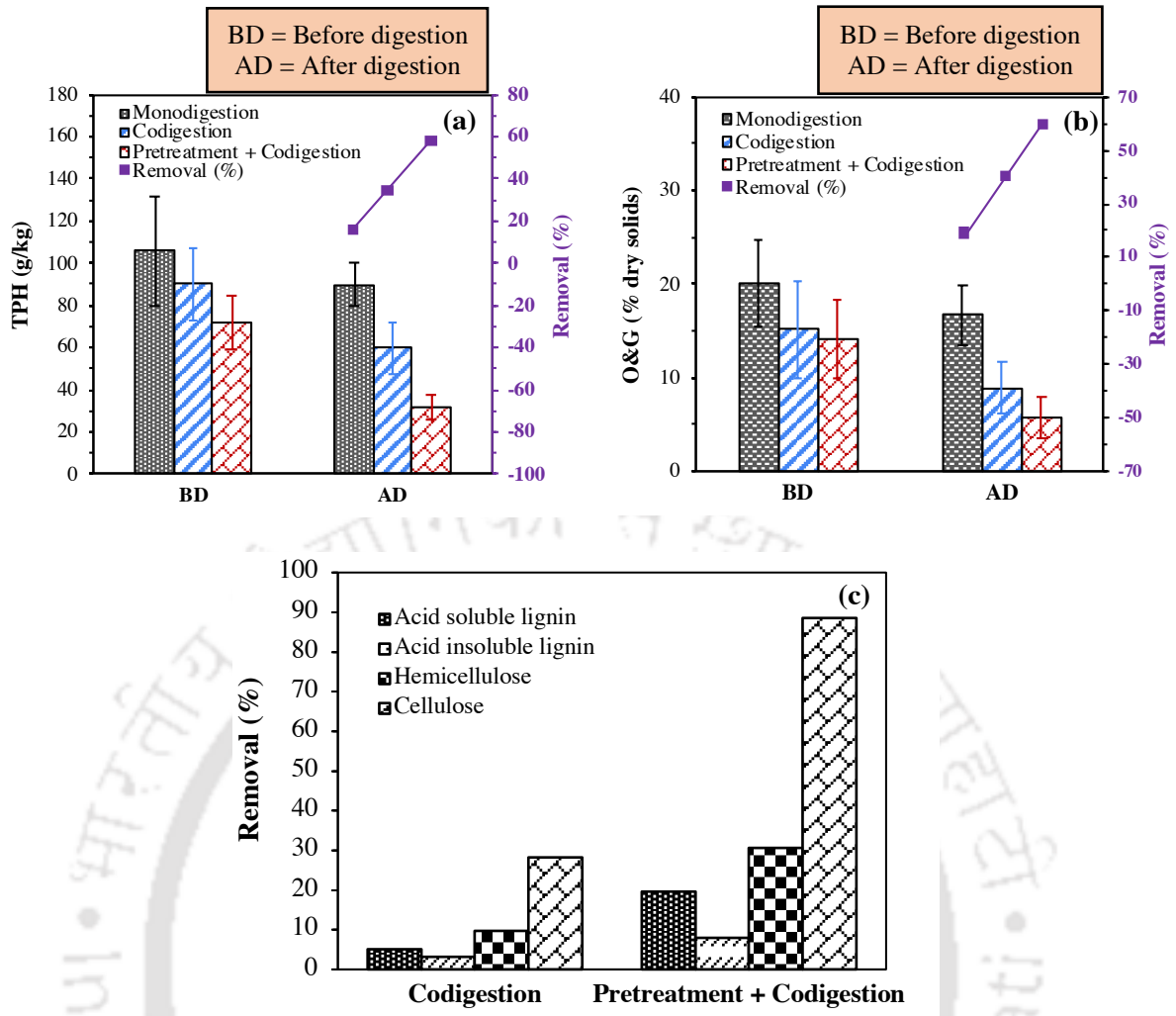

Fig. 6.18 (a) TPH, (b) O&G, and (c) lignocellulosic content degradation during the monodigestion (PRS), co-digestion, and combined pretreatment and co-digestion of PRS and YW

6.3.5.3 Pollutant degradation and mechanism

The conversion of the organic chemical composition during this *B. subtilis* pretreated anaerobic co-digestion of PRS and YW had been preliminarily addressed by GC-MS (Table 6.7). It could be observed that untreated PSYW was primarily composed of alkanes ranging from n-C_{15} to n-C_{54} along with few cyclic alkanes and polyaromatics (hexadecane, octadecane, heptadecane, phytane, nonadecane, heneicosane, eicosane, 2-methylphenanthrene, 1-phenylnaphthalene, 4,5-dimethylphenanthrene, 2,3,5-trimethylphenanthrene, 1-phenylnaphthalene, 4,5-dimethylphenanthrene, 2,3,5-trimethylphenanthrene, dotriacontane, 2-methyltetracosane, benzo[b]triphenylene, tetrapentacontane, 1-benzylpyrene, 1,1':2',1"-terphenyl, 4'-phenyl-) which were also corroborated by [24]. The major fractions consisted of dotriacontane (RT=24.713), benzo[b]triphenylene (RT=26.291), tetrapentacontane (RT=30.196), 1-benzylpyrene (RT=31.206)

and hexadecane (RT=15.471). The affinity of *B. subtilis* to feed onto these hydrocarbon compounds had been reported by Christova et al. (2004) and Wang et al. (2019). The alkanes might have been aerobically oxidized by *B. subtilis* strain during pretreatment through terminal oxidation, sub-terminal oxidation, ω-oxidation, and β-oxidation to secondary alcohols and corresponding ketones and esters to generate alcohols and/or fatty acids. The aromatics, comparatively less biodegradable than saturated hydrocarbons, might have followed diol formation, followed by benzene ring cleavage and dicarboxylic acids formation whereas the cyclic alkanes might have been oxidized to cyclic alcohols and dehydrogenated to ketones (Callaghan, 2013). These might further be utilized by the acetogenic and methanogenic bacteria for conversion to CH_4 and CO_2 during the anaerobic co-digestion process resulting in their biodegradation as observed from the GC-MS of digestate (Varjani, 2017). The remaining compounds such as pyrogallol (RT=11.723) (a plant metabolite that might be sourced from the YW utilized as the co-substrate during this study), 11H-benzo[b]fluorene (RT=24.294) (sourced from petroleum products), and 1,1':2',1"-Terphenyl, 4'-phenyl- (RT=36.682) (aromatic hydrocarbon) might have been either converted to other chemically stable and lesser reactive compounds or degraded during the pretreated anaerobic co-digestion process. During anaerobic degradation, hydrocarbons are activated through four general enzymatic pathways: (a) substrate addition to fumarate, catalyzed by a glycyl radical enzyme, to produce aromatic-substituted succinates, (b) methylation of unsubstituted aromatics, (c) hydroxylation of alkyl substituents by a dehydrogenase, and (d) direct carboxylation. As a result of these activation reactions, pathways for ring saturation, β-oxidation, or ring cleavage are activated, and central metabolites such as benzoyl-CoA are produced either completely getting oxidized or getting incorporated into the biomass (Mbadinga et al., 2011; Varjani and Upasani, 2017). The chromatogram corresponding to untreated PSYW, and the digestate after its pretreated co-digestion comparing the peaks with the NIST library has been shown in Fig. 6.19.

The GC-MS of digestate indicated the presence of 2,4-di-tert-butylphenol (RT= 14.103) (a natural bacterial metabolite converted from *Bacillus subtilis* strain), 1,2,3,5-cyclohexanetetrol (RT=16.778) (plant constituent and might be converted from co-substrate, YW), neophytadiene (RT=19.064) (plant and algal metabolite as mentioned by Castro et al. (2022), might have sourced from YW), n-hexadecanoic acid (RT=20.717) (saturated fatty acid observed in plants might be converted from YW having antibacterial, cancer preventive and anti-microbial properties as reported by Aparna et al. (2012), octadecatrienoic acid (RT=22.982) (polyunsaturated fatty acid, a plant source and observed due to the co-digestion process), phenol, 2,4-bis (1,1-dimethylethyl) (RT=34.007) (a natural plant product converted from co-digestion with YW), and octatriacontyl trifluoroacetate (RT=35.716) (a heavy-molecular-weighted phytochemical compound of plant

constituents having insecticidal properties as reported by Ravi et al. (2018), might be sourced from YW, which proved recalcitrant for efficient microbial activity as reviewed by Ferdeș et al. (2020). This clearly emphasized the utilization of hydrocarbon compounds for bioconversion into biogas remaining with mostly saturated or recalcitrant plant metabolites in the digestate after the pretreated co-digestion process. The mechanism involved behind methanogenic degradation of hydrocarbons (Varjani, 2017), and the depolymerization of lignin present in PSYW (Khan and Ahring, 2019), a primary recalcitrant fraction of lignocellulose under an anaerobic environment, during the *B. subtilis* pretreated co-digestion of PSYW to convert into methane-rich biogas has been illustrated diagrammatically in Fig. 6.20.

Table 6.7. Organic contaminants showed by the GC-MS profile

RT (min)	Compounds	Untreated	Digestate	Formula
11.723	1,2,3-Benzenetriol (pyrogallol)	+	-	$C_6H_6O_3$
14.103	2,4-Di-tert-butylphenol	-	+	$C_{14}H_{22}O$
15.471	Hexadecane	+	-	$C_{16}H_{34}$
16.245	Octadecane	+	-	$C_{18}H_{38}$
16.778	1,2,3,5-Cyclohexanetetrol	-	+	$C_6H_{12}O_4$
17.033	Heptadecane	+	-	$C_{17}H_{36}$
17.121	2,6,10,14-tetramethylhexadecane (phytane)	+	-	$C_{20}H_{42}$
18.396	1-Nonadecane	+	-	$C_{19}H_{40}$
18.489	Heneicosane	+	-	$C_{21}H_{44}$
18.626	Eicosane	+	-	$C_{20}H_{42}$
19.064	Neophytadiene	-	+	$C_{20}H_{38}$
20.582	2-methylphenanthrene	+	-	$C_{15}H_{12}$
20.717	n-Hexadecanoic acid (palmitic acid)	-	+	$C_{16}H_{32}O_2$
21.216	1-phenylnaphthalene	+	-	$C_{16}H_{12}$
21.693	4,5-dimethylphenanthrene	+	-	$C_{16}H_{14}$
22.982	Octadecatrienoic acid	-	+	$C_{18}H_{30}O_2$
23.752	2,3,5-trimethylphenanthrene	+	-	$C_{17}H_{16}$
24.294	11H-Benzo[b]fluorene	+	-	$C_{17}H_{10}O$
24.713	Dotriacontane	+	-	$C_{32}H_{66}$
25.399	2-Methyltetracosane	+	-	$C_{25}H_{52}$
26.291	Benzo[b]triphenylene	+	-	$C_{22}H_{14}$
30.196	Tetrapentacontane	+	-	$C_{54}H_{110}$
31.206	1-Benzylpyrene	+	-	$C_{20}H_{12}$

34.007	Phenol, 2,4-bis (1,1-dimethylethyl)	-	+	$C_{14}H_{22}O$
35.716	Octatriacontyl trifluoroacetate	-	+	$C_{40}H_{77}F_3O_2$
36.682	1,1':2',1''-Terphenyl, 4'-phenyl-	+	-	$C_{24}H_{18}$

(+) Present; (-) Absent

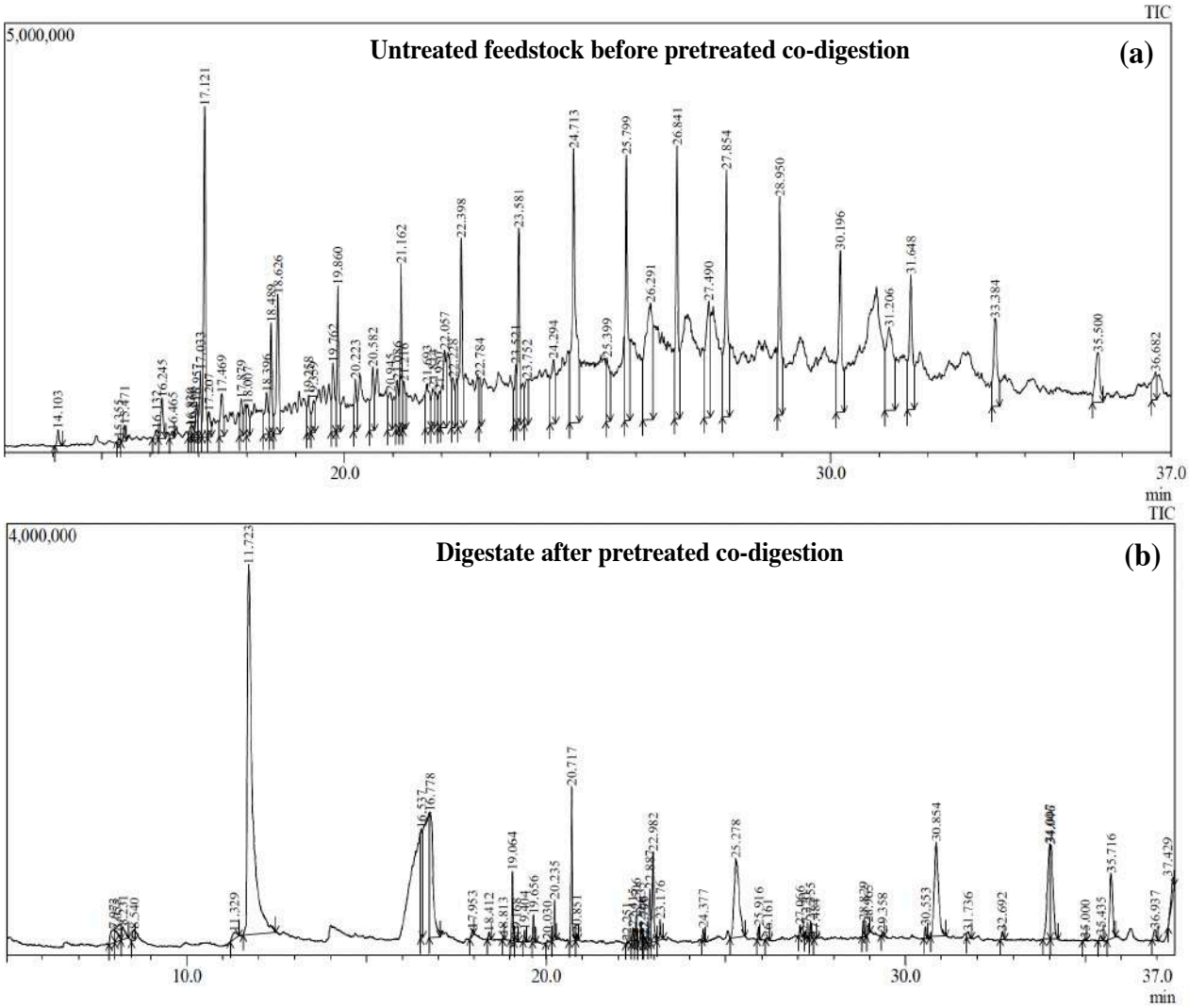

Fig. 6.19. GC-MS analysis of (a) untreated feedstock (PRS mixed with YW at C/N=32.5, pH=7) and (b) digestate of the feedstock after pretreated co-digestion of PRS and YW

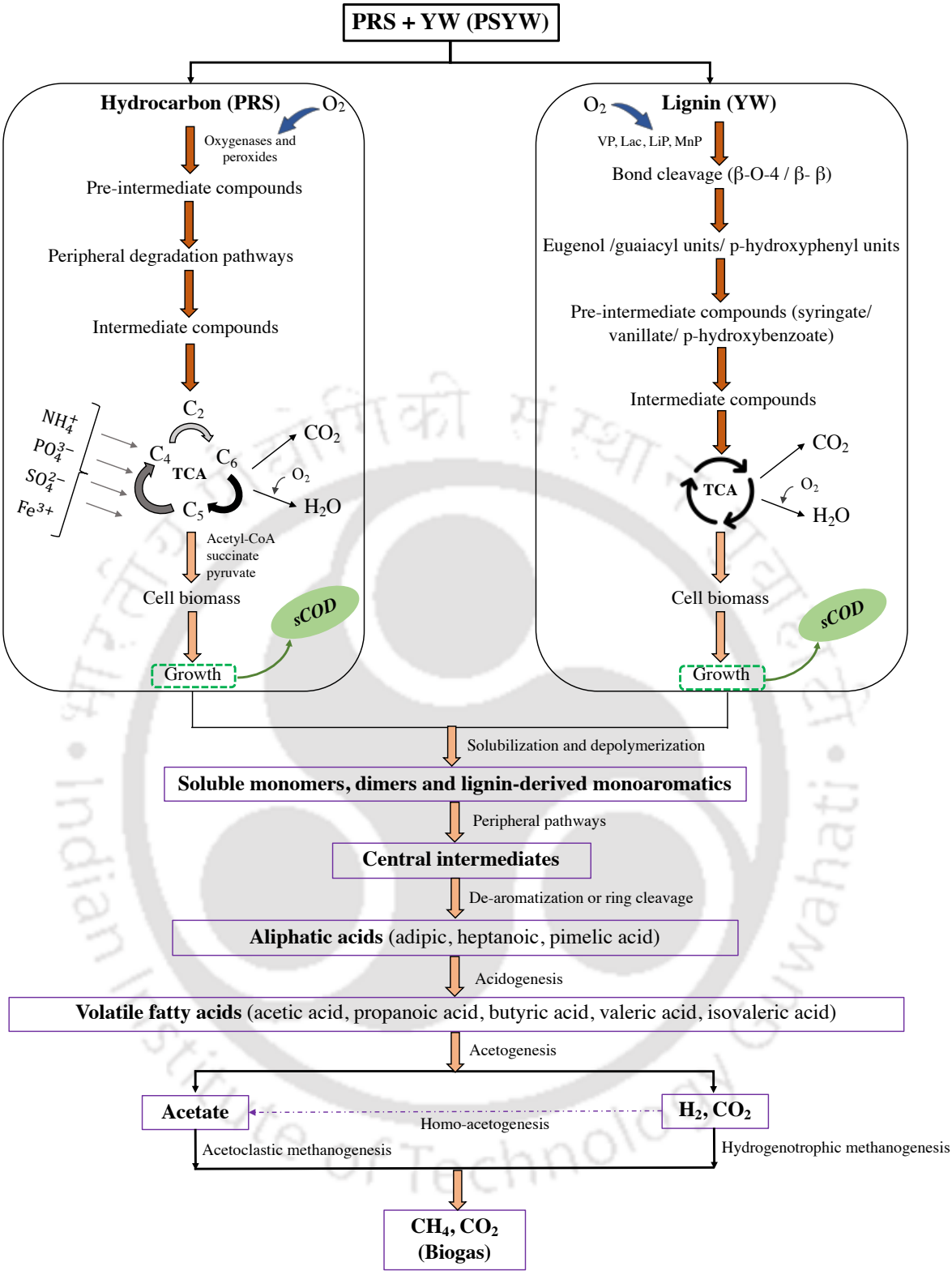

Fig. 6.20. A simplified diagrammatic illustration of the microbially enhanced anaerobic co-digestion of PRS and YW

6.4 COMPARATIVE CONCLUSION

The co-digestion of nitrogen-rich PRS with carbon-rich YW led to optimal microbial proliferation benefiting process stability by adjusting the lack of nutrients, moisture content, and diluting the inhibitors. The microbial diversity of PRS represented major enrichment of *Proteobacteria*, *Bacteroidetes,* and *Chloroflexi* at the phylum level, exhibiting hydrocarbon-degrading properties. The enhancement of co-digestion of hydrocarbon-rich PRS with lignocellulosic YW through electrokinetic and microbial pretreatments with strains isolated from PRB itself, augmented biogas recovery with improved biodegradability of both the recalcitrant substrate and co-substrate. A comparative analysis has been tabulated for assessing the most significant combination study in terms of enhancement in biogas, removal of pollutants, in terms of total petroleum hydrocarbons and emulsions, alongside degradation of lignocellulosic content (Table 6.8). Electrokinetically-assisted co-digestion study augmented maximal biogas production with better biodegradation of pollutants.

Table 6.8. Comparative analysis of combination study

Type of combination	**Operating conditions**	**Biogas enhancement (%)**	**TPH removal (%)**	**O&G removal (%)**	**Lignin degradation (%)**
Electrokinetically pretreated co-digestion	53.5 V, 53 min	84.3	64.7	70.6	34.3
Microbially pretreated co-digestion	10^8 CFU/mL, 5 d	75.9	56.0	60.0	27.7

Chapter 7

OPERATION OF LAB-SCALE SEMI-CONTINUOUS ANAEROBIC REACTOR

This chapter deals with the operation of a lab-scale anaerobic bi-phased baffled reactor (ABBR) of 20 L capacity with 14 L working volume in semi-continuous (daily-fed) mode with PRS. Firstly, the reactor was assessed for methane production using untreated PRS as feedstock followed by electrokinetically pretreated PRS.

7.1 Acclimatization of ABBR and optimization of OLR

Acclimatization of an anaerobic reactor is the process of gradually adapting the microorganisms within the digester to a specific feedstock or operating conditions. Acclimatization of an anaerobic digester enables microbial communities to enhance process stability, improve digestion performance, maximize methane yield, and reduce start-up periods (Xu et al., 2012; Dhamodharan et al., 2015). Acclimatization can take several weeks to months, depending on the complexity of the feedstock and the proliferation of the desired microbial community. It is imperative to allow sufficient time for the microorganisms to adapt and establish a stable population. An inoculum from an already operational, steady-state anaerobic digester already contains a diverse and well-adapted microbial community as observed from Section 4.4 (Treu et al., 2018). These microorganisms had already been acclimated to the specific conditions of anaerobic digestion and the particular feedstock used in that reactor, thereby helping enabling a kickstart to the digestion process by introducing a community of microorganisms that are already adapted to the desired operating conditions (Wojcieszak et al., 2017). In this study, the ABBR was inoculated with a well-acclimated, degassed digested sludge (DS) from an operational fixed-dome type anaerobic digester being fed with animal manure as feedstock. This is the most efficient inoculum selected from the inoculum study. The ABBR was fed with 5 kg DS and sealed for 20 d for acclimatization of microbial communities inside the reactor. DS has a homogeneous characteristic with lesser washout potential, enabling the reactor to be stable within 20 d, following which the reactor feeding was initiated.

The ABBR was initially fed with untreated PRS at an organic loading rate (OLR) of 0.85 kg COD m^{-3} d^{-1} for a duration of 40 d. Once the biogas production became stable, the OLR was elevated to 1.15 kg COD m^{-3} d^{-1} and maintained for 30 d. Subsequently, the OLR was further increased to 1.63 kg COD m^{-3} d^{-1}, and maintained for an additional 30 d. The OLR is an important parameter in biogas digestion, describing the input rate of organic material per unit volume of the

digester. Improper OLR can lead to process inhibition. Increasing the OLR can have economic benefits by increasing energy production and minimizing the capital costs. However, operating digesters at high OLRs can lead to instabilities, such as production of inhibitors and excess acidification (Glanpracha and Annachhatre, 2016). The accumulation of VFAs, long-chain fatty acids (LCFAs), ammonia (NH_3), and pH fluctuations due to high OLR can reduce methane production and even lead to digester failure. Therefore, the digesters need to be operated at optimum OLRs (Nkuna et al., 2023). For untreated PRS, exceeding the OLR of 1.63 kg COD m^{-3} d^{-1} resulted in highly dynamic biogas production, accompanied by instantaneous washout of the feedstock at the reactor outlet. The quantities of feedstock fed during each OLR operation has been shown in Fig. 7.1(a). For electrokinetically pretreated PRS under optimum operating conditions (applied voltage: 60 V, exposure period: 83.5 min, electrode spacing: 11.6 cm) as described in Section 5.2, the ABBR was initially fed at an OLR of 0.8 kg COD m^{-3} d^{-1} for 30 d. Subsequently, the OLR was increased to 1.2 kg COD m^{-3} d^{-1} for another 30 d. Upon achieving stable biogas production, the OLR was further raised to 1.5 kg COD m^{-3} d^{-1} for 25 d, and subsequently to 1.9 kg COD m^{-3} d^{-1} for the next 15 d. The gradual increase in OLR allowed the methanogenic microorganisms to flourish, effectively facilitating the start-up of the anaerobic digester while preventing any shock load resulting from a sudden surge in COD loading. As a result, biogas production initiates almost immediately upon initiating the feeding of the digester (Tsegaye et al., 2023). However, beyond an OLR of 1.9 kg COD m^{-3} d^{-1}, the biogas production became notably unstable with reduced methane composition, leading to the decision not to feed the ABBR beyond this OLR. The quantities of electrokinetically pretreated PRS utilized at each OLR during the operation of ABBR is shown in Fig. 7.1(b).

Overall, the primary objective of the start-up phase was to facilitate the adaptation of the DS as an inoculum with PRS as feedstock resulting in a prompt and stable commencement of biogas production. Glanpracha and Annachhatre (2016) in their anaerobic co-digestion study of cassava pulp from cassava starch industries with pig manure in a semi-continuous digester observed a start-up of 60 d which was much higher than that observed in this study. Also, increasing the OLR beyond the optimal value can negatively impact the stability of a biogas digester. It can lead to process instabilities and reduced biogas productions.

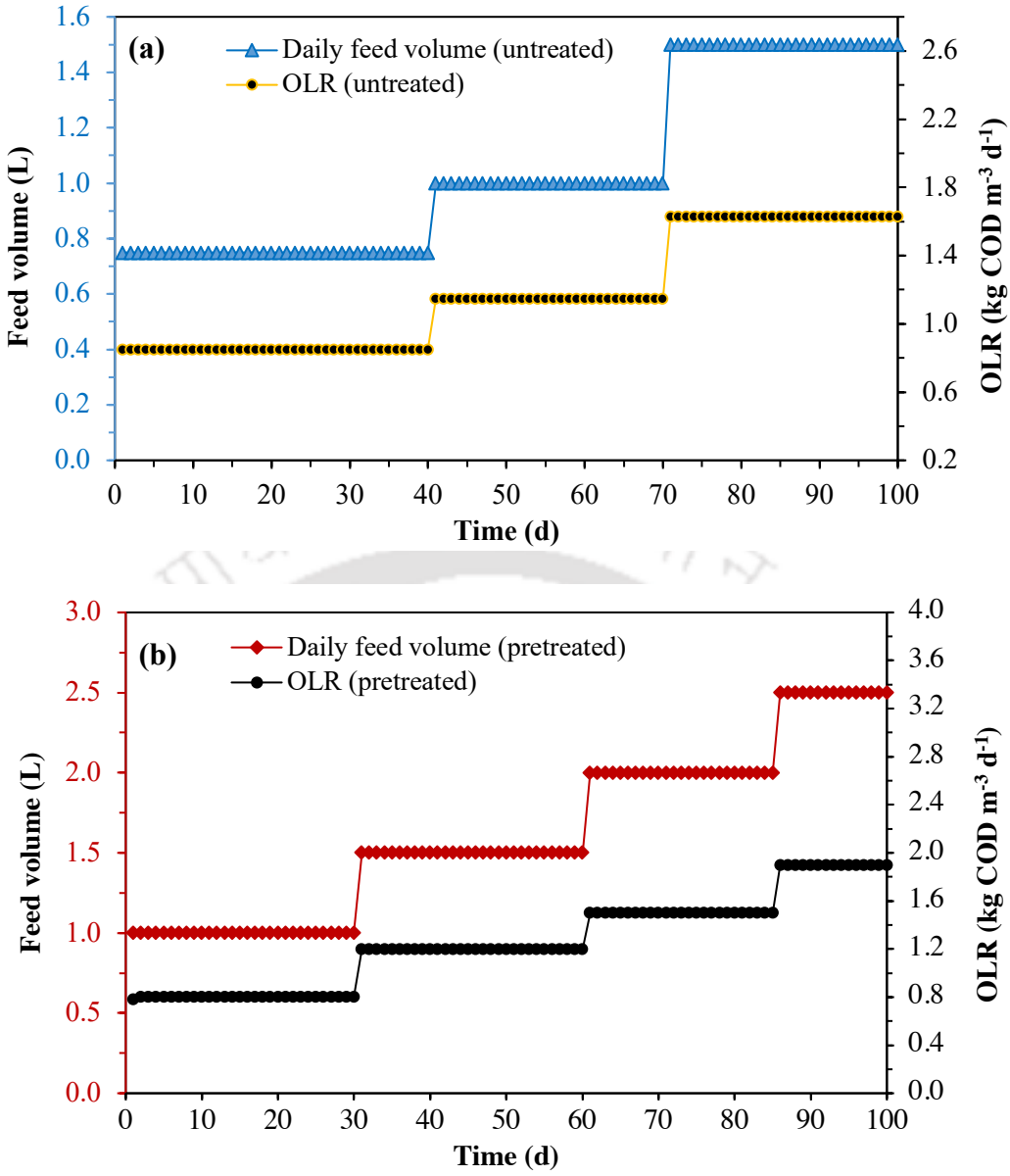

Fig. 7.1. Feed volumes and organic loading rates when the ABBR being fed with (a) untreated PRS and (b) electrokinetically pretreated PRS

7.2 Biogas production profile

The daily biogas production profile during operation of ABBR with untreated and electrokinetically pretreated PRS under optimum conditions is shown in Fig. 7. 2. During the initial operation of ABBR with untreated PRS at an OLR of 0.85 kg COD m^{-3} d^{-1}, the biogas production increased linearly for the first 10 d suggesting a speedy start-up of the reactor (Fig. 7.2a). The acclimated environment created by the microbial community present in DS as an inoculum began utilizing the organic fraction of untreated PRS for converting into biogas. Beyond 10 d, the biogas production remained stable within 40 d of operation of ABBR. Upon increasing the OLR to 1.15 kg COD m^{-3} d^{-1}, the biogas production also increased suggesting the active action of fermentative,

acidogenic and methanogenic bacteria for the biodegradation of the substrate, which became stable by the end of 70 d of operation of ABBR. When the OLR was further increased from 1.15 to 1.63 kg COD m^{-3} d^{-1}, the biogas production further incremented. But the rate of biogas production was quite dynamic during the operation of ABBR from 70th to 100th d. Operation of a reactor beyond an optimum OLR leads to reactor instability with erratic biogas production (Glanpracha and Annachhatre, 2016). Bi-phased anaerobic digestion encompasses distinct hydrolytic-acidogenic and methanogenesis stages, delivering enhanced stability, reduced retention time, and significantly higher methane production rates compared to conventional single-phase anaerobic digestion (Wang et al., 2016). The phase separation contributes to improved hydrolytic-acidogenic performance, making it particularly well-suited for the treatment of substrates with complex intricate composition such as, hydrocarbon-rich PRS (Demirel and Yenigün, 2002).

During the initial operation of ABBR with electrokinetically pretreated PRS under optimum conditions at an OLR of 0.8 kg COD m^{-3} d^{-1} for 30 d, the biogas production kept incrementing for 6 d, after which it became stable. The start-up period of the reactor was inevitably lower compared to the untreated PRS. The conversion of complex insoluble hydrocarbon fraction of PRS to soluble forms due to the pretreatment was easily utilized by the microbial consortium present in the reactor resulting in prompt biogas production and stabilization (Raut et al., 2021). Also, at the time of feeding with pretreated PRS, the ABBR consisted of inoculum and untreated PRS with a wide-range of microorganisms responsible in the metabolic process thereby augmenting biogas. With further increase in OLRs, the biogas production kept rising till 85 d. When the ABBR was operated at an OLR of 1.9 kg COD m^{-3} d^{-1} after 85 d, the biogas production further incremented, but the rate of production was observed to be quite dynamic. This might be attributed to the fact that the ABBR was operated at OLR beyond optimum leading to instability in biogas production (Rajput and Sheikh, 2019). The ratio of methane recovery, VFA concentrations, solid fraction, and soluble COD are responsible for the biogas production dynamics during the operation of an anaerobic digester as discussed in the subsequent sections (Wang et al., 2016; Roy et al., 2016). The cumulative biogas production during operation of ABBR with electrokinetically pretreated PRS at different OLRs for 100 d led to 2.1-fold increment in biogas production compared to operation of ABBR with untreated PRS for 100 d suggesting pretreatment significantly led to higher utilization of organics by the acclimated microbial consortium resulting in augmented biogas production. This enhancement was higher than the anaerobic biodegradability study conducted by Roy et al. (2016), in semi-continuous anaerobic digesters, who observed 1.6-fold increase in methane yield due to ozonation pretreatment of waste activated sludge from petroleum refinery compared to theoretical methane yield evaluated for untreated sludge.

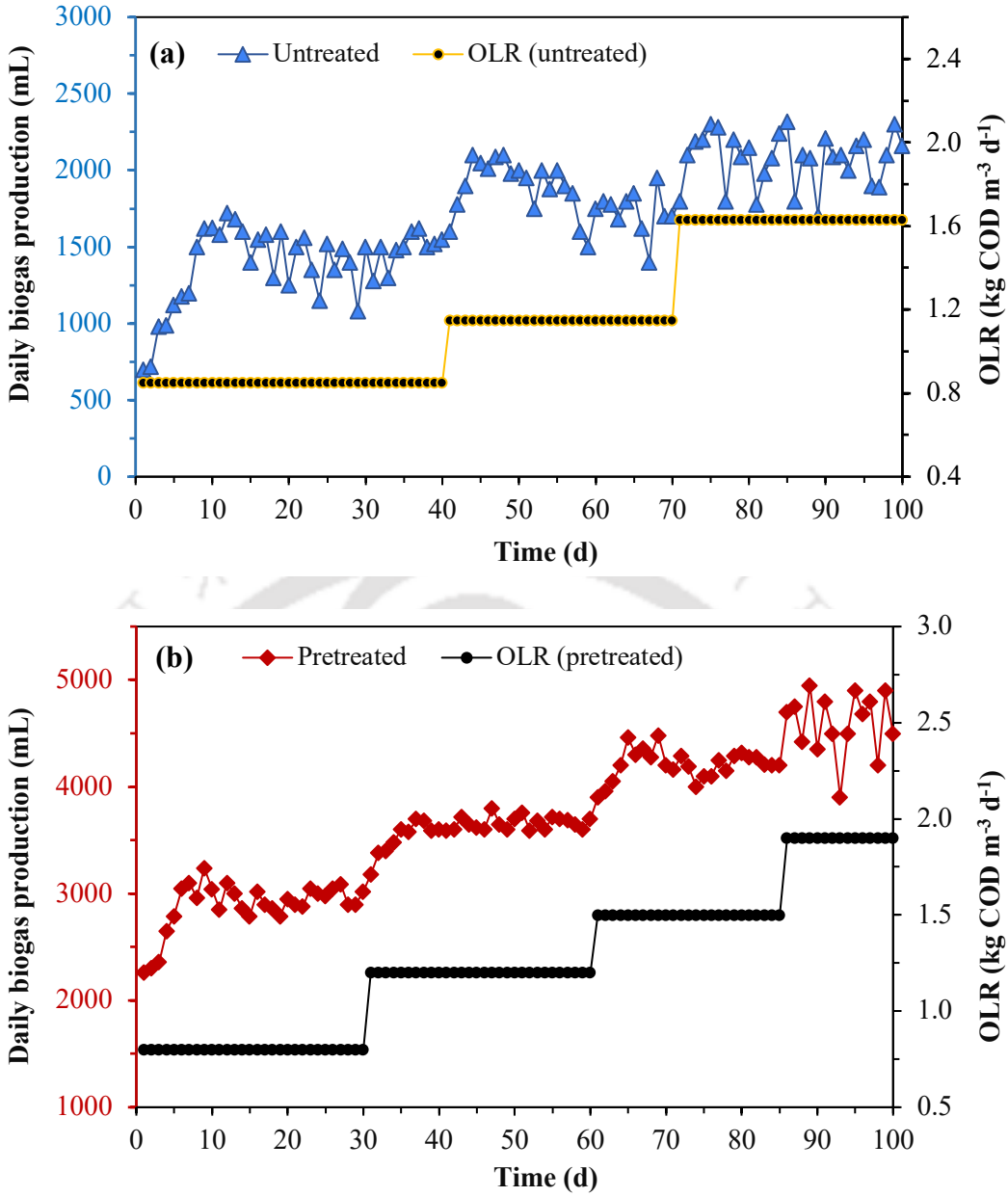

Fig. 7.2. Biogas production profile when ABBR fed with (a) untreated, and (b) electrokinetically pretreated PRS

7.3 Biogas composition profile

The primary constituents of biogas produced during anaerobic digestion are methane (CH_4) and carbon dioxide (CO_2) along with some trace gases. To optimize the performance of an anaerobic digester, it is crucial to monitor and control the process to achieve a higher percentage of methane in the biogas (Chen et al., 2015). The variation in biogas composition profiles during the operation of the ABBR with untreated and electrokinetically pretreated PRS is depicted in Fig. 7.3. During the operation of ABBR with untreated PRS at an OLR of 0.85 kg COD m^{-3} d^{-1}, the methane concentration initially started at 42% and gradually increased to 45.6% within the first 10 d of the

start-up period. Subsequently, the CH_4 concentration fluctuated around 45%, while the average CO_2 concentration was around 35% for the subsequent 30 d (Fig. 7.3a) When the reactor was fed at higher OLRs (1.15 kg COD m^{-3} d^{-1} and 1.63 kg COD m^{-3} d^{-1}), the CH_4 concentration fluctuated around 46-47%, specifying that the increase in OLR contributed to slight increase in methane composition. However, the carbon dioxide concentrations at higher OLR too started to increase resulting in diminishing quality of biogas. Operating biogas digester at higher OLRs results in increased accumulation of volatile and semi-volatile hydrocarbon compounds which increments toxicant concentrations resulting in process inhibition within the digesters (Roy et al., 2016). This complexity makes it challenging for the microorganisms to efficiently utilize and degrade the organic material (Haak et al., 2016).

During the operation of ABBR with electrokinetically pretreated PRS under optimum operating conditions at an OLR of 0.8 kg COD m^{-3} d^{-1}, the biogas showed promising methane content, starting at 50.6%, accompanied by a carbon dioxide content of 33.6%. As the process unfolded, the methane concentration further increased to 57.2%, while the carbon dioxide content decreased from 33.6% to 31.8% within 30 d of operation. These results indicated the efficient hydrolytic, acidogenic, and methanogenic activities of the diverse microbial communities, effectively converting soluble monomers and dimers into higher methane (Schievano et al., 2012). Over the initial 30 d, the average methane composition remained consistently around 54%. Upon increasing the OLR to 1.2 kg COD m^{-3} d^{-1} after 30 d, the methane composition exhibited a noteworthy rise, with the average content remaining steady at around 57.3% until 60 d. This suggested a significant improvement in the biodegradation of the substrate with the higher OLR. As the OLR was further increased to 1.5 kg COD m^{-3} d^{-1} after 60 d, the average methane composition escalated to 61.2%, which was in close accordance with the findings of a two-phased anaerobic digestion study on oil refinery waste activated sludge conducted by Wang et al. (2016). Their study revealed an initial methane concentration of 54.8% within 5d of the start-up period, with the average composition maintained at 60%. Interestingly, as the OLR of the ABBR was further raised from 1.5 to 1.9 kg COD m^{-3} d^{-1} after 85 d, a notable shift occurred in the average methane composition, decreasing from 61.2% to 56.1%. Simultaneously, the average CO_2 composition increased from 29.4% to 32.2%, leading to a reduction in the overall quality of the biogas. These findings highlighted a crucial aspect indicating that an increase in biogas production does not necessarily equate to a rise in methane composition. This could be attributed to various factors, such as feedstock concentration, digester design, operating conditions (such as OLR, HRT), microbial activity, and production of inhibitors (ammonia, hydrogen sulphide) (Glanpracha and Annachhatre, 2016; Baldi et al., 2019; Nkuna et al., 2023). It is worth noting that biogas with a higher percentage of methane holds greater

economic value due to its increased energy content (Kuo and Dow, 2017). Consequently, the optimal OLR for pretreated PRS was observed to be 1.5 kg COD m^{-3} d^{-1}. This careful balance allowed for a significant methane composition while avoiding potential challenges associated with further increasing the OLR and compromising the biogas quality. The above results demonstrated a considerable potential of electrokinetically pretreated PRS in anaerobic digestion, resulting in elevated methane content and the efficient utilization of the substrate by diverse microbial communities.

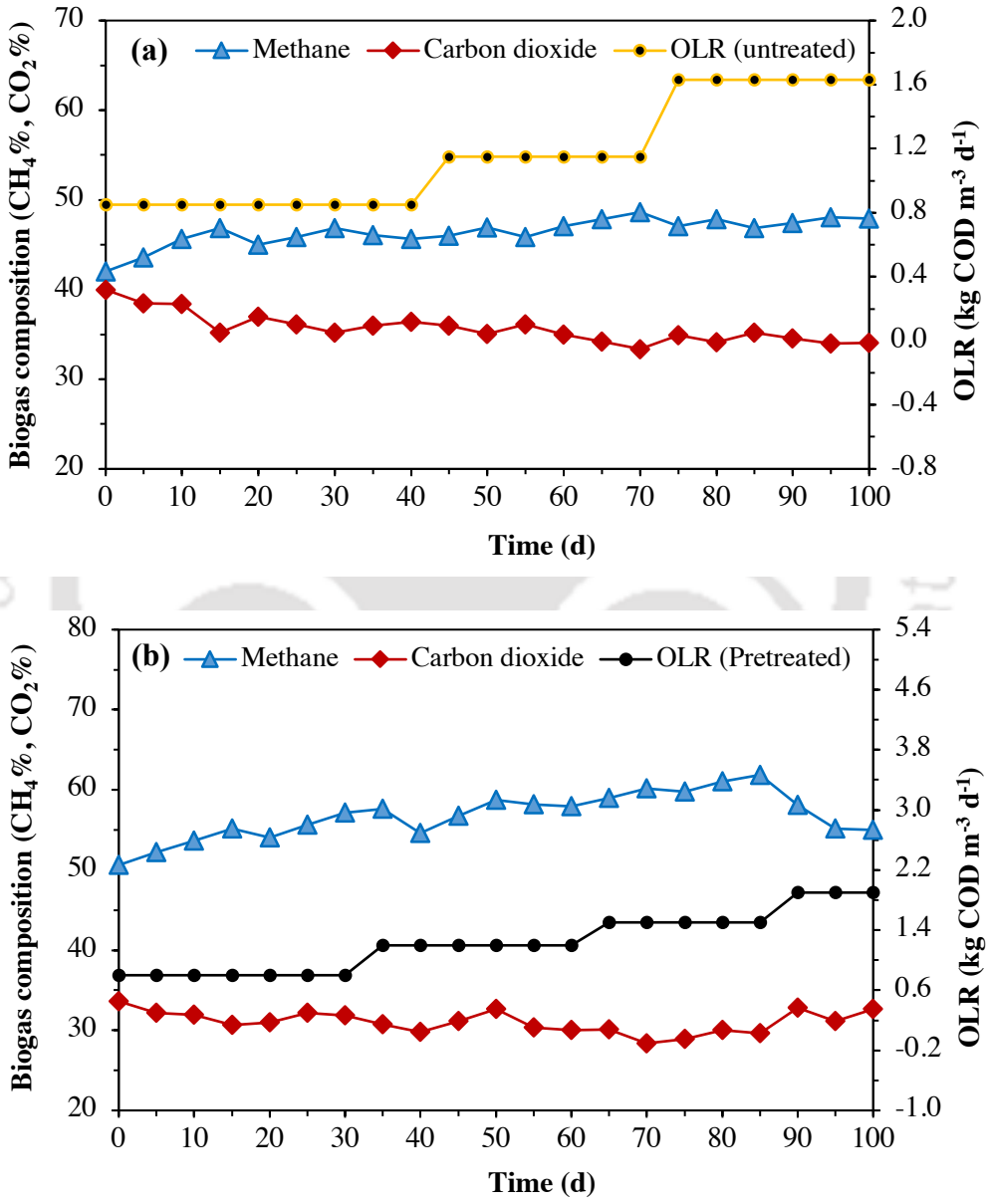

Fig. 7.3. The variation in biogas composition when ABBR was fed with (a) untreated, and (b) electrokinetically pretreated PRS

7.4 sCOD and VFA profile

Evaluating the soluble organic fraction profile during anaerobic digestion is vital for monitoring process efficiency, assessing feedstock characteristics, optimizing operating conditions, and predicting methane yield. It helps understand microbial activity and evaluate the effectiveness of the applied pretreatment for stable operation of a biogas digester (Hallaji et al., 2019). In bioreactors, a greater proportion of sCOD offers more readily biodegradable material, fostering increased methane production. In industrial applications, the emphasis is on high OLR, but excessively high loadings can result in elevated VFA concentrations, decreasing pH and inhibiting the anaerobic digestion process (Chen et al., 2008; Feng et al., 2017). The variation in sCOD and VFA profiles during the operation of ABBR with untreated and pretreated PRS is illustrated in Fig. 7.4 and Fig. 7.5, respectively. The sCOD removal during operation with untreated PRS at an OLR of 0.85 kg COD m^{-3} d^{-1} started at 14% and increased to 16% within 40 d (Fig. 7.4a). With further OLR increase to 1.15 kg COD m^{-3} d^{-1}, the average sCOD removal increased to 18%. By the end of 100 d of ABBR operation, the average sCOD removal reached 19.5%, showing a linear relationship with OLR. Higher sCOD removal indicates better digester stability. However, the average sCOD removal (17.8%) was relatively low, suggesting reduced solubilization during anaerobic digestion of untreated PRS. The organics from untreated PRS included refractory aromatics and heterocyclic compounds becoming toxic for methanogenic activity resulting in lower solubilization (Janejreh et al., 2018). Pretreatment improves solubilization by breaking down complex organic compounds, increasing surface area, releasing soluble compounds, improving dewaterability, and enhancing degradation of pollutants (Gidudu and Chirwa, 2020). It accelerates reaction rates, making the organic material more accessible to microbial degradation. This is evident from the sCOD removals of 61.3%, 66.3%, 70.6% during operation of ABBR with electrokinetically pretreated PRS at OLRs of 0.8, 1.2, and 1.5 kg COD m^{-3} d^{-1} respectively (Fig. 7.4b). This improved sCOD removals could be attributed to the buildup of the robust microbial film around the horizontal baffles in ABBR resulting in improved solubilization and degradation of the substrate. However, at OLR of 1.9 kg COD m^{-3} d^{-1}, the sCOD removal decreased to 60.8%, which might be attributed to the fact that operation of reactor beyond optimum conditions (OLR) leads to inadequate retention time limiting the contact between organic matter and microbial communities, leading to lower solubilization and methane production as corroborated from Fig. 7.3b. Wang et al. (2016) observed 77.8% removal of sCOD during operation of two-phased anaerobic reactor with petroleum refinery waste activated sludge which is in close accordance with the maximum sCOD removal of 70.6% obtained in this study.

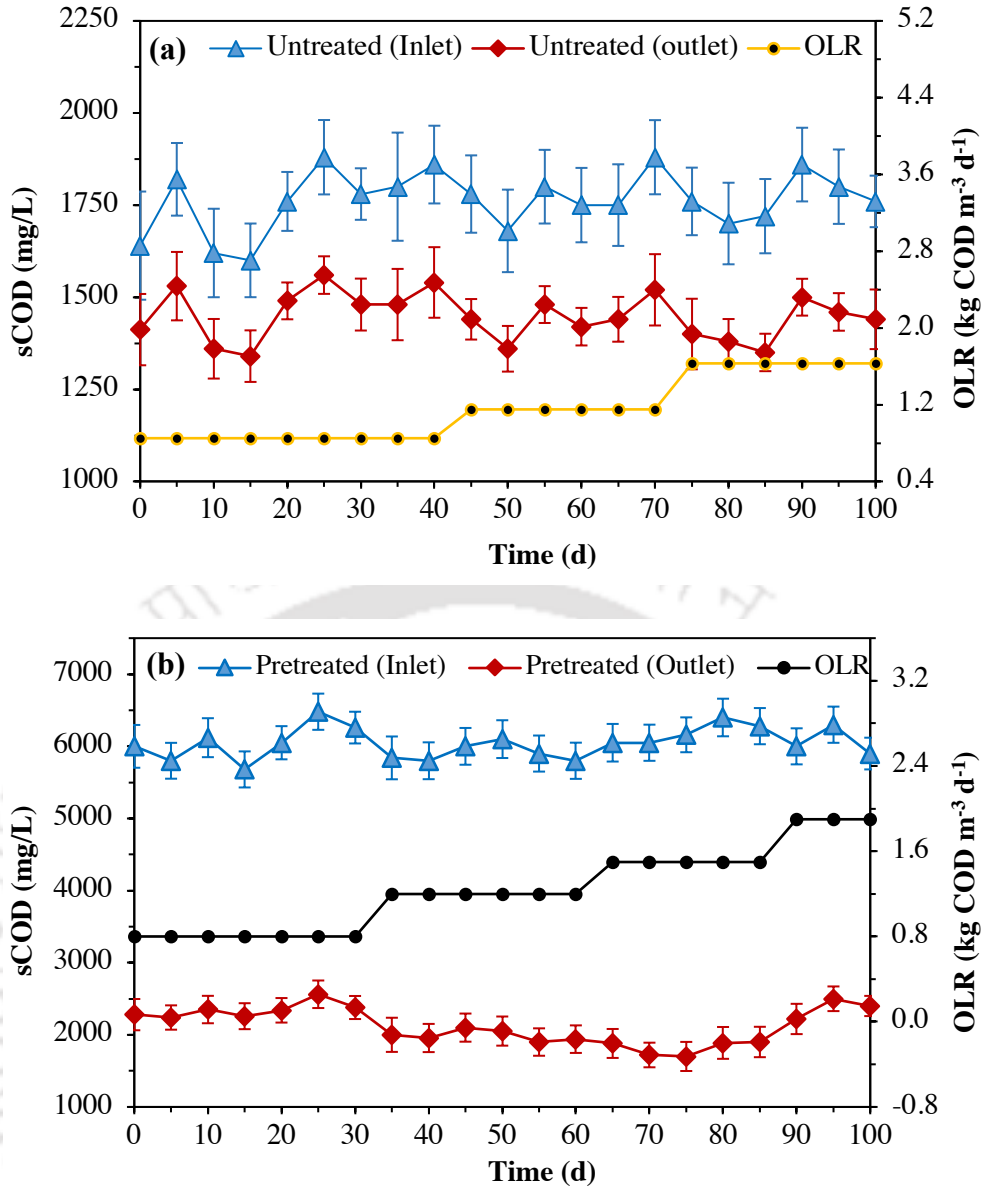

Fig. 7.4. Variation in sCOD during the operation of ABBR with (a) untreated, and (b) electrokinetically pretreated PRS

The relationship between OLR (organic loading rate) and VFA (volatile fatty acid) accumulation in anaerobic digestion shows a typical positive correlation. As the OLR increases, the potential for VFA accumulation also rises, as observed in the operation of the ABBR with untreated PRS over 100 d (Fig. 7.5a). VFA concentrations remained stable at the inlet for all OLRs, while at the outlet, VFAs decreased over time due to the action of fermentative and acidogenic bacteria, converting the substrate towards degradation. However, at an OLR of 1.63 kg COD m^{-3} d^{-1}, VFAs were observed to steeply rise in the outlet. This could be attributed to the digester receiving more organic material than the microbial community could efficiently metabolize, resulting in an organic overload and VFA accumulation (Zhou et al., 2018).

In contrast, during reactor operation with electrokinetically pretreated PRS, VFA concentrations remained stable in both the inlet and outlet until 85 d. Similar trends in VFA production were observed by Roy et al. (2016) in their anaerobic digestion study of ozone pretreated waste activated sludge from a petroleum refinery. After 85 d, VFA accumulation started to increase, suggesting the predominant action of fermentative bacteria over methanogenic bacteria. This resulted in a decrease in methane content and an increase in CO_2 content (Fig. 7.3b). Rapid increases in OLR could cause an imbalance in the microbial community within the digester, where acetogenic bacteria responsible for converting VFAs into methane might not keep up with the increased VFA production, leading to their accumulation (Nkuna et al., 2023). VFA accumulation provides valuable insights into the degree of acidification during the anaerobic digestion of pretreated PRS (Wang et al., 2016).

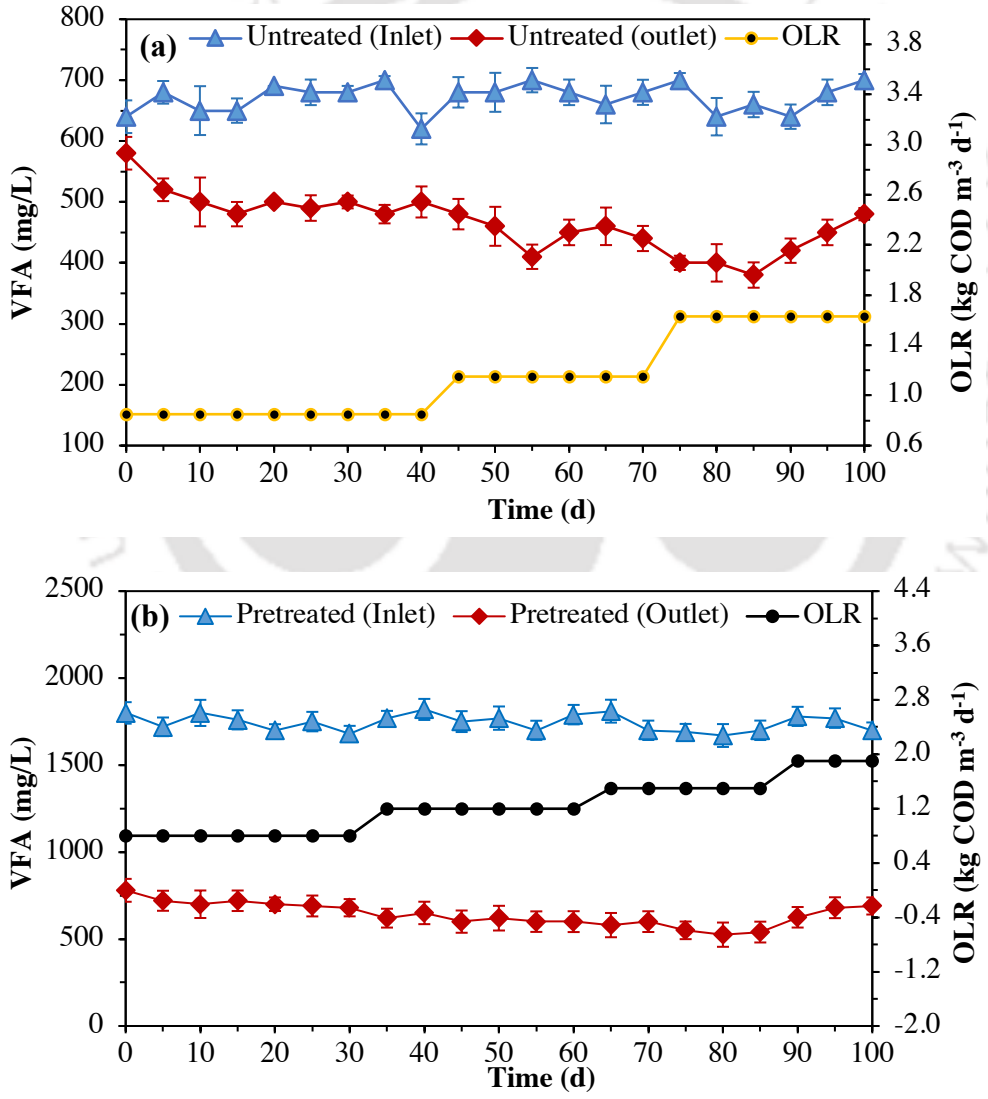

Fig. 7.5. Variation in VFA during the operation of ABBR with (a) untreated, and (b) electrokinetically pretreated PRS

7.5 Total petroleum hydrocarbon degradation profile

Conversion of complex organic matter such as, organic fraction of petroleum hydrocarbons to methane relies on the syntrophic cooperation of various types of microorganisms, where fermentative organisms transfer formate, hydrogen, and acetate to methanogens to yield methane (Mbadinga et al., 2011). Fig. 7.6 (a) and Fig. 7.6 (b) show the total petroleum hydrocarbon (TPH) degradation during the operation of ABBR with untreated and electrokinetically pretreated PRS respectively. During the operation of ABBR with untreated PRS, the TPH content remained stable throughout the digestion period at different OLRs. During the startup period of the reactor, the TPH removal increased gradually from 7% on 0^{th} d to 12% on 10^{th} d suggesting the action of acclimated microorganisms for biodegradation of the complex substrate. The average TPH removal thereafter remained at 12.2% during the first 40 d of operation at an OLR of 0.85 kg COD m^{-3} d^{-1}. Subsequently, the average TPH removals were 12% and 15.5% during ABBR operation at OLRs of 1.15 and 1.63 kg COD m^{-3} d^{-1} respectively. During the anaerobic degradation of PRS, the action of hydrogen-degrading microorganisms created by the acclimated inoculum reduced hydrocarbon equivalents to molecular hydrogen, which thereby got converted to carbon dioxide and methane by the action of methanogenic archaea. The degradation of TPH content could also be ascribed to the synergistic activity of sulfate-reducing, nitrogen-fixing, and methanogenic microbial communities already inherent in the PRS, as documented by Roy et al. (2018). In general, the TPH removal was found to be inadequate during the operation of untreated PRS, indicating that the TPH predominantly existed in recalcitrant forms. This rendered it challenging for microorganisms to effectively utilize these compounds, consequently resulting in lower biogas yields.

When the ABBR was fed with electrokinetically pretreated PRS under optimum operating conditions initially at an OLR of 0.8 kg COD m^{-3} d^{-1}, the TPH removal increased gradually during the startup period of 6 d and became stable in the subsequent days (Fig.7.6b). The average TPH removal was observed to have a positive correlation with the OLRs during 85 d of operation. The average TPH removals were observed to be 45.3%, 50.4% and 54% at OLRs of 0.8, 1.2 and 1.5 kg COD m^{-3} d^{-1} respectively. The removal of TPH can be attributed to either aliphatic (including alicyclic) hydrocarbons, or aromatic hydrocarbons degradation. Aliphatics consist of saturated (alkanes) and unsaturated (alkenes and alkynes) hydrocarbons, which become activated in anaerobic conditions through carboxylation (Wilkes et al., 2016). This transforms C-odd n-alkanes into C-even cellular fatty acids, and vice-versa, during fermentation (Holliger and Zehnder, 1996). The enzymes glutaryl-CoA dehydrogenase and acetyl-CoA acyltransferase play a vital role in the final step of converting fatty acids through β-oxidation to acetyl-CoA and CO_2, which then enter the tricarboxylic acid (TCA) cycle (Mbadinga et al., 2011). Microbial affinity for degradation of

unsaturated hydrocarbons is higher compared to the saturated ones, which is even higher compared to aromatics (Das and Chandran, 2011). Aromatic hydrocarbons can undergo activation through different mechanisms, such as fumarate addition by glycyl-radical enzymes, hydroxylation, or carboxylation. Once activated, the subsequent degradation process involves reductive de-aromatization and hydrolytic ring cleavage. In the anaerobic degradation of activated benzene (benzoyl-CoA), the initial step entails the aromatic reduction of the benzene ring, facilitated by the enzyme benzoyl-CoA reductase, resulting in the de-aromatization of diene benzoyl-CoA. Subsequently, a modified β-oxidation pathway incorporates the addition of (di)enoyl-CoA, leading to ring cleavage. Finally, the process culminates in conventional β-oxidation, leading to the generation of 3-acetyl-CoA and CO_2, both of which enter the tricarboxylic acid (TCA) cycle. (Sierra-Garcia et al., 2014). Upon increasing the OLR further to 1.9 kg COD m^{-3} d^{-1}, the average TPH removal decreased to 48.5%. Operation of reactors at higher OLRs decrease the process efficiency due to longer fermentation periods, thereby delaying the conversion to TPHs leading to decreased TPH removals and thereby, reduced methane concentrations (Fig. 7.3b).

The electrokinetically pretreated PRS exhibited an average maximum TPH removal that was 3.5 times higher compared to untreated PRS. The electrokinetic pretreatment encompasses a comprehensive approach involving electroosmosis, electrokinetic transport, enhanced mass transfer, electrochemical reactions, and pH changes to enhance sludge dewaterability and solubility, resulting in improved mobility of the hydrocarbons (Glendinning et al., 2007; Gill et al., 2014; Westerholm et al., 2016). Consequently, during the operation of pretreated PRS, a higher organic fraction of hydrocarbons becomes readily available to microorganisms, facilitating easier degradation and efficient energy recovery.

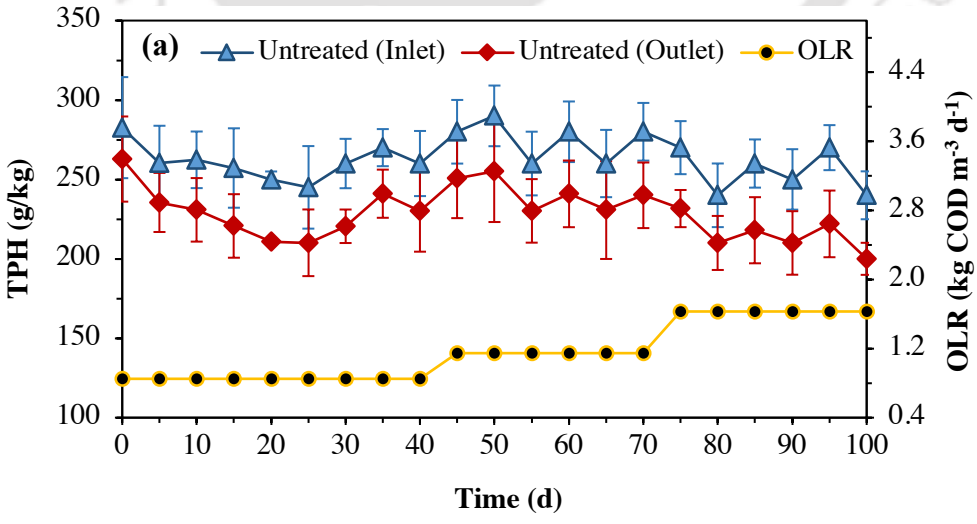

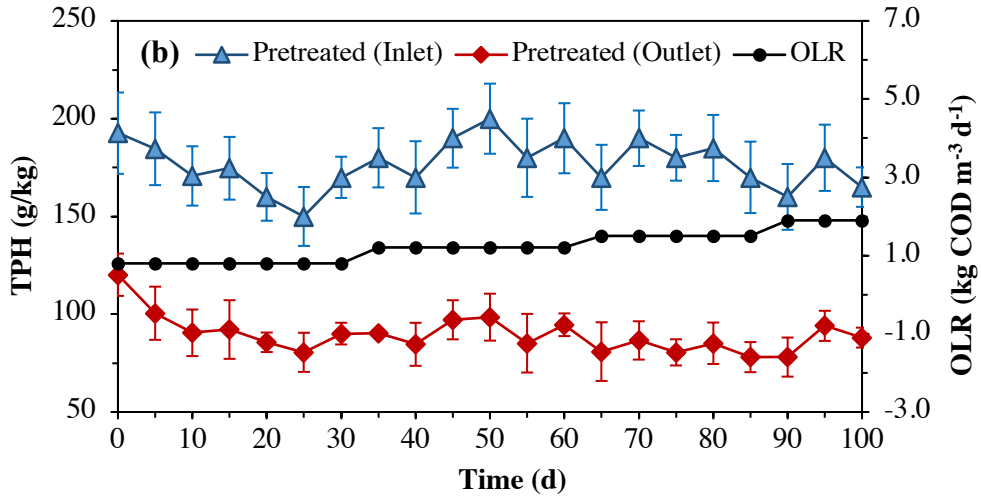

Fig. 7.6. Variation in TPH during the operation of ABBR with (a) untreated, and (b) electrokinetically pretreated PRS

7.6 Oil and grease degradation profile

The degradation profile of oil and grease (O&G) during the operation of ABBR with both untreated and electrokinetically pretreated PRS is illustrated in Fig. 7.7. In the case of untreated PRS, when operated at an OLR of 0.85 kg COD m^{-3} d^{-1}, the O&G removal increased from 9% to 17% over a span of 40 d, with an overall average of 12.3% during the ABBR operation (Fig. 7.7a). However, as the OLR was increased further, there was no significant enhancement in O&G removals observed up to 100 d of operation. At OLRs of 1.15 and 1.63 kg COD m^{-3} d^{-1}, the O&G removals were 13.3% and 14.2% respectively. The challenges faced by microorganisms in accessing hydrocarbons from untreated feedstock were evident from the relatively poor O&G removal rates observed. This underscores the inherent recalcitrance of the feedstock in the absence of any pretreatment, resulting in unsatisfactory O&G removal rates under anaerobic conditions.

During operation with pretreated PRS, the average O&G removals incremented with the increase in OLRs till 85 d of operation. The average O&G degradation percentages for OLRs of 0.8, 1.2, and 1.5 kg COD m^{-3} d^{-1} were observed to be 48%, 53.3%, and 58.5% respectively. The electrokinetic pretreatment technique utilizes electroosmotic flow from a DC power source to mobilize O&G (hydrophobic neutral molecules) within the organic substrate. This electric field-induced oil transport is facilitated by the momentum transfer from the electroosmotic flow of water present on pore surfaces, leading to increased permeability of the substrate through colloidal displacement, widening the capillaries (Elektorowicz et al., 2006). Additionally, the presence of emulsifying substances, such as water-in-oil (W/O), organic acids, asphaltenes, resins, and minerals in the substrate forms a film on scattered water droplets, preventing coalescence. However, the electrokinetic pretreatment effectively removes these finer particles from the W/O

emulsion, resulting in improved water droplet coalescence (Niqui-Arroyo et al., 2012; Ghazanfari et al., 2012; Gill et al., 2014). Therefore, in anaerobic condition, microbial consortium gains access to hydrocarbons through direct microbial adhesion to large oil droplets and by aggregating with emulsified or pseudo solubilized oil. These microorganisms utilize hydrocarbons as carbon source to produce bioemulsifiers or biosurfactants (Ward et al., 2003). The activity of these produced biosurfactants facilitate the extracellular breakdown of substrate during fermentation and the subsequent reduction in O&G content. The decline in the average O&G removal to 56.5% at an OLR of 1.9 kg COD m^{-3} d^{-1} could be attributed to the inhibited activity of methanogenic microorganisms. Operating the reactor at a higher-than-optimum OLR slows down the degradation of organic matter and emulsions, leading to a decrease in biogas production. The optimum OLR represents the ideal balance between the amount of organic material fed into the digester and the microbial capacity to efficiently degrade it. Therefore, operating anaerobic digesters at the optimum organic loading rates ensures balanced microbial activity, reduced risk of inhibition, enhanced biogas production and improved process stability (Nkuna et al., 2023).

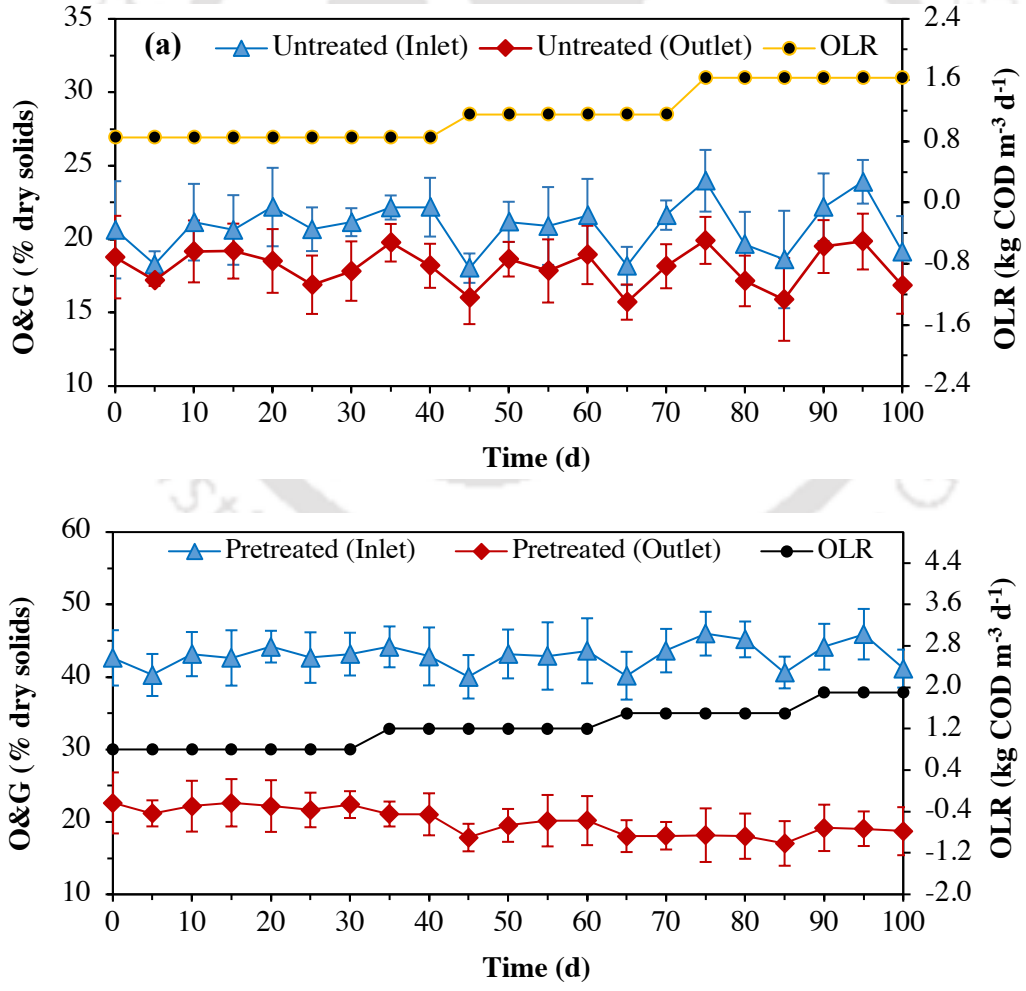

Fig. 7.7. Variation in O&G during the operation of ABBR with (a) untreated, and (b) electrokinetically pretreated PRS

7.7 COMPARATIVE CONCLUSIONS

The ABBR demonstrated note-worthy potential for degrading PRS, with its biphased design showcasing superior methane enhancement compared to single-phased reactors. The incorporation of horizontal baffles facilitated prolonged contact time between the organic substrate and the active inoculum (digested sludge), leading to improved solubilization and subsequent degradation. ABBR enhanced the biodegradability of PRS, particularly in terms of petroleum hydrocarbon and emulsion removals. Electrokinetic pretreatment of PRS resulted in enhanced solubilization, leading to a substantial increase in biogas production. At the optimum OLR for pretreated PRS, the average methane content was 1.3 times higher than that obtained for untreated PRS. Maintaining the reactor at optimal OLRs proved to be crucial for achieving superior process stability. A comparative analysis was conducted to highlight the significant outcomes observed during this study, emphasizing the advantages of operating the ABBR with pretreated PRS over untreated PRS.

Table 7.1. Comparative analysis of the semi-continuous reactor study

Substrate	**Optimum OLR (kg COD m^{-3} d^{-1})**	**Average methane (%)**	**sCOD removal (%)**	**TPH removal (%)**	**O&G removal (%)**
Untreated	1.63	47.5%	19.5	15.5	14.2
Pretreated	1.5	61.2%	70.6	54	58.5

Chapter 8

CONCLUSIONS AND RECOMMENDATIONS

This chapter provides a comprehensive synthesis of significant findings derived from various studies aimed at enhancing biogas production and improving the anaerobic biodegradability of PRS. Furthermore, it includes valuable recommendations for future research endeavors in this area.

8.1 OVERALL CONCLUSIONS

- In **Phase I**, the initial characterization of PRS, collected from the biological treatment unit of the effluent treatment plant of a petrochemical refinery, revealed its potential as a promising feedstock for anaerobic digestion, primarily due to its substantial moisture content and organic matter content. To gauge the anaerobic biodegradability of hydrocarbon-rich PRS, a study was conducted to identify an efficient inoculum, which comprised an undigested residue (UR) from animal manure and an anaerobically acclimated or digested sludge (DS) sourced from a stable operational anaerobic digester. The use of DS as the inoculum fostered a well-balanced environment with favorable microbial communities known to possess hydrocarbon-degrading properties. This contributed to enhanced biogas production and higher removal of organic fractions during the anaerobic digestion process. However, the subpar organic removal percentage (10.7%) indicated the complex and recalcitrant nature of the PRS, leading to prolonged hydrolysis phase.
- In **Phase II**, the hydrolysis phase was expedited using various pretreatment techniques (thermal, electrokinetic, and microbial) in the presence of DS as the inoculum. The application of thermal pretreatment resulted in improved solubilization of PRS, with dry heat at 140°C for 60 min exhibiting the highest enhancement, followed by pressurized moist heat, microwave irradiation, and agitated open moist heat. For untreated PRS, dry heat at 140°C for 60 min maximized solubilization and led to 40% increase in biogas production from pretreated PRS. Similarly, electrokinetic pretreatment at 60V for 83.5 min with an electrode spacing of 11.6 cm achieved a significant 61% enhancement in biogas production through improved solubilization. Microbial pretreatment employing two bacterial strains, Lac enzyme-producing *Pseudomonas putida* 7525 and LiP enzyme-producing *Kosakonia Oryziphila* (MZ605201), also illustrating promising results, with biogas production increasing by 54.6% and 50%, respectively. Chemical characterization (FTIR) showed efficacy in dissociation of hydrocarbon compounds corroborating the improvement in

solubilization of PRS due to the applied pretreatments. Among the different pretreatment methods, electrokinetic pretreatment showcased utmost enhancement in the biodegradability of PRS. This was evidenced by the highest removals of TPH content, and O&G, along with reduction in digestate phytotoxicity.

- In **Phase III**, the nitrogen-rich PRS was co-digested with carbon-rich lignocellulosic YW for balancing the lack of nutrients and moisture content to foster diverse microbial proliferation during the process. The co-digestion at C/N = 33.5 and pH=7.0 resulted in maximum biogas enhancement of 40% compared to the monodigestion of PRS. Considering both the substrate and co-substrate exhibited recalcitrant characteristics, different pretreatment methods (electrokinetic and microbial) were applied to the substrate and co-substrate mix under optimal co-digestion conditions. Electrokinetic pretreatment at 53.5 V and 53 min yielded the highest solubilization, leading to 40.5% enhancement in biogas production compared to untreated co-digestion of PRS and YW. Similarly, microbial pretreatment involved the application of potential bacterial strains isolated from PRS itself (*Bacillus subtilis* IH1, MZ618640 and *Bacillus velezensis* IH2, MZ605121), out of which *B. subtilis* maximized the solubilization with biogas augmentation of 34.2% against untreated co-digestion of PRS and YW. Morphological and chemical characterization (FESEM, FTIR) showcased significant alteration of organic hydrocarbon compounds due to the applied pretreatments suggesting dissociation. The combination of electrokinetic pretreatment and co-digestion proved highly effective, showcasing an 84% enhancement in biodegradability against monodigestion. Additionally, the integrated process demonstrated notably higher degradation of TPH, O&G, and lignin. Electrokinetically-assisted co-digestion resulted in superior biogas recovery with higher degradation of pollutants. Phase III provided a promising avenue of overall sustainability, incorporating an industrial symbiosis approach.
- In **Phase IV**, a laboratory-scale anaerobic biphased baffled reactor (ABBR) with a capacity of 20 L (14 L working volume) was fabricated and operated for 200 d in two stages to assess the anaerobic biodegradability of PRS under semi-continuous (daily-fed) mode. During Stage I, the ABBR was fed with untreated PRS as the feedstock at different OLRs for a period of 100 d. Subsequently, during Stage II, the ABBR was operated with electrokinetically pretreated PRS (applied DC voltage = 60V, exposure period = 83.5 min, electrode spacing = 11.6 cm) at various OLRs for the following 100 d. Notably, the application of electrokinetically pretreated PRS at the optimal OLR of 1.5 kg COD m^{-3} d^{-1} resulted in a significant increase in average methane content, rising from 47.5% for

untreated PRS to 61%, accompanied by a remarkable 3.6-fold enhancement in average COD removal. The ABBR demonstrated its immense potential for the biodegradation of PRS, with its biphased design and horizontal baffled configuration enabling diverse proliferation of the microbial community. This led to improved digestibility of the feedstock and overall enhancement of the anaerobic digestion process showcasing process superiority over single phased anaerobic digesters.

8.2 FUTURE RECOMMENDATIONS

- Use of microbial consortia isolated from the PRS, or genetically engineered microorganisms with enhanced hydrocarbon-degrading capabilities as pretreatments for improved biodegradability of PRS could be performed.
- Advanced pretreatment techniques, such as hydrothermal, ultrasonic, or enzymatic pretreatment, to improve the solubilization of PRS could be explored.
- Co-digestion of PRS with other organic waste streams could be explored.
- Investigation of integration of biogas upgrading technologies, such as anaerobic digestion with microbial electrolysis cells or membrane separation, to enhance the purity of methane in the biogas.
- Pilot-scale studies to assess the feasibility of implementing methane production from PRS at industrial scale to validate the commercial potential and economic viability.
- Economic feasibility and environmental assessment of biogas digesters through cost–benefit analysis and life cycle assessment (LCA) could be performed.

BIBLIOGRAPHY

Aboulfoth, A. M., El Gohary, E. H., El Monayeri, O. D., 2015. Effect of thermal pretreatment on the solubilization of organic matters in a mixture of primary and waste activated sludge, J. Urban Environ. 9 (2015) 82-88. https://doi.org/10.4090/juee.2015.v9n1.082088.

Aburahman H. N., Rosli, M., Yunus, A., 2006. Continuous Microwave Heating of Water-in-oil Emulsions: An Experimental Study. J. Appl. Sci., 6(8), 1868-1872.

Adeniji, A. O., Okoh, O. O., Okoh, A. I., 2017. Analytical methods for the determination of the distribution of total petroleum hydrocarbons in the water and sediment of aquatic systems: A review. J. Chem. 5178937. https://doi.org/10.1155/2017/5178937.

Admon, S., Green, M., Avnimelech, Y., 2001. Biodegradation kinetics of hydrocarbons in soil during land treatment of oily sludge. Bioremediat. J., 5(3), 193-209.

Al-Zahrani, S.M., Putra, M.D., 2013. Used lubricating oil regeneration by various sol-vent extraction techniques. J. Ind. Eng. Chem. 19, 536–539.

Andrade Cruz, I., Chuenchart, W., Long, F., Surendra, K., Renata Santos Andrade, L., Bilal, M., Liu, H., Tavares Figueiredo, R., Khanal, S. K., Fernando Romanholo Ferreira, L., 2022. Application of machine learning in anaerobic digestion: Perspectives and challenges. Bioresour. Technol. 345, 126433. https://doi.org/10.1016/j.biortech.2021.126433.

Aparna, V., Dileep, K.V., Mandal, P.K., Karthe, P., Sadasivan, C., Haridas, M., 2012. Anti-inflammatory property of n-hexadecanoic acid: structural evidence and kinetic assessment. Chem. Biol. Drug Des. 80(3), 434-439. https://doi.org/10.1111/j.1747-0285.2012.01418.x.

APHA, Standard methods for the examination of water and wastewater, 22nd edition edited by E. W. Rice, R. B. Baird, A. D. Eaton and L. S. Clesceri. American Public Health Association (APHA), American Water Works Association (AWWA) and Water Environment Federation (WEF), Washington, D.C., USA, 2012.

Appels, L., Baeyens, J., Degrève, J., Dewil, R., 2008. Principles and potential of the anaerobic digestion of waste-activated sludge. Prog. Energy Combust. 34(6), 755–81. https://doi.org/10.1016/j.pecs.2008.06.002.

Appels, L., Degrève, J., Van der Bruggen, B., Van Impe, J., Dewil, R., 2010. Influence of low temperature thermal pre-treatment on sludge solubilisation, heavy metal release and anaerobic digestion. Bioresour. Technol. 101, 5743-5748. https://doi.org/10.1016/j.biortech.2010.02.068.

Atlas, R. and Bragg, J., 2009. Bioremediation of marine oil spills: when and when not–the Exxon Valdez experience, Microb. Biotechnol. 2, 213-221. https://doi.org/10.1111/j.1751-7915.2008.00079.x

Ayotamuno, M.J., Okparanma, R.N., Nweneka, E.K., Ogaji, S.O.T., Probert, S.D., 2007. Bio-remediation of a sludge containing hydrocarbons. Appl. Energy, 84(9), 936-943.

Baldi, F., Pecorini, I., Iannelli, R., 2019. Comparison of single-stage and two-stage anaerobic co-digestion of food waste and activated sludge for hydrogen and methane production. Renew. Energy. 143, 1755-1765. https://doi.org/10.1016/j.renene.2019.05.122.

Barua, V. B., Raju, V. W., Lippold, S., Kalamdhad, A. S., 2017. Electrohydrolysis pretreatment of water hyacinth for enhanced hydrolysis. Bioresour. Technol. 238, 733-737. https://doi.org/10.1016/j.biortech.2017.04.016.

Bayard, R., Gonzalez-Ramirez, L., Guendouz, J., Benbelkacem, H., Buffière, P., Gourdon, R., 2015. Statistical analysis to correlate bio-physical and chemical characteristics of organic wastes and digestates to their anaerobic biodegradability. Waste Biomass Valorization. 6(5), 759-769. https://doi.org/10.1007/s12649-015-9411-2

Baykara, S. Z., 2018. Hydrogen: A brief overview on its sources, production and environmental impact. Int. J. Hydrog. Energy, 43 (23), 10605-10614. https://doi.org/10.1016/j.ijhydene.2018.02.022.

Behera, S. K., Meena, H., Chakraborty, S., Meikap, B. C., 2018. Application of response surface methodology (RSM) for optimization of leaching parameters for ash reduction from low-grade coal. Int. J. Min. Sci. Technol. 28(4), 621-629. https://doi.org/10.1016/j.ijmst.2018.04.014.

Bhandari, S., Poudel, D. K., Marahatha, R., Dawadi, S., Khadayat, K., Phuyal, S., Shrestha, S., Gaire, S., Basnet, K., Khadka, U., Parajuli, N., 2021. Microbial Enzymes Used in Bioremediation. J. Chem. 2021, 8849512. https://doi.org/10.1155/2021/8849512.

Bhattacharyya, J. K., Shekdar, A. V., 2003. Treatment and disposal of refinery sludges: Indian scenario. Waste Manag. Res. 21, 249–261. https://doi.org/10.1177/0734242X0302100309

Bian, X. Y., Mbadinga, S. M., Liu, Y. F., Yang, S. Z., Liu, J. F., Ye, R. Q., Gu, J. D., Mu, B. Z., 2015. Insights into the anaerobic biodegradation pathway of n-alkanes in oil reservoirs by detection of signature metabolites. Sci. Rep. 5(1), 1-12. https://doi.org/10.1038/srep09801.

Bonten, L.T., Grotenbuis, T.C., Rulkens, W.H., 1999. Enhancement of PAH biodegradation in soil by physicochemical pretreatment. Chemosphere, 38(15), 3627-3636.

Borges, E.S.M. and Chernicharo, C.A.L., 2009. Effect of thermal treatment of anaerobic sludge on the bioavailability and biodegradability characteristics of the organic fraction, Braz. J. Chem. Eng. 26, 469-480. https://doi.org/10.1590/S0104-66322009000300003 .

Bozkurt, Y.C., Apul, O.G., 2020. Critical review for microwave pretreatment of waste-activated sludge prior to anaerobic digestion. Curr. Opin. Environ. Sci. Health. 14, 1-9. https://doi.org/10.1016/j.coesh.2019.10.003.

Brown, D., Li, Y., 2013. Solid state anaerobic co-digestion of yard waste and food waste for biogas production. Bioresour. Technol. 127, 275-280. 10.1016/j.biortech.2012.09.081.

Brown, D.M., Bonte, M., Gill, R., Dawick, J. and Boogaard, P.J., 2017. Heavy hydrocarbon fate and transport in the environment. Q. J. Eng. Geol. 50, 333-346. https://doi.org/10.1144/qjegh2016-142.

Cachot, J., Geffard, O., Augagneur, S., Lacroix, S., Le Menach, K., Peluhet, L., Couteau, J., Denier, X., Devier, M.H., Pottier, D., Budzinski, H., 2006. Evidence of genotoxicity related to high PAH content of sediments in the upper part of the Seine estuary (Normandy, France). Aquat. Toxicol. 79, 257-267. doi: 10.1016/j.aquatox.2006.06.014.

Callaghan, A.V., 2013. Metabolomic investigations of anaerobic hydrocarbon-impacted environments. Curr. Opin. Biotechnol. 24(3), 506-515. https://doi.org/10.1016/j.copbio.2012.08.012.

Cambeilla, A., Benito, J.M., Pazos, C., Coca, J., 2006. Centrifugal Separation Efficiency in the Treatment of Waste Emulsified Oils. Chem. Eng. Res. Des., 84, 69-76.

Carrère, H., Bougrier, C., Castets, D., Delgenès, J.P., 2008. Impact of initial biodegradability on sludge anaerobic digestion enhancement by thermal pretreatment. J. Environ. Sci. Health A, 43(13), 1551-1555.

Castro, T. M. S. D., Cammarota, M. C., Pacheco, E. B. A. V., 2022. Anaerobic co-digestion of oil refinery waste activated sludge and food waste. Environ. Technol. 1-12. https://doi.org/10.1080/09593330.2021.1946598.

Cerqueira, V. S., Hollenbach, E. B., Maboni, F., Vainstein, M. H., Camargo, F. A., Maria do Carmo, R. P., Bento, F. M., 2011. Biodegradation potential of oily sludge by pure and mixed bacterial cultures. Bioresour. Technol. 102 (23), 11003-11010. https://doi.org/10.1016/j.biortech.2011.09.074.

Chaillan, F., Le Flèche, A., Bury, E., Phantavong, Y., Grimont, P., Saliot, A., Oudot, J., 2004. Identification and biodegradation potential of tropical aerobic hydrocarbon-degrading

microorganisms. Res. Microbiol. 155 (7), 587-595. https://doi.org/10.1016/j.resmic.2004.04.006.

Chauhan, P.S., Goradia, B., Saxena, A., 2017. Bacterial laccase: recent update on production, properties and industrial applications. 3 Biotech. 7(5), 1-20. https://dx.doi.org/10.1007%2Fs13205-017-0955-7.

Chen, X.Y., Vinh-Thang, H., Ramirez, A.A., Rodrigue, D., Kaliaguine, S., 2015. Membrane gas separation technologies for biogas upgrading. RSC advances. 5(31), 24399-24448. https://doi.org/10.1039/C5RA00666J.

Christova, N., Tuleva, B., Nikolova-Damyanova, B., 2004. Enhanced hydrocarbon biodegradation by a newly isolated *Bacillus subtilis* strain. Zeitschrift für Naturforschung C, 59(3-4), 205-208. https://doi.org/10.1515/znc-2004-3-414.

Cioabla, A. E., Ionel, I., Dumitrel, G. A., Popescu, F., 2012. Comparative study on factors affecting anaerobic digestion of agricultural vegetal residues. Biotechnol. Biofuels. 5, 39. https://doi.org/10.1186/1754-6834-5-39

Cokkizgin, A., 2012. Salinity stress in common bean (Phaseolus vulgaris L.) seed germination. Notulae Botanicae Horti Agrobotanici Cluj-Napoca. 40 (1), 177-182. https://doi.org/10.15835/nbha4017493.

Colberge, N.O.S., 2004. Microbial Transformation and Degradation of Toxic Organic Chemicals in L. Y. Young, C. E. Caniglia (Eds.), (Wiley-Liss, New York), 27-24.

Conrardy, J., Vaxelaire, J., Olivier, J., 2016. Electro-dewatering of activated sludge: Electrical resistance analysis. Water Res. 100, 194-200. https://doi.org/10.1016/j.watres.2016.05.033.

Costello, D., Greenfield, P., Lee, P., 1991. Dynamic modelling of a single-stage high-rate anaerobic reactor—I. Model derivation. Water Res. 25 (7), 847-858. https://doi.org/10.1016/0043-1354(91)90166-N.

da Silva, L. J., Alves, F. C., de França, F. P., 2012. A review of the technological solutions for the treatment of oily sludges from petroleum refineries. Waste Manag. Res. 30 (10), 1016-1030. https://doi.org/10.1177/0734242X12448517.

Das, K., Mukherjee, A.K., 2007. Crude petroleum-oil biodegradation efficiency of *Bacillus subtilis* and *Pseudomonas aeruginosa* strains isolated from a petroleum-oil contaminated soil from North-East India. Bioresour. Technol. 98(7), 1339-1345. https://doi.org/10.1016/j.biortech.2006.05.032.

Das, N., Chandran, P., 2011. Microbial degradation of petroleum hydrocarbon contaminants: an overview. Biotechnol. Res. Int. 2011, 941810. doi:10.4061/2011/941810.

Daugulis, A. J., McCracken, C. M 2003. Microbial degradation of high and low molecular weight polyaromatic hydrocarbons in a two-phase partitioning bioreactor by two strains of Sphingomonas sp.. Biotechnol. Lett. 25, 1441–1444. https://doi.org/10.1023/A:1025007729355.

De Francisci, D., Kougias, P. G., Treu, L., Campanaro, S., Angelidaki, I., 2015. Microbial diversity and dynamicity of biogas reactors due to radical changes of feedstock composition. Bioresour. Technol. 176, 56-64. https://doi.org/10.1016/j.biortech.2014.10.126.

De Vrieze, J., Raport, L., Willems, B., Verbrugge, S., Volcke, E., Meers, E., Angenent, L.T., Boon, N., 2015. Inoculum selection influences the biochemical methane potential of agro-industrial substrates. Microb. Biotechnol. 8, 776-786. https://dx.doi.org/10.1111%2F1751-7915.12268.

Demirel, B., Yenigün, O., 2002. Two-phase anaerobic digestion processes: a review. J. Chem. Technol. Biotechnol. 77, 743-755. https://doi.org/10.1002/jctb.630.

Dettenmaier, E.M., Doucette, W.J. and Bugbee, B., 2009. Chemical hydrophobicity and uptake by plant roots. Environ. Sci. Technol. 43(2), 324-329. DOI: 10.1021/es801751x.

Dhamodharan, K., Kumar, V., Kalamdhad, A. S., 2015. Effect of different livestock dungs as inoculum on food waste anaerobic digestion and its kinetics. Bioresour. Technol. 180, 237–241. doi: 10.1016/j.biortech.2014.12.066.

Dhamodharan, K., Kumar, V., Kalamdhad, A.S., 2015. Effect of different livestock dungs as inoculum on food waste anaerobic digestion and its kinetics. Bioresour. Technol. 180, 237-241.

DiLallo, R., Albertson, O. E., 1961.Volatile acid by direct titration. Water Pollut. Control Fed. 33, 356–365. https://www.jstor.org/stable/25034391.

Dioha, I.J., Ikeme, C.H., Nafi'u, T., Soba, N.I., Yusuf, M.B.S., 2013. Effect of carbon to nitrogen ratio on biogas production. Int. Res. J. Nat. Sci. 1(3), 1-10.

Distefano, T.D., Ambulkar, A., 2006. Methane production and solids destruction in an anaerobic solid waste reactor due to post-reactor caustic and heat treatment, Water Sci. Technol. 53, 33-41. https://doi.org/10.2166/wst.2006.233.

Diya'uddeen, B.H., Daud, W. M. A.W., Aziz, A. R. A., 2011. Treatment technologies for petroleum refinery effluents: A review. Process Saf. Environ. Prot. 89, 95–105.

Dueholm, M. S., Marques, I. G., Karst, S. M., D'Imperio, S., Tale, V. P., Lewis, D., Nielsen, P. H., Nielsen, J. L., 2015. Survival and activity of individual bioaugmentation strains. Bioresour. Technol. 186, 192-199. https://doi.org/10.1016/j.biortech.2015.02.111.

Dwyer, J., Starrenburg, D., Tait, S., Barr, K., Batstone, D.J., Lant, P., 2008. Decreasing activated sludge thermal hydrolysis temperature reduces product colour, without decreasing degradability. Water Res. 42, 4699–4709. https://doi.org/10.1016/j.watres.2008.08.019.

El-Naas, M. H., Alhaija, M. A., Al-Zuhair, S., 2014. Evaluation of a three-step process for the treatment of petroleum refinery wastewater. J. Environ. Chem. Eng. 2, 56–62.

Elalami, D., Carrere, H., Monlau, F., Abdelouahdi, K., Oukarroum, A., Barakat, A., 2019. Pretreatment and co-digestion of wastewater sludge for biogas production: Recent research advances and trends. Renewable Sustainable Energy Rev. 114, 109287. https://doi.org/10.1016/j.rser.2019.109287.

Elektorowicz, M., Habibi, S., 2005. Sustainable waste management: recovery of fuels from petroleum sludge. Can. J. Civ. Eng. 32(1), 164-169. https://doi.org/10.1139/l04-122.

Elektorowicz, M., Habibi, S., Chifrina, R., 2006. Effect of electrical potential on the electro-demulsification of oily sludge. J. Colloid. Interface Sci., 295, 535–541. https://doi.org/10.1016/j.jcis.2005.08.042.

Ennouri, H., Miladi, B., Zahedi, S., Fdez-Güelfo, L.A., Solera, R., Hamdi, M., Bouallagui, H., 2016. Effect of thermal pretreatment on the biogas production and microbial communities balance during anaerobic digestion of urban and industrial waste activated sludge. Bioresour. Technol. 214, 184-191. https://doi.org/10.1016/j.biortech.2016.04.076.

Fang, C.S., Lai, P.M.C., 1995. Microwave heating and separation of water-in-oil emulsions. J. Microw. Power Electromagn. Energy. 30 (1), 46-57.

Fathepure, B. Z., 2014. Recent studies in microbial degradation of petroleum hydrocarbons in hypersaline environments. Frontiers in microbiology, 5, 173. https://doi.org/10.3389/fmicb.2014.00173.

Feng, J., Zhang, J., Zhang, J., Zhang, J., He, Y., Zhang, R., Chen, C., Liu, G., 2017. Enhanced methane production of vinegar residue by response surface methodology (RSM). AMB Expr, 7, 89. https://doi.org/10.1186/s13568-017-0392-3

Feng, S., Gong, L., Zhang, Y., Tong, Y., Zhang, H., Zhu, D., Huang, X., Yang, H., 2021. Bioaugmentation potential evaluation of a bacterial consortium composed of isolated *Pseudomonas* and *Rhodococcus* for degrading benzene, toluene and styrene in sludge and sewage. Bioresour. Technol. 320, 124329. https://doi.org/10.1016/j.biortech.2020.124329.

Ferdeș, M., Dincă, M. N., Moiceanu, G., Zăbavă, B. Ș., Paraschiv, G., 2020. Microorganisms and Enzymes Used in the Biological Pretreatment of the Substrate to Enhance Biogas Production: A Review. Sustainability. 12(17), 7205. https://doi.org/10.3390/su12177205.

Ferreira-Leitão, V.S., da Silva, J.G., Bon, E.P., 2003. Methylene blue and azure B oxidation by horseradish peroxidase: a comparative evaluation of class II and class III peroxidases. Appl. Catal. B, 42 (2), 213-221. https://doi.org/10.1016/S0926-3373(02)00238-2.

Franke-Whittle, I.H., Walter, A., Ebner, C., Insam, H., 2014. Investigation into the effect of high concentrations of volatile fatty acids in anaerobic digestion on methanogenic communities. Waste Manag. 34 (11), 2080-2089. https://doi.org/10.1016/j.wasman.2014.07.020.

Gargouri, B., Mnif, S., Aloui, F., Karray, F., Mhiri, N., Chamkha, M., Sayadi, S., 2012. Bioremediation of petroleum contaminated water and soils in Tunisia. In Clean Soil and Safe Water (pp. 153-165). Springer Netherlands. https://doi.org/10.1007/978-94-007-2240-8_12.

Gazineu, M.H.P., Araújo de, A.A., Brandão, Y.B., Hazin, C.A., Godoy, J.M., 2005. Radioactivity concentration in liquid and solid phases of scale and sludge generated in the petroleum industry. J. Environ. Radioact. 81, 47-54.

Ghaleb, A.A.S., Kutty, S.R.M., Salih, G.H.A., Jagaba, A.H., Noor, A., Kumar, V., Almahbashi, N.M.Y., Saeed, A.A.H., Saleh Al-dhawi, B.N., 2021. Sugarcane bagasse as a co-substrate with oil-refinery biological sludge for biogas production using batch mesophilic anaerobic co-digestion technology: Effect of carbon/nitrogen ratio. Water, 13 (5), 590. https://doi.org/10.3390/w13050590.

Ghazanfari, E., Shrestha,R. A., Miroshnik, A., Pamukcu, S., 2012. Electrically assisted liquid hydrocarbon transport in porous media. Electrochim. Acta. 86, 185-191. https://doi.org/10.1016/j.electacta.2012.04.077.

Ghimire, N., Wang, S., 2018. Biological treatment of petrochemical wastewater. In Petroleum Chemicals—Recent Insight; Zoveidavianpoor, M., Ed.; IntechOpen: London, UK.

Ghosh, P., Kumar, M., Kapoor, R., Kumar, S.S., Singh, L., Vijay, V., Vijay, V.K., Kumar, V., Thakur, I.S., 2020. Enhanced biogas production from municipal solid waste via co-

digestion with sewage sludge and metabolic pathway analysis. Bioresour. Technol. 296 (2020) 122275. https://doi.org/10.1016/j.biortech.2019.122275.

Gidudu, B., Chirwa, E.M.N., 2020. The combined application of a high voltage, low electrode spacing, and biosurfactants enhances the bio-electrokinetic remediation of petroleum contaminated soil. J. Clean. Prod. 276, 122745. https://doi.org/10.1016/j.jclepro.2020.122745.

Gill, R.T., Harbottle, M.J., Smith, J.W.N., Thornton, S.F., 2014. Electrokinetic-enhanced bioremediation of organic contaminants: A review of processes and environmental applications. Chemosphere. 107, 31-42. https://doi.org/10.1016/j.chemosphere.2014.03.019.

Glanpracha, N., Annachhatre, A.P., 2016. Anaerobic co-digestion of cyanide containing cassava pulp with pig manure. Bioresour. Technol. 214, 112-121. https://doi.org/10.1016/j.biortech.2016.04.079.

Glendinning, S., Lamont-Black, J., Jones, C. J.F.P., 2007. Treatment of sewage sludge using electrokinetic geosynthetics. J. Hazard. Mater., 139 (3), 491-499. https://doi.org/10.1016/j.jhazmat.2006.02.046.

Goering, H.K., Van Soest, P.J., 1975. Forage fibre analysis. U.S. Dep. Agric. (1975), 379, 387-598.

Gojgic-Cvijovic, G. D., Milic, J. S., Solevic, T. M., Beskoski, V. P., Ilic, M. V., Djokic, L. S., Narancic, T. M., Vrvic, M. M., 2012. Biodegradation of petroleum sludge and petroleum polluted soil by a bacterial consortium: a laboratory study. Biodegradation. 23(1), 1-14. https://doi.org/10.1007/s10532-011-9481-1.

Gong, Z., Wang, Z., Wang, Z., 2018. Study on migration characteristics of heavy metals during oil sludge incineration. Pet. Sci. Technol. 36 (6), 469e474.

Granato, D., de Araújo Calado, V.M., 2014. The use and importance of design of experiments (DOE) in process modelling in food science and technology. Math. Stat. Methods Food Sci. Technol. 1, 1-18.

Grishchenkov, V. G., Townsend, R. T., McDonald, T. J., Autenrieth, R. L., Bonner, J. S., Boronin, A.M., 2000. Degradation of petroleum hydrocarbons by facultative anaerobic bacteria under aerobic and anaerobic conditions. Process Biochem. 35 (9), 889-896. https://doi.org/10.1016/S0032-9592(99)00145-4.

Guo, S., Li, G., Qu, J., Liu, X., 2011. Improvement of acidification on dewaterability of oily sludge from flotation. Chem. Eng. J. 168 (2), 746-751. https://doi.org/10.1016/j.cej.2011.01.070.

Güven, G., Perendeci, A., Tanyolaç, A., 2008. Electrochemical treatment of deproteinated whey wastewater and optimization of treatment conditions with response surface methodology. J. Hazard. Mater. 157(1), 69-78. https://doi.org/10.1016/j.jhazmat.2007.12.082.

Haak, L., Roy, R., Pagilla, K., 2016. Toxicity and biogas production potential of refinery waste sludge for anaerobic digestion. Chemosphere. 144, 1170-1176. https://doi.org/10.1016/j.chemosphere.2015.09.099 .

Haider, F. U., Ejaz, M., Cheema, S. A., Khan, M. I., Zhao, B., Liqun, C., Salim, M. A., Naveed, M., Khan, N., Núñez-Delgado, A., Mustafa, A., 2021. Phytotoxicity of petroleum hydrocarbons: sources, impacts and remediation strategies. Environ. Res. 111031. 787 https://doi.org/10.1016/j.envres.2021.111031.

Halalsheh, M., Koppes, J., Elzen, J., Zeeman, G., Fayyad, M., Lettinga, G., 2005. Effect of SRT and temperature on biological conversions and the related scum-forming potential. Water Res. 39, 2475-82.

Hallaji, S.M., Kuroshkarim, M. and Moussavi, S.P., 2019. Enhancing methane production using anaerobic co-digestion of waste activated sludge with combined fruit waste and cheese whey. BMC Biotechnol. 19, 19 (2019). https://doi.org/10.1186/s12896-019-0513-y.

Haq, I., Kalamdhad, A. S., 2021. Phytotoxicity and cyto-genotoxicity evaluation of organic and inorganic pollutants containing petroleum refinery wastewaterusing plant bioassay. Environ. Technol. Inno., 101651. http://dx.doi.org/10.1016/j.eti.2021.101651.

Haq, I., Kumari, V., Kumar, S., Raj, A., Lohani, M., Bhargava, R.N., 2016. Evaluation of the phytotoxic and genotoxic potential of pulp and paper mill effluent using *Vigna radiata* and *Allium cepa*. Adv. Biol. 065736. https://doi.org/10.1155/2016/8065736.

Hardoim, P. R., Nazir, R., Sessitsch, A., Elhottová, D., Korenblum, E., van Overbeek, L. S., van Elsas, J. D., 2013. The new species *Enterobacter oryziphilus* sp. nov. *and Enterobacter oryzendophyticus* sp. nov. are key inhabitants of the endosphere of rice. BMC Microbiol. 13 (1), 1-13. https://doi.org/10.1186/1471-2180-13-164.

Haritash, A., Kaushik, C., 2009. Biodegradation aspects of Polycyclic Aromatic Hydrocarbons (PAHs): A review. J. Hazard. Mater. 169 (1-3), 1-15. https://doi.org/10.1016/j.jhazmat.2009.03.137

He, S., Fan, X., Katukuri, N.R., Yuan, X., Wang, F., Guo, R., 2016. Enhanced methane production from microalgal biomass by anaerobic bio-pretreatment. Bioresour. Technol. 204, 145–151. https://doi.org/10.1016/j.biortech.2015.12.073.

Heider, J., Schühle, K., 2013. Anaerobic biodegradation of hydrocarbons including methane. The Prokaryotes. 605-634. https://doi.org/10.1007/978-3-642-30141-4_80.

Heng, G.C., Isa, M.H., Lim, J.W., Ho, Y.C., Zinatizadeh, A. A. L., 2017. Enhancement of anaerobic digestibility of waste activated sludge using photo-Fenton pretreatment. Environ. Sci. Pollut. Res. Int. 24(35), 27113-27124. doi: 10.1007/s11356-017-0287-5

Hoffmann, T., Troup, B., Szabo, A., Hungerer, C., Jahn, D., 1995. The anaerobic life of *Bacillus subtilis*: cloning of the genes encoding the respiratory nitrate reductase system. FEMS Microbiol. Lett. 131(2), 219-225. doi: 10.1111/j.1574-6968.1995.tb07780.x.

Holliger, C., Zehnder, A.J., 1996. Anaerobic biodegradation of hydrocarbons. Curr. Opin. Biotechnol. 7(3), 326-330. https://doi.org/10.1016/S0958-1669(96)80039-5.

Hu, G., Feng, H., He, P., Li, J., Hewage, K., Sadiq, R., 2020. Comparative life-cycle assessment of traditional and emerging oily sludge treatment approaches. J. Clean. Prod. 251, 119594. https://doi.org/10.1016/j.jclepro.2019.119594.

Hu, G., Li, J., Zeng, G.., 2013. Recent development in the treatment of oily sludge from petroleum industry: A review. J. Hazard. Mater. 261, 470-490. https://doi.org/10.1016/j.jhazmat.2013.07.069.

Huang W, Wang Z, Zhou Y, Ng WJ., 2014. The role of hydrogenotrophic methanogens in an acidogenic reactor. Chemosphere. 140, 40-46.

Hwang, M.H., Jang. N.J., Hyum, S.H., Kim, I.S., 2004. Anaerobic biohydrogen production from ethanol fermentation: the role of pH. J. Biotechnol. 111, 297–309.

International Renewable Energy Agency, 2020. Global Energy Transformation: A Roadmap to 2050. Abu Dhabi: International Renewable Energy Agency.

Islam, B., 2015. Petroleum sludge, its treatment and disposal: A review. Int. J. Chem. Sci. 13 (4), 1584-1602.

J., De Vrieze, L., Raport, B., Willems, S., Verbrugge, E., Volcke, E., Meers, L.T. Angenent, N., Boon, 2015. Inoculum selection influences the biochemical methane potential of agro-

industrial substrates, Microb. Biotechnol. 8, 776-786. https://dx.doi.org/10.1111%2F1751-7915.12268

Jacob, S., Banerjee, R., 2016. Modelling and optimization of anaerobic co-digestion of potato waste and aquatic weed by response surface methodology and artificial neural network coupled genetic algorithm. Bioresour. Technol. 214, 386-395. https://doi.org/10.1016/j.biortech.2016.04.068.

Janajreh, I., Alshehi, A., Elagroudy, S., 2020. Anaerobic co-digestion of petroleum hydrocarbon waste and wastewater treatment sludge. Int. J. Hydrog. 45, 11538-11549. https://doi.org/10.1016/j.ijhydene.2018.05.100 .

Jasmine, J., Mukherji, S., 2014. Evaluation of bioaugmentation and biostimulation effects on the treatment of refinery oily sludge using 2 n full factorial design. Environ. Sci.: Process. Impacts. 16(8), 1889-1896.

Jerez, S., Ventura, M., Molina, R., Pariente, M.I., Martínez, F., Melero, J.A., 2021. Comprehensive characterization of an oily sludge from a petrol refinery: A step forward for its valorization within the circular economy strategy. J. Environ. Manag. 285, 112124. https://doi.org/10.1016/j.jenvman.2021.112124.

Jiménez, J., Guardia-Puebla, Y., Romero-Romero, O., Cisneros-Ortiz, M., Guerra, G., Morgan-Sagastume, J., Noyola, A., 2014. Methanogenic activity optimization using the response surface methodology, during the anaerobic co-digestion of agriculture and industrial wastes. Microbial community diversity. Biomass Bioenergy, 71, 84-97. https://doi.org/10.1016/j.biombioe.2014.10.023

Jin, Y.Q., Zheng, X.Y., Chu, X.L., Chi, Y., Yan, J.H., Cen, K.F., 2012. Oil recovery from oil sludge through combined ultrasound and thermochemical cleaning treatment. Ind. Eng. Chem. Res. 51, 9213–9217.

Johannes, C., Majcherczyk, A., 2000. Natural mediators in the oxidation of polycyclic aromatic hydrocarbons by laccase mediator systems. Appl. Environ. Microbiol. 66 (2), 524-528. https://doi.org/10.1128/AEM.66.2.524-528.2000.

Johnson, O. A., Affam, A.C., 2019. Petroleum sludge treatment and disposal: A review. Environmental Engineering Research. 24 (2), 191-201. https://doi.org/10.4491/eer.2018.134.

Jones, W.J., Leigh, J.A., Mayer, F., Woese, C.R., Wolfe, R.S., 1983. Methanococcus jannaschii sp. nov., an extremely thermophilic methanogen from a submarine hydrothermal vent. Arch. Microbiol. 136(4), 254-261.

Joseph, G., Zhang, B., Harrison, S.H., Graves Jr, J.L., Thomas, M.D., Panchagavi, R., Ewunkem, J.A.J., Wang, L., 2020. Microbial community dynamics during anaerobic co-digestion of corn stover and swine manure at different solid content, carbon to nitrogen ratio and effluent volumetric percentages. J. Environ. Sci. Health A. 55(9), 1111-1124. https://doi.org/10.1080/10934529.2020.1771975.

Joseph, P.J., Joseph, A., 2009. Microbial enhanced separation of oil from a petroleum refinery sludge. J. Hazard. Mater. 161(1), 522-525.

Juhasz, A. L., Naidu, R., 2000. Bioremediation of high molecular weight polycyclic aromatic hydrocarbons: a review of the microbial degradation of benzo[a]pyrene. Int Biodeterior Biodegrad. 45, 57–88.

Kainthola, J., Kalamdhad, A.S., Goud, V.V., 2019. Optimization of methane production during anaerobic co-digestion of rice straw and hydrilla verticillata using response surface methodology. Fuel, 235, 92-99.

Kalra, K., Chauhan, R., Shavez, M., Sachdeva S., 2013. Isolation of laccase producing *Trichoderma* spp. and effect of pH and temperature on its activity. Int. J. Chem. Environ. Technol., 5, 2229-2235.

Kameswari, K. S. B., Kalyanaraman, C., Porselvam, S., Thanasekaran, K., 2012. Optimization of inoculum to substrate ratio for bio-energy generation in co-digestion of tannery solid wastes. Clean Techn. Environ. Policy. 14 (2), 241-250. https://doi.org/10.1007/s10098-011-0391-z.

Kapusta, K., 2018. Effect of ultrasound pretreatment of municipal sewage sludge on characteristics of bio-oil from hydrothermal liquefaction process. Waste Manag. 78, 183-190.

Kargi, F., Catalkaya, E.C., Uzuncar, S., 2010. Hydrogen gas production from waste anaerobic sludge by electrohydrolysis: effects of applied DC voltage. Hydrog. Energy. 6, 1-8. https://doi.org/10.1016/j.ijhydene.2010.11.087.

Karigar, C.S., Rao, S.S., 2011. Role of microbial enzymes in the bioremediation of

Kasoobi,K., 2017. The assessment of treated wastewater quality and the effects of mid-term irrigation on soil physical and chemical properties (case study: bandargaz-treated wastewater). Appl Water Sci. 7, 2385-2396. https://doi.org/10.1007/s13201-016-0420-5.

Kaur, N., Singh, A.K., 2016. Ohmic Heating: Concept and Applications-A Review. Crit. Rev. Food. Sci. Nutr. 56(14), 2338-51. doi:10.1080/10408398.2013.835303.

Kavitha, S., Jayashree, C., Kumar, S. A., Yeom, I. T., Banu, J. R., 2014. The enhancement of anaerobic biodegradability of waste activated sludge by surfactant mediated biological pretreatment. Bioresour. Technol. 168, 159-166. https://doi.org/10.1016/j.biortech.2014.01.118.

Ke, C. Y., Lu, G. M., Wei, Y. L., Sun, W. J., Hui, J. F., Zheng, X. Y., Zhang, Q. Z., Zhang, X. L., 2019. Biodegradation of crude oil by *Chelatococcus daeguensis* HB-4 and its potential for microbial enhanced oil recovery (MEOR) in heavy oil reservoirs. Bioresour. Technol. 287, 121442. https://doi.org/10.1016/j.biortech.2019.121442.

Ke, C. Y., Qin, F. L., Yang, Z. G., Sha, J., Sun, W. J., Hui, J. F., Zhang, Q. Z., Zhang, X. L., 2021. Bioremediation of oily sludge by solid complex bacterial agent with a combined two-step process. Ecotoxicol. Environ. Saf. 208, 111673. https://doi.org/10.1016/j.ecoenv.2020.111673.

Khan, M. U., Ahring, B. K., 2019. Lignin degradation under anaerobic digestion: Influence of lignin modifications- A review. Biomass Bioenergy. 128, 105325. https://doi.org/10.1016/j.biombioe.2019.105325.

Khan, N., Khan, M.D., Sabir, S., Nizami, A.S., Anwer, A.H., Rehan, M., ZainKhan, M., 2019. Deciphering the effects of temperature on bio-methane generation through anaerobic digestion. Environ. Sci. Pollut. Res. 27, 1-12. https://doi.org/10.1007/s11356-019-07245-w.

Kianmehr, P., Parker, W., Seto, P., 2010. An evaluation of protocols for characterization of ozone impacts on WAS properties and digestibility. Bioresour. Technol. 101(22), 8565-8572.

Koch, K., Hafner, S.D., Weinrich, S., Astals, S., Holliger, C., 2020. Power and Limitations of Biochemical Methane Potential (BMP) Tests. Front. Energy Res. 8, 63. https://doi.org/10.3389/fenrg.2020.00063.

Kondusamy, D., Kalamdhad, A.S., 2014. Pre-treatment and anaerobic digestion of food waste for high rate methane production–A review. J. Environ. Chem. Eng., 2 (3), 1821-1830. https://doi.org/10.1016/j.jece.2014.07.024.

Kontogianni, N., Barampouti, E.M., Mai, S., Malamis, D., Loizidou, M., 2019. Effect of alkaline pretreatments on the enzymatic hydrolysis of wheat straw. Environ. Sci. Pollut. Res. 26(35), 35648-35656. https://doi.org/10.1007/s11356-019-06822-3.

Kovács, E., Wirth, R., Maróti, G., Bagi, Z., Rákhely, G., Kovács, K.L., 2013. Biogas production from protein-rich biomass: fed-batch anaerobic fermentation of casein and of pig blood and associated changes in microbial community composition. PLoS One. 8(10), 77265.

Kralova, I., Sjöblom, J., Øye, G., Simon, S., Grimes, B. A., Paso, K., 2011. Heavy crude oils/particle stabilized emulsions. Adv. Colloid Interface Sci., 169(2), 106-127. https://doi.org/10.1016/j.cis.2011.09.001.

Kriipsalu, M., Marques, M., Maastik, A., 2008. Characterization of oily sludge from a wastewater treatment plant flocculation-flotation unit in a petroleum refinery and its treatment implications. J. Mater. Cycles Waste Manage. 10, 79–86. https://doi.org/10.1007/s10163-007-0188-7.

Kuglarz, M., Karakashev, D., Angelidaki, I., 2013. Microwave and thermal pretreatment as methods for increasing the biogas potential of secondary sludge from municipal wastewater treatment plants. Bioresour. Technol. 134, 290-297. https://doi.org/10.1016/j.biortech.2013.02.001.

Kumar, A. G., Vijayakumar, L., Joshi, G., Peter, D. M., Dharani, G., Kirubagaran, R., 2014. Biodegradation of complex hydrocarbons in spent engine oil by novel bacterial consortium isolated from deep sea sediment. Bioresour. Technol. 170, 556-564. https://doi.org/10.1016/j.biortech.2014.08.008.

Kumar, A., Chandra, R., 2020. Ligninolytic enzymes and its mechanisms for degradation of lignocellulosic waste in environment. Heliyon. 6 (2), e03170. https://doi.org/10.1016/j.heliyon.2020.e03170.

Kumar, B., B, R. M., 2013. Petroleum Refinery Oily Sludge: The Quantitative and Qualitative Analysis of Its Composition. Indian Streams Research Journal. 3(10), 2230-7850.

Kuo, J., Dow, J., 2017. Biogas production from anaerobic digestion of food waste and relevant air quality implications. J. Air Waste. Manag. Assoc., 67(9), 1000-1011. https://doi.org/10.1080/10962247.2017.1316326.

Lafitte-Trouqué, S., Forster, C., 2000. Dual anaerobic co-digestion of sewage sludge and confectionery waste. Bioresour. Technol. 71 (1), 77-82. https://doi.org/10.1016/S0960-8524(99)00043-7.

Laherrère, J., Hall, C. A., Bentley, R., 2022. How much oil remains for the world to produce? Comparing assessment methods, and separating fact from fiction. Curr. Opin. Environ. Sustain. 4, 100174.

Lai, J., Wang, H., Wang, D., Fang, F., Wang, F., Wu, T., 2014. Ultrasonic extraction of antioxidants from Chinese sumac (*Rhus typhina* L.) fruit using response surface methodology and their characterization. Molecules. 19 (7), 9019-9032. https://doi.org/10.3390/molecules19079019.

Lee, C., Kim, S., Park, M. H., Lee, Y. S., Lee, C., Lee, S., Yang, J., Kim, J. Y., 2022. Valorization of petroleum refinery oil sludges via anaerobic co-digestion with food waste and swine manure. J. Environ. Manag., 307, 114562. https://doi.org/10.1016/j.jenvman.2022.114562.

Lee, D.J., Lee, S.Y., Bae, J.S., Kang, J.G., Kim, K.H., Rhee, S.S., Park, J.H., Cho, J.S., Chung, J. and Seo, D.C., 2015. Effect of Volatile Fatty Acid Concentration on Anaerobic Degradation Rate from Field Anaerobic Digestion Facilities Treating Food Waste Leachate in South Korea. J. Chem. 640717. https://doi.org/10.1155/2015/640717.

Lee, H., Yun, S.Y., Jang, S., Kim, G.H. and Kim, J.J., 2015. Bioremediation of polycyclic aromatic hydrocarbons in creosote-contaminated soil by *Peniophora incarnata* KUC8836. Bioremediat. J. 19 (1), 1-8. https://doi.org/10.1080/10889868.2014.939136.

Lee, I.S., Rittmann, B.E., 2011. Effect of low solids retention time and focused pulsed pre-treatment on anaerobic digestion of waste activated sludge. Bioresour. Technol. 102(3), 2542-2548. https://doi.org/10.1016/j.biortech.2010.11.082.

Levén, L., Nyberg, K., Schnürer, A., 2012. Conversion of phenols during anaerobic digestion of organic solid waste–a review of important microorganisms and impact of temperature. J. Environ. Manage. 95, S99-S103. https://doi.org/10.1016/j.jenvman.2010.10.021.

Li, C. Y., Zhou, Y. L., Ji, J., Gu, C. T., 2016. Reclassification of *Enterobacter oryziphilus* and *Enterobacter oryzendophyticus* as *Kosakonia oryziphila* comb. nov. and *Kosakonia oryzendophytica* comb. nov. Int. J. Syst. Evol. Microbiol. 66 (8), 2780-2783. https://doi.org/10.1099/ijsem.0.001054.

Li, J., Zhang, X., Zhou, C., Zheng, J., Ge, D., Zhu, W., 2015. New applications of an automated system for high-power LEDs. IEEE-ASME T Mech. 21(2), 1035-1042.

Li, Q., Zuo, W., Zhang, Y., Li, J., He, Z., 2020. Effects of rectangular rib on exergy efficiency of a hydrogen-fueled micro combustor. Int. J. Hydrog. Energy. 45 (16), 10155-10163. https://doi.org/10.1016/j.ijhydene.2020.01.221.

Li, W., Zhang, G., Zhang, Z., Xu, G., 2014. Anaerobic digestion of yard waste with hydrothermal pretreatment. Appl. Biochem. Biotechnol. 172 (5), 2670-2681. 10.1007/s12010-014-0724-6.

Li, Y., Ni, J., Cheng, H., Zhu, A., Guo, G., Qin, Y., Li, Y., 2021. Methanogenic performance and microbial community during thermophilic digestion of food waste and sewage sludge in a high-solid anaerobic membrane bioreactor. Bioresour. Technol. 342, 125938. https://doi.org/10.1016/j.biortech.2021.125938.

Liang, J., Chen, C., Yoza, B.A., Liang, Y., Li, J., Ke, M., Wang, Q., 2019. Hydrolysis and acidification of activated sludge from a petroleum refinery. Pet. Sci. 16, 428-438. https://doi.org/10.1007/s12182-019-0301-2.

Liu, T., Sun, L., Müller, B., Schnürer, A., 2017. Importance of inoculum source and initial community structure for biogas production from agricultural substrates. Bioresour. Technol. 245, 768-777. https://doi.org/10.1016/j.biortech.2017.08.213.

Liu, X., Wang, W., Gao, X., Zhou, Y., Shen, R., 2012. Effect of thermal pretreatment on the physical and chemical properties of municipal biomass waste. Waste Manag. 32, 249-255. https://doi.org/10.1016/j.wasman.2011.09.027.

Lohar, A. K., Sreekrishnan, T. R., 2021. Solubilization of Heavy Metals during Anaerobic Digestion of Sewage Sludge Using Acidogenesis. J. Hazard. Toxic Radioact. Waste. 25 (2), 04020079. https://doi.org/10.1061/(ASCE)HZ.2153-5515.0000593.

Luo, K., Pang, Y., Yang, Q., Wang, D., Li, X., Lei, M., Huang, Q., 2019. A critical review of volatile fatty acids produced from waste activated sludge: enhanced strategies and its applications. Environ. Sci. Pollut. Res. 26, 13984–13998. https://doi.org/10.1007/s11356-019-04798-8.

Machín-Ramírez, C., Okoh, A. I., Morales, D., Mayolo-Deloisa, K., Quintero, R., Trejo-Hernández, M. R., 2008. Slurry-phase biodegradation of weathered oily sludge waste. Chemosphere, 70(4), 737-744.

Malele, I., Nyingilili, H., Lyaruu, E., Tauzin, M., Bernard Ollivier, B., Cayol, J. L., Fardeau, M. L., Geiger, A., 2018. Bacterial diversity obtained by culturable approaches in the gut of Glossina pallidipes population from a non sleeping sickness focus in Tanzania: preliminary results. BMC Microbiol. 18 (1), 107-116. doi: 10.1186/s12866-018-1288-3.

Marin, J. A., Hernandez, T., Garcia, C., 2005. Bioremediation of oil refinery sludge by landfarming in semiarid conditions: Influence on soil microbial activity. Environ. Res. 98 (2), 185-195. https://doi.org/10.1016/j.envres.2004.06.005.

Marín, J.A., Moreno, J.L., Hernández, T., García, C., 2006. Bioremediation by composting of heavy oil refinery sludge in semiarid conditions. Biodegradation. 17, 251–261.

Marsolek, M.D., Kendall, E., Thompson, P.L., Shuman, T.R., 2014. Thermal pretreatment of algae for anaerobic digestion. Bioresour. Technol. 151, 373-377. https://doi.org/10.1016/j.biortech.2013.09.121.

Martin, F., Torelli, S., Le Paslier, D., Barbance, A., Martin-Laurent, F., Bru, D., Geremia, R., Blake, G., Jouanneau, Y., 2012. Betaproteobacteria dominance and diversity shifts in the bacterial community of a PAH-contaminated soil exposed to phenanthrene. Environ. Pollut. 162, 345-353. https://doi.org/10.1016/j.envpol.2011.11.032.

Maspolim, Y., Zhou, Y., Guo, C., Xiao, K. and Ng, W.J., 2015. Comparison of single-stage and two-phase anaerobic sludge digestion systems–Performance and microbial community dynamics. Chemosphere. 140, 54-62.

Mater, L., Sperb, R.M., Madureira, L.A.S., Rosin, A.P., Correa, A.X.R., Radetski, C.M., 2006. Proposal of a sequential treatment methodology for the safe reuse of oil sludge-contaminated soil. J. Hazard. Mater.136(3), 967-971.

Matthews, J.E., Hastings, L., 1987. Evaluation of toxicity test procedure for screening treatability potential of waste in soil. Toxic. Assess. 2, 265–281.

Mbadinga, S. M., Wang, L. Y., Zhou, L., Liu, J. F., Gu, J. D., Mu, B. Z., 2011. Microbial communities involved in anaerobic degradation of alkanes. Int. Biodeterior. Biodegrad., 65(1), 1-13. https://doi.org/10.1016/j.ibiod.2010.11.009.

Meegoda, J.N., Li, B., Patel, K., Wang, L.B., 2018. A Review of the Processes, Parameters, and Optimization of Anaerobic Digestion. Int. J. Environ. Res. Public Health. 15(10), 2224.

Mehryar, E., Ding, W., Hemmat, A., Hassan, M., Talha, Z., Kafashan, J., Huang, H., 2017c. Modeling and multiresponse optimization for anaerobic co-digestion of oil refinery wastewater and chicken manure by using artificial neural network and the Taguchi method. BioMed Res. Int. 2017, 2036737. https://doi.org/10.1155/2017/2036737.

Mehryar, E., Ding, W.M., Hemmat, A., Hassan, M., Bi, J.H., Huang, H.Y., Kafashan, J., 2017a. Anaerobic co-digestion of oil refinery wastewater and chicken manure to produce biogas, and kinetic parameters determination in batch reactors. Agron. Res. 15, 1983–1996. https://doi.org/10.15159/AR.17.072.

Mehryar, E., Ding, W.M., Hemmat, A., Talha, Z., Hassan, M., Mamat, T., Hei, K., 2017b. Anaerobic Co-digestion of oil refinery wastewater with bagasse; evaluating and modeling by neural network algorithms and mathematical equations. BioResources 12.

Merkl, N., Schultze-Kraft, R., Infante, C., 2005. Assessment of tropical grasses and legumes for phytoremediation of petroleum-contaminated soils. Water Air Soil Pollut. 165 (1), 195-209. https://doi.org/10.1007/s11270-005-4979-y.

Merrylin, J., Kumar, S. A., Kaliappan, S., Yeom, I. T., Banu, J. R., 2013. Biological pretreatment of non-flocculated sludge augments the biogas production in the anaerobic digestion of the pretreated waste activated sludge. Environ. Technol., 34 (13-14), 2113-2123. https://doi.org/10.1080/09593330.2013.810294.

Metcalf., Eddy., Inc. (2003). Wastewater engineering: treatment and reuse.

Mishra, S., Jyot, J., Kuhad, R.C., Lal, B., 2001. Evaluation of Inoculum Addition to Stimulate In-Situ Bioremediation of Oily Sludge Contaminated Soil. Appl. Environ. Microbial. 67, 1675-1681.

Mrayyan, B., Battikhi, M.N., 2005. Biodegredation of Total Organic Carbon (TOC) in Jordanian Petroleum Sludge. J. Hazard. Mater. 120, 127-134.

Mudhoo, A., Kumar, S. Effects of heavy metals as stress factors on anaerobic digestion processes and biogas production from biomass. Int. J. Environ. Sci. Technol. 10, 1383–1398 (2013). https://doi.org/10.1007/s13762-012-0167-y.

Mukred, A.M., Hamid, A.A., Hamzah, A., Yusoff, W.W., 2008. Development of three bacteria consortium for the bioremediation of crude petroleum-oil in contaminated water. Online J. Biol. Sci. 8(4), 73-79.

Murto, M., Björnsson, L., Mattiasson, B., 2004. Impact of food industrial waste on anaerobic co-digestion of sewage sludge and pig manure. J. Environ. Manage. 70(2), 101-107.

Nielfa, A., Cano, R., Fdz-Polanco, M., 2014. Theoretical methane production generated by the co-digestion of organic fraction municipal solid waste and biological sludge. Biotechnology reports (Amsterdam, Netherlands), 5, 14–21. https://doi.org/10.1016/j.btre.2014.10.005

Niqui-Arroyo, J.L., Ortega-Calvo, J.J., 2010. Effect of Electrokinetics on the Bioaccessibility of Polycyclic Aromatic Hydrocarbons in Polluted Soils. J. Environ. Qual. 39(6), 1993-8. doi: 10.2134/jeq2010.0101.

Nkuna, R., Roopnarain, A., Rashama, C., Adeleke, R., 2023. Insights into organic loading rates of anaerobic digestion for biogas production: a review. Crit. Rev. Biotechnol. 42 (4), 487-507. https://doi.org/10.1080/07388551.2021.1942778.

OECD, 2003. Guideline for Testing of Chemicals (2003 Draft). Terrestrial Plant Tests: 208: Seedling Emergence and Seedling Growth Test. 1-19.

Oliveira, H., 2012. Chromium as an environmental pollutant: insights on induced plant toxicity. J. Bot., Le 8, 375843. https://doi.org/10.1155/2012/375843.

Passos, F., Ferrer, I., 2015. Influence of hydrothermal pretreatment on microalgal biomass anaerobic digestion and bioenergy production. Water Res. 68, 364–373. https://doi.org/10.1016/j.watres.2014.10.015.

Pellera, F. M., Gidarakos, E., 2016. Effect of substrate to inoculum ratio and inoculum type on the biochemical methane potential of solid agroindustrial waste. J. Env. Chem. Eng. 4 (3), 3217-3229. https://doi.org/10.1016/j.jece.2016.05.026.

Phillips, D.H. and Grover, P.L., 1994. Polycyclic hydrocarbon activation: bay regions and beyond. Drug metabol. reviews. 26, 443-467. doi: 10.3109/03602539409029808

Priac, A., Badot, P.M., Crini, G., 2017. Treated wastewater phytotoxicity assessment using Lactuca sativa: focus on germination and root elongation test parameters. CR. BIOL., 340(3), 188-194. https://doi.org/10.1016/j.crvi.2017.01.002.

Rajasekar, A., Maruthamuthu, S., Nagu, M., Mohanan, S., Subramanian, P., Palaniswamy, N., 2005. Bacterial degradation of naphtha and its influence on corrosion. Corros. Sci. 47, 257-271. https://doi.org/10.1016/j.corsci.2004.05.016.

Rajput, A. A., Sheikh, Z., 2019. Effect of inoculum type and organic loading on biogas production of sunflower meal and wheat straw. Sustain. Environ. Res. 29, 4. https://doi.org/10.1186/s42834-019-0003-x

Raugei, M., Fullana-i-Palmer, P., Fthenakis, V., 2012. The Energy Return on Energy Investment (EROI) of Photovoltaics: Methodology and Comparisons with Fossil Fuel Life Cycles. Energy Policy, 45, 576-582. doi:10.1016/j.enpol.2012.02.033.

Raut, M. P., Pandhal, J., Wright, P. C., 2021. Effective pretreatment of lignocellulosic co-substrates using barley straw-adapted microbial consortia to enhanced biomethanation by anaerobic digestion. Bioresour. Technol. 321, 124437. https://doi.org/10.1016/j.biortech.2020.124437.

Ravi, R., Husna Zulkrnin, N. S., Rozhan, N. N., Nik Yusoff, N. R., Mat Rasat, M. S., Ahmad, M. I., Hamzah, Z., Ishak, I. H., Mohd Amin, M. F., 2018. Evaluation of two different solvents for *Azolla pinnata* extracts on chemical compositions and larvicidal activity against *Aedes albopictus* (Diptera: Culicidae). J. Chem. 2018, 1-8. https://doi.org/10.1155/2018/7453816.

Robertson, F. A., Thorburn, P. J., 2007. Management of sugarcane harvest residues: consequences for soil carbon and nitrogen. Soil Res. 45(1), 13-23.

Robertson, S. J., McGill, W. B., Massicotte, H. B., Rutherford, P. M., 2007. Petroleum hydrocarbon contamination in boreal forest soils: a mycorrhizal ecosystems perspective. Biol. Rev. 82 (2), 213-240. https://doi.org/10.1111/j.1469-185X.2007.00012.x.

Rocha da, O.R.S., Dantas, R.F., Duarte, M.M.M.B., M.M.L., Silva Da, V.L., 2007. Oil Sludge Treatment by Photocatalysis Applying Black and White Light. Chem. Eng. J., 157, 80-85.

Rodan-Carrillo, T., Gastorena-Cortes, G., Zapata-Penasco, I., Reyes-Avila, J., Olgum- Lora, P., 2012. Aerobic Biodegradation of Sludge with High Hydrocarbon Content Generated by a Mexican Natural Gas Processing Facility. J. Environ. Manage. 95, 593-598.

Rostami, I., Juhasz, A.L., 2011. Assessment of persistent organic pollutant (POP) bioavailability and bioaccessibility for human health exposure assessment: a critical review. Crit Rev Environ Sci Technol. 41, 623–656. https://doi.org/10.1080/10643380903044178.

Roy, A., Dutta, A., Pal, S., Gupta, A., Sarkar, J., Chatterjee, A., Saha, A., Sarkar, P., Sar, P., Kazy, S.K., 2018a. Biostimulation and bioaugmentation of native microbial community accelerated bioremediation of oil refinery sludge. Bioresour. Technol. 253, 22-32. https://doi.org/10.1016/j.biortech.2018.01.004.

Roy, A., Sar, P., Sarkar, J., Dutta, A., Sarkar, P., Gupta, A., Mohapatra, B., Pal, S., Kazy, S.K., 2018b. Petroleum hydrocarbon-rich oil refinery sludge of North-East India harbours anaerobic, fermentative, sulfate-reducing, syntrophic and methanogenic microbial populations. BMC Microbiol. 18 (1), 1-22. https://doi.org/10.1186/s12866-018-1275-8.

Roy, R., Haak, L., Li., L., Pagilla, K., 2016. Anaerobic digestion for solids reduction and detoxification of refinery waste streams. Process Biochem. 51 (2016) 1552-1560. https://doi.org/10.1016/j.procbio.2016.08.006 .

Salerno, M.B., Lee, H.S., Parameswaran, P., Rittmann, B.E., 2009. Using a pulsed electric field as a pretreatment for improved biosolids digestion and methanogenesis. Water Environ. Res. 81(8), 831-839. https://doi.org/10.2175/106143009X407366.

Samuel, M. S., Sivaramakrishna, A., Mehta, A., 2014. Bioremediation of p-Nitrophenol by *Pseudomonas putida* 1274 strain. J. Environ. Health Sci. Engineer. 12 (1), 1-8. https://doi.org/10.1186/2052-336X-12-53.

Sánchez Rubal, J., Cortacans Torre, J.A., del Castillo González, I., 2012. Influence of Temperature, Agitation, Sludge Concentration and Solids Retention Time on Primary Sludge Fermentation. Int. J. Chem. Eng. 2012, 861467. https://doi.org/10.1155/2012/861467.

Sangeetha, J., Thangadurai, D., 2014. Effect of biologically treated petroleum sludge on seed germination and seedling growth of *Vigna unguiculata* (L.) Walp. (Fabaceae) Braz. Arch. Biol. Technol. 57, 427-433. https://doi.org/10.1590/S1516-89132014005000011.

Sankaran, S., Pandey, S., Sumathy, K., 1998. Experimental investigation on waste heat recovery by refinery oil sludge incineration using fluidised-bed technique. J. Environ. Sci. Heal. A. 33(5), 829-845. https://doi.org/10.1080/10934529809376764.

Sappl, J., Harders, M., Rauch, W., 2023. Machine learning for quantile regression of biogas production rates in anaerobic digesters. Sci. Total Environ. 872, 161923. https://doi.org/10.1016/j.scitotenv.2023.161923.

Sarkar, P., Roy, A., Pal, S., Mohapatra, B., Kazy, S.K., Maiti, M.K., Sar, P., 2017. Enrichment and characterization of hydrocarbon-degrading bacteria from petroleum refinery waste as potent bioaugmentation agent for in situ bioremediation. Bioresour. Technol. 242, 15-27. https://doi.org/10.1016/j.biortech.2017.05.010.

Schievano, A., Tenca, A., Scaglia, B., Merlino, G., Rizzi, A., Daffonchio, D., Oberti, R., Adani, F., 2012. Two-stage vs single-stage thermophilic anaerobic digestion: comparison of energy production and biodegradation efficiencies. Environ. Sci. Technol. 46 (15), 8502-8510. DOI: 10.1021/es301376n

Shie, J.L., Lin, J.P., Chang, C.Y., Wu, C.H., Lee, D.J., Chang, C.F., Chen, Y.H., 2004. Oxidative thermal treatment of oil sludge at low heating rates. Energ. Fuel. 18, 1272–1281. https://doi.org/10.1021/ef0301811.

Siddique, M. N. I., Munaim, M. S. A., Zularisam, A.W., 2016. Effect of food to microbe ratio variation on anaerobic co-digestion of petrochemical wastewater with manure. J. Taiwan Inst. Chem. Eng. 58, 451-457. https://doi.org/10.1016/j.jtice.2015.06.038.

Siddique, M. N. I., Munaim, M.S.A., Wahid, Z.B.A., 2017. The combined effect of ultrasonic and microwave pre-treatment on bio-methane generation from co-digestion of petrochemical wastewater. J. Clean. Prod. 145, 303-309. https://doi.org/10.1016/j.jclepro.2017.01.061.

Siddique, M., Munaim, M., Zularisam, A., 2014. Mesophilic and thermophilic biomethane production by co-digesting pretreated petrochemical wastewater with beef and dairy cattle manure. J. Ind. Eng. Chem. 20, 331–337.

Siddique, M.N.I., Munaim, M.S.A. and Zularisam, A.W., 2015. Feasibility analysis of anaerobic co-digestion of activated manure and petrochemical wastewater in Kuantan (Malaysia). J. Clean. Prod. 106, 380-388.

Sierra-Garcia, I. N., Correa Alvarez, J., Pantaroto de Vasconcellos, S., Pereira de Souza, A., dos Santos Neto, E.V., de Oliveira, V.M., 2014. New hydrocarbon degradation pathways in the microbial metagenome from Brazilian petroleum reservoirs. PloS one, 9(2), e90087. https://doi.org/10.1371/journal.pone.0090087.

Siles-Castellano, A.B., López, M.J., López-González, J.A., Suárez-Estrella, F., Jurado, M.M., Estrella-González, M.J., Moreno, J., 2020. Comparative analysis of phytotoxicity and compost quality in industrial composting facilities processing different organic wastes. J. Clean. Prod. 252, 119820. https://doi.org/10.1016/j.jclepro.2019.119820.

Silva, C.C., Hayden, H., Sawbridge, T., Mele, P., Kruger, R.H., Rodrigues, M.V., Costa, G.G., Vidal, R.O., Sousa, M.P., Torres, A.P.R., Santiago, V.M., 2012. Phylogenetic and functional diversity of metagenomic libraries of phenol degrading sludge from petroleum refinery wastewater treatment system. AMB Express. 2 (1), 1-13. DOI: 10.1186/2191-0855-2-18

Singh, B., Kumar, P., 2020. Physicochemical characteristics of hazardous sludge from effluent treatment plant of petroleum refinery as feedstock for thermochemical processes. J. Environ. Chem. Eng. 8 (4), 103817. https://doi.org/10.1016/j.jece.2020.103817.

Singh, D., Fulekar, M. H., 2010. Biodegradation of petroleum hydrocarbons by Pseudomonas putida strain MHF 7109. Clean (Weinh). 38 (8), 781-786. https://doi.org/10.1002/clen.200900239.

Srinivasarao Naik, B., Mishra, I. M., Bhattacharya, S. D., 2011. Biodegradation of total petroleum hydrocarbons from oily sludge. Bioremediat. J. 15 (3), 140-147. https://doi.org/10.1080/10889868.2011.598484.

Subramanian, S., Kumar, N., Murthy, S., Novak, J.T., 2007. Effect of anaerobic digestion and anaerobic/aerobic digestion processes on sludge dewatering, J. Residuals Sci. Technol. 4 (1), 17–23.

Sun, L., Liu, T., Müller, B., Schnürer, A., 2016. The microbial community structure in industrial biogas plants influences the degradation rate of straw and cellulose in batch tests. Biotechnol. Biofuels, 9 (1), 1-20. https://doi.org/10.1186/s13068-016-0543-9.

Sun, Z., Xia, F., Lou, Z., Chen, X., Zhu, N., Yuan, H., Shen, Y., 2020. Innovative process for total petroleum hydrocarbons reduction on oil refinery sludge through microbubble ozonation. J. Clean. Prod. 256, 120337. https://doi.org/10.1016/j.jclepro.2020.120337.

Supaphol, S., Jenkins, S. N., Intomo, P., Waite, I. S., O'Donnell, A. G., 2011. Microbial community dynamics in mesophilic anaerobic co-digestion of mixed waste. Bioresour. Technol. 102 (5), 4021-4027. https://doi.org/10.1016/j.biortech.2010.11.124.

Tahhan, R. A., Ammari, T. G., Goussous, S. J., Al-Shdaifat, H. I., 2011. Enhancing the biodegradation of total petroleum hydrocarbons in oily sludge by a modified bioaugmentation strategy. Int. Biodeterior. Biodegradation. 65(1), 130-134. https://doi.org/10.1016/j.ibiod.2010.09.007.

Taiwo, E. A., Otolorin. J.A., 2009. Oil recovery from petroleum sludge by solvent extraction. Pet. Sci. Technol. 27 (8), 836–44.

Tanaka, S., Kobayashi, T., Kamiyama, K.I., Bildan, M.L.N.S., 1997. Effects of thermochemical pretreatment on the anaerobic digestion of waste activated sludge. Water Sci. Technol. 35(8), 209-215.

Tang, J., Lu, X., Sun, Q., Zhu, W., 2012. Aging effect of petroleum hydrocarbons in soil under different attenuation conditions. Agric. Ecosyst. Environ. 149, 109-117. https://doi.org/10.1016/j.agee.2011.12.020.

Tavassoli, T., Mousavi, S. M., Shojaosadati, S. A., Salehizadeh, H., 2012. Asphaltene biodegradation using microorganisms isolated from oil samples. Fuel. 93, 142–148. doi: 10.1016/j.fuel.2011.10.021.

Teng, Z., Hua, J., Wang, C. and Lu, X., 2014. Design and optimization principles of biogas reactors in large scale applications. In Reactor and process design in sustainable energy technology (pp. 99-134). Elsevier.

Throne-Holst, M., Wentzel, A., Ellingsen, T.E., Kotlar, H.K., Zotchev, S.B., 2007. Identification of novel genes involved in long-chain n-alkane degradation by Acinetobacter sp. strain DSM 17874. Appl. Environ. Microbiol. 73(10), 3327-3332.

Toreci, I., Kennedy, K.J., Droste, R.L., 2010. Effect of high-temperature microwave irradiation on municipal thickened waste activated sludge solubilization, Heat Transf. Eng. 31, 766-773. https://doi.org/10.1080/01457630903501039.

Treu, L., Tsapekos, P., Peprah, M., Campanaro, S., Giacomini, A., Corich, V., Kougias, P., Angelidaki, I., 2018. Microbial profiling during anaerobic digestion of cheese whey in

reactors operated at different conditions. Bioresour. Technol. 275, 375-385. https://doi.org/10.1016/j.biortech.2018.12.084.

Trofimov, S.Y., Rozanova, M.S., 2003. Transformation of soil properties under the impact of oil pollution. Eurasian J. Soil Sci. 36, S82-S87.

Tsegaye, B., Balomajumder, C., Roy, P., 2019. Microbial delignification and hydrolysis of lignocellulosic biomass to enhance biofuel production: an overview and future prospect. Bull. Natl. Res. Cent. 43(1), pp.1-16. https://doi.org/10.1186/s42269-019-0094-x.

Tsegaye, D., Khan, M.M., Leta, S., 2023. Optimization of Operating Parameters for Two-Phase Anaerobic Digestion Treating Slaughterhouse Wastewater for Biogas Production: Focus on Hydrolytic–Acidogenic Phase. Sustainability. 15 (6), 5544.

Tufaner, F., Demirci, Y., 2020. Prediction of biogas production rate from anaerobic hybrid reactor by artificial neural network and nonlinear regressions models. Clean Technol. Environ. Policy, 22, 713-724.

Tuhuloula, A., Suprapto, S., Altway, A., Juliastuti, S. R., 2019. Biodegradation of Extractable Petroleum Hydrocarbons by Consortia *Bacillus cereus* and *Pseudomonas putida* in Petroleum Contaminated-Soil. Indones. J. Chem. 19 (2), 347-355. https://doi.org/10.22146/ijc.33765.

Updegraff, D.M., 1969. Semimicro determination of cellulose in biological materials. Anal. Biochem. 32(3), 420-424. https://doi.org/10.1016/S0003-2697(69)80009-6.

Varjani, S. J., 2017. Microbial degradation of petroleum hydrocarbons. Bioresour. Technol. 223, 277-286. https://doi.org/10.1016/j.biortech.2016.10.037.

Varjani, S. J., Upasani, V. N., 2017. A new look on factors affecting microbial degradation of petroleum hydrocarbon pollutants. Int. Biodeterior. Biodegrad. 120, 71-83. https://doi.org/10.1016/j.ibiod.2017.02.006.

Verma, A., Dhiman, K., Shirkot, P., 2016. Hyper-production of laccase *by Pseudomonas putida* LUA 15.1 through mutagenesis. J. Microbiol. Exp. 3 (1), 00080. https://doi.org/10.15406/jmen.2016.03.00080.

Wahidunnabi, A. K., Eskicioglu, C., 2014. High pressure homogenization and two-phased anaerobic digestion for enhanced biogas conversion from municipal waste sludge. Water Res. 66, 430-446. https://doi.org/10.1016/j.watres.2014.08.045

Wang, D., Lin, J., Lin, J., Wang, W., Li, S., 2019. Biodegradation of petroleum hydrocarbons by *Bacillus subtilis* BL-27, a strain with weak hydrophobicity. Molecules, 24(17), 3021. https://doi.org/10.3390/molecules24173021.

Wang, K., Yun, S., Xing, T., Li, B., Abbas, Y., Liu, X., 2021. Binary and ternary trace elements to enhance anaerobic digestion of cattle manure: Focusing on kinetic models for biogas production and digestate utilization. Bioresour. Technol. 323, 124571. https://doi.org/10.1016/j.biortech.2020.124571.

Wang, L., Xu, Y., Zhao, Z., Zhang, D., Lin, X., Ma, B., Zhang, H., 2022. Analysis of Pyrolysis Characteristics of Oily Sludge in Different Regions and Environmental Risk Assessment of Heavy Metals in Pyrolysis Residue. ACS omega. 7 (30), 26265-26274. https://doi.org/10.1021/acsomega.2c01994

Wang, Q., Liang, Y., Zhao, P., Li, Q. X., Guo, S., Chen, C., 2016. Potential and optimization of two-phase anaerobic digestion of oil refinery waste activated sludge and microbial community study. Sci. Rep. 6, 38245. https://doi.org/10.1038/srep38245 .

Wang, W., Keturi, P.H., 1990. Comparative seed germination tests using ten plant species for toxicity assessment of a metal engraving effluent sample. Water, Air, Soil Pollut. 52(1990) 369–376. https://doi.org/10.1007/BF00229444.

Wang, Z., Guo, Q., Liu, X., Cao, C., 2007. Low temperature pyrolysis characteristics of oily sludge under various heating conditions. Energ. Fuel. 21, 957-962. https://doi.org/10.1021/ef060628g.

Ward, O., Singh, A., Van Hamme, J., 2003. Accelerated biodegradation of petroleum hydrocarbon waste. J. Ind. Microbiol. Biotechnol., 30 (5), 260-270. https://doi.org/10.1007/s10295-003-0042-4.

Weiland, P., 2006. Biomass digestion in agriculture: a successful pathway for the energy production and waste treatment in Germany. Eng. Life Sci. 6(3), 302-309. https://doi.org/10.1002/elsc.200620128.

Westerholm, M., Crauwels, S., Houtmeyers, S., Meerbergen, K., Van Geel, M., Lievens, B., Appels, L., 2016. Microbial community dynamics linked to enhanced substrate availability and biogas production of electrokinetically pre-treated waste activated sludge. Bioresour. Technol. 218, 761-770. https://doi.org/10.1016/j.biortech.2016.07.029.

Widdel, F., Rabus, R., 2001. Anaerobic biodegradation of saturated and aromatic hydrocarbons. Curr. Opin. Biotechnol. 12 (3), 259-276. https://doi.org/10.1016/S0958-1669(00)00209-3.

Wilkes, H., Buckel, W., Golding, B.T., Rabus, R., 2016. Metabolism of hydrocarbons in n-alkane-utilizing anaerobic bacteria. J. Mol. Microbiol. Biotechnol. 26 (1-3), 138-151. https://doi.org/10.1159/000442160.

Wojcieszak, M., Pyzik, A., Poszytek, K., Krawczyk, P. S., Sobczak, A., Lipinski, L., Roubinek, O., Palige, J., Sklodowska, A., Drewniak, L., 2017. Adaptation of methanogenic inocula to anaerobic digestion of maize silage. Front. Microbiol. 8, 1881. https://doi.org/10.3389/fmicb.2017.01881.

Wojcieszak, M., Pyzik, A., Poszytek, K., Krawczyk, P.S., Sobczak, A., Lipinski, L., Roubinek, O., Palige, J., Sklodowska, A., Drewniak, L., 2017. Adaptation of Methanogenic Inocula to Anaerobic Digestion of Maize Silage. Front. Microbiol. 8, 1881. https://doi.org/10.3389/fmicb.2017.01881.

Wong, D.W., 2009. Structure and action mechanism of ligninolytic enzymes. Appl. Biochem. Biotechnol. 157(2), 174-209. https://doi.org/10.1007/s12010-008-8279-z.

World Energy Council. (2019). World Energy Resources: 2019 Survey. London: World Energy Council.

Wu, Y., Teng, Y., Li, Z., Liao, X., Luo, Y., 2008. Potential role of polycyclic aromatic hydrocarbons PAHs oxidation by fungal laccase in the remediation of an aged contaminated soil. Soil Biol. Biochem. 40, 789-796. https://doi.org/10.1016/j.soilbio.2007.10.013.

Xu, F., Shi, J., Lv, W., Yu, Z., Li, Y., 2012. Comparison of different liquid anaerobic digestion effluents as inocula and nitrogen sources for solid state anaerobic digestion of corn stover. Waste Manag. 33, 26–32. doi: 10.1016/j.wasman.2012.08.006.

Xu, H., Li, Y., Hua, D., Zhao, Y., Chen, L., Zhou, L., Chen, G., 2021. Effect of microaerobic microbial pretreatment on anaerobic digestion of a lignocellulosic substrate under controlled pH conditions. Bioresour. Technol. 328, 124852. https://doi.org/10.1016/j.biortech.2021.124852.

Xu, N., Wang, W., Han, P., Lu, X., 2008. Effects of ultrasound on oily sludge deoiling, J. Hazard. Mater. 171, 914–917.

Xu, W., Zhao, H., Cao, H., Zhang, Y., Sheng, Y., Li, T., Zhou, S., Li, H., 2020. New insights of enhanced anaerobic degradation of refractory pollutants in coking wastewater: Role of zero-

valent iron in metagenomic functions. Bioresour. Technol. 300, 122667. https://doi.org/10.1016/j.biortech.2019.122667.

Xu, X., Liu, W., Tian, S., Wang, W., Qi, Q., Jiang, P., Gao, X., Li, F., Li, H., Yu, H., 2018. Petroleum hydrocarbon-degrading bacteria for the remediation of oil pollution under aerobic conditions: a perspective analysis. Front. Microbiol., 9, 2885. https://doi.org/10.3389/fmicb.2018.02885.

Xu, Y., Lu, Y., Dai, X., Dai, L., 2018. Enhancing Anaerobic Digestion of Waste Activated Sludge by Solid–Liquid Separation via Isoelectric Point Pretreatment. ACS Sustainable Chemistry & Engineering, 6 (11), 14774-14784.

Xu, Z., Lei, P., Zhai, R., Wen, Z., Jin, M., 2019. Recent advances in lignin valorization with bacterial cultures: microorganisms, metabolic pathways, and bio-products. Biotechnol. Biofuels. 12(1), 1-19. https://doi.org/10.1186/s13068-019-1376-0.

Yan, L., Ye, J., Zhang, P., Xu, D., Wu, Y., Liu, J., Zhang, H., Fang, W., Wang, B., Zeng, G., 2018. Hydrogen sulfide formation control and microbial competition in batch anaerobic digestion of slaughterhouse wastewater sludge: Effect of initial sludge pH. Bioresour. Technol. 259, 67-74. https://doi.org/10.1016/j.biortech.2018.03.011.

Yan, P., Lu, M., Yang, Q., Zhang, H.L., Zhang, Z.Z, Chen R., 2012. Oil recovery from refinery oily sludge using a rhamnolipid biosurfactant-producing Pseudomonas. Bioresour. Technol. 116, 24-28.

Yang, L., Nakhla, G., Bassi, A., 2005. Electro-kinetic dewatering of oily sludges. J. Hazard. Mater. 125, 130–140. https://doi.org/10.1016/j.jhazmat.2005.05.040.

Yang, Q., Zhang, C., Li, L., Xu, W., 2020. Anaerobic co-digestion of oil sludge with corn stover for efficient biogas production. Sustainability. 12 (5), 1861. https://doi.org/10.3390/su12051861.

Yang, Y., Cheng, G., Li, Y., Wang, T., Li, F., Huang, W., 2019. Effect of agitation pretreatment on anaerobic digestion of swine manure. Energy Sources, Part A: Recovery, Utilization, and Environmental Effects. 41, 122-128. https://doi.org/10.1080/15567036.2018.1503758.

Ye, G., Lu, X., Han, P., Peng, F., Wang, Y., Shen, X., 2008. Application of ultrasound on crude oil pretreatment. Chem. Eng. Process. 47(12), 2346-2350.

Yeshanew, M.M., Frunzo, L., Lens, P.N., Pirozzi, F., Esposito, G., 2016. Mass Loss Controlled Thermal Pretreatment System to Assess the Effects of Pretreatment Temperature on

Organic Matter Solubilization and Methane Yield from Food Waste, Front. Environ. Sci. 4, 62. https://doi.org/10.3389/fenvs.2016.00062.

Yılmaz, Ş., Şahan, T., 2020. Utilization of pumice for improving biogas production from poultry manure by anaerobic digestion: A modeling and process optimization study using response surface methodology. Biomass Bioenergy. 138, 105601. https://doi.org/10.1016/j.biombioe.2020.105601.

Yu, B., Xu, J., Yuan, H., Lou, Z., Lin, J., Zhu, N., 2014. Enhancement of anaerobic digestion of waste activated sludge by electrochemical pretreatment. Fuel. 130, 279-285. https://doi.org/10.1016/j.fuel.2014.04.031.

Yuan, C., Weng, C., 2003. Sludge dewatering by electrokinetic technique: effect of processing time and potential gradient. Adv. Environ. Res., 7 (3), 727-732. https://doi.org/10.1016/S1093-0191(02)00030-8.

Zeng, Q., Zan, F., Hao, T., Biswal, B. K., Lin, S., van Loosdrecht, M. C., Chen, G., 2019. Electrochemical pretreatment for stabilization of waste activated sludge: Simultaneously enhancing dewaterability, inactivating pathogens and mitigating hydrogen sulfide. Water Res. 166, 115035. https://doi.org/10.1016/j.watres.2019.115035.

Zeshan, K.O., Visvanathan, C., 2012. Effect of C/N ratio and ammonia-N accumulation in a pilot-scale thermophilic dry anaerobic digester. Bioresour. Technol. 113, 94-302. https://doi.org/10.1016/j.biortech.2012.02.028.

Zhang, D., Feng, Y., Huang, H., Khunjar, W., Wang, Z., 2020. Recalcitrant dissolved organic nitrogen formation in thermal hydrolysis pretreatment of municipal sludge, Environ. Int. 138, 105629. https://doi.org/10.1016/j.envint.2020.105629.

Zhang, G., Zhang, Z., Li, C., 2018. Improvement of solid-state anaerobic digestion of yard waste by co-digestion and pH adjustment. Waste Biomass Valorization. 9 (2), 211-221. https://doi.org/10.1007/s12649-016-9798-4.

Zhang, J., Li, W., Lee, J., Loh, K.C., Dai, Y., Tong, Y.W., 2017. Enhancement of biogas production in anaerobic co-digestion of food waste and waste activated sludge by biological co-pretreatment. Energy, 137, pp.479-486. https://doi.org/10.1016/j.energy.2017.02.163.

Zhang, L., Lee, Y.W., Jahng, D., 2011. Anaerobic co-digestion of food waste and piggery wastewater: focusing on the role of trace elements. Bioresour. Technol. 102, 5048-5059. https://doi.org/10.1016/j.biortech.2011.01.082.

Zhou, H., Wu, C., Onwudili, J.A., Meng, A., Zhang, Y., Williams, P.T., 2015a. Polycyclic aromatic hydrocarbons (PAH) formation from the pyrolysis of different municipal solid waste fractions. Waste Manag. 36, 136-146.

Zhou, J., Xu, W., Wong, J.W., Yong, X., Yan, B., Zhang, X., Jia, H., 2015b. Ultrasonic and Thermal Pretreatments on Anaerobic Digestion of Petrochemical Sludge: Dewaterability and Degradation of PAHs. PloS One. 10, e0136162. https://doi.org/10.1371/journal.pone.0136162.

Zhou, M., Yan, B., Wong, J. W.C., Zhang, Y., 2018. Enhanced volatile fatty acids production from anaerobic fermentation of food waste: A mini-review focusing on acidogenic metabolic pathways. Bioresour. Technol. 248 (Part A), 68-78. https://doi.org/10.1016/j.biortech.2017.06.121.

Zhu, B., Zhang, R., Gikas, P., Rapport, J., Jenkins, B., Li, X., 2010. Biogas production from municipal solid wastes using an integrated rotary drum and anaerobic-phased solids digester system. Bioresour. Technol. 101, 6374-6380. https://doi.org/10.1016/j.biortech.2010.03.075

Zubaidy, E.A.H., Abouelnasr, D.M., 2010. Fuel recovery from waste oily sludge using solvent extraction. Process. Saf. Environ. 88, 318-326.

Zuo, W., Li, J., Zhang, Y., Li, Q., He, Z., 2020. Effects of multi-factors on comprehensive performance of a hydrogen-fueled micro-cylindrical combustor by combining grey relational analysis and analysis of variance. Energy. 199, 117439. https://doi.org/10.1016/j.energy.2020.117439.

Zuo, W., Zhang, Y., Li, Q., Li, J., He, Z., 2021. Numerical investigations on hydrogen-fueled micro-cylindrical combustors with cavity for micro-thermophotovoltaic applications. Energy, 223, 120098. https://doi.org/10.1016/j.energy.2021.120098.

भारतीय प्रौद्योगिकी संस्थान गुवाहाटी
Indian Institute of Technology Guwahati

RESEARCH OUTPUT

JOURNAL PUBLICATIONS

Published articles

- Paul Choudhury, S., Haq, I., Kalamdhad, A.S., 2023. Unleashing Synergistic Potential of Microbially Enhanced Anaerobic Co-Digestion of Petroleum Refinery Biosludge and Yard Waste: Impact of Nutrient Balance and Microbial Diversity. ***Journal of Hazardous Materials***. p. 132361. https://doi.org/10.1016/j.jhazmat.2023.132361
- Paul Choudhury, S., Panda, S., Haq, I., Kalamdhad, A.S., 2022. Microbial pretreatment using *Kosakonia oryziphila* IH3 to enhance biogas production and hydrocarbon depletion from petroleum refinery sludge. ***Renewable Energy***. 194, 1192-1203. https://doi.org/10.1016/j.renene.2022.05.167.
- Paul Choudhury, S., Panda, S., Haq, I., Kalamdhad, A.S., 2022. Enhanced methane production and hydrocarbon removal from petroleum refinery sludge after *Pseudomonas putida* pretreatment and process scale-up. ***Bioresource Technology***. 343, p.126127. https://doi.org/10.1016/j.biortech.2021.126127.
- Paul Choudhury, S., Dalasingh, B., Haq, I., Kalamdhad, A. S., 2021. Methane production and toxicity evaluation of petroleum refinery biosludge through optimization of different modes of heat. ***Process Safety and Environmental Protection***. 154, 236-248. https://doi.org/10.1016/j.psep.2021.08.019.
- Paul Choudhury, S., Kalamdhad, A. S., 2021. Optimization of electrokinetic pretreatment for enhanced methane production and toxicity reduction from petroleum refinery sludge. ***Journal of Environmental Management***. 298, 113469. https://doi.org/10.1016/j.jenvman.2021.113469.

Articles (submitted/under review)

- Paul Choudhury, S., Haq, I., Gautam, P., Kalamdhad, A.S., 2023. Unveiling the Impact of Biological Pretreatment on the Anaerobic Co-Digestion of Petroleum Refinery Biosludge with Yard Waste. *Bioresource Technology*. **(Submitted)**
- Paul Choudhury, S., Kalamdhad, A.S., 2023. Electrokinetically Assisted Anaerobic Co-digestion of Petroleum Refinery Sludge and Yard Waste: Combined Effect of Direct Current Voltage and Exposure Period. *International biodegradation and biodeterioration*. **(Submitted)**

BOOK CHAPTERS

- Paul Choudhury, S., Saha, B., Kalamdhad, A., 2020. **Use of Petroleum Refinery Sludge for the Production of Biogas as an Alterntive Energy Source: A Review**. *Advanced Organic Waste Management: Sustainable Practices and Approaches*. 277-297. Elsevier.

CONFERENCES/TEQUIP/FDP

- **Paul Choudhury, S.**, Kalamdhad, A.S, 2023. Biogas Production from Petroleum Refinery Sludge in Anaerobic Biphased Baffled Reactor (ABBR): A Semi-Continuous Study. *International Conference on Waste Management (RECYCLE 2023)*, Indian Institute of Technology, Guwahati, India.
- **Paul Choudhury, S**., Kalamdhad, A.S., 2022. Microbial Pretreatment using *Pseudomonas putida* for Biogas Augmentation and Hydrocarbon Degradation from Activated Refinery Sludge. *North East Research Conclave Sustainable Science and Technology (NEERC)* May 20-22, 2022; Indian Institute of Technology Guwahati, Assam, India.
- **Paul Choudhury, S.**, Haq, I., Kalamdhad, A.S, 2020. Biological Pretreatment of Petroleum Refinery Sludge for Enhanced Biogas Production. *International Conference on Waste Management (RECYCLE 2020)*, Indian Institute of Technology, Guwahati, India.
- **Paul Choudhury, S.**, Dalasingh, B., Kalamdhad, A.S, 2020. Evaluation of Thermal Pretreatment on Petroleum Sludge to Enhance the Performance of Anaerobic Digestion. *International Conference on Waste Management (RECYCLE 2020)*, Indian Institute of Technology, Guwahati, India.
- TEQUIP-III Short-term Course on **Challenges and Opportunities in Solid and Liquid Waste Management** from 02/11/20 - 06/11/2020.
- Faculty Development Programme (FDP) on **Municipal Solid Waste Management during COVID-19 Pandemic** from 28/05/2020 - 30/05/2020.